

Concepts and Strategies in Plant Sciences  
Series Editor: Chittaranjan Kole

Jianfeng Zhou  
Henry T. Nguyen *Editors*

# High-Throughput Crop Phenotyping

 Springer

# **Concepts and Strategies in Plant Sciences**

## **Series Editor**

Chittaranjan Kole, Raja Ramanna Fellow, Government of India,  
ICAR-National Institute for Plant Biotechnology, Pusa, Delhi, India

This book series highlights the spectacular advances in the concepts, techniques and tools in various areas of plant science. Individual volumes may cover topics like genome editing, phenotyping, molecular pharming, bioremediation, miRNA, fast-track breeding, crop evolution, IPR and farmers' rights, to name just a few. The books will demonstrate how advanced strategies in plant science can be utilized to develop and improve agriculture, ecology and the environment. The series will be of interest to students, scientists and professionals working in the fields of plant genetics, genomics, breeding, biotechnology, and in the related disciplines of plant production, improvement and protection.

**Interested in editing a volume?** Please contact Prof. Chittaranjan Kole, Series Editor, at [ckoleorg@gmail.com](mailto:ckoleorg@gmail.com)

More information about this series at <http://www.springer.com/series/16076>

Jianfeng Zhou · Henry T. Nguyen  
Editors

# High-Throughput Crop Phenotyping

 Springer

*Editors*

Jianfeng Zhou  
University of Missouri  
Columbia, MO, USA

Henry T. Nguyen  
University of Missouri  
Columbia, MO, USA

ISSN 2662-3188

ISSN 2662-3196 (electronic)

Concepts and Strategies in Plant Sciences

ISBN 978-3-030-73733-7

ISBN 978-3-030-73734-4 (eBook)

<https://doi.org/10.1007/978-3-030-73734-4>

© Springer Nature Switzerland AG 2021

This work is subject to copyright. All rights are reserved by the Publisher, whether the whole or part of the material is concerned, specifically the rights of translation, reprinting, reuse of illustrations, recitation, broadcasting, reproduction on microfilms or in any other physical way, and transmission or information storage and retrieval, electronic adaptation, computer software, or by similar or dissimilar methodology now known or hereafter developed.

The use of general descriptive names, registered names, trademarks, service marks, etc. in this publication does not imply, even in the absence of a specific statement, that such names are exempt from the relevant protective laws and regulations and therefore free for general use.

The publisher, the authors and the editors are safe to assume that the advice and information in this book are believed to be true and accurate at the date of publication. Neither the publisher nor the authors or the editors give a warranty, expressed or implied, with respect to the material contained herein or for any errors or omissions that may have been made. The publisher remains neutral with regard to jurisdictional claims in published maps and institutional affiliations.

This Springer imprint is published by the registered company Springer Nature Switzerland AG  
The registered company address is: Gewerbestrasse 11, 6330 Cham, Switzerland

# Preface

Global population is expected to reach 9.8 billion and food demand is expected to be 60% higher than it is today by 2050, which requires a double current yield increase rate to meet the demand. During the past 20 years, molecular profiling and sequencing technologies enabled major advances toward the large-scale characterization of crop genomes. However, the acquisition of crop phenotypic information has lagged behind to allow a better understanding of genotype-to-phenotype relationships and becomes one of the bottlenecks to crop improvement, genetics, and genomic selection (GS). Thanks to the advances in emerging technologies in sensors, machine vision, robotics, Unmanned Aerial Systems (UASs), crop traits (phenotypic data) are able to be acquired in a large-scale and high-throughput manner. Big data processing and analytic technologies (e.g., machine learning and deep learning) and high-performance computation systems are transforming the conventional crop breeding to the next-generation AI-based crop breeding.

This book presents state-of-the-art information on the important innovations of high-throughput crop phenotyping technology in quantifying crop traits of shoots and roots through various applications in field and controlled environments. The applications cover a large range of crops (including soybean, wheat, maize, grains, and potato), various measurements of crop phenotypes in different levels (crop organ, plot, and field), and for different purposes. Different novel technologies and the implementation of these technologies in high-throughput crop phenotyping are reviewed and discussed. The technologies include emerging sensors to measure different crop traits, automated data acquisition platforms for fast and large-scale data collection (e.g., autonomous ground and aerial vehicles, robotic systems), big data processing and analytics, and their integration. Each chapter of the book focuses on different aspects of the high-throughput phenotyping technology and the applications for specific crops. The book starts with a chapter (Chap. 1) that briefly explains the concept, content, and roles of the high-throughput crop phenotyping technology in crop breeding towards yield improvement using the breeder's equation. Chaps. 2 and 3 provide the applications of innovative field-based crop phenotyping systems using ground-based robot systems and a cable-suspended robot system. As one of the key components of image-based phenotyping systems,

Chap. 4 discusses novel methods for developing three-dimensional (3D) architecture of crop plants based on images or videos collected with field crop phenotyping systems. The following chapters (Chaps. 5–8) provide applications in crop breeding of wheat, rice, soybean, and potato, followed by the applications in a controlled environment (Chap. 9) and root phenotyping (Chap. 10). The final chapter (Chap. 11) discusses the challenges in adopting high-throughput crop phenotyping technology into crop breeding pipelines by considering of cost.

This book provides insights into high-throughput crop phenotyping technology from the different perspectives of leading researchers in multiple disciplines, including but not limited to Crop Breeding, Genetics, Engineering, Computer Science, and Data Science. The authors have extensive knowledge and practical experiences in their respective fields and are actively involved in the international community of crop phenotyping. We wish to acknowledge their expert contributions and great efforts in the preparation for the book chapters. Finally, we hope that this book will assist all readers who are working in or associated with the fields of high-throughput crop phenotyping.

Columbia, MO, USA

Jianfeng Zhou  
Henry T. Nguyen

# Contents

<b>1</b>	<b>Solve the Breeder’s Equation Using High-Throughput Crop Phenotyping Technology</b> .....	<b>1</b>
	Jianfeng Zhou and Henry T. Nguyen	
<b>2</b>	<b>Field Robotic Systems for High-Throughput Plant Phenotyping: A Review and a Case Study</b> .....	<b>13</b>
	Yin Bao, Jingyao Gai, Lirong Xiang, and Lie Tang	
<b>3</b>	<b>Cable Suspended Large-Scale Field Phenotyping Facility for High-Throughput Phenotyping Research</b> .....	<b>39</b>
	Geng (Frank) Bai and Yufeng Ge	
<b>4</b>	<b>Structure from Motion and Mosaicking for High-Throughput Field-Scale Phenotyping</b> .....	<b>55</b>
	Hadi AliAkbarpour, Ke Gao, Rumana Aktar, Steve Suddarth, and Kannappan Palaniappan	
<b>5</b>	<b>Experiences of Applying Field-Based High-Throughput Phenotyping for Wheat Breeding</b> .....	<b>71</b>
	Jared Crain, Xu Wang, Mark Lucas, and Jesse Poland	
<b>6</b>	<b>High-Throughput Phenotyping (HTP) and Genetic Analysis Technologies Reveal the Genetic Architecture of Grain Crops</b> .....	<b>101</b>
	Wanneng Yang, Xuehai Zhang, and Lingfeng Duan	
<b>7</b>	<b>High-Throughput Phenotyping in Soybean</b> .....	<b>129</b>
	Asheesh K. Singh, Arti Singh, Soumik Sarkar, Baskar Ganapathysubramanian, William Schapaugh, Fernando E. Miguez, Clayton N. Carley, Matthew E. Carroll, Mariana V. Chiozza, Kevin O. Chiteri, Kevin G. Falk, Sarah E. Jones, Talukder Z. Jubery, Seyed V. Mirnezami, Koushik Nagasubramanian, Kyle A. Parmley, Ashlyn M. Rairdin, Johnathon M. Shook, Liza Van der Laan, Therin J. Young, and Jiaoping Zhang	



**8 High-Throughput Phenotyping in Potato Breeding** ..... 165  
Jagesh Kumar Tiwari, Sushil S. Changan, Tanuja Buckseth,  
Rajesh K. Singh, Brajesh Singh, Satish K. Luthra, Shashi Rawat,  
and Manoj Kumar

**9 High-Throughput Crop Phenotyping Systems for Controlled  
Environments** ..... 183  
Jianfeng Zhou, Jing Zhou, Heng Ye, and Henry T. Nguyen

**10 Phenotyping Root System Architecture, Anatomy,  
and Physiology to Understand Soil Foraging** ..... 209  
Larry M. York

**11 Got All the Answers! What Were the Questions? Avoiding  
the Risk of “Phenomics” Slipping into a Technology Spree** ..... 223  
Vincent Vadez, Jana Kholova, Grégoire Hummel,  
and Uladzimir Zhokhavets

**Index** ..... 243

# Contributors

**Rumana Aktar** University of Missouri-Columbia, Columbia, USA

**Hadi AliAkbarpour** Transparent Sky, Edgewood, USA;  
University of Missouri-Columbia, Columbia, USA

**Geng (Frank) Bai** Department of Biological Systems Engineering, University of  
Nebraska-Lincoln, Nebraska, Lincoln, USA

**Yin Bao** Department of Biosystems Engineering, Auburn University, Auburn, AL,  
USA

**Tanuja Buckseth** ICAR-Central Potato Research Institute, Shimla, Himachal  
Pradesh, India

**Clayton N. Carley** Department of Agronomy, Iowa State University, Ames, IA,  
USA

**Matthew E. Carroll** Department of Agronomy, Iowa State University, Ames, IA,  
USA

**Sushil S. Changan** ICAR-Central Potato Research Institute, Shimla, Himachal  
Pradesh, India

**Mariana V. Chiozza** Department of Agronomy, Iowa State University, Ames, IA,  
USA

**Kevin O. Chiteri** Department of Agronomy, Iowa State University, Ames, IA, USA

**Jared Crain** Department Plant Pathology, Kansas State University, Throckmorton  
Plant Sciences Center, Manhattan, KS, USA

**Lingfeng Duan** College of Engineering, Huazhong Agricultural University,  
Wuhan, People's Republic of China

**Kevin G. Falk** Department of Agronomy, Iowa State University, Ames, IA, USA

**Jingyao Gai** Department of Agricultural and Biosystems Engineering, Iowa State  
University, Ames, IA, USA

**Baskar Ganapathysubramanian** Department of Mechanical Engineering, Iowa State University, Ames, IA, USA

**Ke Gao** University of Missouri-Columbia, Columbia, USA

**Yufeng Ge** Department of Biological Systems Engineering, University of Nebraska-Lincoln, Nebraska, Lincoln, USA

**Grégoire Hummel** Phenospex, Heerlen, The Netherlands

**Sarah E. Jones** Department of Agronomy, Iowa State University, Ames, IA, USA

**Talukder Z. Jubery** Department of Agronomy, Iowa State University, Ames, IA, USA

**Jana Kholova** Crop Physiology Laboratory, ICRISAT, Patancheru, Telangana, India

**Manoj Kumar** ICAR-Central Potato Research Institute, Shimla, Himachal Pradesh, India

**Mark Lucas** Department Plant Pathology, Kansas State University, Throckmorton Plant Sciences Center, Manhattan, KS, USA

**Satish K. Luthra** ICAR-Central Potato Research Institute, Shimla, Himachal Pradesh, India

**Fernando E. Miguez** Department of Agronomy, Iowa State University, Ames, IA, USA

**Seyed V. Mirnezami** Department of Mechanical Engineering, Iowa State University, Ames, IA, USA

**Koushik Nagasubramanian** Department of Electrical Engineering, Iowa State University, Ames, IA, USA

**Henry T. Nguyen** Division of Plant Science and Technology, University of Missouri, Columbia, MO, USA

**Kannappan Palaniappan** University of Missouri-Columbia, Columbia, USA

**Kyle A. Parmley** Department of Agronomy, Iowa State University, Ames, IA, USA

**Jesse Poland** Department Plant Pathology, Kansas State University, Throckmorton Plant Sciences Center, Manhattan, KS, USA;  
Wheat Genetics Resource Center, Kansas State University, Throckmorton Plant Sciences Center, Manhattan, KS, USA

**Ashlyn M. Rairdin** Department of Agronomy, Iowa State University, Ames, IA, USA

**Shashi Rawat** ICAR-Central Potato Research Institute, Shimla, Himachal Pradesh, India

**Soumik Sarkar** Department of Mechanical Engineering, Iowa State University, Ames, IA, USA

**William Schapaugh** Department of Agronomy, Kansas State University, Manhattan, KS, USA

**Johnathon M. Shook** Department of Agronomy, Iowa State University, Ames, IA, USA

**Arti Singh** Department of Agronomy, Iowa State University, Ames, IA, USA

**Asheesh K. Singh** Department of Agronomy, Iowa State University, Ames, IA, USA

**Brajesh Singh** ICAR-Central Potato Research Institute, Shimla, Himachal Pradesh, India

**Rajesh K. Singh** ICAR-Central Potato Research Institute, Shimla, Himachal Pradesh, India

**Steve Suddarth** Transparent Sky, Edgewood, USA

**Lie Tang** Department of Agricultural and Biosystems Engineering, Iowa State University, Ames, IA, USA

**Jagesh Kumar Tiwari** ICAR-Central Potato Research Institute, Shimla, Himachal Pradesh, India

**Vincent Vadez** Institut de Recherche pour le Développement (IRD), UMR DIADE, University of Montpellier, Montpellier, France

**Liza Van der Laan** Department of Agronomy, Iowa State University, Ames, IA, USA

**Xu Wang** Department Plant Pathology, Kansas State University, Throckmorton Plant Sciences Center, Manhattan, KS, USA

**Lirong Xiang** Department of Agricultural and Biosystems Engineering, Iowa State University, Ames, IA, USA

**Wanneng Yang** National Key Laboratory of Crop Genetic Improvement and National Center of Plant Gene Research, Huazhong Agricultural University, Wuhan, People's Republic of China

**Heng Ye** Division of Plant Science and Technology, University of Missouri, Columbia, MO, USA

**Larry M. York** Noble Research Institute, LLC, Ardmore, OK, USA

**Therin J. Young** Department of Mechanical Engineering, Iowa State University, Ames, IA, USA

**Jiaoping Zhang** Department of Agronomy, Iowa State University, Ames, IA, USA

**Xuehai Zhang** National Key Laboratory of Wheat and Maize Crops Science/College of Agronomy, Henan Agricultural University, Zhengzhou, People's Republic of China

**Uladzimir Zhokhavets** Phenospex, Heerlen, The Netherlands

**Jianfeng Zhou** Division of Plant Science and Technology, University of Missouri, Columbia, MO, USA

**Jing Zhou** Division of Plant Science and Technology, University of Missouri, Columbia, MO, USA

# Abbreviations

$\Delta^{13}\text{C}$	Carbon isotope discrimination
$\Delta G_{\text{year}}$	Genetic gain per year
$^{13}\text{C}$	Isotope Carbon 13
2D	Two-dimensional
2-D	2 dimension
3D	Three-dimensional
3-D	3 dimension
AGV	Automatic guided vehicles
AI	Artificial Intelligence
API	Application programming interface
ATV	All-terrain vehicle
BC	Backcross population
BOVW	Bag of Visual Words
CCD	Charge-coupled device
CIMMYT	International Maize and Wheat Improvement Center
CMOS	Complementary metal-oxide-semiconductor
CNN	Convolutional neural networks
$\text{CO}_2$	Carbon dioxide
CPU	Central processing unit
CSS	Cable-suspended system
CT	Computed Tomography
DAE	Day after emerging
DEM	Digital Elevation Model
DH	Double haploid population
DIRT	Digital imaging of root traits
DL	Deep learning
DPS	Global positioning system
DR	Drought tolerance
EKF	Extended Kalman filter
ELM	Extreme Learning Machine
ELR	Extreme learning
EMS	Electromagnetic spectrum

EPV	Estimated processed value
EVI2	Enhanced vegetation index
FIP	Field Phenotyping Platform
$F_m$	Maximum fluorescence value
$F_o$	Minimum fluorescence value
FOV	Field of view
FPP	Field plant phenotyping
$F_v$	Variable fluorescence
G2P	Genotype-to-phenotype
GBS	Genotype-by-sequence
GBS	Genotyping-by-sequencing
GCPs	Ground control points
GEBV	Genomic estimated breeding values
gLAI	green Leaf Area Index
GNSS	Global navigation satellite system
GP	Genomic prediction
GPS	Global positioning system
GS	Genomic selection
GSD	Ground sample distance
GSR	Green super rice
GUIs	Graphic User Interfaces
GVPF	Green Vegetation Pixel Fraction
GWAS	Genome-Wide Association Study
HHIS	High-throughput hyperspectral imaging system
HLS	High-throughput leaf scoring
HPC	High-performance computing
HRPF	High-throughput rice phenotyping facility
HTP	High-throughput phenotyping
HTPP	High-throughput plant phenotyping
IAP	Inbred association panel
IAP	Integrated analysis platform
IDC	Iron deficiency chlorosis
ILs	Introgression lines
IMU	Inertial measurement unit
inGaAs	Indium gallium arsenide
IPK	Leibniz Institute of Plant Genetics and Crop Plant Research
IPPN	International plant phenotyping network
IR	Infrared
IRT	Infrared thermography
IRT	Infrared thermometer
K-NN	K-Nearest Neighbors
LAI	Leaf area index
LAN	Local area network
LAT	Laser ablation tomography
LD	Linkage disequilibrium

LDA	Linear Discriminant Analysis
LEADER	Leaf elemental accumulation for deep roots
LED	Light Emitting Diodes
LiDAR	Light detecting and ranging
LIF	Laser-induced Fluorescence
LQG	Linear-Quadratic-Gaussian
LQR	Linear Quadratic Regulator
LSTM	Long short-term memory
LWIR	Long-wave Infrared
MAE	Mean absolute error
MAGIC	Multiparent advanced generation intercross population
MAS	Marker-assisted selection
MED	Minimum Euclidean Distance
ML	Machine learning
MLP	Multilayer perceptrons
MLR	Multiple linear regression
MPC	Model predictive control
MRI	Magnetic resonance imaging
N	Nitrogen
NAM	Nested association mapping
NARS	National Agriculture Research Systems
NAS	Network-attached storage
NASA	National Aeronautics and Space Administration
NASA	The National Aeronautics and Space Administration
NDRE	Normalized Difference Red Edge
NDVI	Normalized difference vegetation index
NIL	Near isogenic lines
NIR	Near-infrared
NMPC	Nonlinear model predictive control
NPQ	Non-photochemical quenching
NSF	National Science Foundation
PAM	Pulse Amplitude Modulated
PAR	Photosynthetically active radiation
PCB	Printed circuit board
PET	Positron emission tomography
PH	Plant height
PheWAS	Phenome-wide association study
Pi	Phosphate
PID	Proportional-integral-derivative
PLS	Partial least squares
PLSR	Partial least squares regression
PNN	Probabilistic Neural Network
PTS	Plant-to-sensor
QDA	Quadratic Discriminant Analysis
QTL	Quantitative trait loci



RANSAC	Random sample consensus
R-CNN	Region-based convolutional neural networks
REST	Root Estimator for Shovelomics Traits
RF	Random Forest
RGB	Red, Green, Blue
RGB-D	RGB and depth
RH	Relative humidity
RIL	Recombinant inbred lines
RMSE	Root mean square error
RNN	Recurrent neural networks
ROAM	Random-open-parent association mapping
ROI	Region of interest
ROS	Robot Operating System
RSA	Root system architecture
RTK	Real-time kinematic
RTK-GPS	Real-time kinematic global positioning system
RUE	Radiation use efficiency
SAM	Shoot apical meristem
SAM	Spectral Angle Mapper
SCN	Soybean cyst nematode
SEA	Seed Evaluation Accelerator
SfM	Structure from Motion
SMO	Sequential Minimal Optimization
SNP	Single nucleotide polymorphism
STP	Sensor-to-plant
STR	Salt tolerant rate
SVM	Support Vector Machine
SVR	Support Vector regression
SWIR	short-wave infrared
T	Temperature
$T_a$	Air temperature
$T_c$	Canopy temperature
TEB	Timed elastic band
ToF	Time-of-flight
$T_s$	Soil temperature
UAS	Unmanned aerial systems
UAV	Unmanned Aerial Vehicle
UAVs	Unmanned aerial vehicles
UGV	Unmanned ground vehicle
UGVs	Unmanned ground vehicles
UTC	Coordinated universal time
UTM	Universal transverse mercator
UV	Ultraviolet
VI <sub>s</sub>	Vegetation indices
VNIR	Visible near-infrared

VPD	Vapor pressure deficit
VREI2	Vogelmann red edge index 2
X-ray CT	X-ray computed tomography
XRF	X-ray fluorescence
YTS	Yield traits scorer

# Chapter 1

## Solve the Breeder's Equation Using High-Throughput Crop Phenotyping Technology



Jianfeng Zhou and Henry T. Nguyen

**Abstract** This chapter provides an overview of high-throughput crop phenotyping technology on its concept and significance under the context of crop production improvement. The roles of different components in the crop production equation ( $P = G \times E \times M + \varepsilon$ ) toward crop yield, i.e., crop yield ( $P$ ) is a function of crop genotype ( $G$ ), environment ( $E$ ) and management ( $M$ ) is discussed. It is concluded that all components have a great impact on the agriculture yield. Studies suggest that the contribution of crop genetic improvement to yield improvement can be increased substantially upon the breakthroughs in high-efficient crop phenotyping technologies. The potential solutions to improve crop yield gain are discussed and guided by the genetic gain (breeder's) equation. In this chapter, the concept of high-throughput phenotyping technology is introduced and their potential contributions toward genetic improvement are discussed. This chapter also provides some background information for the high-throughput phenotyping technologies discussed in the following chapters.

**Keywords** Crop production · Interaction of genotype, environment and management · Genetic gain equation · High-throughput phenotyping

### 1.1 Crop Production

The world population is estimated to increase by 2 billion in the next 30 years, from 7.7 billion currently to 9.7 billion in 2050, although the growth speed is at a slower pace (UN DESA 2019). It is estimated that global crop production needs to double by 2050 to meet the projected demands from rising population, diet shifts, and increasing biofuels consumption (Alexandratos and Bruinsma 2012a; Hickey et al. 2019; Ray

---

J. Zhou (✉)

Division of Plant Science and Technology, University of Missouri, MO 65211 Columbia, USA  
e-mail: [zhoujianf@missouri.edu](mailto:zhoujianf@missouri.edu)

H. T. Nguyen

Division of Plant Science and Technology, University of Missouri, MO 65211 Columbia, USA  
e-mail: [nguyenhenry@missouri.edu](mailto:nguyenhenry@missouri.edu)

© Springer Nature Switzerland AG 2021

J. Zhou et al. (eds.), *High-Throughput Crop Phenotyping*,  
Concepts and Strategies in Plant Sciences,  
[https://doi.org/10.1007/978-3-030-73734-4\\_1](https://doi.org/10.1007/978-3-030-73734-4_1)

et al. 2013). However, the current yearly increases of crop production for maize (*Zea mays* L.) at 1.6%, rice (*Oryza sativa* L.) at 1.0%, wheat (*Triticum aestivum* L.) at 0.9%, and soybean [*Glycine max* (L.) Merr.] at 1.3% are insufficient to meet the projected demands of  $\sim 2.4\%$  in 2050 (Alexandratos and Bruinsma 2012b; Ray et al. 2013). How to improve the production of the major crops has become an impressive pressure to the global research communities (Hatfield and Walthall 2015).

Crop production is very complicated and determined by many factors, such as crop genotypes (varieties), growing environments (e.g., weather, soil, microclimate, and location), and agronomic management strategies (e.g., seed treatment and placement, planting, fertilizer, and pest management). All the effects of different factors to crop production can be summarized using a crop production equation, i.e., crop production ( $P$ ) is the function of the interactions of genotype ( $G$ ), environment ( $E$ ), and management ( $M$ ), as shown in Eq. 1.1 (Beres et al. 2020; Hatfield and Walthall 2015).

$$P = G \times E \times M + \varepsilon \quad (1.1)$$

where,  $P$  = plant Phenotypes that refer to the observable physical properties of an organism, including yield;  $G$  = Genotype that refers to the genetic makeup of an organism;  $E$  = Environmental factors that affect plant growth, such as climate, soil quality, light, temperature, and water availability; and  $M$  = Management practices of plant and field, such as seed treatment, planting, pest management, nutrition management, and irrigation;  $\varepsilon$  is the total errors of the model. The equation suggests that crop yield can be increased with the improvement in crop genotypes through breeding programs, adoption of crops to environment, and improvement in field and crop management strategies (von Mogel 2013).

The natural environment is not possible to manage, but it has a great impact on crop production. Under climate change, environment is becoming unfavorable to plant growth, such as changes in CO<sub>2</sub> level, global temperature, degradation of soil quality, and extreme weather conditions (e.g., flood and drought). For example, according to the US National Aeronautics and Space Administration (NASA) weather simulation models, there is a predicted 30% increase in heavy precipitation events by the year 2030, which is expected to significantly increase the risk and frequency of flooding (Rosenzweig et al. 2002). Flooding damage to crops can be caused by extreme rainfall events, excess irrigation, or by rainfall that occurs after an irrigation event (Heatherly and Pringle III 1991). Environment will continue generating strong impacts on crop production negatively. According to a recent study (Aggarwal et al. 2019), it is found that global crop yields declines due to climate change starts as early as the 2020s, and yield losses are projected to increase with time, up to 50% by the 2080s. Therefore, there is a pressing need to develop climate-resilient crops and agronomic management strategies to suite for the dynamic environment.

Advances in agronomic management in crops and fields have a great positive impact on crop production. Some studies even suggest that the influence of management is more than the genotype does on the crop yield. For example, it is found that  $N$

and water limit crop yield more than plant genetics (Sinclair and Rufty 2012). A study from Brisson et al. (2010) also suggested that wheat yield was significantly affected by the increased variability in climate during the growing season because of the heat stress during grain-filling and water stress during stem elongation and tillering. Affholder et al. (2013) found that poor soil fertility and weed infestation have more impact on agriculture production than other factors of environment and genotypes. In addition, research also shows that yield of corn and soybean is heavily affected by the planting date and planting depth (Baum et al. 2018; Hu and Wiatrak 2012). With continuous improvement in agronomic management with emerging technologies, using emerging technologies in precision agriculture, sensors, internet of things, big data and artificial intelligence, management will make a greater contribution in crop yield improvement.

Although the production of major commodity crops has been increasing over time due to the improved genetics, improved management, and environmental adaptations, their contributions of each factor are difficult to quantify due to the complicated interactions and the dynamic nature of environment and management practices. However, in a study, Fischer (2009) found that Australian wheat yield had a 1.3% total increase per year over the past 100 years. The author attributed 0.2% of the total increase to the environment, 0.5% to genetic improvement and the interaction of genotype with management, and 0.6% to management alone, which are equivalent to about 30% to genetic improvement, 15% to environment adoption, and 55% to management (Hillel and Rosenzweig 2013). In addition, Duvick (2005) argued that increases in maize yield in the past 50 years were due equally to breeding and improved management. Although the yield gain of the world's staple crops continues improving due to improvement in breeding technologies (Li et al. 2018), the yield increases also depend on the improved agronomic management to realize the potential of these breeding-based improvements in farmer's fields (Fischer and Connor 2018). The potential yield is defined as the yield of the best-adapted cultivar with currently the best agronomic management practices ensuring the absence of manageable abiotic and biotic stresses (Fischer 2015). However, the gap between potential yield and yield in farm yields can be substantial (Beres et al. 2020), for example, the farm yields of rice, wheat, and maize are about 80% of potential yields under irrigated conditions, and 50% or less under rainfed conditions (Lobell et al. 2009). Therefore, it is critical to consider the interaction effects of  $G \times E \times M$  as the key to screening genotypes and closing yield gaps (Hatfield and Walthall 2015).

Field and crop management strategies have been improved significantly thanks to the advances in precision agriculture, sensing technologies, data processing, and analysis (Yost et al. 2019). However, there are practical constraints in management that are needed to be considered when maximizing the crop yield. Management strategies are heavily dependent on accumulative experiences from practices, but climate change makes it difficult to make proper decisions on management for the unpredictable environment, which brings significant challenges in crop management to maintain a stable and high yield production. In addition, although modern agriculture with advanced management has been successful in increasing food production, it has also caused extensive environmental damage. For example, increasing fertilizer

use has led to the degradation of water quality in many regions (Bennett et al. 2001; Matson et al. 1997). It is also evident that some irrigated lands have become heavily salinized, causing the worldwide loss of  $\sim 1.5$  million hectares of arable land per year, along with an estimated \$11 billion losses in production (Wood et al. 2000). Up to  $\sim 40\%$  of global croplands may also be experiencing some degree of soil erosion, reduced fertility, or overgrazing (Wood et al. 2000). Therefore, over-managed agricultural systems may not be beneficial for sustainable agricultural system in long run.

There are very limited natural resources that are available for farmers to make desired management practices to optimize crop production. For example, 92% of the soybean acreage in the United States is under rainfed dryland conditions (Irwin et al. 2017) where crop productivity is always threatened by unpredictable drought but irrigation is not an option. In addition, the management of crops under flooding conditions is always challenging. It was reported that the 2011 Mississippi River flood caused a loss of \$2 billion in crop damages when fewer than 6,500 acres of soybean were harvested in the southern counties of Illinois (Olson and Morton 2013). The situation was even worse in 2015, as more than half of the states' soybean crop was affected and the crop damage caused by the floods of 2019 was even severer than that of 2015. The crop yield loss due to the constraints in management may be compensated through the development of new crop varieties with flood or drought-resilient traits. The conventional breeding programs are transferring to more efficient modern breeding programs through integrating emerging technologies, especially the high-throughput phenotyping technology. It is believed by authors that the contributions of genetic improvement based on high-throughput phenotyping technology will increase crop yield gains significantly in the near future. In the following sections of this chapter, we will focus on how to improve the yield gain in breeding programs using high-throughput phenotyping technology.

## 1.2 Breeder's Equation for Crop Production

Crop yield can be improved through optimal management and breeding new crop varieties with improved traits. The improvement of crop yield and other traits due to artificial or genomic selection is quantified using the genetic gain equation (commonly known as 'breeder's equation') calculated using Eq. 1.2 (Eberhart 1970; Li et al. 2018).

$$\Delta G = \frac{ir\sigma_A}{L} \quad (1.2)$$

where  $\Delta G$  is the genetic gain (yearly gain due to genetic factors),  $i$  is the selection intensity,  $r$  is the selection accuracy,  $\sigma_A$  is the square root of the additive genetic variance within the population, and  $L$  is the length of breeding cycle interval or

generation. The breeder's equation provides general guidance and useful framework for the design of breeding programs leading to the improvement of genetic gain. It can be seen from Eq. 1.2 that genetic gain is positively proportional to the parameters of selection intensity, selection accuracy and genetic variance. Selection intensity is determined by the selection rate, i.e., the proportion of the population selected from the total population (Xu et al. 2017). A larger population size allows a greater selection intensity and improves the probability of identifying progenies with desired traits, such as high yield potential and resilience to stresses. Therefore, the first way to improve the genetic gain is to increase the breeding population. The second favorable factor, the selection accuracy, refers to the accuracy of selection on breeding value. The selection accuracy is determined by heritability and can be increased by increasing the marker density. The advances in high-throughput sequencing technologies and genomic selection (GS) can remarkably improve the selection accuracy (Bhat et al. 2016; Crossa et al. 2017). In addition, the selection accuracy can be increased by increasing repeatability in the breeding population thus increases the selection response for the trait of interest (Araus et al. 2018). For the breeding programs with a fixed budget, it needs to balance between the population and replication to maximize the genetic gain.

In addition, genetic variance is also positive to the increase of genetic gain. Although the vast number of valuable germplasm collections in gene banks can be used as a source to acquire genetic variation, the contribution is limited by the time and resources required to precisely characterize the accessions at large scale, and identifying and transferring the useful alleles into adapted germplasm. Advanced tools are needed to identify more molecular markers that can reveal genetic variation (Xu et al. 2017) and accurately quantify genetic variations due to environment (Araus et al. 2018). In the equation, the length of breeding cycle interval or generation is directly reciprocal to genetic gain. Conventional breeding programs have a fixed timeline for the development of new varieties and it is hard to change the breeding cycles. However, in recent years, researchers are studying a method called 'speed breeding' or 'rapid breeding' to shorten the breeding cycle and accelerate breeding and research programs (Li et al. 2018; Watson et al. 2018). For example, speed breeding technology is potential to achieve up to six generations per year for spring wheat, durum wheat, barley, chickpea, and pea, and four generations for canola under normal glasshouse conditions (Watson et al. 2018). In addition, breeding cycle is also potentially to accelerate by improving the prediction accuracy and discovering more reliable secondary crop traits using emerging phenotyping tools (Araus et al. 2018).

In summary, there are many approaches to increase genetic gain of a breeding program by solving the breeder's equation (Cobb et al. 2019; Hickey et al. 2019; Pieruschka and Schurr 2019). To develop next-generation breeding programs, we should consider some critical factors closely related to genetic gains (Araus et al. 2018; Awada et al. 2018; Cobb et al. 2019; Li et al. 2018; Zhao et al. 2017). Some examples include: (a) how to increase the capacity for larger breeding population to enable higher selection intensity; (b) how to enhance selection accuracy using emerging technologies; (c) how to identify genetic variations; and (d) how to reduce the breeding cycles. While we continue advancing the molecular-based breeding

strategies using genomic technology, special efforts should be taken to eliminate the bottlenecks in current breeding programs, i.e., how to measure plant phenotypes efficiently and accurately for a large breeding population. Current breeding programs are limited by cost, time, human labor, land and other resources to efficiently scan a large population of progenies (Rebetzke et al. 2016), which limit the selection intensity, affect the genetic accuracy, and result in low genetic gain. Therefore, the development and application of low-cost, high-throughput phenotyping tools allow reallocation of resources to manage larger populations, enable an increase in selection intensity within a fixed budget.

### 1.3 High-Throughput Crop Phenotyping

The term “phenotype” as a counterpart concept to “genotypes” was created one century ago (Johannsen 1903, 1911), which has been used to describe a wide range of traits in plants, microbes, fungi and animals (Walter et al. 2015). Plant phenotype is the functional plant body that is formed during plant growth and development from the dynamic interaction between the genetic background (genotype) and the physical world in which plants develop (environment). The term ‘phenotyping’ began using in the 1960s (Walter et al. 2015) and later was referred to as the set of methodologies and protocols used to accurately measure plant growth, architecture, and composition at different scales (Fiorani and Schurr 2013). Traditionally, to select superior progenies or identify gene loci in the genome controlling a trait, usually, hundreds to thousands of plant phenotypes are measured by breeders using low-throughput laboratory assessments, visual observations, and manual tools. Traditional crop phenotyping methods are labor-intensive, time-consuming, subjective, and frequently destructive to plants (Chen et al. 2014; Furbank and Tester 2011). The lags in the advances of emerging technologies and low throughput in plant phenotyping have become a critical constraint to crop breeding and functional genomics studies (Deery et al. 2016).

High-throughput phenotyping (HTP) technologies emerged in the last decade thanks to the advances and reduced cost in sensor, computer vision, automation and advanced machine learning technologies. Crop HTP refers as the gathering of multi-dimensional phenotypic data at multiple levels from cell, organ, plant to population using emerging technologies (Lobos et al. 2017; Zhao et al. 2019). A comprehensive HTP system is consisted of supportive hardware (sensors and platforms) and computation component (data process and analytics). Widely used sensors in HTP technology are primarily non-contact and non-invasive sensors, such as digital cameras (e.g., visible, multispectral, hyperspectral Chlorophyll fluorescence and thermal cameras), three-dimensional depth sensors (LiDAR, time-of-flight camera) (see list of the cameras in Araus et al. 2018 and Zhao et al. 2019). Explorable research is testing and adopting some advanced imaging techniques that are widely used in medical applications, such as magnetic resonance imaging (MRI), positron emission tomography (PET), and computed tomography (CT), to HTP systems in the growth



chamber or greenhouse. The advances in sensor technology are primarily driven by the industry sector, while efforts have been made toward integrating them to crop HTP systems. In addition, supportive hardware also includes automation platforms for efficient data collection. Commonly used automation platforms include track-based automation systems (Zhou et al., 2018a; b), indoor and outdoor robotic systems (Awada et al. 2018; Chapman et al. 2014; Yang et al. 2020; Zhao et al. 2019), unmanned aerial system (UAS) (Yang et al. 2017), which are commercially available or developed by the research team for special need.

The more important component of an HTP system is data processing and analytic system. Current HTP systems, especially high-resolution imaging systems, are ready to collect high-dimensional data of crops of a large population. However, researchers will realize soon that they may be overwhelmed by the huge data that are beyond their ability to handle (Blumenthal et al. 2020; Yang et al. 2020; Zhao et al. 2019). Therefore, one of the urgent tasks for HTP system is to develop frameworks or pipelines for efficient data processing and analytics that can translate sensor data to important crop traits (Blumenthal et al. 2020; Hallowell et al. 2018; Zhou et al. 2018a). More efforts should be taken to develop and integrate emerging technologies such as cloud computing, edge computing, machine learning, deep learning and artificial intelligence (AI) into HTP systems. With the continuous efforts from the community, HTP technology can potentially be the key component to solve the breeder's equation and accelerate the process of breeding new crop varieties with advanced traits. The following examples demonstrate the potential applications of HTP technologies to breeding programs based on the breeder's equation:

- (1) Delivery efficient and objective measurements of crop traits. High-throughput phenotyping systems are able to phenotype breeding fields in a more efficient and cost-effective way, which allows an increase in the capacity of breeding programs to handle a larger breeding population and improve the selection intensity. For example, UAS-based HTP platforms are able to screen breeding fields within a short period (e.g., 30 min for a 5-acre field). The implements of spectrum reflectance, photogrammetry, and computer vision provide consistent criteria to estimate crop traits in multiple dimensions, such as plant height, plant temperature, chlorophyll content.
- (2) Identification of novel crop traits. Advanced sensors (e.g., hyperspectral and infrared cameras) capture crop information beyond human vision and sense. Advanced data analytics and AI models reveal hidden information from human and sensor data and have great potential in discovering novel crop traits. The novel traits can be used to describe crop performance at a specific growth stage (e.g., emerging, flowering or harvesting) or to profile crop dynamic responses to environments along growth seasons. Novel crop traits are able to provide additional information to quantify subtle genetic variations of different genotypes and potentially increase the genetic variance.
- (3) Integration of phenotypic data and genotypic data. HTP-based phenotypes could be integrated into genetic analysis, such as quantitative trait locus (QTL) mapping or genome-wide association study (GWAS) to identify key genetic

elements underlying or associated with the yield gain or stress tolerance. The genetic elements for favorable crop traits could be further incorporated into the current germplasm through marker-assisted selection (MAS) during breeding. The integration will allow accurate selection, reduce breeding cycles and increase the genetic gain.

- (4) Allow advanced models to integrate  $G \times E \times M$ . High-throughput phenotyping technology allows collecting big data of crops in a high spatiotemporal resolution and discovering novel crop traits, which will enable the integration with environment and management to reveal  $G \times E \times M$  interactions. Advanced models based on machine learning and deep learning technologies will transform breeding program from **descriptive** phenotyping, to **predictive** phenotyping and **prescriptive** phenotyping that allow ‘manufacture’ crop traits based on needs.

In summary crop HTP technology provides a potential solution to the breeder’s equation to maximize the genetic gains by increasing the selection intensity and accuracy, improving the identification of genetic variations, and accelerating breeding cycles. Crop HTP technology uses an interdisciplinary and holistic approach to integrate research in agronomy, life sciences, information science, mathematics, and engineering sciences, and combines high-performance computing and artificial intelligence technology. Advanced data analytic methods (e.g., machine learning, deep learning) are used to analyze the multifarious phenotypic information of crops and develop predictive and prescriptive models to phenotype crops in a high-throughput, multi-dimensional, big-data, intelligent and automatically measuring manner. The big data of plant phenotypic data collected by plant HTP systems will be integrated with multi-scale genomic and environmental data to mining genes associated with important agronomic traits, and propose new intelligent solutions for precision breeding (Zhao et al. 2019). This book provides showcases HTP applications in the world-leading research programs and by the active researchers and scientists in the areas of crop breeding, genetics, agronomy, engineering, computers, and information technology. The following chapters will focus on the showcases (a) application of merging sensing technology (sensors), (b) introduction of HTP platforms (hardware), (c) approaches of data mining and analytics (big data and AI) and (d) development of HTP framework and pipeline in various crops. We hope this book provides the state-of-the-art of HTP technology and its applications in plant breeding and genetics and brings some case studies that can help researchers to develop and advance the HTP in their research projects.

## References

- Alexandratos N, Bruinsma J (2012a) World agriculture toward 2030/2050, the 2012 revision. ESA Working Paper 12–03, June 2012. Food and Agriculture Organization of the United Nations (FAO), Rome. <https://www.fao.org/>.
- Alexandratos N, Bruinsma J (2012b). World agriculture toward 2030/2050: the 2012 revision

- Affholder F, Poeydebat C, Corbeels M, Scopel E, Tittone P (2013) The yield gap of major food crops in family agriculture in the tropics: Assessment and analysis through field surveys and modelling. *Field Crops Res* 143:106–118
- Aggarwal P, Vyas S, Thornton P, Campbell BM, Kropff M (2019) Importance of considering technology growth in impact assessments of climate change on agriculture. *Glob Food Secur* 23:41–48
- Araus JL, Kefauver SC, Zaman-Allah M, Olsen MS, Cairns JE (2018) Translating high-throughput phenotyping into genetic gain. *Trends Plant Sci* 23(5):451–466
- Awada L, Phillips PWB, Smyth SJ (2018) The adoption of automated phenotyping by plant breeders. *Euphytica* 214(8)
- Baum M, Archontoulis S, Licht M (2018) Planting date, hybrid maturity, and weather effects on maize yield and crop stage. *Agron J*
- Bennett EM, Carpenter SR, Caraco NF (2001) Human impact on erodable phosphorus and eutrophication: a global perspective: increasing accumulation of phosphorus in soil threatens rivers, lakes, and coastal oceans with eutrophication. *Bioscience* 51(3):227–234
- Beres BL, Hatfield JL, Kirkegaard JA, Eigenbrode SD, Pan WL, Lollato RP, Hunt JR, Strydom S, Porker K, Lyon D, Ransom J, Wiersma J (2020). Toward a better understanding of Genotype  $\times$  Environment  $\times$  Management Interactions—a global wheat initiative agronomic research strategy. *Front Plant Sci* 11(828)
- Bhat JA, Ali S, Salgotra RK, Mir ZA, Dutta S, Jadon V, Tyagi A, Mushtaq M, Jain N, Singh PK (2016) Genomic selection in the era of next generation sequencing for complex traits in plant breeding. *Front Genet* 7:221
- Blumenthal J, Megherbi DB, Lussier R (2020) Unsupervised machine learning via Hidden Markov Models for accurate clustering of plant stress levels based on imaged chlorophyll fluorescence profiles & their rate of change in time. *Comput Electron Agric* 105064
- Brisson N, Gate P, Gouache D, Charmet G, Oury F-X, Huard F (2010) Why are wheat yields stagnating in Europe? a comprehensive data analysis for France. *Field Crops Res* 119(1):201–212
- Chapman S, Merz T, Chan A, Jackway P, Hrabar S, Dreccer M, Holland E, Zheng B, Ling T, Jimenez-Berni J (2014) Pheno-copter: a low-altitude autonomous remote-sensing robotic helicopter for high-throughput field-based phenotyping 4(2):279
- Chen D, Neumann K, Friedel S, Kilian B, Chen M, Altmann T, Klukas C (2014) Dissecting the phenotypic components of crop plant growth and drought responses based on high-throughput image analysis. *Plant Cell* 26(12):4636–4655
- Cobb JN, Juma RU, Biswas PS, Arbelaez JD, Rutkoski J, Atlin G, Hagen T, Quinn M, Ng EH (2019) Enhancing the rate of genetic gain in public-sector plant breeding programs: lessons from the breeder's equation. *Theor Appl Genet* 132(3):627–645
- Crossa J, Pérez-Rodríguez P, Cuevas J, Montesinos-López O, Jarquín D, de los Campos G, Burgueño J, González-Camacho JM, Pérez-Elizalde S, Beyene Y (2017) Genomic selection in plant breeding: methods, models, and perspectives. *Trends Plant Sci* 22(11): 961–975
- Deery DM, Rebetzke GJ, Jimenez-Berni JA, James RA, Condon AG, Bovill WD, Hutchinson P, Scarrow J, Davy R, Furbank RT (2016) Methodology for high-throughput field phenotyping of canopy temperature using airborne thermography. *Front Plant Sci* 7:1808
- Duvick DN (2005) The contribution of breeding to yield advances in maize (*Zea mays* L.). *Adv Agron* 86:83–145
- Eberhart S (1970) Factors effecting efficiencies of breeding methods. *Afr Soils* 15(1/3):655–680
- Fiorani F, Schurr U (2013) Future scenarios for plant phenotyping. *Annu Rev Plant Biol* 64(1):267–291
- Fischer R (2015) Definitions and determination of crop yield, yield gaps, and of rates of change. *Field Crops Res* 182:9–18
- Fischer R, Connor D (2018) Issues for cropping and agricultural science in the next 20 years. *Field Crops Res* 222:121–142
- Fischer RA (2009) Farming systems of Australia: exploiting the synergy between genetic improvement and agronomy.

- Furbank RT, Tester M (2011) Phenomics—technologies to relieve the phenotyping bottleneck. *Trends Plant Sci* 16(12):635–644
- Hallowell N, Parker M, Nellaker C (2018) Big data phenotyping in rare diseases: some ethical issues. *Genet Med*
- Hatfield JL, C. L. Walthall. 2015. Meeting Global Food Needs: Realizing the Potential via Genetics  $\times$  Environment  $\times$  Management Interactions. *Agronomy journal* 107(4).
- Heatherly LG, Pringle H III (1991) Soybean cultivars' response to flood irrigation of clay soil. *Agron J* 83(1):231–236
- Hickey LT, Hafeez AN, Robinson H, Jackson SA, Leal-Bertioli SCM, Tester M, Gao C, Godwin ID, Hayes BJ, Wulff BBH (2019) Breeding crops to feed 10 billion. *Nat Biotechnol* 37(7):744–754
- Hillel D, Rosenzweig C (2013) Handbook of climate change and agroecosystems: global and regional aspects and implications. World Scientific
- Hu M, Wiatrak P (2012) Effect of planting date on soybean growth, yield, and grain quality. *Agron J* 104(3):785–790
- Irwin S, Hubbs T, Good D (2017) US Soybean yield trends for irrigated and non-irrigated production. *Farmdoc daily*, vol 7
- Johannsen W (1903) Über Erblichkeit in Populationen und in reinen Linien. Gustav Fischer Verl, Jena
- Johannsen W (1911) The genotype conception of heredity. *Am Nat* 45(531):129–159
- Li H, Rasheed A, Hickey LT, He Z (2018) Fast-forwarding genetic gain. *Trends Plant Sci* 23(3):184–186
- Lobell DB, Cassman KG, Field CB (2009) Crop yield gaps: their importance, magnitudes, and causes. *Ann Rev Environ Resour* 34.
- Lobos GA, Camargo AV, del Pozo A, Araus JL, Ortiz R, Doonan JH (2017) Plant phenotyping and phenomics for plant breeding. *Front Plant Sci* 8:2181
- Matson PA, Parton WJ, Power AG, Swift MJ (1997) Agricultural intensification and ecosystem properties. *Science* 277(5325):504–509
- Olson KR, Morton LW (2013) Restoration of 2011 flood-damaged Birds Point-New Madrid Floodway. *J Soil Water Conserv* 68(1):13A-18A
- Pieruschka R, Schurr U (2019) Plant Phenotyping: Past, Present, and Future. *Plant Phenomics* 2019:1–6
- Ray DK, Mueller ND, West PC, Foley JA (2013) Yield trends are insufficient to double global crop production by 2050. *PLoS ONE* 8(6):e66428
- Rebetzke GJ, Jimenez-Berni JA, Bovill WD, Deery DM, James RA (2016) High-throughput phenotyping technologies allow accurate selection of stay-green. *J Exp Bot* 67(17):4919–4924
- Rosenzweig C, Tubiello FN, Goldberg R, Mills E, Bloomfield J (2002) Increased crop damage in the US from excess precipitation under climate change. *Global Environ Change* 12(3):197–202
- Sinclair TR, Rufty TW (2012) Nitrogen and water resources commonly limit crop yield increases, not necessarily plant genetics. *Glob Food Secur* 1(2):94–98
- UN-DESA (2019) According to the estimation of the *World Population Prospects* published by the UN Department of Economic and Social Affairs. <https://www.un.org/development/desa/en/news/population/world-population-prospects-2019.html>
- von Mogel KH (2013) Genotype  $\times$  Environment  $\times$  Management: interactions key to beating future droughts. *CSA News* 58(2):4–9
- Walter A, Liebisch F, Hund A (2015) Plant phenotyping: from bean weighing to image analysis. *Plant Methods* 11(1):14
- Watson A, Ghosh S, Williams MJ, Cuddy WS, Simmonds J, Rey M-D, Asyraf Md Hatta M, Hinchliffe A, Steed A, Reynolds D, Adamski NM, Breakspear A, Korolev A, Rayner T, Dixon LE, Riaz A, Martin W, Ryan M, Edwards D, Batley J, Raman H, Carter J, Rogers C, Domoney C, Moore G, Harwood W, Nicholson P, Dieters MJ, DeLacy IH, Zhou J, Uauy C, Boden SA, Park RF, Wulff BBH, Hickey LT (2018) Speed breeding is a powerful tool to accelerate crop research and breeding. *Nat Plants* 4(1):23–29

- Wood S, Sebastian K, Scherr SJ (2000) Pilot analysis of global ecosystems: agroecosystems. World Resources Institute
- Xu Y, Li P, Zou C, Lu Y, Xie C, Zhang X, Prasanna BM, Olsen MS (2017) Enhancing genetic gain in the era of molecular breeding. *J Exp Bot* 68(11):2641–2666
- Yang G, Liu J, Zhao C, Li Z, Huang Y, Yu H, Xu B, Yang X, Zhu D, Zhang X, Zhang R, Feng H, Zhao X, Li Z, Li H, Yang H (2017) Unmanned aerial vehicle remote sensing for field-based crop phenotyping: current status and perspectives. *Front Plant Sci* 8:1111
- Yang W, Feng H, Zhang X, Zhang J, Doonan JH, Batchelor WD, Xiong L, Yan J (2020) Crop phenomics and high-throughput phenotyping: past decades, current challenges, and future perspectives. *Mol Plant* 13(2):187–214
- Yost MA, Kitchen NR, Sudduth KA, Massey RE, Sadler EJ, Drummond ST, Volkmann MR (2019) A long-term precision agriculture system sustains grain profitability. *Precis Agric*
- Zhao C, Liu B, Piao S, Wang X, Lobell DB, Huang Y, Huang M, Yao Y, Bassu S, Ciais P, Durand J-L, Elliott J, Ewert F, Janssens IA, Li T, Lin E, Liu Q, Martre P, Müller C, Peng S, Peñuelas J, Ruane AC, Wallach D, Wang T, Wu D, Liu Z, Zhu Y, Zhu Z, Asseng S (2017) Temperature increase reduces global yields of major crops in four independent estimates. *Proc Natl Acad Sci* 114(35):9326–9331
- Zhao C, Zhang Y, Du J, Guo X, Wen W, Gu S, Wang J, Fan J (2019) Crop phenomics: current status and perspectives. *Front Plant Sci* 10:714
- Zhou J, Chen H, Zhou J, Fu X, Ye H, Nguyen HT (2018a) Development of an automated phenotyping platform for quantifying soybean dynamic responses to salinity stress in greenhouse environment. *Comput Electron Agric* 151:319–330
- Zhou J, Fu X, Schumacher L, Zhou J (2018b) Evaluating geometric measurement accuracy based on 3D reconstruction of automated imagery in a greenhouse. *Sensors (Basel)* 18(7)

# Chapter 2

## Field Robotic Systems for High-Throughput Plant Phenotyping: A Review and a Case Study



Yin Bao, Jingyao Gai, Lirong Xiang, and Lie Tang

**Abstract** Continuous crop improvement is essential to meet the growing demands for food, feed, fuel, and fiber around the globe. High-throughput plant phenotyping (HTPP) aims to break the bottleneck in plant breeding programs where phenotypic data are mostly collected with inefficient manual methods. With the recent rapid advancements and applications of robotics in many industries, field robots are also expected to bring transformational changes to HTPP applications. This chapter presents an updated review of the infield ground-based robotic HTPP systems developed so far. Moreover, we report a case study of an autonomous mobile phenotyping robot PhenoBot 3.0 for row crop phenotyping, focusing on the development and evaluation of the navigation system for the articulated steering, a four-wheel-drive robot with an extremely tall sensor mast. Several navigation techniques were integrated to achieve robustness at different corn plant growth stages. Additionally, we briefly review the major sensing technologies for field-based HTPP and present a vision sensor PhenoStereo to show the promising potential of integrating conventional stereo imaging with the state-of-the-art visual perception techniques for plant organ phenotyping applications. As an example, we show that a highly accurate estimation of sorghum stem diameter can be achieved with PhenoStereo. With this chapter, our goal is to provide valuable insights and guidance on the development of infield ground robotic HTPP systems to researchers and practitioners.

**Keywords** High-throughput plant phenotyping · Field robotics · Robot Operating System · Navigation · Stereo vision · Computational perception

---

J. Gai · L. Xiang · L. Tang (✉)

Department of Agricultural and Biosystems Engineering, Iowa State University, Ames, IA 50011, USA

e-mail: [lietang@iastate.edu](mailto:lietang@iastate.edu)

Y. Bao

Department of Biosystems Engineering, Auburn University, Auburn, AL 36849, USA

e-mail: [yzb0016@auburn.edu](mailto:yzb0016@auburn.edu)

© Springer Nature Switzerland AG 2021

J. Zhou et al. (eds.), *High-Throughput Crop Phenotyping*,

Concepts and Strategies in Plant Sciences,

[https://doi.org/10.1007/978-3-030-73734-4\\_2](https://doi.org/10.1007/978-3-030-73734-4_2)

## 2.1 Introduction

To feed the global population, crop production needs to be doubled by 2050 (Tilman et al. 2011); the yield trend, however, has been found insufficient to meet this requirement (Ray et al. 2013), let alone the rising demand for feed, fuel, and fiber. This growing agricultural crisis must be tackled from many different aspects to boost crop yield in a sustainable way. One of the most effective ways to increase crop yield potential is through plant breeding programs (Duvick 2005; Vermerris et al. 2007). The basic principle of plant breeding is to make crosses between different varieties under different environments, and to select the best progeny based on the plant phenotypes. The rapid advancements in high-throughput genotyping technologies have greatly improved the efficiency and lowered the cost of molecular breeding in the last few decades (Appleby et al. 2009). In contrast, plant phenotyping heavily relies on infield manual measurement and scouting. The process is labor-intensive, time-consuming, prone to human errors, and ergonomically poor. Consequently, the phenotypic data collection lacked spatial and temporal resolutions as well as precision. The massive genomic information acquired with high-throughput DNA sequencing technologies has not been fully utilized for crop improvement due to lack of sufficient information on plant phenotypes. Therefore, there is a strong need for developing high-efficient high-throughput plant phenotyping (HTPP) systems.

During the last decade, various HTPP systems were developed. In controlled environments (e.g., growth chambers and greenhouses), the state-of-the-art HTPP systems realize the plant-to-sensor concept. A plant-to-sensor HTPP system conveys individual plants to a screening station where various imagery data are collected, for instance, the Greenhouse Scanalyzer (LemnaTec GmbH, Aachen, Germany). The conveyor-based system typically has a throughput in the order of hundreds of plants per day. In addition, a key advantage is that a single plant can be imaged with controlled lighting conditions, background color, and viewing angles, which reduces the complexity of subsequent image processing. In the field, sensors must be moved to plants, namely, the sensor-to-plant concept. Field-based HTPP systems can be classified into two categories: aerial systems and ground systems. Aerial HTPP systems use satellites and manned/unmanned aerial vehicles as sensor carriers (Liebisch et al. 2015; Shi et al. 2016; Tattaris et al. 2016; Watanabe et al. 2017). They excel at covering large fields in a short amount of time, but struggle with detailed plant phenotyping, particularly at the individual plant level and at the plant organ level. Several commercial companies offer remote sensing services for agricultural research studies and crop scouting, for example, AgPixel (Johnston, IA, USA) and Precision Hawk (Raleigh, NC, USA). As for ground HTPP systems, sensors can be carried on either a mobile platform or a fixed platform. Mobile platforms and fixed platforms have opposite advantages and disadvantages. Mobile platforms can cover large fields and are easy to transport, but are typically limited to short crops and cannot operate on rainy days or on overly wet soils, whereas fixed platforms can handle a wide range of plant height and various weather conditions, but with the limitations of reduced field size, fixed location, and high cost.

Thanks to the convergence of technologies (e.g., advanced manufacturing, sensing, actuation, controls, edge computing, and artificial intelligence (AI)), robotics has undergone rapid advancements in recent years and is expected to bring transformational changes to every industry and everyday life. In the area of HTPP, infield ground-based robotic systems are likely to impact crop improvement the most. Although greenhouse-based HTPP can be highly automated with a full suite of sensor technologies, the resultant research findings often do not translate well into the field due to the complex outdoor environmental factors. Meanwhile, breeders, agronomists, and plant scientists have begun adopting commercial low-cost aerial HTPP solutions. Aerial HTPP systems are mostly capable of the characterization of top crop canopy. Some agronomic traits such as crop stress responses can be predicted from aerial imagery to different extents. However, a complex trait like yield is influenced by many other traits that require more precise phenotyping beyond the canopy level. Compared to aerial systems, ground-based robotic systems can more easily carry sensors and manipulators to perform complicated measurement tasks like humans. Therefore, this book chapter aims to provide an updated literature review about infield ground-based robotic HTPP systems. The remainder of this chapter is organized as follows. In Sect. 2.2, various types of infield ground-based robotic HTPP platforms are reviewed and discussed. In Sect. 2.3, a case study is presented to provide insights into the development of a mobile ground-based robotic platform PhenoBot 3.0. In Sect. 2.4, we briefly review the major sensing technologies for field-based HTPP and present a vision sensor PhenoStereo for the purposes of plant-organ phenotyping. Lastly, we summarize this chapter, followed by our vision for future research directions in Sect. 2.5.

## 2.2 Infield Ground-Based Robotic HTPP Platforms

### 2.2.1 Fixed Platforms

Fixed ground-based robotic HTPP platforms are essentially infield stationary infrastructures that allow various degrees of sensor mobility. Large-scale ones can be gantry systems and cable-suspended systems. LemnaTec GmbH has built two gigantic gantry systems named Field Scanalyzer in the world, one for the Rothamsted Research center in London, UK (Virlet et al. 2017) and one for the University of Arizona and USDA-ARS in Maricopa, Arizona, USA (Fig. 2.1 top left). The Field Scanalyzer is based on a 3-axis industrial portal crane system where two parallel rails (x-axis) support a mobile portal on which a sensor box can be moved perpendicularly to the rails (y-axis) and vertically (z-axis). It is worth mentioning that rainout shelters can be integrated into a gantry system using the same rail system (Fig. 2.1 bottom left), adding the capability for drought research (Beauchêne et al. 2019). An alternative to a gantry system is a cable-suspended system, which typically consists of four winch towers at each corner of a rectangular field. An overhead sensor carrier



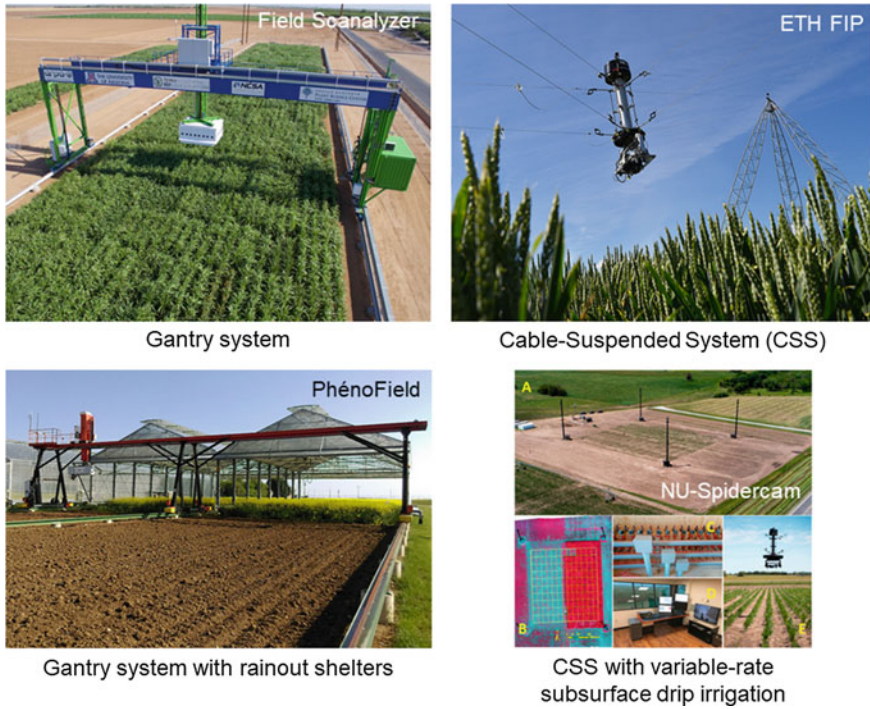


**Fig. 2.1** Fixed infield robotic high-throughput plant phenotyping platforms

within the field is connected to the four winches by four high-strength, lightweight cables. Winding and unwinding the four cables in a coordinated way controls the XYZ position of the sensor carrier. Two large-scale cable-suspended systems have been developed so far, the FIP in Zürich, Switzerland (Kirchgessner et al. 2017) (Fig. 2.1., top right) and the NU-Spidercam in Nebraska, USA (Bai et al. 2019) (Fig. 2.1. bottom right). The main advantage of large-scale fixed robotic HTPP platforms is the ability to quickly move a heavy sensor payload above plants with high positioning accuracy and repeatability. The sensor carrier can move between crop rows, whereas mobile ground platforms must travel out of a crop row before entering the next. Once established, the gantry and cable-suspended systems are unlikely to be relocated. For research programs that involve genotype-environment interactions such as plant breeding, experiments are replicated at multiple field locations, which makes using the large-scale platforms impractical. The extremely high costs limit them to only a handful of research institutes.

### 2.2.2 Mobile Platforms

The design of an infield ground-based mobile robotic HTPP platform depends more on the space available for the platform to travel and for the sensors to capture the regions of interest. A mobile robotic HTPP platform can travel in the field with respect to the crop rows in two fashions, portal and between-rows. Most mobile robotic HTPP platforms adopt the portal design, which can be seen as mobile gantries that straddle one or multiple rows or plots. Some recent robots employ the between-rows design, traveling between two adjacent crop rows. Tall plants and narrow row spacing can pose challenging constraints to the portal type and the between-rows types, respectively.

High-clearance agricultural vehicles (e.g., tractors, sprayers, etc.) can sustain long hours of operation and carry heavy payloads. They naturally serve as convenient bases that can be retrofitted to robotic systems. Hence, we briefly review agricultural vehicle-based HTPP platforms. Commonly, top-viewing sensors are mounted on a boom or a frame rigidly attached to the vehicle (Fig. 2.2 top left). Such a configuration was used for phenotyping wheat (Barker et al. 2016; Deery et al. 2014; Madec et al. 2017; Pérez-Ruiz et al. 2020), cotton (Andrade-Sanchez et al. 2014; Jiang et al. 2018), canola (Bayati and Fotouhi 2018), corn (Peshlov et al. 2017) and early-stage sorghum (Wang et al. 2018). Alternatively, Busemeyer et al. (2013) developed the BreedVision, a custom sensing implement that was pulled by a high-clearance tractor for wheat phenotyping (Fig. 2.2 bottom right). The higher the ground clearance is, the larger the footprint of the vehicle is needed to maintain stability. For extremely tall plants like biomass sorghum, Murray et al. (2016) reported a large custom-built portal vehicle (Fig. 2.2 bottom center). Kicherer et al. (2017) retrofitted a grape harvester that can straddle a trellis with side-viewing hyperspectral and RGB stereo cameras for phenotyping of grapevines and berries. A driver is typically required to operate an agricultural vehicle-based HTPP platform, which makes the system semi-automated. Integrating a commercial off-the-shelf auto-steer module

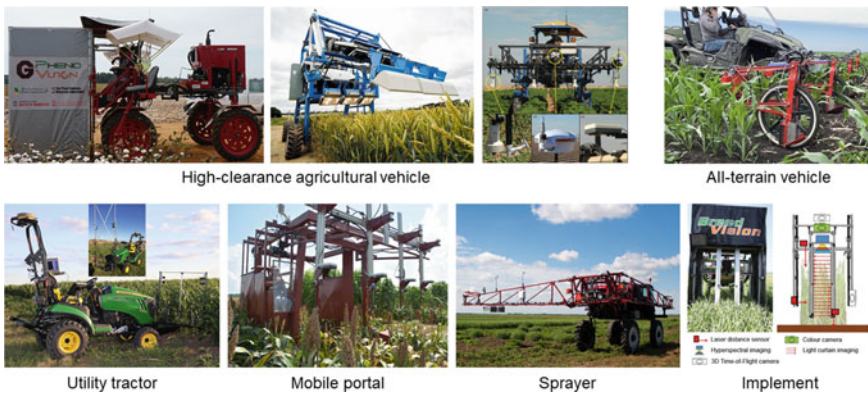
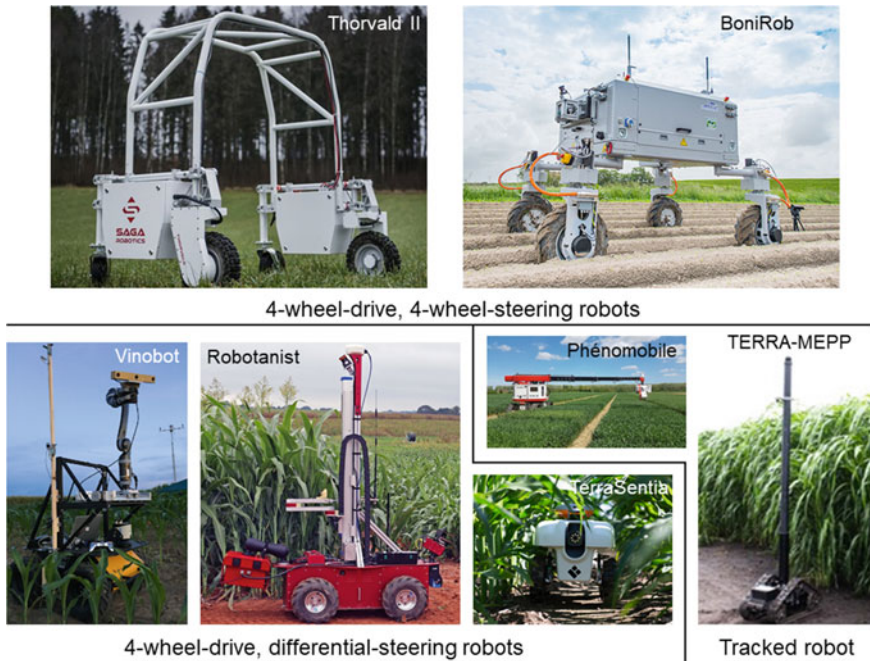


Fig. 2.2 Agricultural vehicle-based infield high-throughput plant phenotyping platforms

can further enable fully automated field-based HTPP. Bao et al. (2019a) retrofitted a utility tractor with an auto-steer system as an automated platform for side-view stereo imaging of sorghum plants (Fig. 2.2 bottom left). In addition to conventional agricultural vehicles, all-terrain vehicles (ATVs) are often used for crop scouting purposes due to their relatively low footprint and ease of transportation. The top right picture in Fig. 2.2 illustrates an ATV-based, multi-row corn stand analyzing system that uses a side-viewing proximity sensor array for corn stand counting and mapping (FieldRobo LLC, IA, USA).

Mobile robot-based HTPP platforms aim to automate sensor data acquisition without human intervention. Removing the human factor can potentially lead to highly repeatable and highly objective HTPP. BoniRob (Klose et al. 2010; Ruckelshausen et al. 2009) was the earliest robot developed for infield individual plant phenotyping of corn and wheat plants (Fig. 2.3 top right). In essence, it is a high-clearance four-wheel-driving four-wheel-steering rover. Each independently steered wheel is connected to the chassis via an articulated arm, enabling an omnidirectional drive mechanism and variable track gauges. The drivetrain of BoniRob is hydraulically powered. Similar mobile robotic HTPP platforms were later developed, i.e., Ladybird (Underwood et al. 2017) and Thorvald II (Grimstad and From 2017). Unlike BoniRob, both Ladybird and Thorvald II (Fig. 2.3 top left) used electric motors. But the three robots share a key design principle, an identical steer and



**Fig. 2.3** Ground robot-based high-throughput plant phenotyping platforms

drive unit for each wheel, which enables highly flexible maneuvers such as crabbing and zero-radius turning. Like powerful high-clearance agricultural vehicles, these large phenotyping robots can handle rough terrains and carry heavy payloads.

For tall plants such as corn and sorghum, side-view sensing can capture information that is occluded from the top-viewing angle. Although the large high-clearance robots can support side-view sensing with additional vertical sensor rigs, it becomes more and more challenging in terms of feasibility and crop damage as the plants grow taller and taller. In contrast, small robots that can navigate between crop rows are better suited in such cases due to their superior maneuverability, flexibility, and portability. Commercial off-the-shelf all-terrain unmanned ground vehicles (UGV) are convenient bases for developing mobile between-row robotic platforms. Shafiekhani et al. (2017) developed Vinobot based on a Husky UGV (Clearpath Robotics, Ontario, Canada) for phenotyping corn plants (Fig. 2.3 bottom left). A robot arm was installed on the UGV to position a stereo camera for 3D plant reconstruction. Ideally, the robot should fit in the standard 0.76-m row spacing. However, Vinobot operates in at least 1.1-m row spacing due to the width of the Husky UGV. This is a trade-off when adopting a general-purpose UGV as an HTPP platform because the design may not be optimized for the narrow row spacing and the crop species. Hence, many research teams designed their mobile robotic phenotyping platforms for their specific crop species and field conditions. For bioenergy sorghum phenotyping, (Young et al. 2019) reported a tracked robot with a high sensor mast (Fig. 2.3 bottom right). The challenges with bioenergy sorghum phenotyping are extremely tall plants (e.g., >3 m), dense canopies, and tillers. A stereo camera was mounted at the top of the mast (up to 3.6 m) for measuring plant height and a Time-of-Flight (ToF) depth camera at the base of the tower for measuring stalk diameter. No sensors were placed between the panicles and the bottom sections of the stems because the dense canopies and the narrow row spacing (i.e., 0.76 m) caused heavy occlusions. Gao et al. (2018) developed a similar tracked robot that travels between rows of soybean plants except that the sensor tower was far shorter. TerraSentia (EarthSense Inc, IL, USA) is a small wheeled robot equipped with a LiDAR and gimbaled side-viewing RGB cameras for general phenotyping of row crops such as corn and soybean (Zhang et al. 2020). The small between-rows mobile robots mostly employ a differential steering mechanism that enables zero-radius turning (Fig. 2.3 bottom center). This design can reduce the complexity and cost of construction. Meanwhile, the differential steering is not as efficient as the Ackermann steering used by agricultural vehicles or the four-wheel-steering of the large robots mentioned above.

Small robots are best suited for even terrains and well-managed fields without excessive weeds due to the low ground clearance. The low payload of small robots can be a limiting factor if there is a need for carrying multiple large sensor modules with multiple viewing angles and even for performing plant manipulation. Mueller-Sim et al. (2017) developed a four-wheel-drive, differential-steering robot Robotanist for bioenergy sorghum phenotyping (Fig. 2.3 bottom center). A tall mast reaching 1.8 m was rigidly mounted on the vehicle to support a real-time kinematic global positioning system (RTK-GPS) module and a pushbroom LiDAR at the top due to the extreme plant height (i.e., over 4 meters). GPS signals and radio communication

signals can be weakened if the antennas are under the canopy. The autonomous navigation relied on the RTK-GPS at the top of the mast and a forward-facing ToF depth camera at the front of the vehicle. The ToF depth camera captured the ground and the bottom sections of the two rows of plants, enabling local navigation. A stereo camera with a high-intensity strobe light was mounted at the rear of the vehicle for stalk detection and stalk diameter estimation. Another unique feature of Robotanist was a stereo vision-guided robot manipulator that can grasp a stalk and measure its strength.

## 2.3 A Case Study

### 2.3.1 *Development of Phenobot 3.0, an Autonomous Ground Vehicle for Field-Based HTPP*

Due to superior autonomy and portability, mobile ground robots have greater potential to become a widely adopted tool for field-based HTPP. The Iowa State University (ISU) PhenoBot Project is a good illustration of the development process of an autonomous ground vehicle for field-based plant phenotyping. The ISU PhenoBot was designed to traverse between corn rows and carry a sensor package mounted on the robot so that phenotypic data of corn plants can be acquired across fields. This case study is based on the dissertation work by Gai (2020) on PhenoBot 3.0. This latest PhenoBot version is capable of self-navigating between corn rows with conventional row spacing of 0.76 m by featuring a narrow body design and a central articulated steering mechanism (Fig. 2.4). The telescoping sensor mast has an adjustable height between 2.1 and 3.7 m. Additionally, the roll angle of the sensor mast was actively controlled to maintain vertical in the presence of the uneven ground surface. Multiple PhenoStereo cameras (Xiang et al. 2020) were mounted on the sensor mast to acquire close-range, side-view stereo images of the two rows of plants. The motorized telescoping mast and the multi-sensor configuration enable the robot to simultaneously image plant sections at different heights. Various organ-level traits such as brace roots, stalks, ears, leaf angles, and tassels/panicles can be imaged for corn and sorghum plants at different growth stages.

During the mechanical design process, different design requirements including structural strength, parts machinability, and Ingress Protection rating were carefully evaluated so that the manufacturing process can be easily scaled up to produce multiple units. The robot is reliable enough to operate in the field. Apart from the mechanical design, robot navigation and image post-processing are two critical functional modules. Efforts were made during the software development of these two modules to ensure that the systems have sufficient robustness against different environments and different plant conditions. Different techniques were employed during the development process.

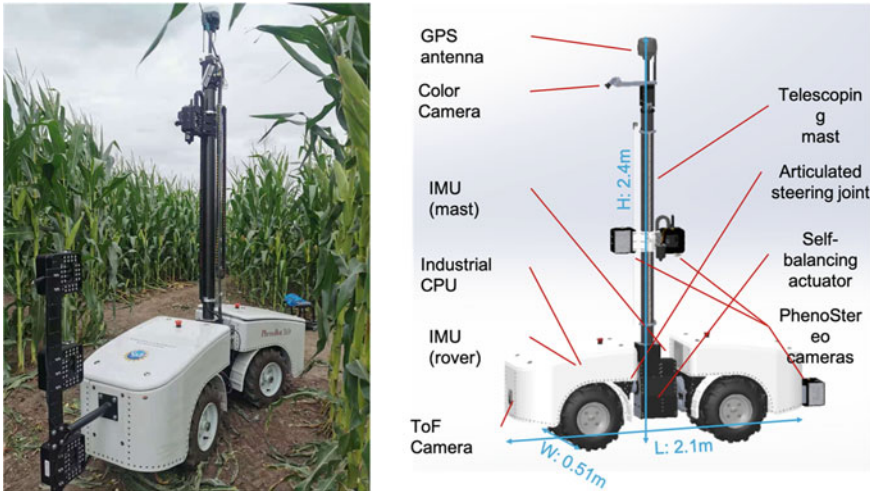


**Fig. 2.4** Illustration of PhenoBot 3.0. PhenoBot 3.0 is an articulated steering vehicle with a self-balancing, telescoping sensor mast. Multiple PhenoStereo sensors are mounted on the sensor mast and attached to the back of the vehicle. Its navigation sensing system includes a GPS module and a color camera at the top of the sensor mast, an IMU module at the bottom of the sensor mast, an IMU module and a ToF camera in the front section of the vehicle, and wheel encoders

### 2.3.1.1 Navigation System Development

The navigation system aims to guide the PhenoBot 3.0 between the corn plant rows, keeping it close to the center of the two crop rows. As for the dataflow of the navigation system (Fig. 2.5), data from multiple navigation sensors were fused for localizing the robot in the field map. And the robot was driven by a path tracking algorithm to correct the position and heading errors relative to the central line between two adjacent crop rows. Finally, the motions of individual motors were controlled based on the kinematic model of the robotic rover. Such a localization-and-tracking strategy was employed by many robotic navigation systems (Li et al. 2009; Mueller-Sim et al. 2017; Young et al. 2019).

Robot localization:

For robots traversing crop rows, accurate estimations of robot pose (i.e., position and orientation) and motion (i.e., speed and acceleration) are critical to avoid crop damage, especially for narrow crop rows. Various position and motion sensors are available for localization, but different information is delivered due to the different working principles. An RTK-GPS unit can measure the global position of a robot in the Universal Transverse Mercator (UTM) coordinate system with a centimeter accuracy (Nagasaka et al. 2009). A compass sensor provides absolute heading information by measuring the magnetic field of the earth. An inertial measurement unit (IMU) sensor is a motion sensor that can track change in position, speed, and heading over time in a local frame. The data from rotary encoders on robot wheels along with

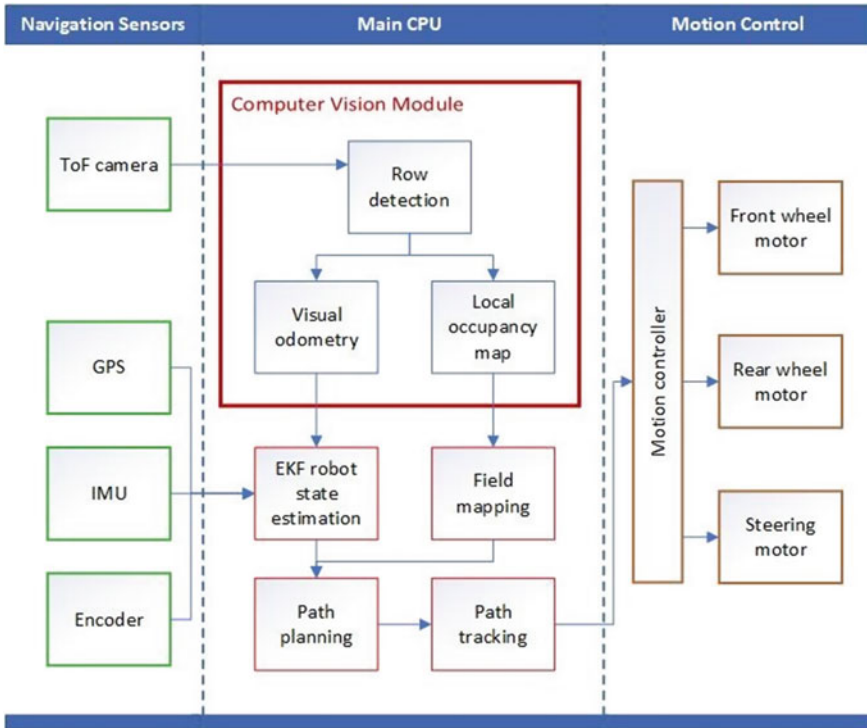


Fig. 2.5 The diagram of the navigation control system of PhenoBot 3.0

the robot's kinematic model can be used to calculate a robot's pose and motion, which is referred to as wheel odometry.

To improve the robustness of robot localization, multiple localization sensors are usually used together rather than relying on a single sensor. Although the sensors may provide redundant data, sensor fusion techniques such as Extended Kalman Filter (EKF) (Hoshiya and Saito 1984) can be used to improve the accuracy and reliability of robot localization. And by referencing the map of the crop rows, the heading and the lateral position relative to the crop rows can be calculated and used to drive the robot.

Another strategy for robot localization within a crop field is visual odometry, which employs computer vision to detect and locate crop rows in real-time images or 3D point clouds, and inversely estimate robot position relative to crop rows. This technique applies to applications where global localization is denied or a field map is not available.

In the PhenoBot 3.0 navigation system, the sensors for explicit robot localization include an RTK-GPS unit mounted at the top of the sensor mast and a forward-facing ToF depth camera. The RTK-GPS unit measures the global location along crop row direction, while the ToF camera provides local 3D environment sensing so that the

robot is constantly aware of its location relative to the two corn rows on the left and right sides. Motor encoders and an IMU were used for vehicle dead-reckoning and heading tracking. Figure 2.6 illustrates the sensor fusion method of PhenoBot 3.0.

Path tracking:

A path tracking algorithm is responsible for determining the appropriate actuation of the robot based on the localization results of the robot to follow a pre-defined or dynamically planned path. Many algorithms were developed and implemented for robotic vehicles operating in the field. Some of them are error-driven feed-back control algorithms, which use the tracking errors at current and previous timestamps to control the steering motion, such as proportional-integral-derivative (PID) control Linear Quadratic Regulator (LQR) control, Fuzzy logic control and sliding mode control. PID control is used in many control applications (Dong et al. 2011; Luo et al. 2009; Malavazi et al. 2018; Underwood et al. 2017). It has a simple structure where the control command is calculated as a weighted sum of the errors, the integral of, and the derivative of the error. However, it has requirements for the simplicity and controllability of the system model. LQR is an optimal control method which operates a dynamic system at minimum cost. It requires a relatively reliable prior knowledge about the dynamic system to achieve high-performance (Olalla et al. 2009). Fuzzy logic is a more intelligent algorithm that allows human knowledge to be integrated as a set of linguistic expressions. It is widely used for steering control due to simplicity

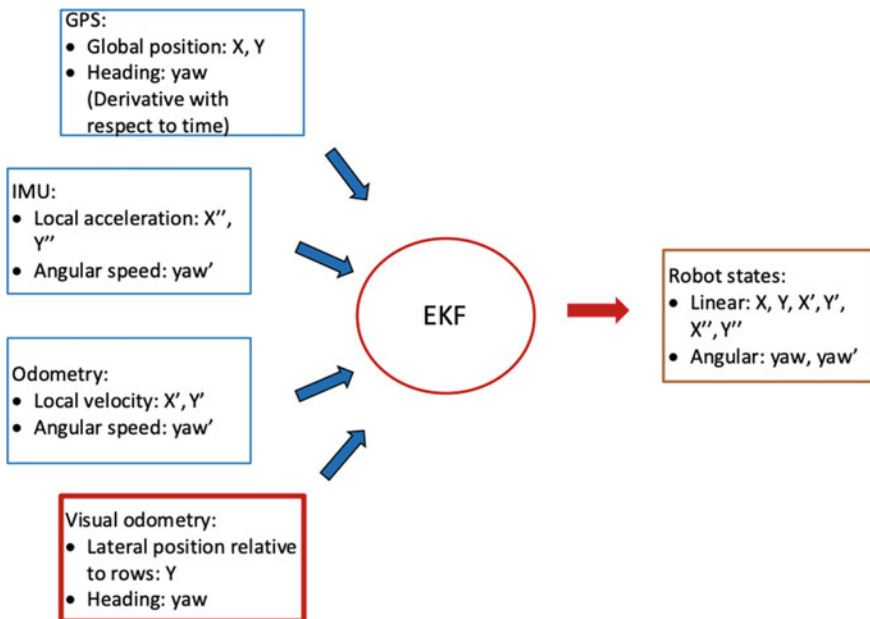


**Fig. 2.6** The sensor fusion diagram for the state estimation of PhenoBot 3.0. The visual odometry is acting as a redundant source to improve the system robustness



and effectiveness (Xue et al. 2012). Sliding mode control is a robust algorithm in which the control input was switched based on the position of the robot states relative to a specified “sliding surface” in the state space. The surface is designed based on the control objective and the robot model, and the robot states are gradually “sliding” to the surface. The algorithm was used in many agricultural navigation applications (Eaton et al. 2008; Tu et al. 2019) due to its high controllability and insensitivity to the model uncertainty and disturbances (Liu and Wang 2011). Another category is the feedforward control, which requires the kinematic or dynamic model of the robot to predict the dynamic response of the system then give the corresponding adjustments. Pure pursuit is a common and effective geometric algorithm mainly for non-holonomic vehicles. It calculates the position and heading errors by comparing with a set point in the path at a certain distance ahead of the robot. And then the algorithm calculates an arc path for the robot to join the path at the set point. The maximum curvature of the path was constrained by the robot steering capability. Because the algorithm does not require the derivative terms of the robot states, it is computationally simple and easy to implement. The algorithm was successfully implemented and validated in many applications (Mueller-Sim et al. 2017; Rains et al. 2014; Zhang et al. 2019).

Model Predictive Control (MPC) refers to a set of optimization-based feed-forward control algorithms, which are more computationally demanding compared to the algorithms mentioned above. The basic concept of MPC is to use a system model to forecast system behavior and optimize the forecast to find the best control decision at the current time. Some variants of MPC such as Nonlinear Model Predictive Control (NMPC) are able to handle constraints, process nonlinearity, uncertainty, or time-delay, thus leading to improved performance and robustness. MPCs were implemented on various autonomous agricultural vehicles and achieved good performance during tracking both straight paths and complex paths (Backman et al. 2012; Kayacan et al. 2018; Utstumo et al. 2015; Zhang et al. 2020). In addition, some optimization-based algorithms such as Timed Elastic Band (TEB Rössmann et al. 2017) were also capable of planning collision-free or space-optimal paths by including a collision or space term in the optimization cost function. These optimization-based algorithms are suitable for critical scenarios during navigation (e.g., head-landing turning) to avoid collisions and adapt to limited space.

The navigation system of PhenoBot 3.0 adopted the LQR, Pure pursuit, and the Time Elastic Band (TEB) algorithms. The LQR and Pure pursuit algorithm handled path tracking in normal conditions, while the TEB algorithm was explicitly used for dynamically path planning for headland turning when the space is limited.

#### Vision-based navigation:

Vision-based navigation can be an alternative to the GPS-based path tracking navigation when the GPS-based localization is denied, or a pre-defined path is not available. In field-based navigation, the strategy is to follow crop rows by identifying the rows using cameras and accordingly steering the robot to keep the robot centered. Two sensor setups are widely adopted in field-based navigation applications. One is using a top-view above-canopy sensor and another a front-view under-canopy sensor.

When using an above-canopy vision sensor, multiple crop rows can be observed at once in the top-view. Most row detection algorithms focus on linear features in the images formed by the crop rows. The most commonly used method for identifying crop rows in the images is the Hough transform (Slaughter et al. 2008). The Hough transform is a computationally efficient procedure for detecting discontinuous lines or parametrical curves in images, and its applications for crop row detection were reported in a number of studies (Abdulsalam et al. 2016; Bossu et al. 2006; Choi et al. 2015; Winterhalter et al. 2018). Other algorithms include linear regression (Benson et al. 2003) and green pixels accumulation (García-Santillán et al. 2018; Li et al. 2020). Furthermore, some applications also fuse local odometry information for row detection using particle filters (Blok et al. 2019; Grisetti et al. 2007).

Row detection algorithms using under-canopy sensors were mainly applied on small robots operating under canopies of tall row crops such as corn and sorghum, or robots operating between tree rows in orchards. When a robot travels under canopies, only two adjacent rows are observable at a time. When using a 2D color camera, the pixels of plants and soil were segmented in the images, and their boundaries were extracted to estimate the position and the direction of the adjacent crop row. Yang et al. (2018) proposed an algorithm to detect the centerlines of maize rows by extracting the base of plants. Compared with the features extracted in 2D color images, 3D features are less prone to varying ambient lighting conditions. Therefore, depth sensors such as a LiDAR sensor and a Time-of-Flight depth camera were often adopted in field-based navigation applications (Higuti et al. 2019; Mueller-Sim et al. 2017). In these applications, the general strategy was to fit two parallel lines or planes representing the crop rows in the point cloud generated from depth sensors. Fitting algorithms such as least squares, RANSAC (Fischler and Bolles 1981), and PEARL (Isack and Boykov 2012) were applied for fitting the model of parallel lines or planes.

A top-view camera and an under-canopy ToF camera were both equipped on PhenoBot 3.0 and are designated for corn plants at earlier growth season and later growth season, respectively (Fig. 2.7). With the row detection results, the current row tracking errors including the lateral position deviation and the heading deviation relative to the row centerlines were determined. A Linear-Quadratic-Gaussian (LQG) controller was applied to steer the robot to correct the tracking error for in-row navigation. The LQG controller combines a Linear-Quadratic Regulator (LQR) with a Kalman filter (a linear-quadratic state estimator), which takes the noise in the linear system and the measurement process into consideration.

### 2.3.1.2 System Implementation and Simulation

ROS-based control system architecture:

ROS (Robot Operating System) was used to integrate different functional processes in the control system of PhenoBot 3.0. ROS is an open-source middleware that provides a framework for connecting many different software components (i.e., ROS nodes) of a complex robotic application. ROS manages a graph-like network of different

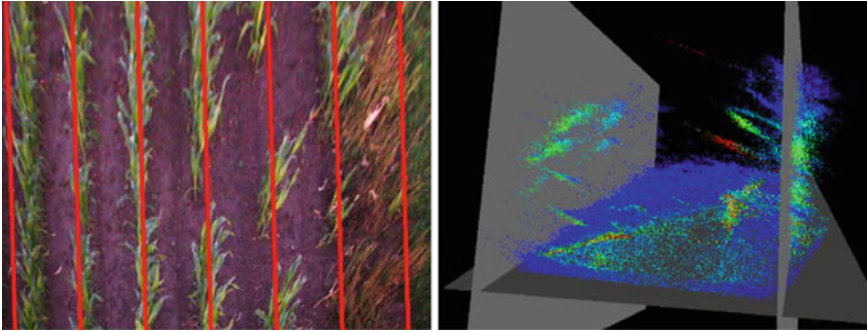


**Fig. 2.7** Vision-based crop row detection methods for PhenoBot navigation. Left: row detection using a top-view camera. Crop rows were detected as parallel lines in the 2D color image. Right: row detection using an under-canopy ToF camera. Crop rows were detected as parallel planes in the 3D point cloud

processes, and the processes are loosely coupled using communication protocols defined by ROS. These protocols were designed for different requirements, including synchronous request/response communication over “service,” asynchronous data streaming over “topics,” and shared parameter storage named “parameter server” (Koubâa 2019).

The control program of PhenoBot 3.0 consisted of several modules (i.e., ROS nodes), including hardware control, robot localization, robot navigation, and mission planning. The hardware control module controls each individual motor by listening to the robot movement commands according to the robot kinematic model. The robot localization module reads the sensor outputs from different navigation sensors, including the encoders, the IMU, the GPS unit, and the vision sensors, then calculates the current position and direction in both the vehicle local coordinate frame and the UTM coordinate frame. The robot navigation module plans and computes motion commands to follow a series of paths to specific targets during the mission. The mission planning module creates plans for accomplishing user-specified tasks such as traversing the crop rows or navigating to a certain location in the field. With the modules above, a “graph” of ROS nodes was established in the control system (Fig. 2.8).

#### Robot simulation:

Simulation technology and evaluation within virtual environments can provide frameworks to test and evaluate the functionality and performance of the developed systems in dynamic scenarios, therefore accelerating the development process. Various types of simulation software such as Gazebo (“Gazebo,” n.d.), V-REP (Rohmer et al. 2013), and ARGos (Pincirolì et al. 2012) are available and were proven capable of simulating field environments for field robotic system development.

The Gazebo simulator was developed specifically for simulation of robotic systems. It is widely used for robot simulation as it easily interfaces with ROS, which

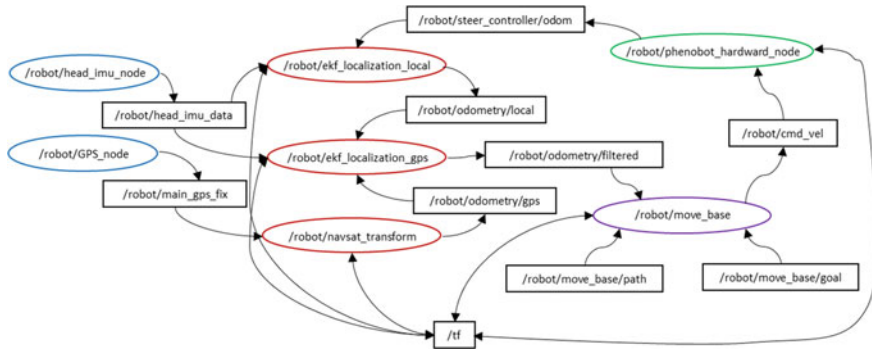


**Fig. 2.8** The ROS node network of the PhenoBot 3.0 control system when working in GPS-based path tracking mode. The ellipses represent ROS nodes including sensor nodes (blue), localization nodes (red), a navigation node (purple), and a motion control node (green). The rectangles represent the ROS message topics for data interchanges between nodes. “/tf” is a series of messages tracking the transformations of different coordinate frames related to the robot

enables the development of software in the context of testing the developed code with a simulated robot and a virtual environment. Gazebo features a time-efficient physical engine to simulate the interaction between the robot and the environment. The descriptions of the robot and the environment are input through an XML file which contains the physical properties and geometry parameters that describe the bodies of the robot and the objects in the environment.

When using Gazebo with ROS, Gazebo loads a series of ROS plugins, which turns Gazebo into a ROS node. The ROS plugins use Gazebo API to simulate sensors, actuate motors, and provide interfaces to dynamically re-configure parameters in the simulation. The rest of the ROS nodes for robot control can be migrated into the real-world robot with little extra effort after being verified and tuned in the simulation.

Gazebo was used to simulate the PhenoBot in a virtual corn field for debugging and validating the functionality of the control algorithms. In the simulation, the robot and the world were modeled into bodies and joints, based on the minimum degree-of-freedom requirement of the simulation. In the case of PhenoBot, the rover with differential gears and the articulated body design was simplified to a 2D bicycle model. The navigation sensors introduced above were included in the navigation system and were also simulated in the Gazebo software. In the virtual environment, a realistic corn plant model was duplicated into a plot, a crop row, and the entire corn field. The virtual ground was made up of an uneven surface, which aimed to simulate real-world soil conditions. The uneven virtual ground also enabled the simulation of the mast balancing on a tilted vehicle body as the vehicle moved through the field.

The simulation of PhenoBot 3.0 in Gazebo was carried out in several steps. At first, the robot model and the simulated sensors were verified by using ROS visualization tools. Specifically, RViz, which is a visualization tool in ROS, was used to inspect the robot model, and the sensor output. Then, the developed ROS programs were attached to the Gazebo simulation environment and each individual module

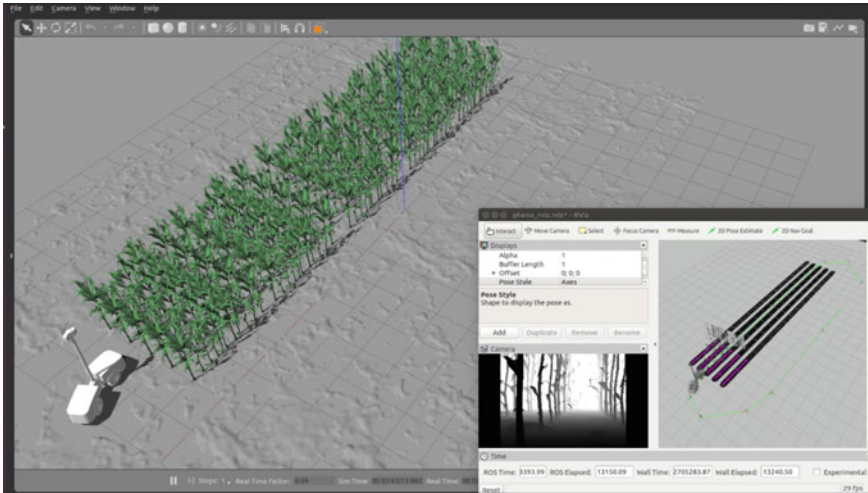


**Fig. 2.9** Simulation of a PhenoBot 3.0 entering a virtual corn field in Gazebo. The robot pose, the map, the planned trajectory and the sensor output are displayed on the Rviz-based control panel on the bottom right

was tested. The robot hardware control module was tested by inspecting the robot movement with a user-specified speed command. As for the localization module, the parameters in the module were tuned to achieve the best accuracy and stability for robot pose estimation. The navigation module was validated by observing the performance of robot navigation behaviors, such as path planning, path following, and obstacle avoidance gave a virtual scene and a target pose. Finally, the mission planning module was attached to the ROS network, and the overall performance of the integrated navigation system with all modules active was evaluated (Fig. 2.9).

### 2.3.1.3 Verification by Field Tests

After the development and evaluation in the simulation environment, the performance of the robot navigation system was finally tested in the field. Field tests were conducted at Iowa State University Agricultural Engineering and Agronomy Research Farm located in Boone, Iowa in 2020. After verifying the functionality of each module, different navigation strategies were tested and evaluated in the field. For instance, the GPS-based path tracking was evaluated by operating on a patch of grass field with compacted and uneven terrain, which is worse than the conditions of most fields. The path to follow during the experiment was defined as a series of cubic splines. The path is composed of straight path sections as the centerlines of the crop rows, c-shape turn path section, and bulb turn path sections for the transition between crop rows. These path sections are the common elements in paths for field-based operations. The path tracking lateral position error was measured for different

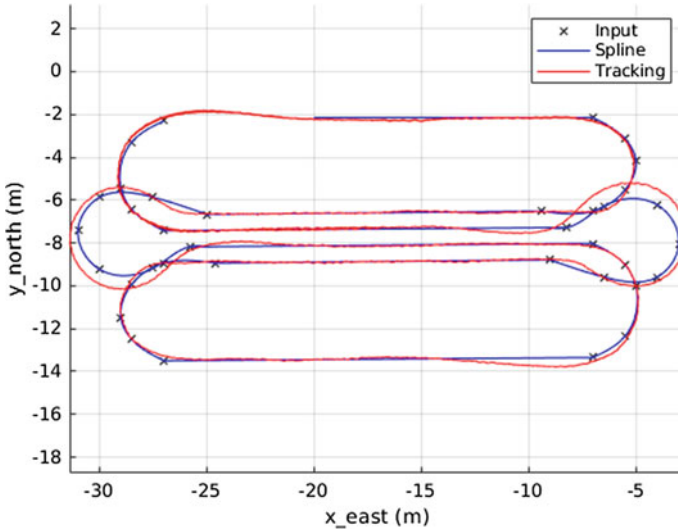


**Fig. 2.10** A reference path and the robot trajectory in the field test using Pure Pursuit Control (PPC) algorithm for GPS-based path tracking

tracking algorithms by comparing the GPS-based localization with the referenced path.

The field results demonstrated that PhenoBot 3.0 with the designed control system is feasible for navigation in the field. The robot is capable of following standard 30'' crop rows using both GPS-based tracking (Fig. 2.10) and vision-based row following with minor crop damages (Lateral error less than 8 cm for 90% of the cases). However, the performance of the navigation control system is still challenged by the semi-structured environment in the field, including the uneven terrain, variable plant shapes, and the weed infection. The reliability and performance of field-based navigation control can further be improved.

## 2.4 Sensors

The process that transforms raw sensor data into meaningful phenotypic data is essentially machine perception. Plant traits can be quantified with sensing technologies at different levels of integration (i.e., plot, plant, or organ). Plot-level traits are often generic and can be applied to a wide range of crop species and crop growth stages. Such traits include plant morphological measurements (e.g., canopy height, canopy width and leaf area) and plant physiological indicators (e.g., vegetation indices and canopy temperature), which require low-level machine perception. All plot-level traits can be adopted as plant-level traits if the sensor data of individual plants can be delineated, namely plant segmentation. Plant segmentation itself also enables

an important plant-level trait, stand count. Other plant-level traits are based on the measurement of a particular plant organ. In the case of cereal crops, for instance, plant height is measured from the ground to the flag leaf of a plant before the panicle becomes visible or to the panicle apex afterward. Since one plant only has one panicle and one flag leaf, machine perception of such special organs enables plant-level trait characterization. Stem diameter is another example of the plant-level trait. If the plant of interest can grow multiple organs of the same type (e.g., leaves, branches, internodes, flowers, fruits, bean pods, corn ears, cotton bolls, grape berries), accurate machine perception of these organs allows for organ-level phenotyping and lays the foundation for higher levels of integration. Due to the small sizes and occlusion issues in the crop fields, machine perception at the organ level remains a challenging research area. Leaf disease assessment is another type of organ-level trait, which can be based on multi- or hyper-spectral analysis or visual perception. Some plant organs are components of larger plant organs, for instance, the spikelets on a wheat spike.

The majority of sensors used in HTPP are imaging-based. A thorough review of imaging techniques for plant phenotyping was given by Li et al. (2014). Five key imaging techniques were identified: visible imaging, fluorescence imaging, thermal imaging, spectroscopic imaging, and LiDAR. Visible imaging has been used to characterize various plant morphological and architectural traits of leaf, stem, panicle, root, and seed (Brichet et al. 2017; Bucksch et al. 2014; Miller et al 2017; Zhang et al. 2017). Fluorescence imaging is typically used to measure photosynthesis and plant stress response (Bresson et al. 2015). Thermal imaging can measure surface temperature, which is related to stomatal conductance and water stress (Buitrago et al. 2016; Struthers et al. 2015). Spectroscopic imaging such as hyperspectral imaging can indicate water and health statuses of leaf and canopy (Ge et al. 2016; Liang et al. 2017; Pandey et al. 2017). LiDAR is mostly used to estimate canopy height, leaf surface area, volume, and biomass (Greaves et al. 2015; Madec et al. 2017; Sun et al. 2017). In addition to imaging sensors, other sensors often provide an average response in the field of view. Such sensors include ultrasonic and laser distance sensors, NDVI spectrometers (e.g., Crop Circle), and infrared radiometers.

### ***2.4.1 Side-View Versus Top-View Imaging***

Ground-based HTPP opens more possibilities of sensor viewing angles in comparison to its aerial counterpart. For short crops, the majority of HTPP systems employ a top-view imaging strategy. Top-view imaging is efficient and effective in quantifying plot-level traits such as NDVI, LAI, and leaf temperature. However, for some tall crops, imaging from a side-viewing angle can capture information that cannot be accessed by top-view imaging due to occlusion. For instance, imaging cereal crops (e.g., wheat, corn, and sorghum) from the side can reveal plant architecture traits such as plant height (Busemeyer et al. 2013; Montes et al. 2011), biomass (Busemeyer et al. 2013; Montes et al. 2011), stem diameter (Bao et al. 2019a; b), and leaf angle (Bao et al. 2019b). In addition, a light curtain can be used to generate side-view binary

images of crop rows to estimate plant height and biomass (Busemeyer et al. 2013; Montes et al. 2011). Another useful application of side-view imaging was sensing plant population and inter-plant spacing. A push-cart system was developed to detect stem lines for early-stage corn plants using side-view 3D imaging by Nakarmi and Tang (2012, 2014). Compared to earlier studies using top-view imaging (Jin and Tang 2009; Shrestha et al. 2004; Shrestha and Steward 2003, 2005; Tang and Tian 2008a, b), the plant architecture of each stand was better exposed in the side-view images.

#### ***2.4.2 PhenoStereo—A Case Study of Plant Organ Phenotyping by Computational Perception***

Sub-canopy phenotyping can provide important agronomic traits such as plant count, stem diameter, plant height, fruit count, and light interception (Baweja et al. 2018; Gage et al. 2019; Mueller-Sim et al. 2017; Nellithimaru and Kantor 2019; Zhang et al. 2020). It also poses unique challenges to off-the-shelf imaging sensors regarding short working distance and low light conditions. Stereo vision in synchronization with a high-intensity strobe light has shown promising potential for sub-canopy high-resolution RGB and depth (RGB-D) imaging, which enabled fruit counting (Pothen and Nuske 2016; Wang et al. 2013) and stem diameter estimation (Baweja et al. 2018). Here we briefly report the development and evaluation of such a stereo imaging module named PhenoStereo (Fig. 2.1) for sub-canopy plant architecture phenotyping. PhenoStereo featured a self-contained embedded design, which made it capable of capturing images at 14 6-megapixel stereoscopic frames per second. The integration of strobe lights enabled the application of the PhenoStereo under various environmental conditions (i.e., direct sunlight, backlighting, shadow, and wind). The PhenoStereo mainly consisted of a developer kit, two RGB cameras, a printed circuit board (PCB), and a set of LED strobe lights. The developer kit includes a Jetson TX2 embedded platform (NVIDIA, California, USA), an Elroy carrier board (Connect Tech Inc., Ontario, Canada), and other accessories on the carrier board. Jetson is able to simultaneously take image pairs from the stereo camera through a high-speed interface (PCIe) and save them to a solid-state drive. The stereo camera has a horizontal view angle of  $85.8^\circ$  and a vertical view angle of  $63.6^\circ$ . The customized LED strobe lights were integrated to overcome lighting variation and enabled the use of an extremely high shutter speed to overcome motion blurs. An electronic circuit was designed to synchronize and trigger the camera pair and the strobe lights. By using the Robot Operating System (ROS) JavaScript Library, a web-based user interface was developed to control the cameras and visualize the images. The interface allows a user to adjust camera parameters (e.g., exposure time, white balance, etc.), send trigger commands, and view live images on a smartphone/laptop browser (Fig. 2.11a). The live images and commands are published over a local area network using Robot Operating System (ROS).



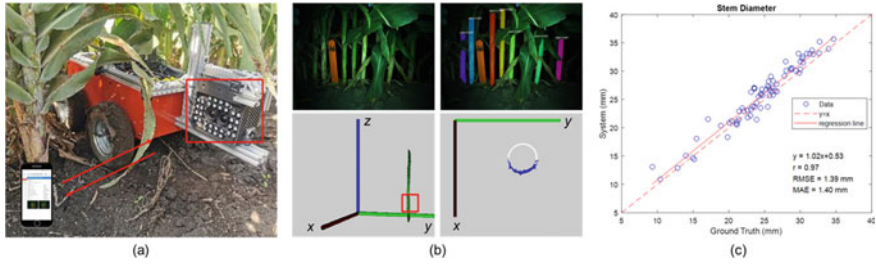


**Fig. 2.11** PhenoStereo for sorghum stem diameter phenotyping. **a** PhenoStereo is mounted on a small ground robot and can be controlled on mobile devices via a web interface. **b** The image processing pipeline for sorghum stem diameter estimation. A Mask R-CNN model was used to detect individual stems from original RGB images. The reconstructed point cloud of a selected stem section was projected onto the  $x$ - $y$  plane, where a circle was detected to quantify the stem diameter. **c** Correlation between system-derived stem diameter and ground truth

Stem diameter of a sorghum plant is an important trait for stalk strength and biomass potential evaluation but has been identified as a challenging sensing task to automate in the field due to high planting densities with heavy tillering (i.e., secondary plants originated from the base of a primary plant). To that connection, PhenoStereo was used to acquire a set of sorghum plant images and an automated point cloud data processing pipeline was developed to automatically extract the stems and then quantify their diameters via an optimized 3D modeling process (Fig. 2.11b). The pipeline employed a Mask Region Convolutional Neural Network (He et al. 2017) for detecting stalk contours and a Semi-Global Block Matching algorithm (Hirschmuller 2007) for reconstructing 3D models. The 2D detections were projected onto 3D point cloud to segment individual stems. After that, each stem was modeled as a cylinder and circle fitting was carried out on the projected point cloud of the selected stem section. The correlation coefficient ( $r$ ) between the image-derived stem diameters and the ground truth measurements was 0.97 with a mean absolute error (MAE) of 1.44 mm (Fig. 2.11c), which outperformed any previously reported sensing approaches. These results demonstrated that a properly customized stereo vision system can be a highly desirable sensing method for field-based plant phenotyping using high-fidelity 3D models reconstructed from stereoscopic images. With the proving results from sorghum plant stem diameter sensing, this proposed stereo sensing approach can likely be extended to characterize a broad spectrum of plant phenotypes such as leaf angle, ear height, and tassel shape of corn plants and seed pods and stem nodes of soybean plants.

## 2.5 Summary

In this chapter, we presented an updated review of infield ground-based robotic HTPP systems. Additionally, we described the development and evaluation of PhenoBot

3.0 and PhenoStereo as a case study for corn plant phenotyping. Our goal is to facilitate the design process of any new robotic HTPP systems for specific applications. Based on the rapid recent advancements in robotics, sensors, and AI, we envision that autonomous, compact, mobile robots or robot fleets are more likely to become the “boots on the ground” for assessing crop performance in the field. The commercialization of legged robots such as the Spot from Boston Dynamics could provide new possibilities for reliable mobility in rough crop fields and actively controlled sensor deployment that maximizes capturing of useful information. On the other hand, AI is beginning to shift the paradigm of phenotypic traits extraction from sensor data. “Hand engineered” algorithms are being surpassed by deep learning algorithms that can automatically learn hierarchical feature representation in raw data and the domain knowledge of a phenotyping task. We believe that AI-powered machine perception will eventually enable the integration of knowledge about plants and “artificial super vision” (i.e., fusion of different sensing technologies) for high-throughput plant phenotyping.

**Acknowledgments** We greatly appreciate the following individuals and organizations for allowing us to include their pictures in Figs. 2.1, 2.2 and 2.3 of this chapter: Dr. Arno Ruckelshausen, Dr. Scott Noble, Dr. David Deery, Dr. Joshua Peschel, Dr. Seth Murray, Dr. Girish Chowdhary, Claire Benjamin (TERRA-MEPP), Dr. Guilherme DeSouza, Dr. Norbert Kirchgessner, Peter Rüegg (ETH Zürich), Christophe Rousset (Robopec), Dr. Pedro Andrade Sanchez, Dr. George Kantor, Dr. Yu Jiang, and Dr. Yufeng Ge.

## References

- Abdulsalam A, Dittman S, Kjessler O, Levy S, Zimbron-alva M, Armstrong DG, Jigar P, Savan V, Bhagat K, Deshmukh S, Dhonde S, Ghag S, Cain D, Layng B, McNulty K, Connor RO, Chen Y, Chip M, Christian H, Wikipedia S (2016) Obstacle avoidance robotic vehicle using ultrasonic sensor, android and bluetooth for obstacle detection. *Int Res J Eng Technol* 5:2395–2456. <https://doi.org/10.3965/j.issn.1934-6344.2009.03.001-016>
- Andrade-Sanchez P, Gore MA, Heun JT, Thorp KR, Carmo-Silva AE, French AN, Salvucci ME, White JW (2014) Development and evaluation of a field-based high-throughput phenotyping platform. *Funct Plant Biol* 41(1):68–79
- Appleby N, Edwards D, Batley J (2009) New technologies for ultra-high throughput genotyping in plants. In: *Plant genomics*. Springer, pp 19–39. [https://doi.org/10.1007/978-1-59745-427-8\\_2](https://doi.org/10.1007/978-1-59745-427-8_2)
- Backman J, Oksanen T, Visala A (2012) Navigation system for agricultural machines: nonlinear model predictive path tracking. *Comput Electron Agric* 82:32–43. <https://doi.org/10.1016/j.compag.2011.12.009>
- Bai G, Ge Y, Scoby D, Leavitt B, Stoerger V, Kirchgessner N, Irmak S, Graef G, Schnable J, Awada T (2019) NU-Spidercam: a large-scale, cable-driven, integrated sensing and robotic system for advanced phenotyping, remote sensing, and agronomic research. *Comput Electron Agric* 160:71–81
- Bao Y, Tang L, Breitzman MW, Salas Fernandez MG, Schnable PS (2019a) Field-based robotic phenotyping of sorghum plant architecture using stereo vision. *J Field Robot* 36(2):397–415
- Bao Y, Tang L, Srinivasan S, Schnable PS (2019b) Field-based architectural traits characterisation of maize plant using time-of-flight 3D imaging. *Biosys Eng* 178:86–101

- Barker J, Zhang N, Sharon J, Steeves R, Wang X, Wei Y, Poland J (2016) Development of a field-based high-throughput mobile phenotyping platform. *Comput Electron Agric* 122:74–85. <https://doi.org/10.1016/j.compag.2016.01.017>
- Baweja HS, Parhar T, Mirbod O, Nuske S (2018) StalkNet: a deep learning pipeline for high-throughput measurement of plant stalk count and stalk width. In: *Field and service robotics. Springer proceedings in advanced robotics*, vol 5, pp 271–284
- Bayati M, Fotouhi R (2018) A mobile robotic platform for crop monitoring. *Adv Robot Autom* 07(01). <https://doi.org/10.4172/2168-9695.1000186>
- Beauchêne K, Leroy F, Fournier A, Huet C, Bonnefoy M, Lorgeou J, De Solan B, Piquemal B, Thomas S, Cohan J-P (2019) Management and characterization of abiotic stress via PhénoField@, a high-throughput field phenotyping platform. *Front Plant Sci* 10:904
- Benson ER, Reid JF, Zhang Q (2003) Machine vision-based guidance system for agricultural grain harvesters using cut-edge detection. *Biosys Eng* 86(4):389–398. <https://doi.org/10.1016/j.biosystemseng.2003.07.002>
- Blok PM, van Boheemen K, van Evert FK, IJsselmuiden J, Kim GH (2019) Robot navigation in orchards with localization based on Particle filter and Kalman filter. *Comput Electron Agric* 157:261–269. <https://doi.org/10.1016/j.compag.2018.12.046>
- Bossu J, Gée C, Guillemain J-P, Truchetet F (2006) Development of methods based on double Hough transform or Gabor filtering to discriminate between crop and weed in agronomic images. In: Meriaudeau F, Niel KS (eds), *Machine vision applications in industrial inspection XIV*, vol 6070. SPIE, p 60700N. <https://doi.org/10.1117/12.642908>
- Bresson J, Vasseur F, Dauzat M, Koch G, Granier C, Vile D (2015) Quantifying spatial heterogeneity of chlorophyll fluorescence during plant growth and in response to water stress. *Plant Methods* 11(1):23. <https://doi.org/10.1186/s13007-015-0067-5>
- Brichet N, Fournier C, Turc O, Strauss O, Artzet S, Pradal C, Welcker C, Tardieu F, Cabrera-Bosquet L (2017) A robot-assisted imaging pipeline for tracking the growths of maize ear and silks in a high-throughput phenotyping platform. *Plant Methods* 13(1):96. <https://doi.org/10.1186/s13007-017-0246-7>
- Bucksch A, Burrige J, York LM, Das A, Nord E, Weitz JS, Lynch JP (2014) Image-based high-throughput field phenotyping of crop roots. *Plant Physiol* 166(2):470–486. <https://doi.org/10.1104/pp.114.243519>
- Buitrago MF, Groen TA, Hecker CA, Skidmore AK (2016) Changes in thermal infrared spectra of plants caused by temperature and water stress. *ISPRS J Photogramm Remote Sens* 111:22–31. <https://doi.org/10.1016/j.isprsjprs.2015.11.003>
- Busemeyer L, Mentrup D, Möller K, Wunder E, Alheit K, Hahn V, Maurer HP, Reif JC, Würschum T, Müller J (2013) BreedVision—a multi-sensor platform for non-destructive field-based phenotyping in plant breeding. *Sensors* 13(3):2830–2847. <https://doi.org/10.3390/s130302830>
- Choi KH, Han SK, Han SH, Park K-H, Kim K-S, Kim S (2015) Morphology-based guidance line extraction for an autonomous weeding robot in paddy fields. *Comput Electron Agric* 113:266–274. <https://doi.org/10.1016/j.compag.2015.02.014>
- Deery D, Jimenez-Berni J, Jones H, Sirault X, Furbank R (2014) Proximal remote sensing buggies and potential applications for field-based phenotyping. *Agronomy* 4(3):349–379. <https://doi.org/10.3390/agronomy4030349>
- Dong F, Heinemann W, Kasper R (2011) Development of a row guidance system for an autonomous robot for white asparagus harvesting. *Comput Electron Agric* 79(2):216–225. <https://doi.org/10.1016/j.compag.2011.10.002>
- Duvick DN (2005) The contribution of breeding to yield advances in maize (*Zea mays* L.). *Adv Agron* 86:83–145. [https://doi.org/10.1016/S0065-2113\(05\)86002-X](https://doi.org/10.1016/S0065-2113(05)86002-X)
- Eaton R, Katupitiya J, Siew KW, Howarth B (2008) Autonomous farming: modeling and control of agricultural machinery in a unified framework. In: *15th international conference on mechatronics and machine vision in practice, M2VIP'08*, pp 499–504. <https://doi.org/10.1109/MMVIP.2008.4749583>

- Fischler MA, Bolles RC (1981) Random sample consensus: a paradigm for model fitting with applications to image analysis and automated cartography. *Commun ACM* 24(6):381–395
- Gage JL, Richards E, Lepak N, Kaczmar N, Soman C, Chowdhary G, Gore MA, Buckler ES (2019) In-field whole-plant maize architecture characterized by subcanopy rovers and latent space phenotyping. *Plant Phenome J* 2(1):1–11
- Gai J, Tuel T, Xiang L, Tang L (2020) PhenoBot 3.0 - an Autonomous Robot for Field-based Maize/Sorghum Plant Phenotyping, Phenome 2020, Tucson, AZ, February 24–2
- Gao T, Emadi H, Saha H, Zhang J, Lofquist A, Singh A, Ganapathysubramanian B, Sarkar S, Singh AK, Bhattacharya S (2018) A novel multirobot system for plant phenotyping. *Robotics* 7(4):61
- García-Santillán I, Guerrero JM, Montalvo M, Pajares G (2018) Curved and straight crop row detection by accumulation of green pixels from images in maize fields. *Precis Agric* 19(1):18–41. <https://doi.org/10.1007/s11119-016-9494-1>
- Ge Y, Bai G, Stoerger V, Schnable JC (2016) Temporal dynamics of maize plant growth, water use, and leaf water content using automated high throughput RGB and hyperspectral imaging. *Comput Electron Agric* 127:625–632. <https://doi.org/10.1016/j.compag.2016.07.028>
- Greaves HE, Vierling LA, Eitel JUH, Boelman NT, Magney TS, Prager CM, Griffin KL (2015) Estimating aboveground biomass and leaf area of low-stature Arctic shrubs with terrestrial LiDAR. *Remote Sens Environ* 164:26–35. <https://doi.org/10.1016/j.rse.2015.02.023>
- Grimstad L, From PJ (2017) The Thorvald II agricultural robotic system. *Robotics* 6(4):24
- Grisetti G, Stachniss C, Burgard W (2007) Improved techniques for grid mapping with Rao-Blackwellized particle filters. *IEEE Trans Rob* 23(1):34–46. <https://doi.org/10.1109/TRO.2006.889486>
- He K, Gkioxari G, Dollár P, Girshick R (2017) Mask r-cnn. In: 2017 IEEE international conference on computer vision (ICCV), pp 2980–2988
- Higuti VAH, Velasquez AEB, Magalhaes DV, Becker M, Chowdhary G (2019) Under canopy light detection and ranging-based autonomous navigation. *J Field Robot* 36(3):547–567
- Hirschmuller H (2007) Stereo processing by semiglobal matching and mutual information. *IEEE Trans Pattern Anal Mach Intell* 30(2):328–341
- Hoshiya M, Saito E (1984) Structural identification by extended Kalman filter. *J Eng Mech* 110(12):1757–1770
- Isack H, Boykov Y (2012) Energy-based geometric multi-model fitting. *Int J Comput Vision* 97(2):123–147. <https://doi.org/10.1007/s11263-011-0474-7>
- Jiang Y, Li C, Robertson JS, Sun S, Xu R, Paterson AH (2018) GPhenoVision: a ground mobile system with multi-modal imaging for field-based high throughput phenotyping of cotton. *Sci Rep* 8(1):1213
- Jin J, Tang L (2009) Corn plant sensing using real-time stereo vision. *J Field Robot* 26(6–7):591–608
- Kayacan E, Young SN, Peschel JM, Chowdhary G (2018) High-precision control of tracked field robots in the presence of unknown traction coefficients. *J Field Robot* 35(7):1050–1062. <https://doi.org/10.1002/rob.21794>
- Kicherer A, Herzog K, Bendel N, Klück HC, Backhaus A, Wieland M, Rose JC, Klingbeil L, Läbe T, Hohl C, Petry W, Kuhlmann H, Seiffert U, Töpfer R (2017) Phenoliner: a new field phenotyping platform for grapevine research. *Sensors (Switzerland)* 17(7). <https://doi.org/10.3390/s17071625>
- Kirchgessner N, Liebisch F, Yu K, Pfeifer J, Friedli M, Hund A, Walter A (2017) The ETH field phenotyping platform FIP: a cable-suspended multi-sensor system. *Funct Plant Biol* 44(1):154–168. <https://doi.org/10.1071/FP16165>
- Klose R, Möller K, Vielstädte C, Ruckelshausen A (2010) Modular system architecture for individual plant phenotyping with an autonomous field robot. In: Proceedings of the 2nd international conference of machine control & guidance, pp 299–307.
- Koubâa A (2019) Robot Operating System (ROS), vol 1. Springer
- Li L, Zhang Q, Huang D (2014) A review of imaging techniques for plant phenotyping. *Sensors* 14(11):20078–20111

- Li M, Imou K, Wakabayashi K, Yokoyama S (2009) Review of research on agricultural vehicle autonomous guidance. *Int J Agric Biol Eng* 2(3):1–16. <https://doi.org/10.3965/j.issn.1934-6344.2009.03.001-016>
- Li S, Zhang Z, Du F, He Y (2020) A new automatic real-time crop row recognition based on SoC-FPGA. *IEEE Access* 8:37440–37452. <https://doi.org/10.1109/access.2020.2973756>
- Liang Z, Pandey P, Stoerger V, Xu Y, Qiu Y, Ge Y, Schnable JC (2017) Conventional and hyperspectral time-series imaging of maize lines widely used in field trials. *GigaScience*. <https://doi.org/10.1093/gigascience/gix117>
- Liebisch F, Kirchgessner N, Schneider D, Walter A, Hund A (2015) Remote, aerial phenotyping of maize traits with a mobile multi-sensor approach. *Plant Methods* 11(1):9. <https://doi.org/10.1186/s13007-015-0048-8>
- Liu J, Wang X (2011) Advanced sliding mode control for mechanical systems. In: *Advanced sliding mode control for mechanical systems*. Springer, Berlin. <https://doi.org/10.1007/978-3-642-20907-9>
- Luo X, Zhang Z, Zhao Z, Chen B, Hu L, Wu X (2009) Design of DGPS navigation control system for Dongfanghong X-804 tractor. *Nongye Gongcheng Xuebao/Trans Chin Soc Agric Eng* 25(11). <https://doi.org/10.3969/j.issn.1002-6819.2009.11.025>
- Madec S, Baret F, Solan B, De Thomas S, Dutartre D, Jezequel S, Hemmerlé M, Colombeau G, Comar A (2017) High-throughput phenotyping of plant height: comparing Unmanned Aerial Vehicles and ground LiDAR estimates. *Front Plant Sci* 8. <https://doi.org/10.3389/fpls.2017.02002>
- Malavazi FBP, Guyonneau R, Fasquel JB, Lagrange S, Mercier F (2018) LiDAR-only based navigation algorithm for an autonomous agricultural robot. *Comput Electron Agric* 154:71–79. <https://doi.org/10.1016/j.compag.2018.08.034>
- Miller ND, Haase NJ, Lee J, Kaeppeler SM, Leon N, Spalding EP (2017) A robust, high-throughput method for computing maize ear, cob, and kernel attributes automatically from images. *Plant J* 89(1):169–178. <https://doi.org/10.1111/tpj.13320>
- Montes JM, Technow F, Dhillon BS, Mauch F, Melchinger AE (2011) High-throughput non-destructive biomass determination during early plant development in maize under field conditions. *Field Crops Res* 121(2):268–273. <https://doi.org/10.1016/j.fcr.2010.12.017>
- Mueller-Sim T, Jenkins M, Abel J, Kantor G (2017) The Robotanist: a ground-based agricultural robot for high-throughput crop phenotyping. 2017 IEEE international conference on robotics and automation (ICRA), pp 3634–3639
- Murray SC, Knox L, Hartley B, Méndez-Dorado MA, Richardson G, Thomasson JA, Shi Y, Rajan N, Neely H, Bagavathiannan M (2016) High clearance phenotyping systems for season-long measurement of corn, sorghum and other row crops to complement unmanned aerial vehicle systems. In: *Autonomous air and ground sensing systems for agricultural optimization and phenotyping*, vol 9866, p 986607
- Nagasaka Y, Saito H, Tamaki K, Seki M, Kobayashi K, Taniwaki K (2009) An autonomous rice transplanter guided by global positioning system and inertial measurement unit. *J Field Robot* 26(6–7):537–548
- Nakarmi AD, Tang L (2012) Automatic inter-plant spacing sensing at early growth stages using a 3D vision sensor. *Comput Electron Agric* 82:23–31
- Nakarmi AD, Tang L (2014) Within-row spacing sensing of maize plants using 3D computer vision. *Biosys Eng* 125:54–64
- Nellithimaru AK, Kantor GA (2019) ROLS: Robust Object-level SLAM for grape counting. In: *Proceedings of the IEEE conference on computer vision and pattern recognition workshops*, 0
- Olalla C, Leyva R, El Aroudi A, Queinnec I (2009) Robust LQR control for PWM converters: an LMI approach. *IEEE Trans Industr Electron* 56(7):2548–2558
- Pandey P, Ge Y, Stoerger V, Schnable JC (2017) High throughput in vivo analysis of plant leaf chemical properties using hyperspectral imaging. *Front Plant Sci* 8:1348. <https://doi.org/10.3389/fpls.2017.01348>

- Pérez-Ruiz M, Prior A, Martínez-Guanter J, Apolo-Apolo OE, Andrade-Sanchez P, Egea G (2020) Development and evaluation of a self-propelled electric platform for high-throughput field phenotyping in wheat breeding trials. *Comput Electron Agric* 169:105237
- Peshlov B, Nakarmi A, Baldwin S, Essner S, French J (2017) Scaling up high throughput field phenotyping of corn and soy research plots using ground rovers. In: *Autonomous air and ground sensing systems for agricultural optimization and phenotyping II*, vol 10218, pp 1021802
- Pincioli C, Trianni V, O'Grady R, Pini G, Brutschy A, Brambilla M, Mathews N, Ferrante E, Di Caro G, Ducatelle F, Birattari M, Gambardella LM, Dorigo M (2012) ARGoS: a modular, parallel, multi-engine simulator for multi-robot systems. *Swarm Intell* 6(4):271–295. <https://doi.org/10.1007/s11721-012-0072-5>
- Pothen ZS, Nuske S (2016) Texture-based fruit detection via images using the smooth patterns on the fruit. 2016 IEEE international conference on robotics and automation (ICRA), pp 5171–5176
- Rains GC, Faircloth AG, Thai C, Raper RL (2014) Evaluation of a simple pure pursuit path-following algorithm for an autonomous, articulated-steer vehicle. *Appl Eng Agric*, 30(3):367–374. <https://doi.org/10.13031/aea.30.10347>
- Ray DK, Mueller ND, West PC, Foley JA (2013) Yield trends are insufficient to double global crop production by 2050. *PLoS ONE* 8(6):e66428
- Rohmer E, Singh SPN, Freese M (2013) V-REP: a versatile and scalable robot simulation framework. In: *IEEE international conference on intelligent robots and systems*, pp 1321–1326. <https://doi.org/10.1109/IROS.2013.6696520>
- Rösman C, Hoffmann F, Bertram T (2017) Integrated online trajectory planning and optimization in distinctive topologies. *Robot Auton Syst* 88:142–153. <https://doi.org/10.1016/j.robot.2016.11.007>
- Ruckelshausen A, Biber P, Dorna M, Gremmes H, Klose R, Linz A, Rahe F, Resch R, Thiel M, Trautz D et al (2009) BoniRob—an autonomous field robot platform for individual plant phenotyping. *Precision Agric* 9(841):1
- Shafiekhani A, Kadam S, Fritschi FB, DeSouza GN (2017) Vinobot and vinoculer: two robotic platforms for high-throughput field phenotyping. *Sensors* 17(1):214
- Shi Y, Thomasson JA, Murray SC, Pugh NA, Rooney WL, Shafian S, Rajan N, Rouze G, Morgan CLS, Neely HL et al (2016) Unmanned aerial vehicles for high-throughput phenotyping and agronomic research. *PLoS ONE* 11(7):e0159781
- Shrestha DS, Steward BL (2003) Automatic corn plant population measurement using machine vision. *Trans ASAE* 46(2):559–565
- Shrestha DS, Steward BL (2005) Shape and size analysis of corn plant canopies for plant population and spacing sensing. *Appl Eng Agric* 21(2):295–303
- Shrestha DS, Steward BL, Birrell SJ (2004) Video processing for early stage maize plant detection. *Biosys Eng* 89(2):119–129
- Slaughter DC, Giles DK, Downey D (2008) Autonomous robotic weed control systems: a review. *Comput Electron Agric* 61(1):63–78. <https://doi.org/10.1016/j.compag.2007.05.008>
- Struthers R, Ivanova A, Tits L, Swennen R, Coppin P (2015) Thermal infrared imaging of the temporal variability in stomatal conductance for fruit trees. *Int J Appl Earth Obs Geoinf* 39:9–17. <https://doi.org/10.1016/j.jag.2015.02.006>
- Sun J, Shi S, Gong W, Yang J, Du L, Song S, Chen B, Zhang Z (2017) Evaluation of hyperspectral LiDAR for monitoring rice leaf nitrogen by comparison with multispectral LiDAR and passive spectrometer. *Sci Rep* 7(1):1–9. <https://doi.org/10.1038/srep40362>
- Tang L, Tian L (2008a) Plant identification in mosaicked crop row images for automatic emerged corn plant spacing measurement. *Trans ASABE* 51(6):2181–2191
- Tang L, Tian L (2008b) Real-time crop row image reconstruction for automatic emerged corn plant spacing measurement. *Trans ASABE* 51(3):1079–1087
- Tattaris M, Reynolds MP, Chapman SC (2016) A direct comparison of remote sensing approaches for high-throughput phenotyping in plant breeding. *Front Plant Sci* 7:1131. <https://doi.org/10.3389/fpls.2016.01131>

- Tilman D, Balzer C, Hill J, Befort BL (2011) Global food demand and the sustainable intensification of agriculture. *Proc Natl Acad Sci* 108(50):20260–20264
- Tu X, Gai J, Tang L (2019) Robust navigation control of a 4WD/4WS agricultural robotic vehicle. *Comput Electron Agric* 164. <https://doi.org/10.1016/j.compag.2019.104892>
- Underwood JP, Wendel A, Schofield B, McMurray L, Kimber R (2017) Efficient in-field plant phenomics for row-crops with an autonomous ground vehicle. *J Field Robot* 34(6):1061–1083
- Ustumo T, Berge TW, Gravdahl JT (2015) Non-linear model predictive control for constrained robot navigation in row crops. 2015 IEEE international conference on industrial technology (ICIT), 2015-June(June), pp 357–362. <https://doi.org/10.1109/ICIT.2015.7125124>
- Vermerris W, Saballos A, Ejeta G, Mosier NS, Ladisch MR, Carpita NC (2007) Molecular breeding to enhance ethanol production from corn and sorghum stover. *Crop Sci* 47(Supplement\_3): S-142–S-153. <https://doi.org/10.2135/cropsci2007.04.0013IPBS>
- Virlet N, Sabermanesh K, Sadeghi-Tehran P, Hawkesford MJ (2017) Field Scanalyzer: an automated robotic field phenotyping platform for detailed crop monitoring. *Funct Plant Biol* 44(1):143–153
- Wang Q, Nuske S, Bergerman M, Singh S (2013) Automated crop yield estimation for apple orchards. *Exp Robot* 745–758.
- Wang X, Singh D, Marla S, Morris G, Poland J (2018) Field-based high-throughput phenotyping of plant height in sorghum using different sensing technologies. *Plant Methods* 14(1):53. <https://doi.org/10.1186/s13007-018-0324-5>
- Watanabe K, Guo W, Arai K, Takanashi H, Kajiya-Kanegae H, Kobayashi M, Yano K, Tokunaga T, Fujiwara T, Tsutsumi N et al (2017) High-throughput phenotyping of sorghum plant height using an unmanned aerial vehicle and its application to genomic prediction modeling. *Front Plant Sci* 8:421
- Winterhalter W, Fleckenstein FV, Dornhege C, Burgard W (2018) Crop row detection on tiny plants with the pattern hough transform. *IEEE Robot Autom Lett* 3(4):3394–3401. <https://doi.org/10.1109/LRA.2018.2852841>
- Xiang L, Tang L, Gai J, Wang L (2020) PhenoStereo: a high-throughput stereo vision system for field-based plant phenotyping-with an application in sorghum stem diameter estimation. In: 2020 ASABE annual international virtual meeting, vol 1
- Xue J, Zhang L, Grift TE (2012) Variable field-of-view machine vision based row guidance of an agricultural robot. *Comput Electron Agric* 84:85–91. <https://doi.org/10.1016/j.compag.2012.02.009>
- Yang S, Mei S, Zhang Y (2018) Detection of maize navigation centerline based on machine vision. *IFAC-PapersOnLine* 51(17):570–575
- Young SN, Kayacan E, Peschel JM (2019) Design and field evaluation of a ground robot for high-throughput phenotyping of energy sorghum. *Precision Agric* 20:697–722. <https://doi.org/10.1007/s11119-018-9601-6>
- Zhang W, Gai J, Zhang Z, Tang L, Liao Q, Ding Y (2019) Double-DQN based path smoothing and tracking control method for robotic vehicle navigation. *Comput Electron Agric* 166. <https://doi.org/10.1016/j.compag.2019.104985>
- Zhang X, Huang C, Wu D, Qiao F, Li W, Duan L, Wang K, Xiao Y, Chen G, Liu Q, Xiong L, Yang W, Yan J (2017) High-throughput phenotyping and QTL mapping reveals the genetic architecture of maize plant growth. *Plant Physiol* 173(3):1554–1564
- Zhang Z, Kayacan E, Thompson B, Chowdhary G (2020) High precision control and deep learning-based corn stand counting algorithms for agricultural robot. *Auton Robots* 1–14

# Chapter 3

## Cable Suspended Large-Scale Field Phenotyping Facility for High-Throughput Phenotyping Research



Geng (Frank) Bai and Yufeng Ge

**Abstract** Field-based high-throughput phenotyping (HTP) research has evolved rapidly in recent years. Various HTP platforms are developed with the aim of improving the phenotyping efficiency for plant breeding. To the best of our knowledge, field HTP systems, which have been widely integrated into breeding research, have not been reported yet. In this chapter, we started explaining why researchers are doing this research and briefly introduced the state of arts of the development of different types of field HTP systems. A general comparison between large-scale ground systems, ground vehicles, and aerial platforms was also carried out based on their pros and cons. Then, we introduced a cable suspended large-scale HTP facility at the University of Nebraska-Lincoln, which has been used as a core research facility to explore different research frontiers in field HTP research. The integration of the hardware and software, the information of onboard instruments, and its unique features were described. We also showed several innovative datasets captured by the system at high spatial and temporal resolutions. Phenotypic parameters at canopy and leaf levels can be retrieved from these datasets, which would deepen our understanding of the interactions between genetics, phenomics, and the growing environment. At last, we end this chapter with a concise summary and truly believe that all relevant research progress in this field will incubate new generations of field HTP systems, which could dramatically increase the efficiency of field phenotyping for plant breeding at an unprecedented scale.

**Keywords** Field phenotyping · NU-Spidercam · Leaf level · Spatial-temporal resolution · RGB · Multispectral · LiDAR · 3D reconstruction · Multi-angle imaging · Hyperspectral imaging

---

G. Bai (✉) · Y. Ge

Department of Biological Systems Engineering, University of Nebraska-Lincoln, Nebraska, Lincoln, USA

e-mail: [gbai2@unl.edu](mailto:gbai2@unl.edu)

Y. Ge

e-mail: [yge2@unl.edu](mailto:yge2@unl.edu)

© Springer Nature Switzerland AG 2021

J. Zhou et al. (eds.), *High-Throughput Crop Phenotyping*,

Concepts and Strategies in Plant Sciences,

[https://doi.org/10.1007/978-3-030-73734-4\\_3](https://doi.org/10.1007/978-3-030-73734-4_3)



### 3.1 Introduction

Undoubtedly, improving crop yield and quality through plant breeding plays a significant role in feeding the increasing global population with declining resources, vulnerable environment, and changing climate (FAO 2018). High throughput plant phenotyping, as an emerging research field, has developed rapidly with the aim of relieving the efficiency bottleneck of conventional phenotyping work in plant breeding (Pieruschka and Schurr 2019). Numerous phenotypic parameters can be quantitated by new phenotyping systems using modern sensor technologies in the lab, greenhouse, and field environments.

Field phenotyping is a vital component to select the best breeding lines, and it is conventionally done by breeders using portable tools while trying out different phenotyping systems developed by collaborators. The traditional phenotyping work is labor-intensive, and results can be subjective due to the systematic bias introduced by human observers (Bai et al. 2018). Furthermore, the throughput of the traditional phenotyping methods has become the rate-limiting factor of the entire plant breeding cycle with the development of the high-throughput genotyping tools (Furbank and Tester 2011). Modern sensor packages with data processing algorithms have been developed to estimate phenotypic parameters, including plant growth rate, height, flowering, and maturity date, lodging, tolerance to abiotic and biotic stresses (Li et al. 2014; Zhang and Zhang 2018). Figure 3.1 illustrates the undergoing transition of Field Plant Phenotyping (FPP) from traditional manual phenotyping to fully automated systems.

Field HTP systems can measure different phenotypic parameters at the canopy level. For example, the dynamics of the vegetation coverage, average height, color distribution, and vegetation indices can be measured on a daily or weekly basis. Although plant scientists use plot-averaged parameters to screen breeding lines, more detailed information could be retrieved if the HTP systems can carry out the leaf-level measurement. However, it is still challenging to accurately measure

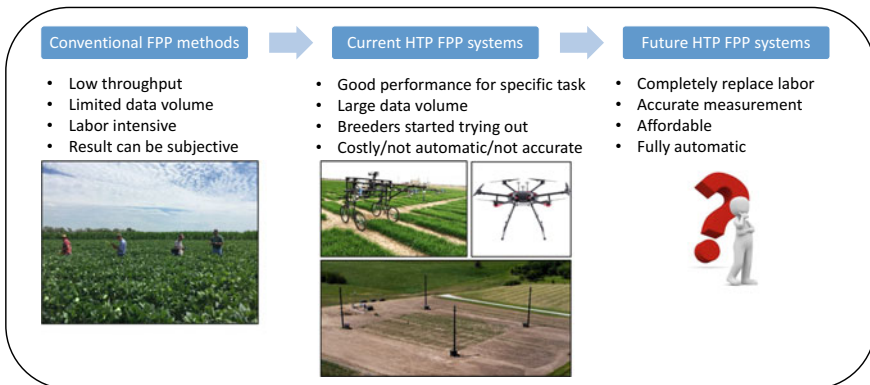


**Fig. 3.1** The transition from conventional field plant phenotyping to future systems

phenotypic parameters at the leaf level in the field condition with accuracy and high spatiotemporal resolution. The environmental factors like wind disturbance, changing incoming solar radiation, and repeatable positioning of sensors are the main constraints.

Field HTP systems can be categorized into ground-based large-scale facilities and mobile platforms. Table 3.1 lists the pros and cons of large-scale ground systems, ground vehicles, and aerial platforms. The most common field HTP systems include movable ground and aerial systems. On one hand, ground vehicles usually have a superior payload capacity for onboard instrumentation and power supplies, comparing to the aerial platforms, ranging from low-cost manually pushed carts to specifically designed fully automated field robots (Andrade-Sanchez et al. 2013; Wendel and Underwood 2016). On the other hand, aerial platforms have the highest phenotyping throughput and full-season field accessibility (Li et al. 2019; Shi et al. 2016). The large-scale ground system could play a vital role in testing different sensor combinations under different working conditions due to its advantages of sensor payload, battery life, positioning accuracy. However, the cost of the large-scale system usually is much higher than that of mobile platforms (Kirchgessner et al. 2017).

A large-scale field HTP system has the capacity to carry out data collection at unprecedented spatiotemporal resolutions with high repeatability without field disturbance. Also, it could be used to test new sensor modules and new data collection protocols by leveraging their superior performance. In the following, we would like to introduce a large-scale field phenotyping system, NU-Spidercam, at the University of Nebraska-Lincoln. An overview of the facility regarding its design and development is first provided, followed by the different datasets at canopy and leaf levels with finer spatial and temporal resolution.

**Table 3.1** Pros and cons of different field HTP systems

Aspects	Large-scale ground system	Ground vehicle	Aerial platform
Payload	Good	Good	Limited
Power supply	Good	Good	Limited
Measurement repeatability	Good	Limited	Limited
Full-season accessibility	Good	Limited	Good
Automation of data collection	Good	Good	Good
Stationary measurement	Good	Limited	Limited
Coverage area	Limited	Good	Good
Affordability	Limited	Good	Good

### 3.2 System Introduction

The main components of the facility include a multi-winch system, a sensing platform, a control station, a subsurface drip irrigation system, and an on-site weather station. A more detailed description of NU-Spidercam could be found in (Bai et al. 2019). The sensing platform could be moved to any location in the 0.4-ha scanning area with a clearance over 9 m. The accurate motion control system enables the fast and precise movement of the platform with a maximum speed of 2 m/s and an estimated accuracy of  $\pm 5$  cm. A maximum of 30 kg of sensor packages could be mounted on a 2D gimbal frame at its lower part with Pan and Tilt flexibility. Figure 3.2 shows the details of the sensing platform and the GUIs (Graphic User Interfaces) of the control software. The onboard instruments include a multispectral camera, a LiDAR, a thermal infrared camera, a spectrometer-fiber system, and a hyperspectral camera. Table 3.2 shows the raw datasets collected using these instruments and their potential applications. Modern sensors have been extensively investigated in plant phenotyping, and new sensing technologies are being constantly applied in this research area (Fahlgren et al. 2015; Li et al. 2014; Paulus 2019). Optic sensors have the advantage for rapid and non-destructive sensing. Besides, cameras with imaging capacity could provide data with high spatial resolution than non-imaging sensors. Spectral reflectance of crops from visual, near-infrared, and thermal infrared wavelengths have been well studied and different phenotypic traits were applied or developed to help breeders monitor the crop performance. With the technology advancing, the hyperspectral camera shows the potential to outperform most of the cameras combined. Also, sensors like Light Detection and Ranging (LiDAR) are widely used for specific phenotypic traits.

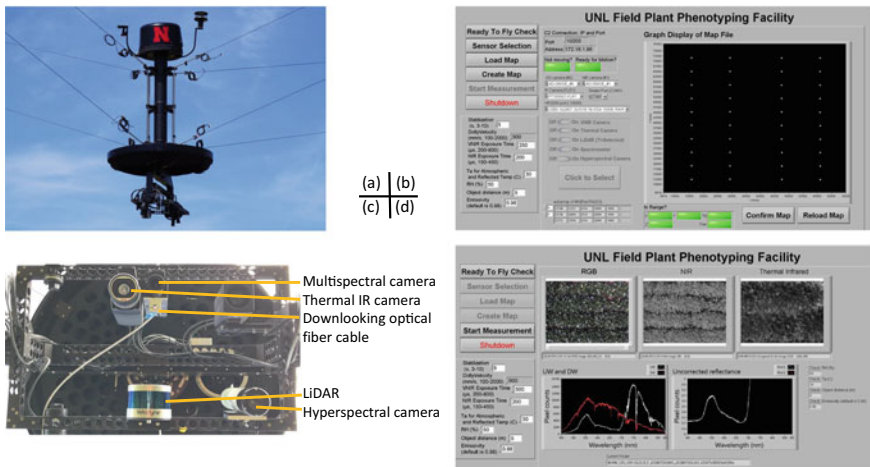


**Fig. 3.2** Hardware and software integration of NU-Spidercam. **a** sensing platform; **b** Interactive GUI of the control software; **c** onboard instrument; **d** GUI for real-time feedback of the control software

**Table 3.2** Onboard sensors of NU-Spidercam and the potential applications

Sensor type	Raw dataset	Parameters/applications
RGB and multispectral camera	Images at Red, Green, Blue, and Near-infrared spectral bands	Vegetation coverage Average canopy NDVI Average soil NDVI Canopy structure parameters
Thermal infrared camera	Temperature matrix	Average canopy temperature Average soil temperature
Spectrometer	Reflectance spectra	Broad-band vegetation indices Narrow-band vegetation indices
LiDAR	3D point cloud	Average canopy height Canopy structure parameters
Hyperspectral camera	Hyperspectral image cube	Reflectance spectra and vegetation indices at the leaf level

### 3.3 Example Results

#### 3.3.1 Data Delivery Pipeline

The data delivery pipeline is an essential part of NU-Spidercam, which enables scientists to carry out further data analysis with no delay. Figure 3.3 illustrates the high-level data delivery pipeline of NU-Spidercam (Bai et al. 2019). Datasets from the onboard cameras, spectrometer, and on-site weather station are processed individually and integrated into a data sheet to be delivered to facility users. A flowchart of the image processing work is shown in Fig. 3(a). The automatic segmentation of the crop from the soil background was realized using the multispectral images. Image registration between multispectral and thermal infrared images enabled the crop segmentation of the thermal infrared image. Then, parameters related to canopy coverage and temperature were extracted. More technical details about the data processing could be found in (Bai et al. 2019).

#### 3.3.2 Estimation of Vegetation Growth at Canopy Level

Numerous studies have been carried out to monitor the dynamics of vegetation growth using different plant phenotyping systems. Generally, ground and aerial vehicles are capable of measuring canopy coverage rate, canopy height, and color-based parameters at high spatial resolution (Bai et al. 2016; Sankaran et al. 2015; Shi et al.

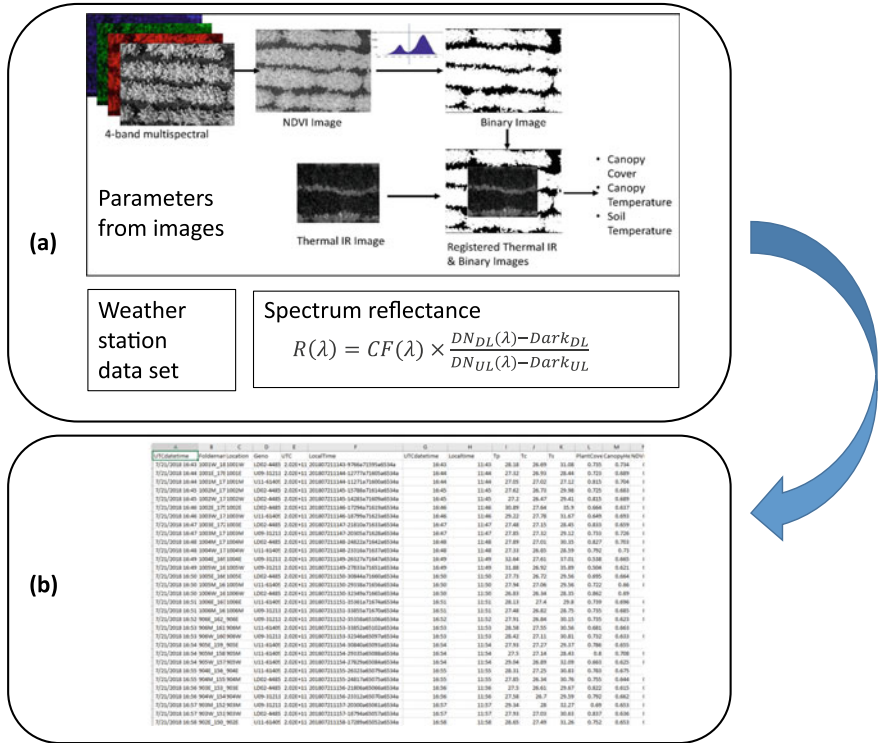


**Fig. 3.3** The high-level flowchart of the data processing of NU-Spidercam, including data collection, processing, and delivery. **a** illustrates there are image, spectral, and weather datasets; **b** shows a snapshot of the dataset delivered to facility users along with the raw dataset

2016; Yang et al. 2017). The onboard sensor package of NU-Spidercam has been used to monitor canopy growth in a similar fashion with a slightly higher temporal resolution.

Figure 3.4 illustrates the result of the dynamics of the green vegetation throughout the growing season from four six-row maize plots with two different maturity days and two planting densities. This preliminary dataset was selected here to show the ability of the imaging and spectral sensors to distinguish different maturity dates and planting densities. The assumption was the sensors could capture the difference of the vegetation growth between planting densities and the difference of senescence between maturity groups at the late growing season. We also expected to differentiate the above-ground biomass, which should be closely related to planting densities. Green Vegetation Pixel Fraction (GVPF) and Normalized Difference Vegetation Index (NDVI) were calculated from the raw images and spectral readings collected by the VNIR camera and the spectrometer on the sensing platform. The image processing protocol introduced in Fig. 3.3a was adopted to segment the green pixels from the background for the calculation of GVPF, while NDVI was also calculated from the

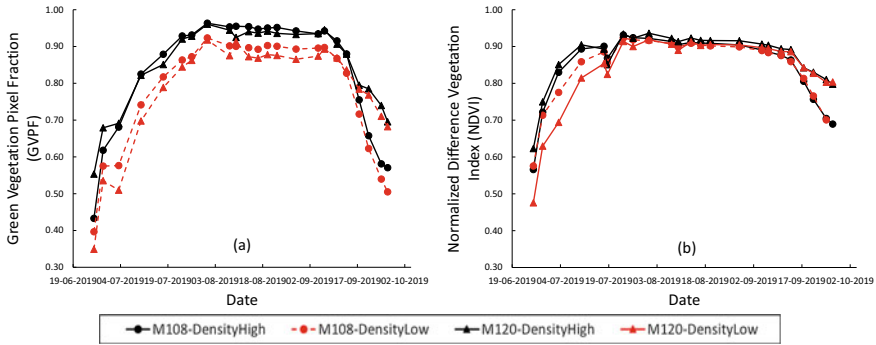


**Fig. 3.4** Green Vegetation Pixel Fraction (GVPF) and Normalized Difference Vegetation Index (NDVI) of four maize plots with two maturity dates (108 and 120 days) and two planting densities (24,000 and 36,000 plants/acre). **a** GVPF difference between different planting densities until the late growing season and GVPF difference between different maturity groups at the late growing season. **b** Similar patterns are observed using NDVI except saturation in the middle of the growing season

equation of spectral reflectance in Fig. 3.3a. The lens of the VNIR camera and the fiber tip of the spectrometer-fiber system were placed near each other for maximum overlap of their Field of Views (FOV).

GVPF was found to have a better performance to differentiate the above-ground biomass and the maturity dates in this experiment (un-published dataset). GVPRs under low planting densities show lower values than that of high planting densities consistently throughout the growing season. NDVI calculated from the spectrometer-fiber system show the potential to indicate the planting densities at the early and the late season. A reason for the better performance of GVPR values can be that the image could cover most of the plot area while the standard fiber optics covers a much smaller area under the same measuring height. The early mature varieties (M108) in this example show earlier senescence than M120 from all figures based on the increasing gap between the GVPRs and NDVIs of two varieties at the late growing season. It should be emphasized that GVPF and NDVI values estimate the above-ground green vegetation biomass rather than the total above-ground biomass.

Figure 3.5 shows the estimation of the above-ground biomass and canopy height by the onboard LiDAR. A ratio was calculated from the LiDAR point count of above-ground vegetation and the total count of the LiDAR points. A similar result was found in Fig. 3.5 compared to Fig. 3.4, except for a less sharp decrease during the plant senescence. The result indicates that LiDAR could detect the difference of the above-ground biomass without excluding the non-green part of the canopy to a certain degree. The varietal difference made a clear contribution to the height difference while planting density did not. Essential information like the height growth rate can be further extracted from the dataset. Thus, these parameters could be used

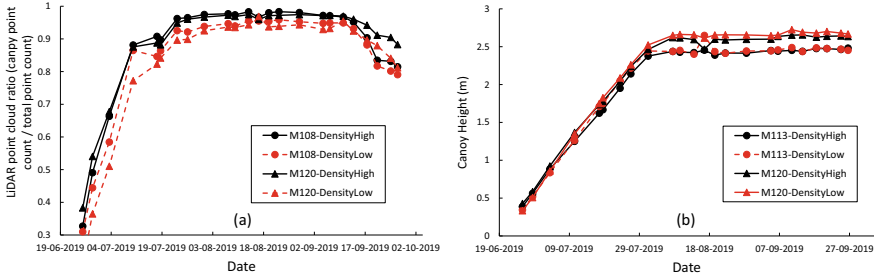


**Fig. 3.5** Relative comparison of above-ground biomass and height measurement by LiDAR for four maize plots with two maturity dates and two planting densities. **a** shows an obvious difference of the above-ground biomass between two planting densities, and also the difference between two maturity rates when plants were entering the end of the reproduction stage. **b** shows a constant difference in canopy height between two maize genotypes after achieving the maximum height

to estimate the above-ground biomass and canopy height across the whole growth season. We believe that these dynamic curves could provide more insight to plant scientists about the crop growth at high temporal resolution.

### 3.3.3 Measurement of Highly Variable Parameters

Some phenotypic parameters are highly influenced by the fluctuating environment, like solar radiation and air temperature, hourly or even shorter time intervals. Among these parameters, canopy temperature has been regarded as an indicator of water stress when combining with environmental parameters (Irmak et al. 2000; Jackson et al. 1981). Canopy temperature is highly influenced by the surrounding micro-climatic condition, especially the air temperature and solar radiation. However, the measurements were usually limited to a single measurement per day (Gonzalez-Dugo et al. 2015). Thus, the ideal way is to measure canopy temperature at a higher spatiotemporal resolution in breeding experiments (Bai et al. 2019).

Figure 3.6 shows an example of measuring temperature-related parameters multiple times in a single afternoon. NU-Spidercam could carry out repeated measurements for each experiment plot by precisely revisiting the same measurement position multiple times during the day. This dataset was collected on an early season soybean plot on a sunny afternoon without clouds. Air temperature and radiation flux density, collected from a dedicated weather station next to the scanning area, were combined with canopy and soil temperature in Fig. 3.6b. The figure shows that canopy temperature is closely related to the air temperature, while soil temperature was closely related to solar radiation. The most substantial difference between canopy and air temperature occurred in the early afternoon around local solar noon. We believe that this kind of data could help researchers to study the interactions among these parameters at an unprecedented resolution.

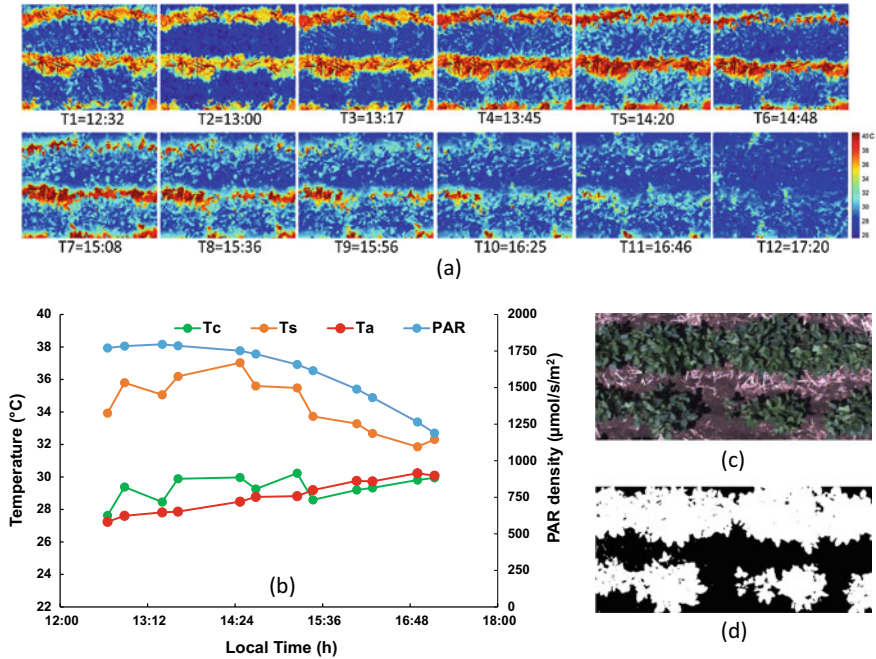


**Fig. 3.6** Measurement of the canopy (Tc) and soil temperature (Ts) for a two-row soybean plot at high temporal resolution with corresponding air temperature (Ta) and Photosynthetically Active Radiation (PAR). **a** illustrates the dynamics of Tc and Ts with local time stamps. **b** combined all measurements to show the close relationships between parameters. **c** provides the RGB images of the target plot with partial canopy coverage, and **d** is a binary image from crop segmentation with crop in white color and bare soil in black color

### 3.3.4 Canopy Structure Parameters Beyond Height

Canopy height information can be accurately retrieved using different sensors on the ground and aerial phenotyping systems (Jimenez-Berni et al. 2018; Madec et al. 2017; Sun et al. 2017; Yuan et al. 2018). However, other canopy structure parameters, like leaf angle, leaf area, and panicle size, could be critical information for accurately estimating primary plant physiological activities and yield. High-density LiDAR scanning and multi-angle imaging are two of the promising technologies to retrieve the canopy structure properties mentioned above. The stable sensing platform of NU-Spidercam with pan-tilt capacity and flexible movement pattern provides an excellent opportunity to explore these measurements.

#### Canopy structure by LiDAR

More parameters related to canopy structure beyond canopy height have been investigated using a high-density point cloud from LiDAR. The parameters include above-ground biomass and leaf area (Su et al. 2019; Walter et al. 2019), size of sorghum



panicles (Malambo et al. 2019), segmentation of plant organs (Jin et al. 2019), and leaf angles (Itakura and Hosoi 2019).

Figure 3.7 shows an example of point clouds generated by the onboard LiDAR when the sensing platform was moving at a constant speed over a maize plot. A denser point cloud was collected comparing with static scans, especially the density along the traveling direction of the sensing platform. Figure 3.7a shows the raw point clouds obtained by the proposed method. Figure 3.7b shows the row centers can be detected by observing the peaks and valleys of the pixel count across multiply rows. Figure 3.7c indicates that a relative comparison of leaf area index or above-ground biomass among different genotypes could be realized by comparing the vertical distribution of the pixel count with considerations of over/under scanning. Figure 3.7d shows a 0.2 m slice of the point cloud along the travel direction of the sensing platform. Leaf-level parameters could be extracted from this raw dataset, including leaf count, leaf angle distribution, etc.

### 3D reconstruction by multi-angle imaging

3D reconstruction technology is one of the promising tools to extract more structure-related parameters quantitatively. A few studies used LiDAR and stereo-vision cameras to estimate the geometric dimension of the top canopy at leaf level under field conditions (Bao et al. 2019; Malambo et al. 2019).

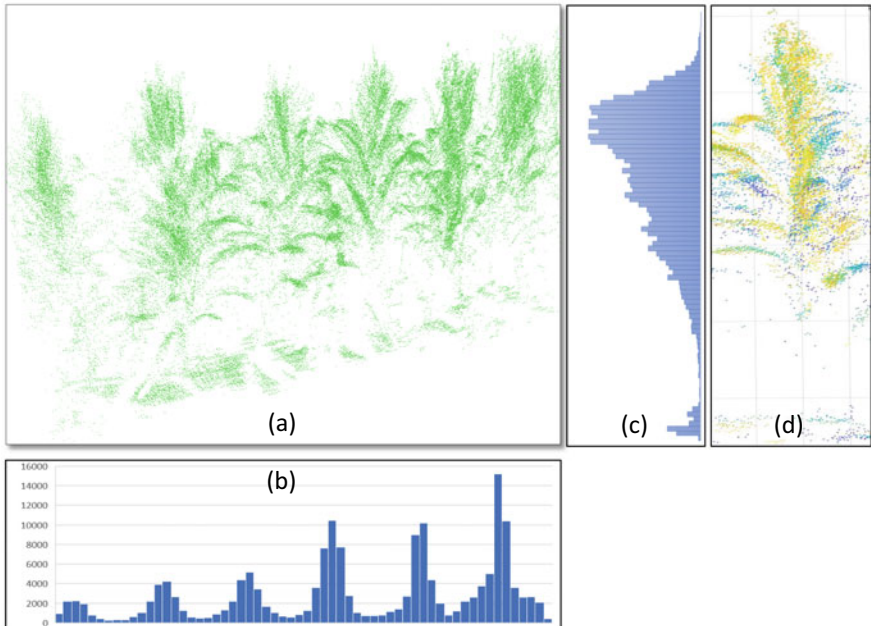


**Fig. 3.7** LiDAR point cloud (a) and its distribution at horizontal (b) and vertical (c) orientations. (d) indicates that more information at the leaf level could be extracted

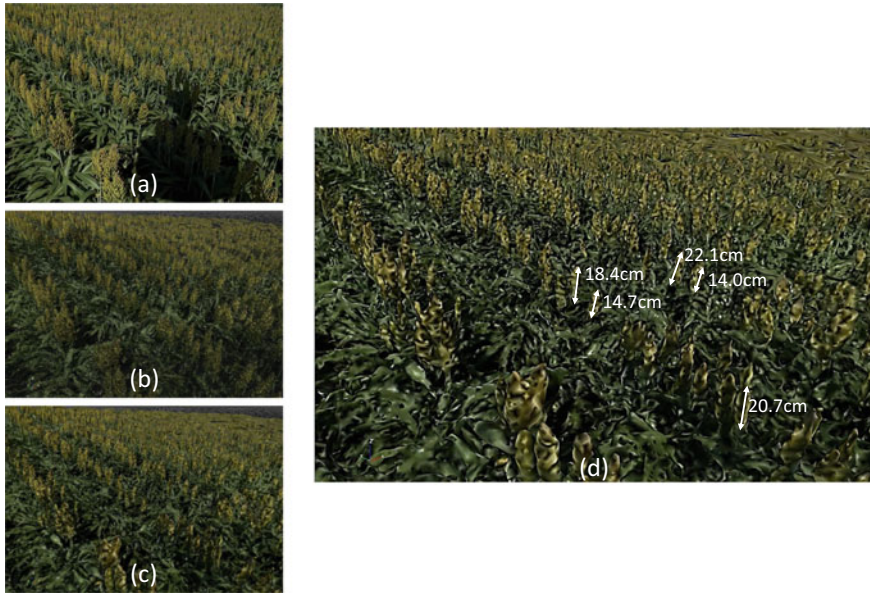


**Fig. 3.8** Length estimation of sorghum panicles by 3D reconstruction technology based on multi-angle RGB imaging (With help of Dr. Abbas Atefi). Figure a–c show an RGB image at one imaging angle, a snapshot of the generated point cloud, and a snapshot of the mesh file based on the point cloud. Figure (d) illustrates the length measurement of five sorghum panicles by this method

Multi-angle images were taken above a sorghum plot by moving NU-Spidercam around the plot, while the onboard RGB camera was always facing the target with a slanted angle. Figure 3.8 shows a preliminary result, which used multi-angle RGB imaging data with 3D reconstruction tools (3DF Zephyr, 3DFlow, Italy) to estimate the panicle length of sorghum plants. No validation data is available for this initial trial, but the estimated length is within the appropriate range (Malambo et al. 2019). More work is needed to improve the quality of the reconstruction result of the sorghum panicles.

### 3.3.5 Hyperspectral Imaging

The hyperspectral imager provides a much higher volume of data by combining the spectral information of the spectrometer and the spatial information of the camera. It has been applied in indoor HTP systems (Fahlgren et al. 2015; Pandey et al. 2017). It has also been widely used in the remote sensing community on different platforms, mostly crewed airplanes and satellites, to collect vegetation reflectance for ecology studies (Wang and Gamon 2019). With the decrease of the camera weight and size, researchers focusing on field plant phenotyping is leveraging the advantages of

hyperspectral imaging in recent years (Campbell et al. 2018; Virlet et al. 2017). Two kinds of hyperspectral cameras have been used for field plant phenotyping, namely, mirror-scanning and push-broom. The mirror-scanning camera can be massive and heavy, comparing to the already pricy push-broom type. The platform can be static when using the mirror-scanning camera to capture 2D hyperspectral image because the motion of the internal mirror replaces the movement of the platform itself. Only one line of the target is scanned by the push-broom camera at once. Thus, the constant moving of the platform across the target is necessary to form a 2D image when using a push-broom camera. The latest publication shows that parameters related to plant physiological activities could be estimated from the full reflectance spectrum at leaf level in the field condition (Fu et al. 2020).

Hyperspectral images of two maize plots were acquired using a push-broom hyperspectral camera while moving the sensing platform of NU-Spidercam at a constant speed along the crop row. White reference was collected before the measurement by setting up the reference panel in the one-acre field. Figure 3.9 shows an example image with the full spectrum of the different components in the image. The sunlit and shadowed leaves show a significant difference in the reflectance percentage, while the tassel has a distinctive spectrum pattern. Thus, these images could provide much more information than multispectral images at the leaf level. There are a few challenges of using hyperspectral cameras in the field condition close to the canopy. The moving speed of the sensing platform for this preliminary study was set to 0.1 m/s or even slower to avoid stretched images. A proper reflectance calibration is also quite challenging for cloudy days due to the constant fluctuation of solar radiation. In addition, crop movement by wind could lead to distortion of the image.

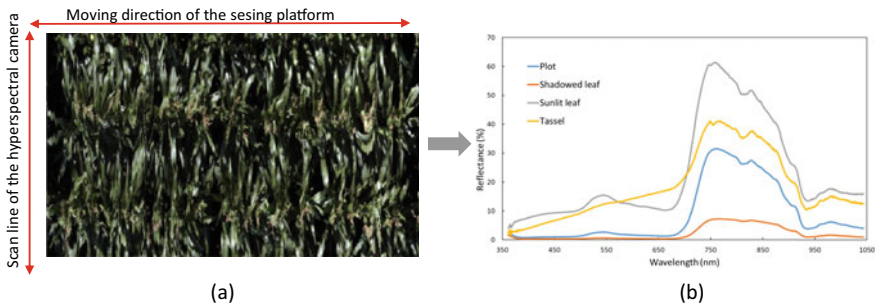


**Fig. 3.9** Example images and spectrum characteristics of vegetation and tassels of a 2-row maize plot. Figure (a) shows the RGB image of the two-row maize plot extracted from the hyperspectral data cube. Figure (b) illustrates the full spectrum of the whole plot (Plot), shaded leaf, sunlit leaf, and tassel

### 3.4 Summary and Future Scenarios

In this section, we started with a systematic comparison of field HTP systems, followed by an introduction of a cable suspended large-scale HTP facility at the University of Nebraska-Lincoln (NU-Spidercam). The focus was on showing the new datasets collected at canopy and leaf levels at high spatial and temporal resolution. A large number of phenotypic parameters could be retrieved from these datasets for a deeper understanding of the interactions between genetics, phenomics, and growing environments.

Large-scale field phenotyping facilities, like NU-Spidercam, have been utilized as core research facilities to develop different data collection pipelines due to its unique advantages. We expect that fully automated systems will be designed to replace most of the conventional phenotyping work in the near future with the continuous advancement of the instrumentation and data analysis capacity. Advanced sensors with different data processing methods need to be continuously developed to equip the sensing platforms to meet this anticipation. Reliable field systems, which can deliver high-quality data hourly and at leaf-level resolution with an affordable cost, will be the milestone to realize the fast adoption of field HTP technology by the breeding community.

### References

- Andrade-Sanchez P, Gore MA, Heun JT, Thorp KR, Carmo-Silva AE, French AN, White JW (2013) Development and evaluation of a field-based high-throughput phenotyping platform. *Funct Plant Biol* 41(1):68–79. <https://doi.org/10.1071/FP13126>
- Bai G, Ge Y, Hussain W, Baenziger PS, Graef G (2016) A multi-sensor system for high throughput field phenotyping in soybean and wheat breeding. *Comput Electron Agric* 128:181–192. <https://doi.org/10.1016/j.compag.2016.08.021>
- Bai G, Ge Y, Scoby D, Leavitt B, Stoerger V, Kirchgessner N, Awada T (2019) NU-Spidercam: A large-scale, cable-driven, integrated sensing and robotic system for advanced phenotyping, remote sensing, and agronomic research. *Comput Electron Agric* 160:71–81. <https://doi.org/10.1016/j.compag.2019.03.009>
- Bai G, Jenkins S, Yuan W, Graef GL, Ge Y (2018) Field-Based Scoring of Soybean Iron Deficiency Chlorosis Using RGB Imaging and Statistical Learning. *Front Plant Sci* 9:1002–1002. <https://doi.org/10.3389/fpls.2018.01002>
- Bao Y, Tang L, Breitzman MW, Salas Fernandez MG, Schnable PS (2019) Field-based robotic phenotyping of sorghum plant architecture using stereo vision. *J Field Robotics* 36(2):397–415. <https://doi.org/10.1002/rob.21830>
- Campbell ZC, Acosta-Gamboa LM, Nepal N, Lorence A (2018) Engineering plants for tomorrow: how high-throughput phenotyping is contributing to the development of better crops. *Phytochem Rev* 17(6):1329–1343. <https://doi.org/10.1007/s11101-018-9585-x>
- Fahlgren N, Gehan MA, Baxter I (2015) Lights, camera, action: high-throughput plant phenotyping is ready for a close-up. *Curr Opin Plant Biol* 24:93–99. <https://doi.org/10.1016/j.pbi.2015.02.006>
- FAO (2018) Transforming food and agriculture to achieve the SDGs. Retrieved from Rome

- Fu P, Meacham-Hensold K, Guan K, Wu J, Bernacchi C (2020) Estimating photosynthetic traits from reflectance spectra: A synthesis of spectral indices, numerical inversion, and partial least square regression. *Plant Cell Environ*. <https://doi.org/10.1111/pce.13718>
- Furbank RT, Tester M (2011) Phenomics—technologies to relieve the phenotyping bottleneck. *Trends Plant Sci* 16(12):635–644. <https://doi.org/10.1016/j.tplants.2011.09.005>
- Gonzalez-Dugo V, Hernandez P, Solis I, Zarco-Tejada P (2015) Using high-resolution hyperspectral and thermal airborne imagery to assess physiological condition in the context of wheat phenotyping. 7(10), 13586. Retrieved from <http://www.mdpi.com/2072-4292/7/10/13586>
- Irmak S, Haman DZ, Bastug R (2000) Determination of crop water stress index for irrigation timing and yield estimation of corn. *Agron J* 92(6):1221–1227. <https://doi.org/10.2134/agronj2000.9261221x>
- Itakura K, Hosoi F (2019) Estimation of leaf inclination angle in three-dimensional plant images obtained from lidar. *Remote Sens* 11(3):344. <https://www.mdpi.com/2072-4292/11/3/344>
- Jackson RD, Idso SB, Reginato RJ, Pinter PJ Jr (1981) Canopy temperature as a crop water stress indicator. 17(4):1133–1138. <https://doi.org/10.1029/WR017i004p01133>
- Jimenez-Berni JA, Deery DM, Rozas-Larraondo P, Condon ATG, Rebetzke GJ, James RA, Sirault XRR (2018) High throughput determination of plant height, ground cover, and above-ground biomass in wheat with LiDAR. *Front Plant Sci* 9:237. <https://doi.org/10.3389/fpls.2018.00237>
- Jin S, Su Y, Wu F, Pang S, Gao S, Hu T, Guo Q (2019) Stem-leaf segmentation and phenotypic trait extraction of individual maize using terrestrial LiDAR data. *IEEE Trans Geosci Remote Sens* 57(3):1336–1346. <https://doi.org/10.1109/TGRS.2018.2866056>
- Kirchgeßner N, Liebisch F, Yu K, Pfeifer J, Friedli M, Hund A, Walter A (2017) The ETH field phenotyping platform FIP: a cable-suspended multi-sensor system. *Funct Plant Biol* 44(1). <https://doi.org/10.1071/fp16165>
- Li J, Veeranampalayam-Sivakumar A-N, Bhatta M, Garst ND, Stoll H, Stephen Baenziger P, Shi Y (2019) Principal variable selection to explain grain yield variation in winter wheat from features extracted from UAV imagery. *Plant Methods* 15(1):123. <https://doi.org/10.1186/s13007-019-0508-7>
- Li L, Zhang Q, Huang D (2014) A review of imaging techniques for plant phenotyping. *Sensors (Basel)* 14(11):20078–20111. <https://doi.org/10.3390/s141120078>
- Madec S, Baret F, de Solan B, Thomas S, Dutartre D, Jezequel S, Comar A (2017) High-throughput phenotyping of plant height: comparing unmanned aerial vehicles and ground LiDAR estimates. *Front Plant Sci* 8:2002. <https://doi.org/10.3389/fpls.2017.02002>
- Malambo L, Popescu SC, Horne DW, Pugh NA, Rooney WL (2019) Automated detection and measurement of individual sorghum panicles using density-based clustering of terrestrial lidar data. *ISPRS J Photogrammetry Remote Sens* 149:1–13. <https://doi.org/10.1016/j.isprsjprs.2018.12.015>
- Pandey P, Ge Y, Stoerger V, Schnable JC (2017) High throughput in vivo analysis of plant leaf chemical properties using hyperspectral imaging. *Front Plant Sci* 8:1348. <https://doi.org/10.3389/fpls.2017.01348>
- Paulus S (2019) Measuring crops in 3D: using geometry for plant phenotyping. *Plant Methods* 15(1):103. <https://doi.org/10.1186/s13007-019-0490-0>
- Pieruschka R, Schurr U (2019) Plant phenotyping: past, present, and future. *Plant Phenomics* 2019:6. <https://doi.org/10.1155/2019/7507131>
- Sankaran S, Khot LR, Espinoza CZ, Jarolmasjed S, Sathuvalli VR, Vandemark GJ, Pavek MJ (2015) Low-altitude, high-resolution aerial imaging systems for row and field crop phenotyping: a review. *Eur J Agron* 70:112–123. <https://doi.org/10.1016/j.eja.2015.07.004>
- Shi Y, Thomasson JA, Murray SC, Pugh NA, Rooney WL, Shafian S, Yang C (2016) Unmanned aerial vehicles for high-throughput phenotyping and agronomic research. *PLoS ONE* 11(7):e0159781–e0159781. <https://doi.org/10.1371/journal.pone.0159781>
- Su Y, Wu F, Ao Z, Jin S, Qin F, Liu B, Guo Q (2019) Evaluating maize phenotype dynamics under drought stress using terrestrial lidar. *Plant Methods* 15(1):11. <https://doi.org/10.1186/s13007-019-0396-x>

- Sun S, Li C, Paterson A (2017) In-field high-throughput phenotyping of cotton plant height using LiDAR. *Remote Sens* 9(4). <https://doi.org/10.3390/rs9040377>
- Virlet N, Sabermanesh K, Sadeghi-Tehran P, Hawkesford MJ (2017) Field scanalyzer: An automated robotic field phenotyping platform for detailed crop monitoring. *Funct Plant Biol* 44(1). <https://doi.org/10.1071/fp16163>
- Walter JDC, Edwards J, McDonald G, Kuchel H (2019) Estimating biomass and canopy height with LiDAR for field crop breeding. *Front Plant Sci* 10(1145). <https://doi.org/10.3389/fpls.2019.01145>
- Wang R, Gamon JA (2019) Remote sensing of terrestrial plant biodiversity. *Remote Sens Environ* 231: <https://doi.org/10.1016/j.rse.2019.111218>
- Wendel A, Underwood J (2016) Self-supervised weed detection in vegetable crops using ground based hyperspectral imaging. In: Paper presented at the 2016 IEEE international conference on robotics and automation (ICRA)
- Yang G, Liu J, Zhao C, Li Z, Huang Y, Yu H, Yang H (2017) Unmanned aerial vehicle remote sensing for field-based crop phenotyping: current status and perspectives. *Front Plant Sci* 8(1111). <https://doi.org/10.3389/fpls.2017.01111>
- Yuan W, Li J, Bhatta M, Shi Y, Baenziger PS, Ge Y (2018) Wheat height estimation using LiDAR in comparison to ultrasonic sensor and UAS. *Sensors (Basel)* 18(11). <https://doi.org/10.3390/s18113731>
- Zhang N, Zhang Y (2018) Imaging technologies for plant high-throughput phenotyping: a review. *Front Agricul Sci Eng* 0(0). <https://doi.org/10.15302/j-fase-2018242>

# Chapter 4

## Structure from Motion and Mosaicking for High-Throughput Field-Scale Phenotyping



Hadi AliAkbarpour, Ke Gao, Rumana Aktar, Steve Suddarth,  
and Kannappan Palaniappan

**Abstract** This work presents a 3D-enabled method to register aerial image sequences. Our approach is based on a novel Bootstrapped Structure-from-Motion (BSfM) followed by analytical homography reprojection or georegistration. BSfM is a fast and robust method to recover the 3D exterior orientation of the camera poses and the scene 3D structure from image sequences. The recovered 3D parameters are used in an analytical approach to estimate homography matrices that project the input images onto the dominant ground plane in the scene to produce a global mosaic of the field and plants. Preliminary experimental results validate the approach and show satisfactory results suitable for scaling up to support high-throughput field phenotyping (HTP) for agricultural crop field experiments.

**Keywords** Structure-from-Motion (SfM) · Video stabilization · Image registration · Orthorectification · Mosaicking

### 4.1 Introduction

Population growth and the increasing demand for food production require improved cultivars adapted for changing environmental conditions and better field manage-

---

H. AliAkbarpour (✉) · S. Suddarth  
Transparent Sky, Edgewood, USA  
e-mail: [hadi@transparentskey.net](mailto:hadi@transparentskey.net); [akbarpour@missouri.edu](mailto:akbarpour@missouri.edu)

S. Suddarth  
e-mail: [director@transparentskey.net](mailto:director@transparentskey.net)

H. AliAkbarpour · K. Gao · R. Aktar · K. Palaniappan  
University of Missouri-Columbia, Columbia, USA  
e-mail: [kegao@mail.missouri.edu](mailto:kegao@mail.missouri.edu)

R. Aktar  
e-mail: [rayy7@mail.missouri.edu](mailto:rayy7@mail.missouri.edu)

K. Palaniappan  
e-mail: [pal@missouri.edu](mailto:pal@missouri.edu)

ment practices at the single plant scale. High-throughput phenotyping (HTP) of whole plants and organs *in vivo* in the field using image analysis and machine learning would enable large-scale data collection at high spatial and temporal resolution to better characterize and select for desirable plant morphology and physiology-related traits as part of crop improvement strategies. Remote sensing with unmanned aerial vehicles (UAVs) provides unprecedented multispectral data and accelerates the progress of precision agriculture applications such as drought stress detection, weed detection, yield prediction, and nutrient status assessment. However, it requires comprehensive image processing to generate measurements (Maes and Steppe 2019). To perform HTP on a large scale, computer vision techniques must advance to take advantage of the data from unmanned vehicles. Holman et al. (2016) developed a high throughput phenotyping method for estimating wheat plant height and growth rate using aerial imagery collected by RGB cameras mounted on UAVs. Measurements were extracted from high resolution 3D models generated using Structure-from-Motion (SfM). Cooper et al. (2017) examined SfM photogrammetry and Terrestrial Laser Scanning (TLS) for measuring grass above ground biomass (AGB) which can be used for analysis of natural grassland systems. Metrics obtained from TLS and 3D point clouds produced by SfM were evaluated against destructive measurements and showed promising performance. Han et al. (2019) evaluated the performance of various machine learning approaches, including support vector machines (SVMs) and random forest, for maize AGB estimation using structural and spectral data provided by UAVs and demonstrated the potential of machine learning methods in this application. To assist in quantifying plant disease, Stewart et al. (2019) trained a Mask R-CNN model for segmentation of UAV imagery to detect northern leaf blight (NLB) disease lesions. Their work showed the efficacy of deep learning on UAV data for high-throughput measurements of plant disease by yielding reasonable detection results with respect to the ground truth. Ampatzidis and Partel (2019) achieved high accuracy for tree detection, geolocalization, categorization, tree health indices analysis, and citrus varieties evaluation by utilizing convolutional neural networks on UAV images. Maimaitijiang et al. (2020) demonstrated that deep neural network (DNN) can be effectively used for crop yield prediction and provided adaptive performance across different soybean genotypes.

Local feature extraction and matching are essential components of many computer vision applications such as video analytics, image retrieval, Structure-from-Motion, and Multi-view Stereo. A basic feature matching pipeline consists of three stages—detecting local feature keypoints from two images, creating descriptors for keypoints, and establishing feature correspondences by matching descriptors from both images. Fortunately, the past few decades have led to tremendous progress in the development of such feature descriptors and matching techniques. SIFT (Lowe 2004) and SURF (Bay et al. 2006) are good-performing hand-crafted floating-point features that are widely used. They provide reliable feature matches despite their relatively high computational cost. To improve computational efficiency and target for real-time applications, several binary feature descriptors were also developed such as BRISK (Leutenegger et al. 2011), ORB (Rublee et al. 2011), and AKAZE (Alcantarilla et al. 2013). However, high speed approaches compromise the matching accu-



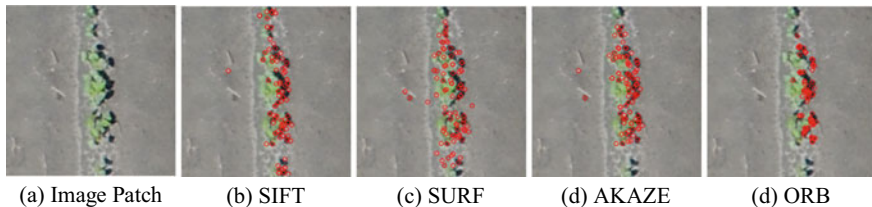


**Fig. 4.1** Feature point detection results for a sample image patch ( $256 \times 256$  pixels) cropped from the first frame ( $4864 \times 3648$  pixels) in the cotton emergence data sequence 3. 100 feature points are detected by each method

racy for binary descriptors, especially in challenging scenarios where large scale or perspective changes exist in the images. Local keypoint detection results by several state-of-the-art hand-crafted features introduced above are visualized in Fig. 4.1. Some frequency-based features like a recent DCT-based in Gao et al. (2020) showed merit in aerial SfM applications. In recent years, many deep learning-based feature matching methods were proposed to improve upon the hand-crafted features (Zagoruyko and Komodakis 2015; Simo-Serra et al. 2015; Balntas et al. 2016; Tian et al. 2017; DeTone et al. 2018; Ono et al. 2018). The advent of convolutional neural networks (CNNs) significantly increases the performance of learned features for applications like matching, image retrieval, object detection, etc. Dusmanu et al. (2019). However, deep learning-based requires a large amount of training data and its performance exhibits high variance across different tasks and datasets (Schönberger et al. 2017). A comprehensive review of different features and their effects on SfM pipelines is presented in our recent work (Gao et al. 2020).

**Problem Statement:** A sequence of  $n$  ordered images (video)  $\mathcal{I} = \{I_i | i = 1 \dots n\}$  is given as input. The images were captured from an airborne camera observing a scene while the UAV is flying over it. For each image frame  $I_i$  we consider a camera geometry corresponding to the pose of the camera at time  $t = i$ . The pose (geometry) of  $i$ th camera (frame/image) is defined by its orientation  $\mathbf{R}_i \in SO(3)$  and its location (position) at  $\mathbf{t}_i \in \mathbb{R}^3$ , jointly denoted as  $\mathbf{C}_i = (\mathbf{R}_i, \mathbf{t}_i)$ . With no prior knowledge of the coordinate systems, we assume the pose of the first camera as our world coordinate system by  $\mathbf{C}_1 = (\mathbf{I}_{3 \times 3}, \mathbf{0}_{3 \times 1})$ , and seek to estimate the pose of the remaining “cameras” (image frames) in the sequence expressed in the world coordinate system. Furthermore, we assume all images were taken by the same physical camera with a constant focal length.

Our proposed method for camera pose recovery is called B-SfM and its pipeline is shown in Fig. 4.2. It starts with choosing two frames at the beginning of an image sequence (video) with a sufficient angular diversity to establish a 3D coordinate system. Given this 3D coordinate system and sparse set of triangulated 3D points, the poses of subsequent frames are estimated using 2D-3D correspondences. A periodical local optimization (local BA) is performed within small window of frames. A robust

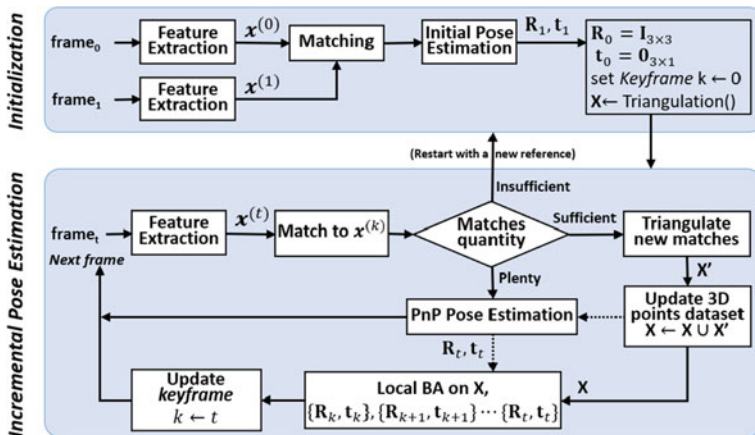


Fig. 4.2 Diagram of the proposed camera pose recovery pipeline. The bootstrapping takes place first to initialize the system (top block), followed by an incremental pose estimation (bottom block)

global optimization (BA) is applied to larger set of frames during the process to enforce a global consistency between the recovered camera poses.

The rest of this article is arranged as follows: Feature extraction and correspondence establishment is discussed in Sect. 4.2. Recovering camera poses is introduced in Sect. 4.3 and our experimental results are presented in Sect. 4.4.

## 4.2 Correspondence Establishment

SfM begins with the establishment of feature correspondences. Assume a set of sequential images (video) as input  $\mathcal{I} = \{I_i | i = 1 \dots n\}$ ,  $n$  being number of frames. On each image a feature extraction method identifies distinguishable image points (features). The features are ideally unique and invariant to image illumination, rotation, and scale. SIFT, SURF, and AKAZE which were introduced earlier are good options for this purpose. Some recent Deep Learning (DL) based feature descriptors have also proved to be good candidates (Dusmanu et al. 2019). Binary features such as ORB (Rublee et al. 2011) can be also used to gain efficiency with the cost of lower robustness. Let  $\mathcal{F}_i$  be the set of features extracted from  $I_i$ . Then the set of all features can be defined as

$$\mathcal{F} = \{\mathcal{F}_i | \mathcal{F}_i \subset [1..height] \times [1 \dots width]\}. \quad (4.1)$$

Feature matching is the next step after extracting the features. A feature matching algorithm receives two set of features corresponding to two input images ( $I_k, I_l$ ) and for each feature in  $I_k$ , it search for the best corresponding feature in  $I_l$  which satisfies

a distance (or similarity) metric. The set of matched features (correspondences) is defined as

$$\mathcal{M} = \{\mathcal{M}_{ij} | \mathcal{M}_{ij} \subset \mathcal{F}_i \times \mathcal{F}_j, i \neq j\}. \quad (4.2)$$

One common practice in the literature is to match every frame within an image dataset to every other frame, however this has computational complexity of  $\mathcal{O}(n^2)$ . Since the image frames in a video are sequentially ordered, one can take advantage of their temporal coherency and drastically reduce the computational cost for feature matching [xx TGRS]. Meaning that features of a frame  $I_i$  is only matched to the features from the next frame in the sequence,  $I_{(i+1)}$ , resulting in a reduced computational complexity of  $\mathcal{O}(n)$ . In other words, Eq. (xx) becomes as

$$\mathcal{M} = \{\mathcal{M}_{i,i+1} | \mathcal{M}_{i,i+1} \subset \mathcal{F}_i \times \mathcal{F}_{i+1}\}. \quad (4.3)$$

Thus the point correspondences can be established as a set of feature tracks (concatenated pairwise matches)  $\mathcal{T} = \{\tau_j | j = 1 \dots m\}$ , where  $m$  is total number of tracks and a track  $\tau_j$  is defined as

$$\tau_j = \{\mathbf{x}_{j,i} | \mathbf{x}_{j,i} \subset \mathcal{F}_i, i = h_j, h_j + 1, \dots, h_j + \gamma_j - 1\}, \quad (4.4)$$

where  $h_j$  and  $\gamma_j$ , respectively, are the indices of the starting view (frame/camera) and the length (or number of elements) in track  $\tau_j$ .  $\mathbf{x}_{j,i}$  represents the 2D pixel coordinates of the feature correspondence in view  $i$  within track  $j$ .

### 4.2.1 Matching Strategies

There are three common strategies to find matches between two image frames once their descriptors are built.

**Nearest Neighbor Matching:** For a keypoint  $\mathbf{p}$  in the reference image, its feature descriptor is compared against all the candidate descriptors in the matching image in terms of  $L_2$  or Hamming distance. The best match for  $\mathbf{p}$  is its nearest neighbor in the matching image. Nearest neighbor is defined as the feature descriptor that produces the smallest matching distance with respect to  $\mathbf{p}$ .

**Distance Ratio Matching:** This method is an effective feature matching strategy between a reference image and a matching image (Lowe 2004). It is widely used by many feature matching approaches including SIFT (Lowe 2004), SURF (Bay et al. 2006), and AKAZE (Alcantarilla et al. 2013). The nearest neighbor of keypoint  $\mathbf{p}$  is first determined using the scheme discussed in the nearest neighbor matching strategy. The matching distance of the nearest neighbor is denoted as  $D_1$ . In addition, the second nearest neighbor is identified in a similar manner and its matching distance is denoted as  $D_2$ . After that, the nearest neighbor distance ratio is computed as follows:

$$\rho = D_1/D_2. \quad (4.5)$$

The nearest neighbor is identified as the match for keypoint  $\mathbf{p}$  if ratio  $\rho$  is smaller than a threshold, *e.g.* 0.8 for SIFT. Distance ratio matching strategy has proven successful for reducing the number of false-positive matches caused by ambiguous or repetitive structures in the image.

**Threshold-based Matching:** Similar to nearest neighbor matching and distance ratio matching, a keypoint  $\mathbf{p}$  in the reference image is compared against all keypoints in the matching image using a distance metric. The best match for  $\mathbf{p}$  is the one whose matching distance is below a pre-defined threshold. Threshold-based matching is adopted by some methods such as one of the pioneering works on deep learning-based features (Zagoruyko and Komodakis 2015). However, one major drawback of threshold-based matching is that the threshold largely depends on the input data and determining an optimal threshold for a particular type of images can be laborious.

### 4.3 Camera Pose Recovery

Knowledge about the geometry of camera pose corresponding to each view (frame) is essential for approaches dealing with 3D information such as multi-view stereo scene (MVS) 3D reconstruction, navigation, tracking, and 3D-enabled registration. In airborne imaging systems the pose of the aircraft and sometimes the pose of the camera are measured via onboard sensors (INS). These measurements are known as *metadata* which include the position (by GPS) and orientation (by IMU), together known as *3D pose*. Although the metadata are recorded in UAVs, in majority of low-end UAVs the precision of the 3D poses are far below to be directly used in downstream processes (*e.g.*, in registration). In the absence of high-quality camera pose information in aerial imagery, a common approach is to use a Structure-from-Motion (SfM) method which tries to estimate the pose of each view in the collection along with estimating a set of sparse 3D points from the scene. Although, the classical SfM is a well studied problem in computer vision literature, it is still considered a hard problem and is actively investigated. Some challenges in SfM in plant aerial imagery include the large image size, high number of views (long sequence of videos) and difficulty in identifying unique features in the images (due to homogeneous underlying textures in the scene). Despite these challenges, there are a few advanced commercial GIS software products that perform well recovering the camera poses from aerial imagery, however, they lack robustness and speed.

**Camera Model:** We use a pinhole camera model in which the homogeneous 2D point  $\mathbf{x} = [x \ y \ 1]^T$  represents the image of a homogeneous 3D point  $\mathbf{X} = [X \ Y \ Z \ 1]^T$  on the 2D camera focal plane and obtained by

$$\mathbf{x} = \mathbf{K} [\mathbf{R}|\mathbf{t}]\mathbf{X}, \quad (4.6)$$

where  $\mathbf{R}_{3 \times 3}$  and  $\mathbf{t}_{3 \times 1}$  are the rotation matrix and translation vector from the world coordinate system to the camera one, respectively.  $\mathbf{K}_{3 \times 3}$  in (4.6) defines the camera calibration (intrinsic) matrix

$$\mathbf{K} = \begin{bmatrix} f & 0 & u \\ 0 & f & v \\ 0 & 0 & 1 \end{bmatrix}, \quad (4.7)$$

$f$  being the camera focal length in pixels and  $(u, v)$  is the principal point.

### 4.3.1 Bootstrapping

In the B-SfM initialization, the goal is to estimate the 2th camera pose  $\mathbf{C}_2$  using first two images  $I_1$  and  $I_2$ . In case of a calibrated camera, the geometric relation between two images  $I_1$  and  $I_2$  can be expressed by the *essential matrix*  $\mathbf{E}$  defined as

$$\mathbf{E} = \mathbf{t}_2 \times \mathbf{R}_2 \quad (4.8)$$

and it can be estimated by having a set of feature correspondences between the two views. Having  $\mathbf{E}$  one can directly extract rotation matrix  $\mathbf{R}_2$  and translation vector  $\mathbf{t}_2$  (up to a scale factor). The essential matrix enforces the relation between the corresponding image points  $\mathbf{x}_{j,1}$  and  $\mathbf{x}_{j,2}$  in  $I_1$  and  $I_2$  as

$$\tilde{\mathbf{x}}_{j,2} \mathbf{E} \tilde{\mathbf{x}}_{j,1} = 0. \quad (4.9)$$

The geometric implication of (4.9) is that the feature point  $\mathbf{x}_{j,2}$  lies on a line (known as *epipolar line*) corresponding to its pair  $x_{j,1}$  determined by the epipolar constraint (4.9). Note that  $\tilde{\mathbf{x}}$  represents the normalized image coordinates of  $\mathbf{x}$ , defined as  $\tilde{\mathbf{x}} = [u, v]^T$ , which can be obtained by multiplying the inverse of the intrinsic matrix  $\mathbf{K}$  by the feature coordinates. Nister in Nistér (2004) proposed a method called 5-point algorithm which requires just five-point correspondences (minimal solution) between the two images to estimate the essential matrix  $\mathbf{E}$ . There exist other methods such as the 8-point method proposed by Longuet-Higgins Longuet-Higgins (1981); Hartley (1997) that requires minimum of eight noncoplanar point correspondences between the views to estimate a relative of the essential matrix known as *fundamental matrix*. Unlike the 5-point algorithm, the 8-point algorithm does not require camera calibration. In the case of plant field multi-view analysis, using the 5-point algorithm is preferred over the 8-point one as it relaxes the requirement of having the points to be noncoplanar. Once the essential matrix between the two views is estimated, the rotation and translation components can be extracted by decomposing it as described in Nistér (2004). Doing so provides four solutions (combinations) of  $\mathbf{R}_2$  and  $\mathbf{t}_2$  among which just one is a valid solution. The correct solution can be determined by triangulating the point correspondences using all four geometrically possible

solutions and identifying the configuration that provides a physically valid (feasible) solution by counting the number of the triangulated 3D points which fall into the front of both cameras.

### 4.3.2 Robust Pose Recovery

After performing the Bootstrapping, the first two camera coordinates in the sequence are estimated in an arbitrary reference. Having the matches between the two views,  $\mathcal{M}_{1,2}$ , one can estimate their corresponding 3D points using triangulation. Ideally, all matched 2D points  $\mathbf{x}_{j,1}$  and  $\mathbf{x}_{j,2}$  define the image coordinates of an identical 3D point  $\mathbf{X}_j$  in the scene. In other words, if the 3D coordinates of a point like  $\mathbf{X}_j$  is known, then all its corresponding 2D image points could be computed by projecting  $\mathbf{X}_j$  onto the  $i$ th and  $j$ th views using (4.6). In real scenarios, the coordinates of 3D point  $\mathbf{X}_j$  are not available, however, one can estimate it by casting ray passing through the camera center and the image point in each camera. In a perfect model (no noise), the two rays cast must intersect at an identical point in 3D which would be equivalent to  $\mathbf{X}$ . However, in real scenarios this is not the case and therefore an optimal solution for  $\mathbf{X}$  must be estimated. Such a method is known as *triangulation* and there are several methods in the literature to perform it, among which we use the Direct Linear Transformation (DLT) (Hartley et al. 2013). The output of the triangulation stage is a set of sparse 3D point cloud which all are expressed in the coordinate system of the first camera. For a next image frame  $I_i$  in the sequence, the goal is to estimate the coordinate system of the camera pose corresponding to the  $i$ th view. There are generally two methods for doing so. One is to keep doing the bootstrapping on every adjacent view in the scene and then concatenate their estimated rotation and translation vectors to express them in the coordinate of the first camera. A problem that has to be solved in this method is to identify the relative scale factors between the translation vectors estimated between each two pair. This technique is called *pairwise incremental camera pose estimation*. Although there are several methods which use this technique (Schönberger et al. 2016; Mur-Artal et al. 2015), however, for the case of recovering camera poses in a continuous set of frames, it is more robust if a *Perspective-n-Point (PnP)* method (Moreno-Noguer et al. 2007) is used to estimate the subsequent cameras after the bootstrapping. Based on an existing 3D model obtained from triangulation of the feature matches between the first two views, a sequential camera pose estimation can be done by incrementally registers new cameras from 2D-3D correspondences. Using PnP will reduce the unnecessary computational complexity of essential matrix estimation as it requires only four correspondences between the image features of the current frame and the know (previously estimated) 3D points (Gao et al. 2003).

### 4.3.3 Optimization by Bundle Adjustment

As mentioned earlier, the 3D points associated with the tracks (for each  $\tau_j$  there is a 3D point  $X_j$  assigned to it) are all estimations from the observations (feature points) using the geometry of involving cameras (views). The camera poses used to cast the rays and estimate the 3D points in the triangulation process are often highly imprecise, however, there is a common optimization method called Bundle Adjustment (BA) to improve the estimation. BA refers to the problem of jointly refining the estimated camera poses and 3D points in an optimal manner using reprojection error as the quality metric. Given a set of  $n$  cameras with initial poses (translations and orientations) and,  $m$  3D points, BA optimization is defined as a least squares minimization using the  $L_2$ -norm or sum-of-squared reprojection errors:

$$E = \min_{\mathbf{R}_i, \mathbf{t}_i, \mathbf{K}_i, \mathbf{X}_j} \sum_{i=1}^n \sum_{j=1}^m \|\mathbf{x}_{ji} - g(\mathbf{X}_j, \mathbf{R}_i, \mathbf{t}_i, \mathbf{K}_i)\|^2, \quad (4.10)$$

where  $\mathbf{R}_i$ ,  $\mathbf{t}_i$ ,  $\mathbf{K}_i$  are, respectively, the rotation matrix, translation vector, and (intrinsic) calibration matrix of the  $i$ th camera,  $\mathbf{X}_j$  is the  $j$ th 3D point in the scene and observation  $\mathbf{x}_{ji}$  is the 2D image coordinates of feature  $\mathbf{X}_j$  in camera  $i$ . The mapping  $g(\mathbf{X}_j, \mathbf{R}_i, \mathbf{t}_i, \mathbf{K}_i)$  is the reprojection model defined in (4.6). The reprojection error basically measures the Euclidean distances between the projection of an estimated 3D point on its corresponding views using the estimated camera poses (rotation and translation). In an ideal case (noise free),  $E$  must be zero, however, this is not the case due to presence of noise both in the feature correspondences (e.g., low localization precision) and also in the estimated camera poses. In order to optimize these estimations and mitigate the noise level, Levenberg Marquardt (LM) is the most widely used solver in BA process (Aliakbarpour et al. 2015, 2017).

## 4.4 Experiments

We use the Orchard dataset (Li and Isler 2016) which contains images of UMN Horticulture Field Station taken from a flying drone. The UAV altitude was around 13 m with a speed of 1m/s and the video was recorded at 29 fps with the frame size of  $1920 \times 1080$  resolution. Figure 4.3 shows a few sample frames corresponding to this dataset. The frames from this dataset are used and their corresponding camera geometry is recovered using the proposed pipeline, B-SfM.

With no metadata (i.e., GPS and IMU measurements), the recovered camera poses are all expressed with respect to the coordinate system of the first camera in the sequence. Using the other product of B-SfM, the sparse 3D points, the dominant ground plane in the scene is estimated (i.e., the plane's normal and distance to the world coordinate system). Figure 4.4 right depicts the projection of the borders of the image frames onto the estimated ground plane. To visualize the quality of the



**Fig. 4.3** A few sample frames from Orchard (Li and Isler 2016) dataset

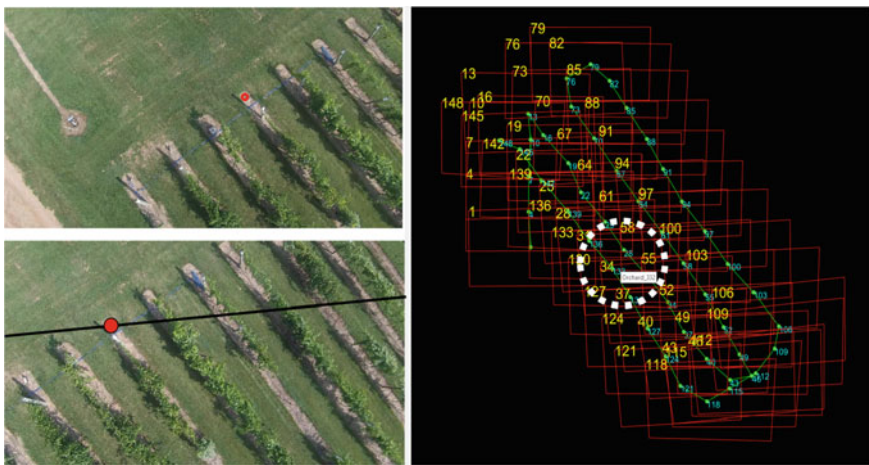


**Fig. 4.4** Epipolar verification between two temporally distant frames that correspond to the same geolocation. Left-top: frame #32 with a red marked point. Left-bottom: The epipolar line on frame #56, corresponding to the red marked point in frame #32 (Left-top). Right: The flight trajectory which has a serpentine pattern. The dotted white circle depicts a geo-spatial area where drone revisits the same place. The temporally distant frames #32 and #56 fall within this area

recovered camera poses in this experiment, the epipolar line between two sample views (frames) is plotted in Fig. 4.4 left. The top image in this figure shows an exemplary point marked by a red dot in frame #56. The corresponding epipolar line is computed using the recovered came poses and plotted on frame #32 (Fig. 4.4 left-bottom). As shown on 4.4 right, these two image frames are from two sub-trajectories that revisit the same spot of the scene after a sharp turn at the corner. The plotted epipolar line for these two sample views which passes through the ground truth marker (the big red dot in Fig. 4.4 left-bottom) indicates a good quality of the recovered poses by our algorithm with a loop closure. More qualitative epipolar plots are presented in Fig. 4.5 on the same frames showing the difference with and without





**Fig. 4.5** Epipolar verification between two temporally distant frames that correspond to the same geolocation. Left: frame #56 with a red marked point. Middle: The corresponding epipolar line on frame #98 corresponding to the red marked point in the left frame (#32). Right: The same epipolar line but plotted after applying loop closure in the pose estimation. As one can see, the epipolar line passes through the ground truth point, in this case

a loop closure. As shown, without a loop closure, the drift between the two frames which are geolocationally apart causes inaccuracy in the recovered camera poses. For loop closure detection, we utilized the recovered camera poses by our B-SfM algorithm in the first pass, estimate the dominant ground plane using the reconstructed sparse 3D point cloud, and then project the view frustum on the estimated ground plane. The feature points between the distant views that have overlaps between their projected polygons are then matched against each other. This will create some new short feature tracks and also merge some existing tracks (from the first pass). Then we run another optimization for a fast final tuning by enforcing new constraints defined by the new tracks after loop closure. Our fast pose-based loop closure technique results in significant improvement on the global consistency of the recovered poses and mitigates the drift issue which is a common problem in most SfM algorithms.

The recovered camera poses are also used to produce a mosaic of the scene. Figure 4.6 shows two such mosaics. The one at the left shows a mosaic created when no loop closure was applied. As one can see, the projection of the apart frames onto the ground manifest some misalignment due to the drift issue. However, as shown in Fig. 4.6 right, our fast loop closure technique has significantly improved the quality of the generated mosaic.

In addition to low-altitude drone aerial imagery datasets, we also run our BSfM algorithm on some Wide Area Motion Imagery (WAMI) datasets where the images were captured from much higher altitude. Figure 4.7 shows some exemplary frames from one of such datasets, with a flight altitude of about 1,500m observing the downtown area of Albuquerque, NM. Although this dataset has metadata acquired by an onboard INS system, in our experiments here we have not used them at all. Our algorithm, BSfM, just took less than 2 min to precisely recover the camera poses in

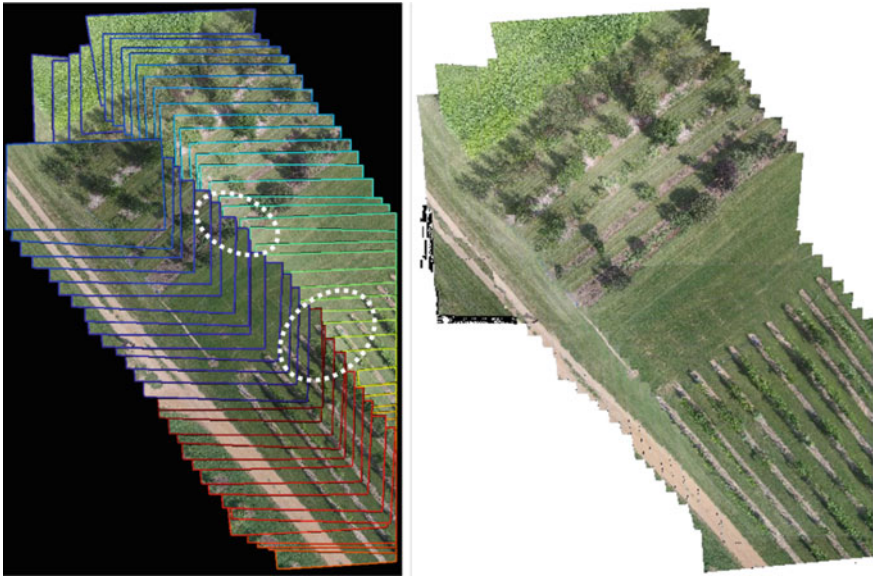


**Fig. 4.6** Mosaic created from geoprojection of the images using the camera poses estimated using our algorithm. Left: when no loop closure is used, Right: after using loop closure. The misalignment (the two white ellipsoid regions) caused by incremental drift on the camera pose estimation on the left mosaic is addressed on the right mosaic after using loop closure technique



**Fig. 4.7** A few sample frames in a high-altitude WAMI dataset corresponding to the downtown of Albuquerque, NM. The actual image frame sizes are  $6600 \times 4400$  pixels

this dataset. Figure 4.8 top shows the recovered camera coordinates for each frame (left) and the corresponding sparse 3D point cloud reconstructed (right). An epipolar line corresponding to ground truth points (marked in red) between two very distant views within this sequence is plotted in Fig. 4.8 bottom, which indicate a high quality of the recovered poses.

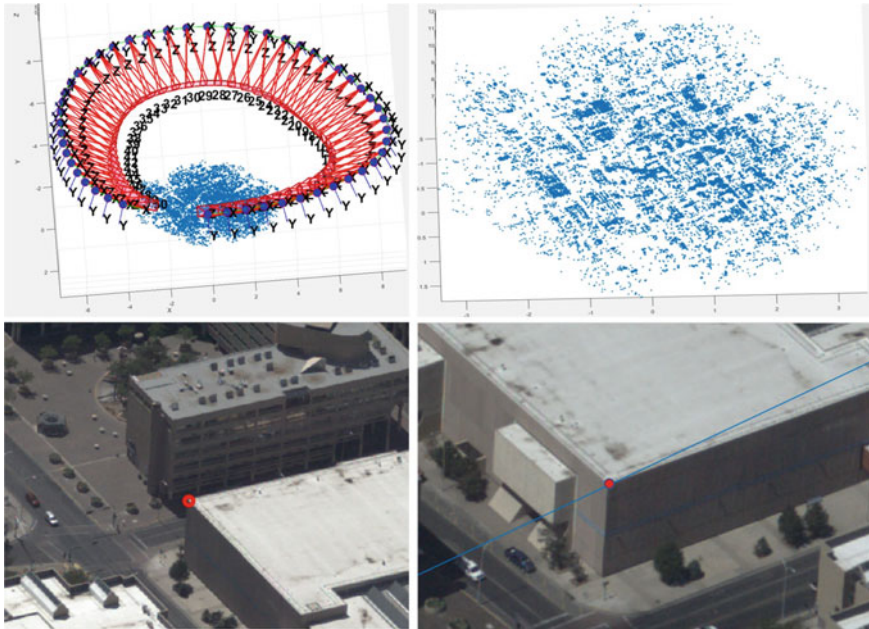


**Fig. 4.8** Results of applying BSfM on a high-altitude WAMI dataset (Albuquerque downtown, NM). Top: the recovered camera coordinate frames (left) and the reconstructed sparse 3D points (right). Bottom: the epipolar line corresponding to a pair of ground truth points (in red) between two distant views in the sequence (they are zoomed and cropped for better visualization)

## 4.5 Conclusions

We proposed a robust and fast method, called BSfM, to recover camera poses in aerial video sequences and register the views. Its effectiveness in generating a mosaic of a plant field for high-throughput phenotyping applications was demonstrated. In addition to the low-altitude aerial datasets, we applied our algorithm on a high-altitude WAMI dataset, which showed its robustness and precision.

**Acknowledgements** This work was partially supported by awards from U.S. Army Research Laboratory W911NF-1820285 and Army Research Office DURIP W911NF-1910181. Support for Transparent Sky was provided by the Office of Naval Research N6833519C0188. Any opinions, findings, and conclusions or recommendations expressed in this publication are those of the authors and do not necessarily reflect the views of the U.S. Government or agency thereof.

## References

- Aktar R (2017) Automatic geospatial content summarization and visibility enhancement by dehazing in aerial imagery. In: MS thesis, University of Missouri–Columbia
- Aktar R, Kharismawati DE, Palaniappan K, Aliakbarpour H, Bunyak F, Stapleton AE, Kazic T (2020) Robust mosaicking of maize fields from aerial imagery. *Appl Plant Sci* 8(8):e11387
- Aktar R, AliAkbarpour H, Bunyak F, Kazic T, Seetharaman G, Palaniappan K (2018a) Geospatial content summarization of uav aerial imagery using mosaicking. In: *Geospatial informatics, motion imagery, and network analytics VIII*, vol 10645. International society for optics and photonics, p 1064501
- Aktar R, Aliakbarpour H, Bunyak F, Seetharaman G, Palaniappan K (2018b) Performance evaluation of feature descriptors for aerial imagery mosaicking. In: *IEEE applied imagery pattern recognition workshop*
- Aktar R, Prasath VBS, Aliakbarpour H, Sampathkumar U, Seetharaman G, Palaniappan K (2016) Video haze removal and poisson blending based mini-mosaics for wide area motion imagery. In: *IEEE applied imagery pattern recognition workshop*
- Alcantarilla PF, Nuevo J, Bartoli A (2013) Fast explicit diffusion for accelerated features in nonlinear scale spaces. In: *British machine vision conference (BMVC)*
- Aliakbarpour H, Palaniappan K, Seetharaman G (2015) Robust camera pose refinement and rapid SfM for multiview aerial imagery—without RANSAC. *IEEE Geosci Remote Sensing Lett* 12(11):2203–2207
- AliAkbarpour H, Palaniappan K, Seetharaman G (2017) Parallax-tolerant aerial image georegistration and efficient camera pose refinement—without piecewise homographies. *IEEE Trans Geosci Remote Sensing* 55(8):4618–4637
- Ampatzidis Y, Partel V (2019) UAV-based high throughput phenotyping in citrus utilizing multi-spectral imaging and artificial intelligence. *Remote Sensing* 11(4):410
- Balntas V, Riba E, Ponsa D, Mikolajczyk K (2016) Learning local feature descriptors with triplets and shallow convolutional neural networks. In: *British machine vision conference (BMVC)*
- Bay H, Tuytelaars T, Van Gool L (2006) SURF: Speeded up robust features. In: *European conference on computer vision*. Springer, pp 404–417
- Complete solution classification for the perspective-three-point problem. 25(8):930–943
- Cooper SD, Roy DP, Schaaf CB, Paynter I (2017) Examination of the potential of terrestrial laser scanning and structure-from-motion photogrammetry for rapid nondestructive field measurement of grass biomass. *Remote Sensing* 9(6):531
- DeTone D, Malisiewicz T, Rabinovich A (2018) SuperPoint: self-supervised interest point detection and description. In: *IEEE conference on computer vision and pattern recognition workshops*, pp 224–236
- Dusmanu M, Rocco I, Pajdla T, Pollefeys M, Sivic J, Torii A, Sattler T (2019) D2-net: a trainable cnn for joint description and detection of local features. In: *Proceedings of the IEEE conference on computer vision and pattern recognition*, pp 8092–8101
- Gao K, Akbarpour HA, Fraser J, Nouduri K, Bunyak F, Massaro R, Seetharaman G, Palaniappan K (2020a) Local feature performance evaluation for structure-from-motion and multi-view stereo using simulated city-scale aerial imagery. *IEEE Sensors J* 1–1
- Gao K, AliAkbarpour H, Seetharaman G, Palaniappan K (2020b) Dct-based local descriptor for robust matching and feature tracking in wide area motion imagery. *IEEE geoscience and remote sensing letters*, pp 1–5
- Han L, Yang G, Dai H, Xu B, Yang H, Feng H, Li Z, Yang X (2019) Modeling maize above-ground biomass based on machine learning approaches using UAV remote-sensing data. *Plant Methods* 15(1):10
- Hartley RI (1997) In defense of the eight-point algorithm. *IEEE Trans Pattern Anal Mach Intel* 19(6):580–593
- Hartley R, Trunpf J, Dai Y, Li H (2013) Rotation averaging. *Int J Comput Vis* 103(3):267–305. [Online]. Available: <http://link.springer.com/10.1007/s11263-012-0601-0>

- Holman FH, Riche AB, Michalski A, Castle M, Wooster MJ, Hawkesford MJ (2016) High throughput field phenotyping of wheat plant height and growth rate in field plot trials using UAV based remote sensing. *Remote Sensing* 8(12):1031
- Leutenegger S, Chli M, Siegwart RY (2011) BRISK: binary robust invariant scalable keypoints. In: *IEEE international conference on computer vision*, pp 2548–2555
- Li Z, Isler V (2016) Large scale image Mosaic construction for agricultural applications. *IEEE Robotics Autom Lett* 1:295–302
- Longuet-Higgins HC (1981) A computer algorithm for reconstructing a scene from two projections. *293(133–135):1981*
- Lowe DG (2004) Distinctive image features from scale-invariant keypoints. *Int J Comput Vis* 60(2):91–110
- Maes WH, Steppe K (2019) Perspectives for remote sensing with unmanned aerial vehicles in precision agriculture. *Trends Plant Sci* 24(2):152–164
- Maimaitijiang M, Sagan V, Sidike P, Hartling S, Esposito F, Fritschi FB (2020) Soybean yield prediction from UAV using multimodal data fusion and deep learning. *Remote Sensing Environ* 237:111599
- Moreno-Noguer F, Lepetit V, Fua P (2007) Accurate non-iterative  $O(n)$  solution to the PnP problem. In: *Proceedings of the IEEE international conference on computer vision*, pp 1–8
- Mur-Artal R, Montiel JMM, Tardós JD (2015) Orb-slam: a versatile and accurate monocular slam system. *IEEE Trans Robotics* 31(5):1147–1163
- Nistér D (2004) An efficient solution to the five-point relative pose problem. *IEEE Trans Pattern Anal Mach Intel* 26(6):756–770
- Ono Y, Trulls E, Fua P, Yi KM (2018) LF-net: learning local features from images. In: *Advances in neural information processing systems*, pp 6237–6247
- Rublee E, Rabaud V, Konolige K, Bradski G (2011) ORB: an efficient alternative to SIFT or SURF. In: *IEEE international conference on computer vision*, pp 2564–2571
- Schönberger JL, Hardmeier H, Sattler T, Pollefeys M (2017) Comparative evaluation of hand-crafted and learned local features. In: *IEEE conference on computer vision and pattern recognition*, pp 1482–1491
- Schönberger M, Lutz J, Price and True and Sattler and Torsten and Frahm and Jan-Michael and Pollefeys (2016) A vote-and-verify strategy for fast spatial verification in image retrieval. In: *Asian conference on computer vision (ACCV)*
- Simo-Serra E, Trulls E, Ferraz L, Kokkinos I, Fua P, Moreno-Noguer F (2015) Discriminative learning of deep convolutional feature point descriptors. In: *IEEE international conference on computer vision (ICCV)*, pp 118–126
- Stewart EL, Wiesner-Hanks T, Kaczmar N, DeChant C, Wu H, Lipson H, Nelson RJ, Gore MA (2019) Quantitative phenotyping of Northern Leaf Blight in UAV images using deep learning. *Remote Sensing* 11(19):2209
- Tian Y, Fan B, Wu F (2017) L2-net: deep learning of discriminative patch descriptor in euclidean space. In: *IEEE conference on computer vision and pattern recognition*, pp 661–669
- Zagoruyko S, Komodakis N (2015) Learning to compare image patches via convolutional neural networks. In: *IEEE conference on computer vision and pattern recognition*, pp 4353–4361

# Chapter 5

## Experiences of Applying Field-Based High-Throughput Phenotyping for Wheat Breeding



Jared Crain, Xu Wang, Mark Lucas, and Jesse Poland

**Abstract** High-throughput phenotyping (HTP) is poised to fundamentally transform plant breeding through increased accuracy, spatial, and temporal resolution in measuring breeding trials. In this chapter, we examine different types of phenotyping platforms, data management, and data utilization for decision making using HTP in plant breeding, with case studies from wheat breeding programs. Development of HTP platforms, both ground-based and aerial vehicles requires evaluating the traits to be measured as well as the resources available. Data management is a critical part of the overall research process, and an example data management program is provided. Finally, examples of HTP use within crop breeding and plant science are presented. This chapter provides an overview of the entire HTP process from system conception to decision making within research programs based on HTP data.

**Keywords** Phenomics · High-throughput phenotyping · Data management · Wheat · Plant breeding · Sensors · Unmanned aerial vehicles UAV

### 5.1 Introduction

Technological advances in DNA sequencing have driven many biological fields, including plant breeding, from limited genomic resources to an information rich

---

J. Crain (✉) · X. Wang · M. Lucas · J. Poland  
Department Plant Pathology, Kansas State University, 4024 Throckmorton Plant Sciences Center,  
Manhattan 66506, KS, USA  
e-mail: [jcrain@ksu.edu](mailto:jcrain@ksu.edu)

X. Wang  
e-mail: [xuwang@ksu.edu](mailto:xuwang@ksu.edu)

J. Poland  
e-mail: [jpoland@ksu.edu](mailto:jpoland@ksu.edu)

J. Poland  
Wheat Genetics Resource Center, Kansas State University, 4024 Throckmorton Plant Sciences  
Center, Manhattan 66506, KS, USA

science. While the ability to generate genomic data has expanded exponentially since the early 2000s, the phenotypic information needed to unlock the potential of data driven breeding has lagged behind and has only begun to evolve into its own high-throughput, data rich endeavor. Phenotypic data at this scale is needed to connect the genotype-to-phenotype relationships which has been labeled the G2P problem (Cooper et al. 2002), and the lack of phenotypic information is often cited as the bottleneck to plant improvement (Richards et al. 2010), genetics and genomics studies, including implementation of genomic selection (GS) (Cobb et al. 2013). Historically, collecting phenotypic data has been laborious, time consuming, and expensive, with many phenotypic constraints remaining today.

Phenomics has emerged as a suite of technologies to help alleviate the slow rate and low throughput associated with phenotyping (Furbank and Tester 2011). Phenomics tools have been used for in field and controlled environments at multiple levels of plant organization from whole plant canopies to individual leaves. While there is no standard definition for field based high-throughput phenotyping (HTP), there is common consensus that HTP must provide cost-effective, accurate, and high-throughput manner of plant measurements (Furbank and Tester 2011; Cobb et al. 2013). In general, HTP technologies can be characterized by one or several of the following characteristics: ability to non-invasively measure plants (Reynolds and Langridge 2016), automation to reduce labor (Cabrera-Bosquet et al. 2012; Cobb et al. 2013), ability to measure multiple traits, plots, or both simultaneously (Bai et al. 2016; Barker et al. 2016), and have efficient automated or semi-automated data processing pipelines (Araus and Cairns 2014; Haghghattalab et al. 2016; Coppens et al. 2017).

The goal of this chapter is to present an outline for researchers embarking in field phenomics from conception of HTP platforms through data analysis and breeding decisions based on HTP application in wheat (*Triticum aestivum*). Particular attention will be devoted to developing sound methods that will help researchers achieve success in incorporating HTP into their breeding programs.

## 5.2 Current Phenotyping Systems and Considerations

### 5.2.1 Overview of Platforms

Many different phenotyping platforms have been used in breeding and research programs. The simplest HTP systems have been hand carried (Crain et al. 2016) or carts mounted with sensors that are pushed in the field (White and Conley 2013; Bai et al. 2016; Crain et al. 2016). These systems are often quite affordable, portable, and have been used throughout the world. Sensor integration and data collection from vehicles offer an increasing level of complexity and throughput (Busemeyer et al. 2013a; Andrade-Sanchez et al. 2014; Barker et al. 2016). Several large scale, mobile phenotyping units have been reported in wheat research including systems that can

measure three plots simultaneously for spectral reflectance, canopy temperature, and crop height (Barker et al. 2016) and the “Phenomobile” which is equipped with LiDAR and stereocameras among other systems (Deery et al. 2014). One of the most autonomous and automated systems that has been used to collect phenotypic data, interacts with plants by measuring stem strength in sorghum (Mueller-Sim et al. 2017).

In addition to ground-based platforms, many airborne systems have been described, particularly unmanned aerial vehicles (UAVs). Both fixed wing (plane type) and rotary wing (helicopters and multicopters) UAVs have been used to carry color, multispectral, and thermal cameras for field-based phenotyping (Haghighattalab et al. 2016; Shi et al. 2016; Tattaris et al. 2016). Piloted small, airplanes equipped with hyperspectral cameras mounted for crop observation (Montesinos-López et al. 2017) have likewise been used for phenotyping, as well as tethered balloons or aerostats (Jensen et al. 2007).

While ground and airborne systems are usually quite portable, cranes or gantry systems have been proposed, with the LemnaTech GmbH (Germany) Field Scanner being a high-end option. This system incorporates many sensor modules, infrared, hyper and multispectral, cameras, environmental sensors, and laser scanning systems into a gantry crane system that allows precision movement along three axes. Wheat research programs at Rothamsted Research Center, UK (Virlet et al. 2017) and Maricopa, AZ, USA (Burnette et al. 2018) have used this system. A cable suspended phenotyping platform has also been deployed that can cover 1 ha and carry up to 12 kg in payload (Kirchgessner et al. 2017). In addition, many commercial smart sensors (i.e., Smartfield™ FIT System, Lubbock, TX and Agrela Ecosystems™ PheNode, <https://www.agrelaeco.com>) are field deployable and able to monitor plant traits in real-time. While these platforms can offer detailed data from a variety of sensors, they are often limited to small areas that are fixed in size and location.

While phenomics was initially limited to deliver magnitudes of data beyond hand measurements, there currently exists numerous HTP platforms that can meet this problem (Table 5.1). Currently, the challenge is to choose an appropriate system that can measure desired traits at an affordable cost. For programs embarking on HTP, researchers should begin by defining the size and scope of the program. The desired traits to be measured should be identified, and an appropriate measurement device should be selected, as conclusions will only be valid for what is measured, potentially differing from the stated objectives. Along with time and monetary resources available to run the phenotyping initiative, programs should consider any specialized training or licensing, such as a pilot’s license to fly a UAV, that would be required for safe and legal HTP platform operation.

Matching HTP platform to the anticipated use is critical to obtaining useful data, Fig. 5.1. For example, if a program is interested in measuring thousands of breeding plots for canopy temperature, a measurement that is greatly affected by ambient conditions, a UAV or platform measuring multiple plots at the same time within a very small-time frame would be needed. Additionally, if canopy temperature measurements were to be taken in an area prone to rain or irrigation, a UAV may be the



**Table 5.1** Non-exhaustive list of high-throughput phenotyping (HTP) platforms, selected notes and information about their capabilities and sensor systems that have been reported in wheat phenomics research

Type of platform	Measured crops	Data acquired	Simultaneous plot measurements	Data storage	Rate of data measurement	Sensor adjustability	Selected notes	References
Hand and pushcart	Wheat	NDVI, canopy temperature, RGB images, GNSS coordinates	1 plot	computer	10 Hz NDVI, CT, GNSS 3 Hz RGB	Adjust height and row position		Crain et al. (2016)
Push cart	Wheat, barley (Hordeum vulgare), camelina (Camelina sativa) upland cotton (Gossypium hirsutum)	Monochrome cameras, GNSS, ultrasonic sensors, infrared thermometers, radiometers	1 plot	Data loggers (Campbell Scientific, Inc.)	1 and 5 Hz	Adjust row width, sensor height and position. Published version assessment showed that crops could grow taller than cart	Moved from field to field on a trailer	White and Conley (2013)
Push cart	Wheat, soybean (Glycine max)	Ultrasonic sensor, NDVI, infrared radiometers, RGB camera, spectrometer	3 plots	Computer with data acquisition board for analog signals	1 Hz at using a stop-measure-go motion	Flexible sensor position and height		Bai et al. (2016)
Mobile unit, tractor pulled	Wheat, triticale (Triticosecale)	Light curtains, hyperspectral imaging, 3-D time of flight cameras, laser distance sensors, RGB camera	1 plot	Industrial computer using MySQL database	1 Hz GNSS, RGB camera, 5 Hz time of flight camera, 100 Hz hyperspectral images	Flexible height adjustment		Busenmeyer et al. (2013a)

(continued)

Table 5.1 (continued)

Type of platform	Measured crops	Data acquired	Simultaneous plot measurements	Data storage	Rate of data measurement	Sensor adjustability	Selected notes	References
Mobile unit (Mudmaster)	Wheat, soybean, sorghum (Sorghum bicolor)	NDVI sensors, ultrasonic, infrared, GNSS	3 plots	Computer with data acquisition for analog signals	5 Hz GNSS 10 Hz other sensors	Adjustable row spacing for sensor, height adjustment, wheel spacing possible		Barker et al. (2016)
Mobile unit (Phenomobile)	Wheat, Brassica napus, maize (Zea mays)	LiDAR, GNSS, RGB cameras, thermal infrared camera, infrared thermometers, spectroradiometers, and hyperspectral cameras	1 plot		1 Hz spectroradiometer	Adjustable height sensor bar		Deery et al. (2014)
Mobile unit (PhenoTrac 4)	Wheat	NDVI sensors, RGB cameras, GNSS, multispectral sensor			Up to 70 readings per plot			Kipp et al. (2014)
Mobile unit LeeAgra sprayer	cotton ( <i>Gossypium barbadense</i> )	NDVI sensors, sonar, infrared thermometers, GNSS	3 plots	Data loggers	1 Hz GNSS and analog sensor data	Height adjustable boom		Andrade-Sanchez et al. (2014)
Mobile unit of a horizontal boom mounted to tractor	wheat	RGB cameras, spectrophotometers	1 plot		10 Hz GNSS, up to 80 spectra per plot	Horizontal rail to measure neighboring plot		Alexis et al. (2012)

(continued)

Table 5.1 (continued)

Type of platform	Measured crops	Data acquired	Simultaneous plot measurements	Data storage	Rate of data measurement	Sensor adjustability	Selected notes	References
Gantry system (LemnaTech GmbH)	wheat	Chlorophyll fluorescence imager, hyperspectral scanners, laser scanner, RGB, thermal cameras	1 plot	Database with transfer through optical cables		Sensor view adjustable along 3 axis	No simultaneous sensor operation	Virlet et al. (2017)
Cable suspended phenotyping platform	Wheat, maize, soybean	Spectrometers, RGB, infrared, thermal camera, terrestrial laser scanner	Multiple	4 computers controlling sensors		Sensor adjustment over 1 ha field	90 kg payload	Kirchgeßner et al. (2017)
Field camera track	Wheat, barley, oat (Avena sativa)	360 FLY hemispherical video	Multiple			Operates under windy conditions, 360 degree field of view	Up to 22 kg payload	Susko et al. (2018)
Fixed wing UAV	Wheat	Multispectral camera	Multiple				150 g payload	Haghighattalab et al. (2016)
Fixed wing UAV	Wheat, sorghum, corn, cotton	Multispectral camera	Multiple		Varied on flight speed	Gimbal for stability, up to 45 min flight,	Camera triggered by onboard controller	Shi et al. (2016)
Rotary wing UAV octocopter	Wheat, sorghum, corn, cotton	RGB cameras	Multiple		0.3-0.5 s per frame	2.8 kg max payload, 10 min flight	Camera triggered by operator	Shi et al. (2016)

(continued)

Table 5.1 (continued)

Type of platform	Measured crops	Data acquired	Simultaneous plot measurements	Data storage	Rate of data measurement	Sensor adjustability	Selected notes	References
Pheno-Copter (gas powered)	Wheat, sorghum, cotton, sugar cane ( <i>Saccharum officinarum</i> )	Thermal camera, RGB, and near infrared camera	Multiple	Cameras and then computer		1.5 kg for 30 min flight	1.78 m rotor diameter	Chapman et al. (2014)
Quadcopter	Wheat	RGB camera	Multiple			custom gimbal	Max payload 400 grams 0.9 cm per pixel resolution	Haghighattalab et al. (2016) Holman et al. (2016)
Octocopter	Wheat	RGB cameras	Multiple					
Multicopter	Wheat	RGB high resolution video clips	Multiple	On board system	30 Frames per second	Gimbal with view 20° from nadir	0.5 mm per pixel	Wang et al. (2019a)

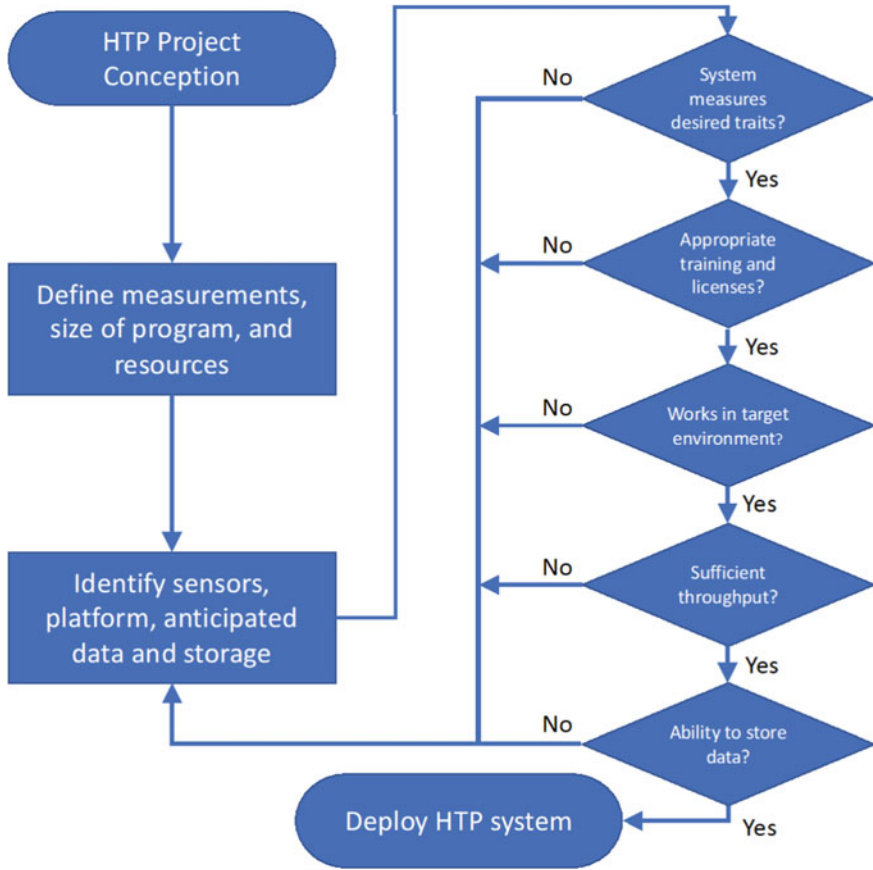


**Fig. 5.1** Flowchart for selecting high-throughput phenotyping system that meets experimenters needs through matching system components with desired trait measurements, resource constraints, and environmental conditions

only viable option to adequately obtain the data as UAVs would avoid compacting moist soil or disturbing plants compared to ground-based vehicles. Alternatively, a ground-based, mobile phenotyping unit may be needed if the desired data included high resolution imagery of individual plots or plants or the sensors were too heavy for UAV platforms. For researchers wanting to use phenotyping tools at remote locations portability of the HTP system should be considered. Carefully, matching the HTP system to the desired data output will ensure that resources are used as efficiently as possible and the best results are obtained.

## 5.2.2 Overview of Phenotypic Measurements

Data from HTP platforms is used to describe the growth and development of plants (Fiorani and Schurr 2013; Fahlgren et al. 2015). Many phenological traits have been measured using non-destructive imaging or sensor techniques such as canopy temperature, stay green, and ground cover (Pask et al. 2012). Often measurements rely on using various wavelengths of the electromagnetic spectrum from color (400–700 nm) for RGB (red, green, blue) digital imagery, infrared radiation for spectral indices (700–1000 nm), to hyper spectral (350–2500 nm) for full spectrum readings (Fahlgren et al. 2015). In addition, light detection and ranging (LiDAR) and thermal readings using infrared thermometers (IRT) use the electromagnetic spectrum (Fahlgren et al. 2015).

By carefully choosing sensors to match the desired target, researchers have been successful in evaluating plant growth. For wheat, Pask et al. (2012) reviewed a large number of phenotyping techniques including canopy temperature, spectral reflectance, chlorophyll fluorescence, and direct growth measurements such as plant height and maturity. These measurements were taken with a variety of point and image sensors (Sect. 5.2.3.2), to provide information about plant growth and development that can inform breeding selection decisions. For example, spectral reflectance indices and canopy temperature can be used for indirect selection of grain yield in wheat (Amani et al. 1996; Babar et al. 2006a, 2007).

Image data from RGB and active spectrophotometers have been used for measuring early plant vigor (Kipp et al. 2014), canopy cover (Mullan and Reynolds 2010), and plant height and lodging (Chapman et al. 2014; Tattaris et al. 2016). Along with analyzing data at a single time point, temporal plant growth has been monitored using hyperspectral imaging in Triticale (*Triticosecale*) and the results mapped to quantitative trait loci (QTL) controlling biomass accumulation showing dynamic effects of QTL controlling plant growth (Busemeyer et al. 2013b). Machine learning algorithms (Yu et al. 2017) have used digital images throughout the growing season to classify plant growth.

As phenotyping methods improved, researchers have successfully quantified stay green traits (Lopes et al. 2012; Crain et al. 2017), 3-D canopy architecture (Aasen et al. 2015), tiller density and crop growth (Du and Noguchi 2017), abiotic (Crain et al. 2017) and biotic stresses (Shakoor et al. 2017). Imaging technologies have been used to evaluate other complex traits, such as lodging (Singh et al. 2019), ear density (Madec et al. 2019), and flowering time (Wang et al. 2019b) in wheat. Many of these traits provide researchers with opportunities to better understand and select crop performance.

The range of traits that could be measured using HTP methods is only limited to the ability to identify a sensor system that accurately evaluates a desired trait. For example, over 100 vegetation indices (VIs) have been reviewed by Xue and Su (2017), and the interest in hyperspectral imaging will probably increase the number of VIs that are used in crop assessment. Any trait that does not have a strong body of literature supporting the method of measurement should be carefully verified that the

protocol method is indeed measuring the trait of interest. For example, significant correlations between UAV measured and ground truth data were observed for growth stages from stem elongation to late grain fill (Hassan et al. 2018) providing evidence that the UAV system was providing similar data to ground-based information.

While many traits have been amenable to HTP application, advancing sensor technology and data analysis methods will most likely lead to more traits being able to be measured or estimated through non-destructive measures. For research programs implementing HTP methods, deciding which target traits to measure and how they will be assessed is important to obtain optimal results. A common challenge with HTP is that data collection is often very easy, facilitating building large datasets; however, these data sets may not answer the questions researchers posited resulting in inefficient use of resources within research programs.

### **5.2.3 Overview of Sensors**

A typical field-based HTP platform normally incorporates a suite of sensing units, global navigation satellite system (GNSS) receivers, and a data acquisition system. Positioning data is used to georeference the HTP observations, effectively linking the measurement to the experimental unit (Wang et al. 2016). Cameras, IRTs, spectrometers, and other sensors that record data form the sensing unit, and provide data for analysis. The data acquisition system communicates with sensors, GNSS units, and computers or data loggers to translate sensor data signals into data files. Plot-level assessment of HTP data requires a combination of these systems working in harmony to accurately measure and report crop parameters.

#### **5.2.3.1 Positioning Sensors**

The GNSS receiver provides the HTP platform with positioning information that is critical for deriving the phenotypic data sampling time and positions. The GNSS can also facilitate auto-navigation, though this is not a necessary component of every phenotyping platform. Suitable GNSS units will provide both Coordinated Universal Time (UTC) information and the antenna's geographic position.

Selection of a GNSS unit for field-based HTP should consider many factors, such as the positioning precision and the sampling frequency. These factors can result in large differences in cost. For field-based HTP, the positioning precision determines how accurately the individual measurements can be linked to the experimental units. More accurate positions can link the individual phenotypic measurements to the correct plot or even plant which may be especially important for breeding programs evaluating lines in small-plots. For that purpose, a GNSS with differential correction which will achieve precision within 10–15 cm is preferred as the minimum level of precision for typical plots sizes of 1 m × 1 m. As plot size decreases, from standard

yield plot (~1 m × 3 m) to single rows or single plants, the precision of the GNSS will need to increase to accurately assign data to the correct plot or plant.

The sampling frequency of the GNSS determines the measurements resolution in the region of interest (ROI) as well as the maximum moving velocity of the HTP platform. As the sampling frequency decreases or the velocity of the HTP vehicle increases, the absolute error of the measurements between the observed measurement and actual geographic location will increase. Sampling time stamps can also be used to query the meteorological data, such as solar irradiance, wind speed, air temperature, and relative humidity from weather stations. These ambient environmental conditions can be used in conjunction with HTP data to control for known covariates that may affect data quality. Ensuring sensor specifications across integrated systems will be compatible with downstream data analysis and is crucial for creating pipelined analysis that can report in-season or real time results.

In addition to positioning precision and sampling rate, other factors to consider include the dimension and the weight of the GNSS system as various HTP platforms have different payload capacity and space to attach the GNSS units. Recently, many low-cost real-time kinematic (RTK) GNSS have been released into the market, such as EMLID REACH GNSS ([www.emlid.com/reachrs](http://www.emlid.com/reachrs)) and TERSUS GNSS ([www.tersus-gnss.com](http://www.tersus-gnss.com)). One important factor when selecting the low-cost RTK GNSS is the GNSS frequency band. A single-frequency RTK GNSS (i.e., only L1 band) can only allow precision accuracy when the distance between the base station and the rover is less than 3 km, therefore, the field scale and the location of the base station should be examined.

### 5.2.3.2 Phenotyping Sensors

Remote sensing is the key technology that enables field-based HTP. This includes proximal sensing close to the canopy (e.g. <2 m). Two common types of phenotypic data are point-based sensor observations and multi-dimensional data set (i.e., images and point cloud data) that are determined by the type of sensors utilized. Point-based sensors usually provide easily derived trait measurements, such as canopy temperature and VIs. These sensors are relatively low-cost compared to imaging sensors, and mostly used on ground platforms.

To achieve a higher throughput (i.e., to measure several plots at the same time) and a higher spatial resolution, imaging sensors are becoming more prominent than point-based sensors for field-based HTP. Zhang and Zhang (2018) have reviewed most commonly used imaging technologies for plant HTP. For multi- and hyperspectral cameras, the number of spectrum bands, the band width, and the overlap between two consecutive spectral bands should be considered. Multi-spectral generally refers to sensors with 4-10 bands, while hyperspectral can often contain hundreds or thousands of bands. Hyperspectral bands are often narrower in band width than multispectral cameras. For thermal camera, the measurement resolution (i.e., ±5 °C) needs to be evaluated to determine if the measurements can reflect the dynamic temperature variation.



During RGB image acquisition, especially from a moving platform, the shutter speed, aperture value, and white balance should be set carefully according to the platform speed, the distance between the camera and the target, and the ambient light condition. Shutter speed affects the amount of time that the lens is open, allowing exposure for the image. If a camera is on a moving platform, the shutter speed must be fast enough that image blur does not occur. Aperture of the lens affects the range of depth (i.e., on the canopy) where objects can be focused, with narrow aperture allowing more of the photo to be in focus. Aperture and camera view angle can be adjusted according to the target and desired data usage. For example, nadir view may be better for imaging crop canopies, while off-nadir view may be better for detecting flowers and fruit. Controlling ambient light conditions, through external light sources or shades, will help with the post image processing and maintain accurate white balance. While vehicle HTP platforms may be able to control light conditions, UAV platforms often rely on post image processing to control for changes in ambient light conditions. Consulting camera manuals or photography experts, early in the HTP process, will help ensure camera settings are appropriate for the HTP platform and the data can be used to answer HTP objectives.

In addition to defining sensors by point or image data, a second category is active or passive sensors. Active sensors have their own light source and are not affected by ambient environmental conditions such as cloud cover. Active sensors often include the Trimble GreenSeeker (Trimble Inc., Sunnyvale, CA) and Holland Scientific Crop Circle (Holland Scientific, Lincoln, NE). While passive sources rely on ambient light, and thus are influenced by changing environmental conditions, they often have a larger range of measurement options. Most cameras are passive sensors, although light curtains can be used to eliminate environmental noise (Montes et al. 2011; Busemeyer et al. 2013a). For image data, radiometric calibration may help standardize data sets from fluctuating environmental conditions (Haghighattalab et al. 2016; Shi et al. 2016; Yang et al. 2017), yet for other sensors like IRT there may be no way to easily calibrate data if HTP evaluation occur when environmental conditions are variable or windy. Due diligence of understanding sensors, their mode of action, and the factors that can affect measurement results will help ensure that the data collected is tractable for downstream analysis.

Sensor selection should include evaluating field-of-view (FoV), measurement resolution, and expandability. The FoV determines the amount of area that a sensor observes when it takes a measurement. Wide FoV may include noise from non-vegetative targets such as soil, while narrow FoV may not reflect the common plant trait within a small ROI. When the FoV for a camera or sensor is fixed, the ROI can be manipulated by the distance that the sensor is from the target, increasing or decreasing ROI by sensor placement. Taken together, these important consideration for the ROI must be accounted for a well-functioning HTP system.

Sensor resolution refers to how precisely a trait may be measured and can influence if certain dynamic traits can accurately be assessed for genotypic discrimination. For example, if canopy temperature is expected to have only a few degrees difference between all genotypes, an IRT with a resolution of  $\pm 1.00$  °C would not as efficiently differentiate between genotypes as an IRT with a resolution of  $\pm 0.25$  °C. For all

cameras, the imaging sensor size is the most important factor in considering camera resolution. Sensor size determines the effective pixels included in the raw image and the ground sample distance (GSD). The GSD is the limitation of image resolution and refers to the distance on the ground between two adjacent pixels. As sensor size increases or FoV decreases the area included in each pixel decreases, resulting in higher GSD resolution. While high-resolution is often desired, the higher the resolution increases sensor cost as well as the volume of data generated increasing storage and data curating requirements.

Expandability allows sensors to have the potential to provide different measurements based on user needs. For example, the Trimble GreenSeeker provides fixed spectral bands whereas the Holland Scientific Crop Circle has interchangeable filters allowing the user to determine which spectral bands to be recorded. The ability to fine-tune sensor measurements, could allow one sensor system to perform multiple task.

### 5.2.3.3 Data Acquisition Systems

Data acquisition systems form the connections between different sensors and immediate data storage. For simple HTP systems, users may not even need to consider the data acquisition system. For single sensors, such as the Trimble GreenSeeker, data acquisition occurs automatically, with the user being able to download a final file of observations. Some UAV platform autopilot systems perform a similar task by automating image collection by consistent time or space intervals, i.e. every 5 s an image is collected regardless of UAV or target position. However, as the HTP systems become more complex, integrating more sensors, users will most likely have to develop protocols for combining sensor data.

LabView (National Instruments, Austin, TX, USA) has been used on several phenotyping platforms (Bai et al. 2016; Barker et al. 2016; Crain et al. 2016) as it has the capabilities to interact with sensors outputting different rates and types of signals. Computing languages like Python have also been used to interact and record data from multiple sensors (McGahee 2016). While data acquisition systems may not be at the forefront of users of already developed HTP systems, users building their own systems should be aware of potential issues in connecting many and often disparate sensors. Often the most direct solution is to partner with engineers or computer programmers that have the requisite skill set to quickly resolve potential problems.

### 5.2.4 Future Sensors and Application

Advancing technology may soon make the ability to obtain super high-resolution and throughput phenotypic data possible with videos (i.e., 6 K video) and satellite photos (i.e., GSD <10 cm). As these technologies improve, they will become more popular for field-based HTP. These advances will allow for more high-dimensional

phenotypic dataset to be generated through sensor fusion techniques (Jiang et al. 2018). For example, using sensor fusion technologies, a LiDAR point cloud can be registered with pixel information from cameras (i.e., GeoSLAM Hub and Draw, <https://geoslam.com>), which can be used to differentiate plant tissues. In addition, more advanced sensing techniques, such as radar could be used to collect phenotypic data underneath plant canopies and X-ray micro computed tomography was used to reconstructing the wheat grain structure without physically harming the wheat spike (Hughes et al. 2017). All these novel sensing technologies will bring more discoveries for field phenomics research, while at the same time bring more challenges for data processing.

### 5.3 Data Processing

A hallmark of HTP platforms is the ability to produce massive amounts of data. Even a small HTP system of two sensors reading at 10 Hz can produce over 72,000 data points per hour, and image-based systems can routinely produce gigabytes of data in a single flight. While numerous HTP platforms have been proposed and developed, the ability to handle the inundation of data has often received less attention. While the exact processing steps may look different for each platform, in general data should be processed for quality control and trait extraction as soon as possible to check for potential errors (White et al. 2012).

In the literature, several data management practices are described, but the reported information is often limited especially from a perspective of long-term storage and preservation of the data as well as exact methods used. For example, the Field Scanner (Virlet et al. 2017) uses proprietary software to manage up to 800 MB of data that can be collected on a single plot per measurement. Once the raw data is processed, extracted information such as VIs are then stored in databases which can be accessed by users. Another example is the ETH field phenotyping platform (cable system) which uses a MySQL database with different tables to store data sensor readings, ground truth, and weather data (Kirchgeßner et al. 2017). While these two examples highlight certain aspects of data management, HTP data often has many steps from data collection to knowledge.

All HTP data requires processing to move from a raw data observation to a value that can be used in modeling. Point data is often paired with GNSS information based on the time of data collection (Barker et al. 2016). Image or multi-dimensional, data is often more challenging and requires several steps to process raw images into indices or values. Several processing pipelines have been presented for image data with the common themes including format conversion and image correction, ortho-mosaicking, radiometric calibration, followed by data extraction (Haghighattalab et al. 2016; Shi et al. 2016; Yang et al. 2017).

Regardless of the type of data, the first objective is the correct assignment of data points or images to a plot to be subsequently used in statistical analysis or crop models. While GNSS tagging through point data or generation of ortho-mosaic

image data is nearly universal, the link between where a data point is geographically located and which plot it belongs to is essential. Several plot identifying methods have been utilized in literature. At the most basic level, coordinates for each of the plot corners can be measured forming a polygon, or polygons can be drawn from orthomosaic photos (Shi et al. 2016). Both of these methods are quite low throughput and laborious. However, plot delineation only has to be completed one time per season so the number of plots phenotyped could dictate the time and resources spent on extracting plot boundaries. Another simple strategy has been to use the rectangular nature of plots to grid the experimental area to the number of plots, followed by trimming to insure that bare ground is not included in the plots (Chapman et al. 2014; Haghigattalab et al. 2016). For point data such as VIs, which offers contrast between green plots and bare alleys simple algorithms to define the start and end of plots followed by extrapolation of plot size can be used (Crain et al. 2016). In a more robust method for image data, a classification into plant or non-plant can be used to segment the image and apply plot identifications (Haghigattalab et al. 2016). If early season imagery is available, with few artifacts, this method could be very accurate, but there is the potential need to manually edit misclassifications. Wang et al. (2016) demonstrated methods to assign HTP point data to plots and delineate plots based on vehicle heading and sensor position. These methods were applicable to varying plots sizes and can be used after data collection to quickly georeference HTP phenotypic measurements to GNSS data.

While much effort has been devoted to extracting values from data and pairing phenotypic data with plot information for immediate analysis, less effort has been devoted to how crop phenotypes should be stored with emphasis on long-term utilization. Unfortunately, data standards to store and curate data are often secondary to phenomics goals of QTL mapping, dissecting traits, or increasing the rate of genetic gains in crops. Similar to public repositories for DNA data (e.g. Short Read Archive (Leinonen et al. 2011)) there have been several resources developed for storing phenomic data; however, at a cost of central repositories (Coppens et al. 2017). Some phenomics data facilities have been built for specific users including the Phenomics Ontology Driven Data (PODD) for Australian phenomics work (Li et al. 2010) and the Phenopsis DB for data produced from the PHENOPSIS HTP platform for *Arabidopsis thaliana* (Fabre et al. 2011). A more generalized version has been the Plant Genomics and Phenomics data repository hosted by the Leibniz Institute of Plant Genetics and Crop Plant Research (Arend et al. 2016). This data repository is consistent with FAIR (findable, accessible, interoperable, reusable) data principles (Wilkinson et al. 2016).

While these repositories allow researchers to store data and their associated metadata, these databases may not allow for full reproduction of analysis, as many intermediary processing steps or raw data may not be stored. To make research more reproducible, with the ability to evaluate the data and methods of analysis (Peng 2011), experimenters should consider the entire lifecycle of data from collection to storage, with particular emphasis on a future vision that could reuse the data. Each phenomics program will probably look different in terms of exact data curating, but

storing raw data, backups, extracted traits, and the processes used to develop them, along with plot information should be included in every data management plan.

### 5.4 Data Management Example

Maintaining millions of HTP data points for numerous field trials and experiments each year requires a dedicated effort in terms of both software and personnel actions. Data management is comprised of a series of tasks that provide the means to validate the integrity of incoming data, standardize data format, and archive data with sufficient metadata to support reliable backup and retrieval of specific data sets. The following sections describe and highlight the most important aspects of the data management tasks and supporting system architecture employed by the Poland Lab in order to avoid drowning in the deluge of HTP data. This model is built to be flexible to different HTP platforms, sensors, and experiment types, and should be a useful reference to scientists pursuing HTP projects.

The data management workflow for UAV-based includes collecting, verifying, and storing information, Fig. 5.2. After the data has been collected in the field, the image data sets are uploaded to a central server. After upload, a basic check is made to verify that all images and associated log files are present in each data set. Since raw images only have a numeric identifier that is not unique, images are renamed with date and time information to provide a unique file name for each image. If image Exchangeable image file format (Exif) metadata does not contain reliable position data, the images are geo-referenced using information from a trusted external log file. For each image that was collected during the phenotyping run, the rename and geo-referencing process generates metadata that is stored in a MySQL (MySQL Server version 5.6.34. 2016-10-12 Oracle Corporation, Redwood Shores, CA, USA) relational database with the metadata providing a pointer to the image file. For point

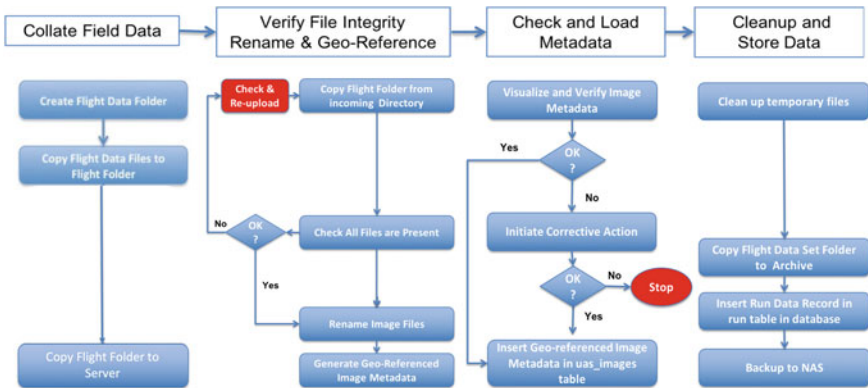
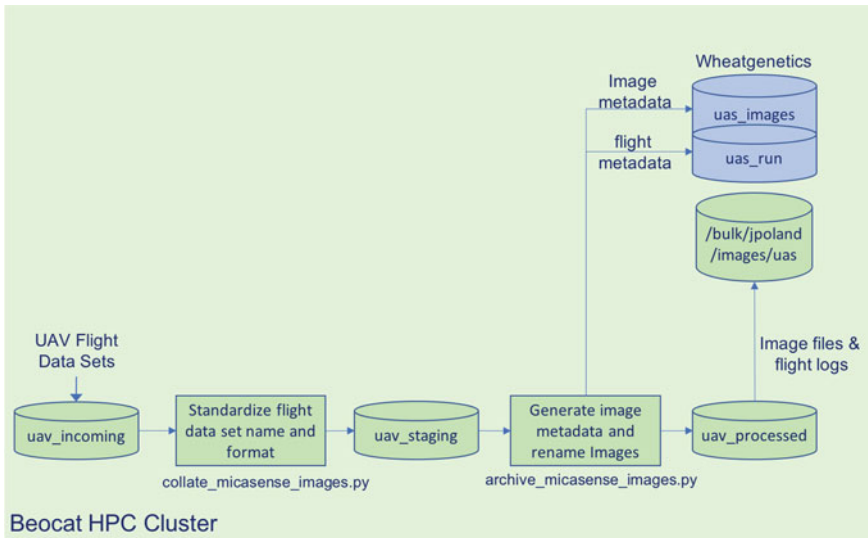


Fig. 5.2 Example UAV image data management workflow from data collection to long-term storage

data generated by ground-based systems, the system is nearly identical, only the recorded measurements are stored in the database instead of metadata. Finally, the data sets are backed up to an external network-attached storage (NAS) to provide protection against data loss on the main high-performance computing (HPC) cluster.

### 5.4.1 Data Management Architecture

An example of currently implemented data management system architecture for UAV-based image data is shown in Fig. 5.3. All data sets collected in the field are first uploaded to the `uav_incoming` directory. Prior to archiving, the data sets are collated into a standard format and then moved into the `uav_staging` directory. A scheduled task, Python program, is then initiated which archives any data sets found in the `uav_staging` directory. Archiving consists of renaming the image files with unique date and time-based names, updating the database with metadata for each flight and each image and then moving the updated data set files into the `uav_processed` folder where final checks of the archive artifacts are made. Finally, each data set is moved into a standard archive folder. Scheduled tasks are then invoked to backup both the database and image files to external (NAS) storage.



**Fig. 5.3** UAV image data management system architecture documenting raw data from sensors to processed and renamed data stored for retrieval

### 5.4.2 Database Design

The database has been designed to be highly flexible to maintain current data, while at the same time being able to adapt to new sources of data. The goal of the database, is to create sufficient record of experiments, including data collected, that any user can completely reconstruct when and where a field experiment occurred, along with all of the data that was collected allowing for full statistical analysis. The latest iteration of the database design for HTP data is shown in Fig. 5.4.

While there are many tables that share relationships to link each source of data, Fig. 5.4, the overarching element is a unique experiment ID. Every experiment maintains a unique ID, with most IDs being a combination of year, location, and purpose of the experiment (e.g. 19-RKY-AM is the 2019, Rocky Ford Association Mapping experiment). Even if an experiment is planted in multiple years or sites, this naming convention maintains that each year of the experiment is a unique entity. The experiment ID is maintained in a table of experiments that records all experiments, location, planting date, and notes that describe the experiment. While this table can be searched using keywords, years, or location through SQL commands, it is also small enough

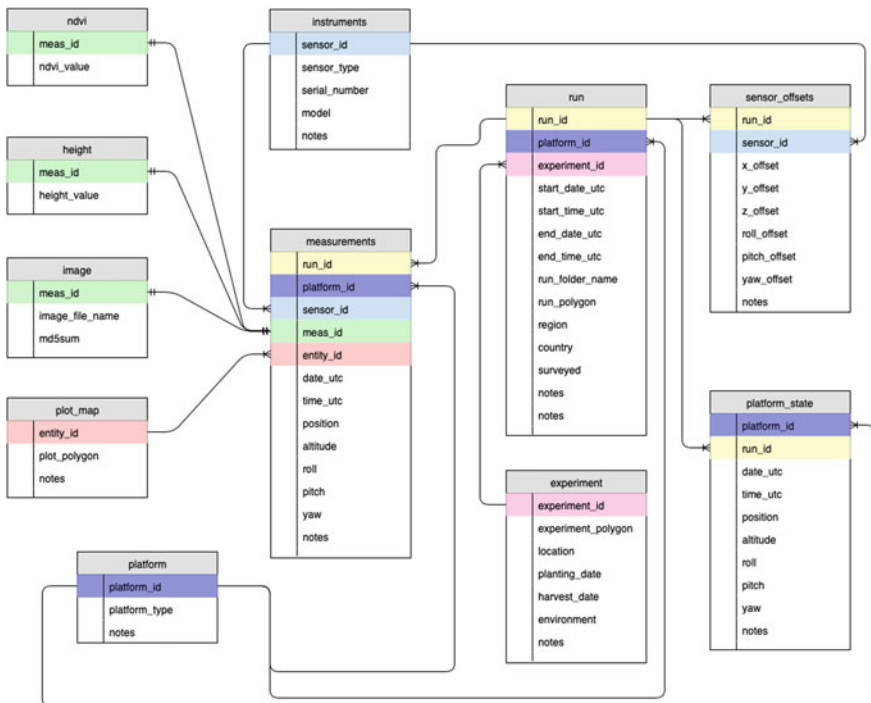


**Fig. 5.4** Example of high-throughput phenotyping database schema. Each table is linked to other tables through relationships (colored column names linked by lines)

to allow visual inspection to find experiments as needed. Experiment field dimensions and location are defined as a latitude and longitude based spatial object i.e. an experiment polygon. All geographical coordinates in the database are specified using latitude and longitude coordinate pairs. MySQL spatial objects such as points and polygons are utilized to define the position associated with an image or sensor measurement, as well as the dimensions and location of experiments and plots.

Once an experiment is identified, the experiment ID can be used to find plots IDs in the plot table. Each plot ID is unique consisting of a combination of year, location, and plot number. The plot table details each plot in an experiment, the cultivar name of the plot, row, column, replicate, and block number for statistical analysis. For plots with HTP data, the plot dimensions and location are defined as latitude and longitude based spatial objects i.e. plot polygon.

The unique plot ID can then be used to query tables that store hand-measured phenotypic data, HTP data, and genotypic data. Hand measured phenotype data, such as grain yield and plant height, are needed to correlate HTP measurements to standard field practices. The database schema for hand-based phenotype data is shown in Fig. 5.5 along with experiment and plot tables. The experiment table is the same as Fig. 5.4, demonstrating how information can be found by utilizing the experiment ID, and how additional tables, such as a genotype table, can be added to meet the users need.

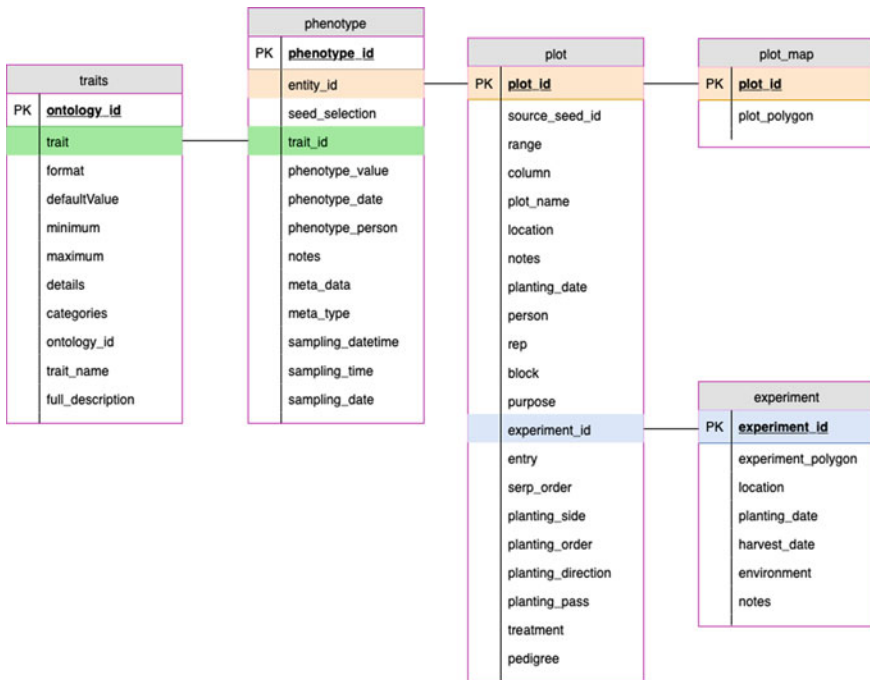


Fig. 5.5 Hand-measured phenotype database tables linked to the plot and experiment tables



The hand-measured phenotype table consist of the entity ID (linking plots to phenotypes), a trait ID, and the phenotype value or character. Each plot can have multiple measurements of the same trait or different traits allowing all phenotypic data to be stored in one table. The trait IDs are unique and described in a trait ID table. To further standardize trait measurements, crop ontology (Shrestha et al. 2010) terms can be used to define traits allowing data from different experiments to be shared using the same measurement protocols.

The trait and phenotype tables (experiment and plot table as another example) represent a common theme of the database that one table lists a high level human readable overview of information, while a larger table (plot and phenotype tables) list all values associated with a database term. This allows users to query the database from different perspectives. For example, a user could find all data for one specific experiment while another user can find all measurements of grain yield in the database without concern for the experiments where the data was collected.

The final aspect of the database relating plot information and hand-measured phenotypes to HTP are a set of tables for HTP measurements as illustrated in Fig. 5.4. To accurately track the sheer volume of data, each collection time of HTP data receives a unique (data acquisition) run ID in an HTP run (or acquisition) table. This ID is composed of the date and time of the start of data collection along with the date and time for the end of data collection. Along with the run ID, the HTP platform is recorded as it could consist of ground based or aerial platforms. Finally, the experiment ID that was measured is linked to the run and platform ID. The HTP run table provides the high-level overview, with experiment ID linking back to the plot and phenotype tables. The HTP platform ID links to a table that describes the platform such as a ground based or UAV system allowing one program to operate many different HTP systems.

While the HTP run table overviews each time of data collection, point and image data is stored in an HTP measurement table. This table lists the HTP run and platform ID, along with a sensor ID and if the measurement value is within a defined plot, the corresponding plot ID. The coordinates of the measurement are also listed along with the UTC time when the measurement was collected. Due to the different types of data, the actual data value is not stored, but a meta data measurement ID is stored. This measurement ID can be used to find the value in several different output tables depending on sensor type. A measurement ID that corresponds to an ultrasonic table would store the point data as a height measurement. Data from normalized difference vegetation index (NDVI) sensors are stored in an NDVI table, with tables being added for different traits or sensor output. For point data, the actual value from the sensor is stored in the output tables. For image or multi-dimensional data, such as full spectrum data, the output table consist of the measurement ID, the image or output file, and the md5sum of the file.

A standard practice of naming the image file consist of adding the date, time, sensor ID, and original name which prevents any duplicate image names. After a unique name is added to each image, the images are stored outside of the database, currently on an HPC cluster. By providing a pointer to the files, rather than storing

the files themselves, the database can store millions of data points while maintaining a small size, whereas image data can quickly exceed terabytes of data.

For image data, or other data that requires significant processing time such as ortho-mosaic images, additional tables could be built to store processed data. Advancing the described database, ortho-mosaic images may be stored in a table like image data that points to the ortho-mosaic file. Either in the table or associated tables, the parameters files that were used to make the processed image and the extracted results could be saved. This would allow a full reconstruction of any published data to evaluate the methods and results for accuracy.

### ***5.4.3 Data Integrity***

Throughout the HTP data processing pipeline, there are numerous built in checks to maintain data integrity. Some of the checks that are performed are making sure that point data values are within standard ranges, for example if NDVI values are above one, the data point is set to missing. For each type of sensor, basic operations can be used to check the sensor output and remove or flag output that may indicate sensor or HTP platform problems. For image and file data, the md5sum is calculated on the original images, and any copied or moved images ensuring that there was no data corruption. In practice, many of these checks have been added to scripts that run automatically to download the data from sensor devices, check data integrity, perform renaming and formatting for the database, uploading information to the database or appropriate locations, and often reporting the results of the operation to the user. For programs wanting to use such a system, a first step would be to curate much of the data using command line tools. Once the process for each particular program is in place, the command line operations can be incorporated into a scripting language such as Python to automate the procedures. While developing automated procedures takes an upfront investment of time, it prevents mistakes that can occur manually and speeds up the data processing pipeline allowing near real time data analysis.

### ***5.4.4 Data Backups***

Data backups are another part of the overall management strategy for HTP data. Scripts to backup databases as well as new data can be developed to automatically run every day, or any time interval, limiting the amount of data that could be lost in a catastrophe. In addition to storing data on an HPC cluster, data is also backed up to a NAS providing two separate physical locations for data storage. Cloud-based backup solutions are another potential option to provide reliable off-site archiving of data for purposes of disaster recovery in the event of massive data loss.

### **5.4.5 Laboratory Procedures**

Along with data management and processing pipelines, laboratories should also be keen on making sure users follow documented protocols. Especially for processing daily HTP measurements, the more standardized protocols can be from file naming conventions to transferring data from HTP platforms to computer, the easier and faster downstream data processing can be. Some of the areas where standardization can work are in file naming at the site of data collection. By using a standardized file name, scripts can be written to automatically parse the file with minimal human intervention. In addition to file names, enforcing rules within the database can also prevent data loss, such as only allowing traits with a defined and valid trait ID to be added to the database. This prevents a user from simply inputting data that does not have descriptions of how the data was collected.

### **5.4.6 Summary**

Data processing forms a key part of phenomics and is essential to moving data from raw measurements on an HTP platform to information that can be used for analysis. While a single trial or project may be able to be managed in an ad hoc manner; to fully realize the genetic gains of HTP integrated data systems must be used. By carefully determining how data should be stored and curated, data collected today could be viable for analysis years into the future.

## **5.5 Data and Trait Analysis**

High-throughput phenotyping provides users with large volumes of data that can help plant breeders be more effective, yet the challenge is transforming the data into decisions. Within the wheat community, there are several examples of deriving biological insights and breeding decisions from phenotypic data. At the most basic level, HTP data can be used to correlate to traits of interest, specifically grain yield. Several studies show significant correlations of NDVI and canopy temperature to grain yield, with correlations sufficiently high for indirect selection (Crain et al. 2017, 2018; Montesinos-López et al. 2017). Relationships between these two traits and grain yield have been well established (Ball and Konzak 1993; Amani et al. 1996; Babar et al. 2006b) for various crop growth stages (Pask et al. 2012). For a breeding program interested in deploying HTP quickly, traits such as NDVI and canopy temperature for which a large body of literature and methods exist may be the easiest and fastest route to increasing selection gains. While grain yield can only be measured at the end of the growing season, the ability to take HTP measurements

like NDVI and canopy temperature multiple times can provide a more thorough assessment of a cultivars yield potential.

While HTP can be used in only a phenotypic setting, the full power of phenotyping will be found in associating HTP and genotypic data. Combining both dense phenotypic data and genetic data from next generation sequencing, researchers have the ability to understand plant dynamics and employ this information in marker assisted selection. Phenotypic data from HTP can be used for QTL mapping which associates genetic locations with a trait of interest. Using HTP data that defined crop growth (Busemeyer et al. 2013b) mapped QTL controlling the biomass accumulation of triticale, with their results showing that the QTL effect was dependent on time. This dynamic control of the trait, resulted in one QTL being important early in the growing season, but having little effect on biomass yield at later times. In addition to wheat, HTP data from several other crops have been used for QTL analysis including drought and well-watered cotton (*Gossypium hirsutum*) to identify genetic regions of abiotic tolerance (Pauli et al. 2016). In rice (*Oryza sativa*) Tanger et al. (2017) showed that many QTL that were identified by hand measurements were highly correlated to QTLs measured by HTP platforms. These examples highlight the power of HTP to collect precision data that can be combined with molecular marker data to investigate the control of quantitative traits.

Genomic selection is another promising area to apply HTP data. In typical GS settings, a training population that has been both phenotyped and genotyped is used to develop a model, and then the model can be used to predict the phenotypic value of ungenotyped individuals. While most of the gains from GS are the result of reduced breeding cycle time (Heffner et al. 2010), increasing the accuracy with which plants are selected would also increase breeding efficiency. While this is an active area of research two studies show the potential for gains incorporating GS and HTP. Rutkoski et al. (2016) used multi-trait GS to incorporate canopy temperature and NDVI as secondary traits into GS models resulting in up to a 70% increase in model accuracy. Crain et al. (2018) found an average of 12% increase in model accuracy by combining canopy temperature and NDVI from HTP platforms in GS models. These approaches combining GS and HTP data show great promise for increasing accuracy and power for selection in breeding programs.

High-throughput phenotyping provides the ability to collect data at multiple time points opening new opportunities for longitudinal studies and understanding plant dynamics over the entire life cycle. While data is often assessed at a single time point e.g. (Busemeyer et al. 2013b; Pauli et al. 2016; Rutkoski et al. 2016; Crain et al. 2017, 2018; Tanger et al. 2017), the processes controlling plant growth are not static, supporting that plant status should be analyzed over time. One method to analyze the longitudinal data provided from HTP is functional trait mapping (Ma et al. 2002; Wu and Lin 2006). This approach fits a mathematical model (such as a sigmoid function) to the data and decomposes the phenotype values into a few parameters that describe the model. These parameters can then be used for QTL analysis, reflecting dynamic changes across multiple measurements. Jiang et al. (2019) used spectral reflectance measurements collected through a mobile, ground based HTP platform to map nitrogen stress dynamics in wheat. The QTLs identified showed a range of

response for how wheat responded to nitrogen deficiency throughout the growing season.

Machine learning may also provide another way to use temporally dependent data sets. Wang et al. (2019b) used machine learning to classify the date of heading in wheat by analyzing images with a convolutional neural network. Using information from the neural network, a model was built that reported heading date within three days of manual phenotype measurements. Heading date is a common phenotypic measurement within breeding programs, and the ability to automate this measurement to HTP collection could standardize data collection and reduce the time and effort associated with measuring this trait.

Data from HTP platforms has the ability to fundamentally alter the plant breeding paradigm. At one extreme, the quantity and quality of data that can be collected in-season would enable breeding programs to grow larger populations, yet selectively harvest plots or individual plants with desired characteristics. At the other extreme, HTP data could be used in early generations with GS allowing plants to be selected years earlier than phenotypic selection. While the most practical and actual applications of HTP will probably result somewhere between these extremes, the ability to increase genetic gains will hinge on the ability to analyze data quickly and efficiently. Programs will need to have resources to quickly analyze data and pipelines must be developed to handle the flow of data so that results can be reported in-season. If the data cannot be analyzed in-season the ability to selectively harvest plots (example above) would not be feasible. Programs wanting to routinely, deploy HTP should be aware of the significant lead time required to develop a smooth pipeline that can be used for in-season data analysis and decision making.

## 5.6 Summary

High-throughput phenotyping is still in its infancy. While there are some arguments that the promises of HTP have not been realized sufficiently fast (Araus et al. 2018), in only a decade the field has moved from a few concept HTP platforms to an abundance of different platforms that can be modified for the desired measurements and deployed at the scale of entire breeding programs. While choosing the correct platform and sensor configurations are import for success, the ability to translate data to genetic gains includes comprehensive downstream aspects for data management and analysis. Successful applications of HTP will require teams of individuals (Shi et al. 2016) composed of skills ranging from genetics, agronomy, engineering, computer science, plant science, and statistics to obtain the most benefit from time and money invested. While the future of HTP research will continue to advance HTP platform and sensor development, it is more likely that data analysis and manipulation will be key to driving gains in plant breeding. By utilizing the latest machine learning and statistical techniques, researchers will be able to effectively translate raw data into informed breeding decisions.

**Acknowledgements** This material is based upon work supported by the National Science Foundation Plant Genome Research Program (PGRP) under Grant No. (1238187)—‘A Field-Based High-Throughput Phenotyping Platform for Plant Genetics,’ the United States Agency for International Development (USAID) Feed the Future Innovation Lab for Applied Wheat Genomics (Cooperative Agreement No. AID-OAA-A-13-00051), EARly-concept Grants for Exploratory Research (EAGER) Grant No. 2019-67013-29008 from the USDA National Institute of Food and Agriculture (NIFA), and NIFA International Wheat Yield Partnership Grant No. 2017-67007-25933/project accession no. 1011391. Any opinions, findings, conclusions, or recommendations expressed in this publication are those of the authors and do not necessarily reflect the view of the U.S. Department of Agriculture.

## References

- Aasen H, Burkart A, Bolten A, Bareth G (2015) Generating 3D hyperspectral information with lightweight UAV snapshot cameras for vegetation monitoring: From camera calibration to quality assurance. *ISPRS J Photogramm Remote Sens* 108:245–259. <https://doi.org/10.1016/j.isprsjprs.2015.08.002>
- Alexis C, Philippe B, Benoit de S, et al (2012) A semi-automatic system for high throughput phenotyping wheat cultivars in-field conditions: description and first results. *Funct Plant Biol* 39:914–924. <https://doi.org/10.1071/FP12065>
- Amani I, Fischer RA, Reynolds MP (1996) Canopy temperature depression association with yield of irrigated wheat cultivars in a hot climate. *J Agron Crop Sci* 176:119–129
- Andrade-Sanchez P, Gore MA, Heun JT et al (2014) Development and evaluation of a field-based, high-throughput phenotyping platform. *Funct Plant Biol* 41:68–79. <https://doi.org/10.1071/FP13126>
- Araus JL, Cairns JE (2014) Field high-throughput phenotyping: The new crop breeding frontier. *Trends Plant Sci* 19:52–61. <https://doi.org/10.1016/j.tplants.2013.09.008>
- Araus JL, Kefauver SC, Zaman-Allah M et al (2018) Translating high-throughput phenotyping into genetic gain. *Trends Plant Sci* 23:451–466. <https://doi.org/10.1016/j.tplants.2018.02.001>
- Arend D, Junker A, Scholz U et al (2016) PGP repository: a plant phenomics and genomics data publication infrastructure. *Database* 2016:1–10. <https://doi.org/10.1093/database/baw033>
- Babar MA, Reynolds MP, Van Ginkel M et al (2006a) Spectral reflectance to estimate genetic variation for in-season biomass, leaf chlorophyll, and canopy temperature in wheat. *Crop Sci* 46:1046–1057. <https://doi.org/10.2135/cropsci2005.0211>
- Babar MA, Reynolds MP, Van Ginkel M et al (2006b) Spectral reflectance indices as a potential indirect selection criteria for wheat yield under irrigation. *Crop Sci* 46:578–588. <https://doi.org/10.2135/cropsci2005.0059>
- Babar MA, van Ginkel M, Reynolds MP et al (2007) Heritability, correlated response, and indirect selection involving spectral reflectance indices and grain yield in wheat. *Aust J Agric Res* 58:432. <https://doi.org/10.1071/ar06270>
- Bai G, Ge Y, Hussain W et al (2016) A multi-sensor system for high throughput field phenotyping in soybean and wheat breeding. *Comput Electron Agric* 128:181–192. <https://doi.org/10.1016/j.compag.2016.08.021>
- Ball ST, Konzak CF (1993) Relationship between grain yield and remotely-sensed data in wheat breeding experiments. *Plant Breed* 110:277–282. <https://doi.org/10.1111/j.1439-0523.1993.tb00590.x>
- Barker J, Zhang N, Sharon J et al (2016) Development of a field-based high-throughput mobile phenotyping platform. *Comput Electron Agric* 122:74–85. <https://doi.org/10.1016/j.compag.2016.01.017>

- Burnette M, Kooper R, Maloney JD et al (2018) TERRA-REF data processing infrastructure. In PEARC'18: Practice & Experience in Advanced Research Computing. ACM, New York, NY, Pittsburgh, PA, pp 1–7
- Busemeyer L, Mentrup D, Möller K et al (2013a) Breedvision - A multi-sensor platform for non-destructive field-based phenotyping in plant breeding. *Sensors (Switzerland)* 13:2830–2847. <https://doi.org/10.3390/s130302830>
- Busemeyer L, Ruckelshausen A, Möller K et al (2013b) Precision phenotyping of biomass accumulation in triticale reveals temporal genetic patterns of regulation. *Sci Rep* 3:2442. <https://doi.org/10.1038/srep02442>
- Cabrera-Bosquet L, Crossa J, von Zitzewitz J et al (2012) High-throughput phenotyping and genomic selection: the frontiers of crop breeding converge. *J Integr Plant Biol* 54:312–320. <https://doi.org/10.1111/j.1744-7909.2012.01116.x>
- Chapman S, Merz T, Chan A et al (2014) Pheno-Copter: a low-altitude, autonomous remote-sensing robotic helicopter for high-throughput field-based phenotyping. *Agronomy* 4:279–301. <https://doi.org/10.3390/agronomy4020279>
- Cobb JN, DeClerck G, Greenberg A et al (2013) Next-generation phenotyping: requirements and strategies for enhancing our understanding of genotype-phenotype relationships and its relevance to crop improvement. *Theor Appl Genet* 126:867–887. <https://doi.org/10.1007/s00122-013-2066-0>
- Cooper M, Chapman SC, Podlich DW, Hammer GL (2002) The GP problem: quantifying gene-to-phenotype relationships. *Silico Biol* 2:151–64
- Coppens F, Wuyts N, Inzé D, Dhondt S (2017) Unlocking the potential of plant phenotyping data through integration and data-driven approaches. *Curr Opin Syst Biol* 4:58–63. <https://doi.org/10.1016/j.coisb.2017.07.002>
- Crain J, Mondal S, Rutkoski J et al (2018) Combining high-throughput phenotyping and genomic information to increase prediction and selection accuracy in wheat breeding. *Plant Genome* 11:1–14. <https://doi.org/10.3835/plantgenome2017.05.0043>
- Crain J, Reynolds M, Poland J (2017) Utilizing high-throughput phenotypic data for improved phenotypic selection of stress-adaptive traits in wheat. *Crop Sci* 57:648–659. <https://doi.org/10.2135/cropsci2016.02.0135>
- Crain JL, Wei Y, Barker J et al (2016) Development and deployment of a portable field phenotyping platform. *Crop Sci* 56:965–975. <https://doi.org/10.2135/cropsci2015.05.0290>
- Deery D, Jimenez-Berni J, Jones H et al (2014) Proximal remote sensing buggies and potential applications for field-based phenotyping. *Agronomy* 4:349–379. <https://doi.org/10.3390/agronomy4030349>
- Du M, Noguchi N (2017) Monitoring of wheat growth status and mapping of wheat yield's within-field spatial variations using color images acquired from UAV-camera System. *Remote Sens* 9. <https://doi.org/10.3390/rs9030289>
- Fabre J, Dauzat M, Nègre V et al (2011) PHENOPSIS DB: an information system for Arabidopsis thaliana phenotypic data in an environmental context. *BMC Plant Biol* 11. <https://doi.org/10.1186/1471-2229-11-77>
- Fahlgren N, Gehan MA, Baxter I (2015) Lights, camera, action: High-throughput plant phenotyping is ready for a close-up. *Curr Opin Plant Biol* 24:93–99. <https://doi.org/10.1016/j.pbi.2015.02.006>
- Fiorani F, Schurr U (2013) Future scenarios for plant phenotyping. *Annu Rev Plant Biol* 64:267–91. <https://doi.org/10.1146/annurev-arplant-050312-120137>
- Furbank RT, Tester M (2011) Phenomics - technologies to relieve the phenotyping bottleneck. *Trends Plant Sci* 16:635–644. <https://doi.org/10.1016/j.tplants.2011.09.005>
- Haghighattalab A, González Pérez L, Mondal S et al (2016) Application of unmanned aerial systems for high throughput phenotyping of large wheat breeding nurseries. *Plant Methods* 12:35. <https://doi.org/10.1186/s13007-016-0134-6>
- Hassan MA, Yang M, Rasheed A et al (2018) A rapid monitoring of NDVI across the wheat growth cycle for grain yield prediction using a multi-spectral UAV platform. *Plant Sci*. <https://doi.org/10.1016/j.plantsci.2018.10.022>

- Heffner EL, Lorenz AJ, Jannink JL, Sorrells ME (2010) Plant breeding with genomic selection: gain per unit time and cost. *Crop Sci* 50:1681–1690. <https://doi.org/10.2135/cropsci2009.11.0662>
- Holman FH, Riche AB, Michalski A, et al (2016) High throughput field phenotyping of wheat plant height and growth rate in field plot trials using UAV based remote sensing. *Remote Sens* 8:1–24. <https://doi.org/10.3390/rs8121031>
- Hughes N, Askew K, Scotson CP et al (2017) Non-destructive, high-content analysis of wheat grain traits using X-ray micro computed tomography. *Plant Methods* 13:1–16. <https://doi.org/10.1186/s13007-017-0229-8>
- Jensen T, Apan A, Young F, Zeller L (2007) Detecting the attributes of a wheat crop using digital imagery acquired from a low-altitude platform. *Comput Electron Agric* 59:66–77. <https://doi.org/10.1016/j.compag.2007.05.004>
- Jiang L, Sun L, Ye M, et al (2019) Functional mapping of N deficiency-induced response in wheat yield-component traits by implementing high-throughput phenotyping. *Plant J* 97:1105–1119. <https://doi.org/10.1111/tpj.14186>
- Jiang Y, Li C, Paterson AH, et al (2018) Quantitative analysis of cotton canopy size in field conditions using a consumer-grade RGB-D camera. *Front Plant Sci* 8:1–20. <https://doi.org/10.3389/fpls.2017.02233>
- Kipp S, Mistele B, Baresel P, Schmidhalter U (2014) High-throughput phenotyping early plant vigour of winter wheat. *Eur J Agron* 52:271–278. <https://doi.org/10.1016/j.eja.2013.08.009>
- Kirchgessner N, Liebisch F, Pfeifer J (2017) The ETH field phenotyping platform FIP : A. 1347–1351. <https://doi.org/10.1071/FP16165>
- Leinonen R, Sugawara H, Shumway M (2011) The sequence read archive. *Nucleic Acids Res* 39:2010–2012. <https://doi.org/10.1093/nar/gkq1019>
- Li Y-F, Kennedy G, Davies F, Hunter J (2010) PODD: an ontology-driven data repository for collaborative phenomics research. In: Chowdhury G, Koo C, Hunter J (eds) *The Role of Digital Libraries in a Time of Global Change*. Springer, Berlin Heidelberg, Berlin, Heidelberg, pp 179–188
- Lopes MS, Reynolds MP, Jalal-Kamali MR et al (2012) The yield correlations of selectable physiological traits in a population of advanced spring wheat lines grown in warm and drought environments. *F Crop Res* 128:129–136. <https://doi.org/10.1016/j.fcr.2011.12.017>
- Ma CX, Casella G, Wu R (2002) Functional mapping of quantitative trait loci underlying the character process: a theoretical framework. *Genetics* 161:1751–1762
- Maded S, Jin X, Lu H et al (2019) Ear density estimation from high resolution RGB imagery using deep learning technique. *Agric For Meteorol* 264:225–234. <https://doi.org/10.1016/j.agrformet.2018.10.013>
- Mcgahee K (2016) Image-based mapping system for transplanted seedlings. Dissertation Kansas State University. Kansas State University
- Montes JM, Technow F, Dhillon BS et al (2011) High-throughput non-destructive biomass determination during early plant development in maize under field conditions. *F Crop Res* 121:268–273. <https://doi.org/10.1016/j.fcr.2010.12.017>
- Montesinos-López OA, Montesinos-López A, Crossa J et al (2017) Predicting grain yield using canopy hyperspectral reflectance in wheat breeding data. *Plant Methods* 13:4. <https://doi.org/10.1186/s13007-016-0154-2>
- Mueller-Sim T, Jenkins M, Abel J, Kantor G (2017) The Robotanist: a ground-based agricultural robot for high-throughput crop phenotyping. In: *IEEE International Conference on Robotics and Automation (ICRA)*. Singapore, Singapore
- Mullan DJ, Reynolds MP (2010) Quantifying genetic effects of ground cover on soil water evaporation using digital imaging. *Funct Plant Biol* 37:703–712. <https://doi.org/10.1071/FP09277>
- Pask A, Pietragalla J, Mullan D, Reynolds MP (2012) Physiological breeding II: a field guide to wheat phenotyping. Mexico City, Mexico



- Pauli D, Andrade-Sanchez P, Carmo-Silva AE, et al (2016) Field-based high-throughput plant phenotyping reveals the temporal patterns of quantitative trait loci associated with stress-responsive traits in cotton. *Genes/Genomes/Genetics* 6:865–879. <https://doi.org/10.1534/g3.115.023515>
- Peng RD (2011) Reproducible research in computation science. *Science* (80) 334:1226–1227
- Reynolds MP, Langridge P (2016) Physiological breeding. *Curr Opin Plant Biol* 311:1162–171. <https://doi.org/10.1016/j.pbi.2016.04.005>
- Richards RA, Rebetzke GJ, Watt M et al (2010) Breeding for improved water productivity in temperate cereals: Phenotyping, quantitative trait loci, markers and the selection environment. *Funct Plant Biol* 37:85–97. <https://doi.org/10.1071/FP09219>
- Rutkoski J, Poland J, Mondal S et al (2016) Canopy temperature and vegetation indices from high-throughput phenotyping improve accuracy of pedigree and genomic selection for grain yield in wheat. *Genes/Genomes/Genetics* 6:2799–2808. <https://doi.org/10.1534/g3.116.032888>
- Shakoor N, Lee S, Mockler TC (2017) High throughput phenotyping to accelerate crop breeding and monitoring of diseases in the field. *Curr Opin Plant Biol* 38:184–192. <https://doi.org/10.1016/j.pbi.2017.05.006>
- Shi Y, Thomasson JA, Murray SC et al (2016) Unmanned aerial vehicles for high-throughput phenotyping and agronomic research. *PLoS One* 1–26. <https://doi.org/10.5061/dryad.65m87>
- Shrestha R, Arnaud E, Mauleon R et al (2010) Multifunctional crop trait ontology for breeders' data: field book, annotation, data discovery and semantic enrichment of the literature. *AoB Plants*. <https://doi.org/10.1093/aobpla/plq008>
- Singh D, Wang X, Kumar U et al (2019) High-throughput phenotyping enabled genetic dissection of crop lodging in wheat. *Front Plant Sci* 10:1–11. <https://doi.org/10.3389/fpls.2019.00394>
- Susko AQ, Gilbertson F, Heuschele DJ et al (2018) An automatable, field camera track system for phenotyping crop lodging and crop movement. *HardwareX* 4:1–13. <https://doi.org/10.1016/j.ohx.2018.e00029>
- Tanger P, Klassen S, Mojica JP et al (2017) Field-based high throughput phenotyping rapidly identifies genomic regions controlling yield components in rice. *Sci Rep* 7:1–8. <https://doi.org/10.1038/srep42839>
- Tattaris M, Reynolds MP, Chapman SC (2016) A direct comparison of remote sensing approaches for high-throughput phenotyping in plant breeding. *Front Plant Sci* 7:1131. <https://doi.org/10.3389/fpls.2016.01131>
- Virlet N, Sabermanesh K, Sadeghi-Tehran P, Hawkesford MJ (2017) Field Scanalyzer: an automated robotic field phenotyping platform for detailed crop monitoring. *Funct Plant Biol* 44:143–153. <https://doi.org/10.1071/FP16163>
- Wang X, Amos C, Lucas M, et al (2019a) Small plot identification from video streams for high-throughput phenotyping of large breeding populations with unmanned aerial systems. In: *Autonomous Air and Ground Sensing Systems for Agricultural Optimization and Phenotyping IV*. International Society for Optics and Photonics, p 110080D
- Wang X, Thorp KR, White JW, et al (2016) Approaches for geospatial processing of field-based high-throughput plant phenomics data from ground vehicle platforms. *Trans ASABE* 59:1053–1067. <https://doi.org/10.13031/trans.59.11502>
- Wang X, Xuan H, Evers B, et al (2019b) High-throughput phenotyping with deep learning gives insight into the genetic architecture of flowering time in wheat. *Gigascience* 8:. <https://doi.org/10.1093/gigascience/giz120>
- White JW, Andrade-sanchez P, Gore MA et al (2012) Field-based phenomics for plant genetics research. *F Crop Res* 133:101–112. <https://doi.org/10.1016/j.fcr.2012.04.003>
- White JW, Conley MM (2013) A flexible, low-cost cart for proximal sensing. *Crop Sci* 53:1646–1649. <https://doi.org/10.2135/cropsci2013.01.0054>
- Wilkinson MD, Dumontier M, Aalbersberg IJJ, et al (2016) The FAIR Guiding Principles for scientific data management and stewardship. *Sci data* 3:1–9
- Wu RL, Lin M (2006) Opinion - functional mapping - how to map and study the genetic architecture of dynamic complex traits. *Nat Rev Genet* 7:229–237. <https://doi.org/10.1038/nrg1804>

- Xue J, Su B (2017) Significant remote sensing vegetation indices: A review of developments and applications. *J Sensors*. <https://doi.org/10.1155/2017/1353691>
- Yang G, Liu J, Zhao C et al (2017) Unmanned aerial vehicle remote sensing for field-based crop phenotyping: current status and perspectives. *Front Plant Sci* 8:1111. <https://doi.org/10.3389/fpls.2017.01111>
- Yu K, Kirchgessner N, Grieder C et al (2017) An image analysis pipeline for automated classification of imaging light conditions and for quantification of wheat canopy cover time series in field phenotyping. *Plant Methods* 13:1–13. <https://doi.org/10.1186/s13007-017-0168-4>
- Zhang Y, Zhang N (2018) Imaging technologies for plant high-throughput phenotyping: a review. *Front Agric Sci Eng* 5:406–419. <https://doi.org/10.15302/j-fase-2018242>

# Chapter 6

## High-Throughput Phenotyping (HTP) and Genetic Analysis Technologies Reveal the Genetic Architecture of Grain Crops



Wanneng Yang, Xuehai Zhang, and Lingfeng Duan

**Abstract** Both functional genomics studies and crop breeding have reached the large-scale and high-throughput stage. However, compared with the rapid progress in sequencing technologies, the traditional measurement of crop traits is still labor intensive and inefficient. To address this issue, several phenotyping platforms and freely available phenotyping techniques have been developed in recent years. In this chapter, we discuss phenotyping research for important grain crop traits using multidisciplinary technologies and then introduce some pioneering work on combining high-throughput phenotyping and quantitative trait locus (QTL) mapping or genome-wide association study (GWAS) to uncover the genetic information of various traits in grain crops. In addition, by addressing some key issues in bridging phenotype-genotype gaps, we hope to provide useful information and alternative phenotyping solutions to crop scientists. We believe that such endeavors in high-throughput phenotyping will accelerate crop genetic improvement, such as drought resistance and increased yield.

**Keywords** High-throughput · Phenotyping · GWAS · QTL · Genetic architecture · Genome selection · Grain crop

---

W. Yang (✉)

National Key Laboratory of Crop Genetic Improvement and National Center of Plant Gene Research, Huazhong Agricultural University, Wuhan 430070, People's Republic of China  
e-mail: [ywn@mail.hzau.edu.cn](mailto:ywn@mail.hzau.edu.cn)

X. Zhang

National Key Laboratory of Wheat and Maize Crops Science/College of Agronomy, Henan Agricultural University, Zhengzhou 450002, People's Republic of China  
e-mail: [xuehai85@126.com](mailto:xuehai85@126.com)

L. Duan

College of Engineering, Huazhong Agricultural University, Wuhan 430070, People's Republic of China  
e-mail: [duanlingfeng@mail.hzau.edu.cn](mailto:duanlingfeng@mail.hzau.edu.cn)

## 6.1 Introduction

With the rapid progress in sequencing technologies, genome projects for certain important grain crops, such as rice (Goff et al. 2002) and maize (Schnable et al. 2009), have been accomplished with the generation of accurate and large genome maps. With such large-scale sequencing data, the next challenge is to dissect genes controlling important crop traits, i.e., crop functional genomics, which requires not only robust genome sequencing tools but also high-throughput phenotyping technologies. In addition to crop genetic studies, crop breeders also seek to identify the best progeny in a large number of lines using high-throughput and reliable phenotyping in the field (Araus and Cairns 2014).

‘Plant phenomics’ has been defined as the non-destructive and accurate acquisition of high-dimensional phenotypic data on an organism-wide scale throughout plant development (Houle et al. 2010) and is no longer a new term. ‘Plant phenotyping’, a buzzword in recent years, refers to the set of methodologies and protocols which measure plant growth traits from organs to the canopy (Fiorani and Schurr 2013). In recent years, many high-throughput phenotyping (HTP) facilities have been constructed, with a strong effort to promote this field of study, such as genetic improvement, genome selection, and assistant breeding.

In this chapter, we first introduce phenotyping research of important crop traits, including shoot traits and root system architectures (in greenhouse and in field), yield and quality-related traits. Next, we introduce some pioneering work combining high-throughput phenotyping with quantitative trait locus (QTL) mapping or genome-wide association study (GWAS) to reveal the genetic basis of these traits. For most crop scientists, the development of a high-throughput phenotyping facility requires multidisciplinary teamwork and is a challenging project (Yang et al. 2013). Thus, in this chapter, by addressing phenotyping studies and the key points in bridging phenotype-genotype gaps, we hope to provide useful information and alternatives for crop scientists and benefit crop genetic improvement.

## 6.2 High-Throughput Phenotyping in Controlled Environments

### 6.2.1 Automated Phenotyping Platforms in Greenhouse Conditions

Significant developments have been made in developing automated phenotyping platforms employed in growth chambers and greenhouses over the last few years. Granier et al. used an automated platform, named PHENOPSIS, to phenotype traits under water deficit conditions in *Arabidopsis thaliana* (Granier et al. 2006). For rapid optical phenotyping of seedling leaf area and relative growth rate, GROWSCREEN

was also established and used to quantify the dynamics of seedling growth acclimation under altered light conditions (Walter et al. 2007). Combining chlorophyll fluorescence imaging and automated plant growth analysis, GROWSCREEN FLUORO allows simultaneous phenotyping of leaf growth and chlorophyll fluorescence in *Arabidopsis thaliana* and other rosette plants with a throughput of approximately 60 plants per hour (Jansen et al. 2009). To dissect ‘yield-enhancement’ genes from a plethora of transgenic cereal materials, a phenotyping platform, TraitMill, was developed by CropDesign (Reuzeau et al. 2010). TraitMill can be used to screen plants weekly and count and weigh seeds after harvest and determine phenotypic traits (aboveground biomass, plant height, total number of seeds, total number of filled seeds, total weight of seeds and harvest index) that, combined with genotypic data, were analyzed to identify genes that improve the yield of cereals. Incorporating color imaging, X-ray computed tomography (CT), automatic controls, and computers, the joint group from Huazhong Agricultural University and Huazhong University of Science and Technology (Wuhan, China) has been developed as a high-throughput rice phenotyping facility (HRPF, Fig. 6.1), which was used to monitor 4 morphology-related traits, 2 biomass-related traits, and 9 yield-related traits. Both the quantitative evaluation of the performance and the construction details of the HRPF were discussed, and its maximum throughput was reported to be 1920 pot-grown rice plants per day out of a greenhouse capacity of 5472 pots (Yang et al. 2014). Another highly intelligent phenotyping robot, GROWSCREEN-Rhizo, was capable of imaging plant roots and shoots simultaneously, and the throughput of the setup was 60 rhizotrons per hour out of a total capacity of 72 rhizotrons (Nagel et al. 2012).

### **6.2.2 RGB Imaging, 3D Imaging and Modeling for Crop Shoot Traits**

Several modern optical imaging technologies have been utilized in plant phenotyping. Visible light imaging (RGB imaging) of plants enables measurement of plant morphological traits in a non-destructive manner and therefore makes it possible to measure dynamic shoot growth. The technical difficulty lies in developing imaging processing and data analysis algorithms to extract useful information from the RGB images. Plants with mere overlapping problems, such as *Arabidopsis*, are generally imaged from above for the evaluation of biomass or leaf area (Walter et al. 2007; Fabre et al. 2011). Side view images from two perpendicular angles and an image from above are used for cereal crops because the leaves overlap in cereal crops, especially when the plants grow older (Honsdorf et al. 2014; Petrozza et al. 2014; Hairmansis et al. 2014). The biomass can be predicted using the projected shoot area with three images and linear models, but the accuracy of the predictive model for

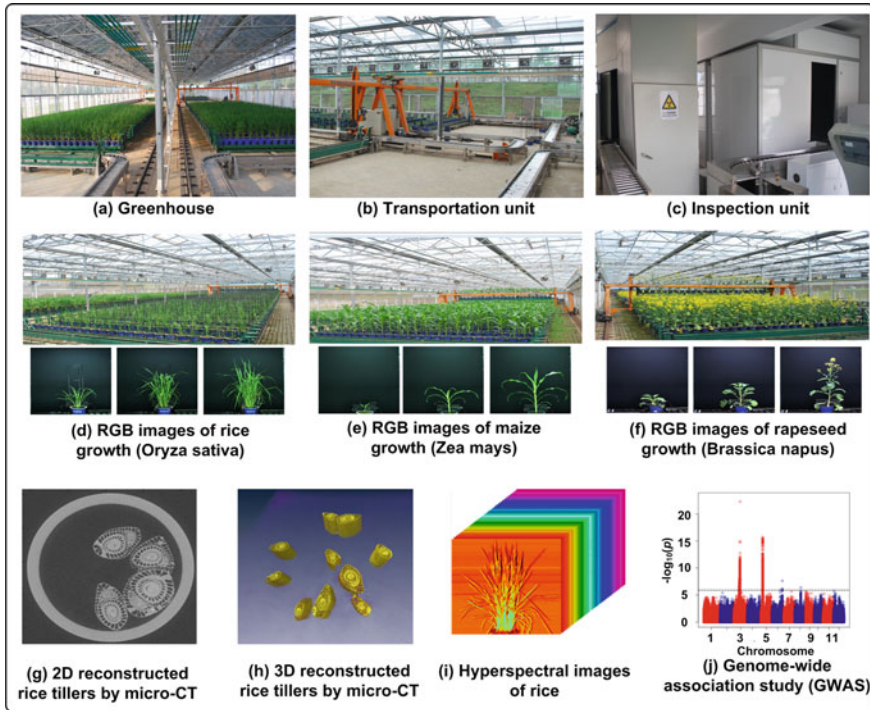


**Fig. 6.1** The high-throughput rice phenotyping facility (HRPF) in Huazhong Agricultural University, China: **a** greenhouse for rice cultivation; **b** cultivation unit and transportation unit with two automatic guided vehicles (AGV); **c** inspection chamber; **d** acquired RGB images of rice growth; **e** acquired RGB images of maize growth; **f** acquired RGB images of rapeseed growth; **g** 2D reconstructed rice tillers by micro-CT; **h** 3D reconstructed rice tillers by micro-CT; **i** acquired hyperspectral images of one rice plant (400–1000 nm); **j** new loci were dissected with a combination of novel phenotypic traits and genome-wide association study (GWAS). (Figure 6.1a–j are courtesy of Wanneng Yang, Huazhong Agricultural University, China)

biomass may decline when cereal plants produce more multiple shoots and overlapping leaves. However, adding the growth date (Golzarian et al. 2011) or new morphological features (Yang et al. 2014) to the model can improve its accuracy.

Plant growth monitoring over a period of plant development by visible light imaging enables assessment of the sum of stress response mechanisms, which offers the possibility to tease apart these responses, such as leaf rolling of drought stress in rice (Duan et al. 2018). Meanwhile, rapid visible light imaging allows growth measurement of large populations and therefore enables the use of a genetic approach to identify the genes responsible for variation under abiotic stress. Visible light imaging can also provide information on plant color, thus allowing quantification of senescence arising from biotic stress, such as pathogen infections (Rajendran et al. 2009).

Because of its low cost, ease of maintenance and fast imaging, visible light imaging technology has become the most widely used imaging technology in plant phenotyping. The plant architecture (the plant shape in three dimensions), which provides information on the adaptation of a plant to environmental conditions, is a key parameter of a plant's phenotype. Moreover, the plant architecture conveys meaningful information concerning the developmental stage of the vegetation period or yield-producing parameters. 3D reconstruction from multiple images acquired by RGB cameras is a good choice (Paprocki et al. 2012). However, it requires a considerable amount of post-processing. Laser scanning provides a satisfying resolution and accuracy and is another convenient technique for acquiring the 3D geometry of plant architecture. Current applications of 3D laser scanning include the measurement of biomass (Keightley and Bawden 2010) and the root volume of trees (Wagner et al. 2011) and growth monitoring for barley plants (Paulus et al. 2014). Compared with the 3D reconstruction method, the cost of laser scanning is relatively high. A recent work demonstrated that by carefully selecting a low-cost sensor, it is possible to substitute an expensive laser scanner in many plant phenotyping tasks (Paulus et al. 2014).

### 6.2.3 Crop Root System Architecture

Roots are crucial organs that directly provide nutrients and water to crops and impact the crop yield; thus, rapid phenotyping of crop root system architecture (RSA) is essential for crop scientists (de Dorlodot et al. 2007). One feasible solution is to implement color cameras to phenotype the RSA in a transparent growth medium, such as gellan gum in a glass cylinder (Topp et al. 2013). The RhizoChamber-Monitor (Fig. 6.2), which includes an automatic imaging system, an irrigation system and an image analysis pipeline, is developed to extract root growth traits, such as the dynamics of length and diameter (Wu et al. 2018). Another alternative is to use aerated nutrients in a transparent plexiglass rhizobox (Courtois et al. 2013). Indeed, using 3D *in vivo* imaging of rice in a gellan gum medium and the free software pipeline, GiA Roots (Galkovskiy et al. n.d.), 25 RSA traits (2D or 3D) were identified, and these relevant quantitative phenotypes can benefit from the genetic dissection of the RSA. However, these methodologies have several pitfalls, such as the lack of consideration of microbial interactions, soil structure and mechanical impedances, and the identification of the natural RSA under soil conditions is urgently needed. One solution is to screen 2D root images of plants grown in transparent soil-filled containers. A highly intelligent root phenotyping robot, GROWSCREEN-Rhizo, was developed to image plant roots and shoots simultaneously, and the throughput of the setup was 60 rhizotrons per hour out of a total capacity of 72 rhizotrons (Nagel et al. 2012).

Roots are notoriously difficult to phenotype in the soil. X-ray CT is capable of detecting the inner structure of an object; thus, it could be a promising solution to recover 3D root architecture in soil environments (Fig. 6.2d). Equipped with a high-resolution X-ray  $\mu$ CT system, robust software using RooTrak (Mairhofer et al. 2012)

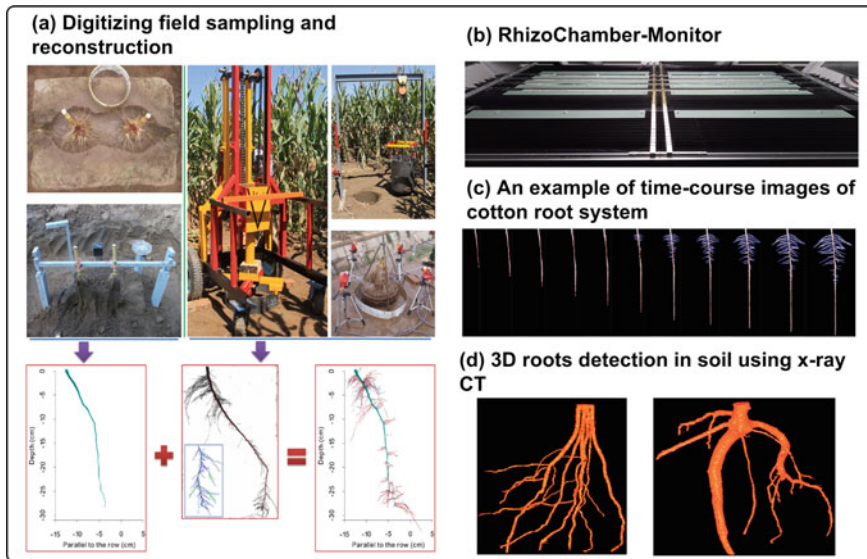


**Fig. 6.2 Root phenotyping in field and lab:** **a** integrated methods for quantifying 3D maize root architecture in field using field sampling and a reconstruction algorithm; **b** RhizoChamber-Monitor: a robotic platform to determine root growth in transparent polycarbonate (PC) panels; **c** an example of time-course images of a cotton root system (Fig. 6.2a–c are courtesy of Jie Wu, Nanjing Agricultural University, China); **d** 3D root detection in soil using X-ray CT (Fig. 6.2d is courtesy of Xuecheng Zhou, South China Agricultural University, China)

visual tracking was developed to distinguish both gravitropic and plagiotropic root branches and recover the full range of RSA (Mairhofer et al. 2013). RooTrak was also shown to extract both coarse and fine roots (the resolution was up to 24  $\mu\text{m}$ ) in different soil textural types. In addition, soil pore architectures can also be imaged *in vivo* to explore the interactions between RSA and soil compaction (Tracy et al. 2012). Unlike the purpose of using X-ray CT in clinical applications (such as reconstructing human tissues with high resolution for a better diagnosis), the ultimate purpose of root phenotyping is to provide more digital traits with high throughput and high reliability. Thus, in our opinion, reducing the time and cost of CT scanning and RSA trait extraction and automating the entire CT scanning procedure will promote the inspection of RSAs with micro-CT at a high-throughput level. X-ray CT was also applied for the phenotyping of multi-tiller plants (such as rice plants) (Wu et al. 2019).

#### 6.2.4 Novel Sensors for Physiological Traits

Thermal infrared imaging (IR) provides information on the temperature of leaves or plants. Because the rate of transpiration or evaporation from the leaf is a major



determinant of leaf temperature, thermal imaging is also appropriate for screening plants for variation in stomatal conductance, especially under laboratory conditions (Jones et al. 2009). IR serves as a useful tool in the diagnosis and quantification of plant responses to water stress. Near infrared (NIR) imaging is a promising technology for measuring plant water content. However, NIR is now most widely used to calculate classical vegetation indices using NIR reflectance ranging from 850 nm to 1200 nm. NIR imaging using NIR cameras still remains in the technical development stages. The main factors that hinder the popularization of NIR cameras are their high price and relatively low spatial resolution. Kobori and Tsuchikawa used an NIR camera to image individual leaves of *Ligustrum japonicum* with highly varying water contents, but the sensitivity of the setup to subtle differences in plant water content needs to be further confirmed (Kobori and Tsuchikawa 2009). Fluorescent imaging enables measurement of differences in the maintenance of photosynthetic function under stresses, such as salt and drought stress, before the reduction in plant growth can be detected (Baker 2008). However, fluorescence imaging using 2D fluorescence cameras is still restricted to *Arabidopsis* or other rosette plants. To extend its application to larger plants with different shoot geometries, substantial improvements such as advanced 3D reconstructions are needed. Fluorescence imaging is also capable of determining leaf area, and measurements over time can be used to calculate the growth rate (Barbagallo et al. 2003).

Hyperspectral reflectance measurement allows the identification of spectral signatures related to plant stress levels and other plant growth characteristics. Hyperspectral imaging using a camera provides both spectral and spatial information and was used to measure the biomass of individual rice plants (Feng et al. 2013). Another interesting study combined magnetic resonance imaging (MRI) and positron emission tomography (PET) to reveal the dynamic changes in plant structures and functions such as growth and carbon allocation within complex root systems (Jahnke et al. 2009). However, because of the high cost and relatively long imaging time, MRI and PET are not appropriate for screening large plant populations at high frequency and high throughput. Furthermore, MRI is particularly sensitive to the moisture content of the sample and the presence of paramagnetic ions.

### **6.2.5 Key Points in Designing Phenotyping Experiments in Greenhouse Conditions**

Design of greenhouse experiments is an important step in achieving a phenotype-genotype map. Using smaller blocks or adjusting for microclimate differences in the greenhouse would be better than relocating plants during an experiment (Brien et al. 2013). In our opinion, for some experiments, such as for drought resistance or yield improvement studies, growing and testing plants in a movable shelter (with climate similar to the outdoors) would be better than experiments in an environment-controlled greenhouse, which will bring more unwanted microclimate differences. To

measure certain physiological traits (such as canopy temperature) that are susceptible to environmental variation (such as air temperature and wind speed) (Jones et al. 2009), moving the camera and keeping the plants stationary would be better than transporting the plants to the inspection chamber via a long belt conveyor. Besides, construction difficulties and costs may be reduced. Normally, individual pot-grown plants are transported via conveyor to a stable imaging chamber, which benefits the image analysis. However, when measuring some physiological traits easily influenced by environments or inspecting large plants that are inconvenient to move, moving the sensors would be preferable. Moreover, plant phenotypes are the result of the interaction of genotypes and the environment. Therefore, environmental monitoring during the experiments is vital and should receive the at least the same amount of attention as the traits that are measured.

In addition, there are some other essential factors in the design of phenotyping experiments, such as a flexible image analysis pipeline (Hartmann et al. 2011), a meticulous experimental setup (Poorter et al. 2012) and even the choice of the proper pot (or growth container) (Poorter et al. 2012). Another consideration is the management of the huge amount of image data from multi-optical sensors. The use of the open-source image analysis pipeline (HTPheno) (Hartmann et al. 2011) and integrated analysis platform (IAP) (Klukas et al. 2014) should be encouraged. In addition to commercial solutions and some specific software, IAP offers freely available data management and data processing for different images of several species (maize, barley and *Arabidopsis*) and allows users to extend the functions of IAP by adding new algorithms in terms of plug-ins.

## 6.3 High-Throughput Phenotyping in Field Conditions

### 6.3.1 *Why Field Phenotyping Is Urgently Needed*

Field phenotyping and greenhouse phenotyping are applied for different goals, and there are several differences between greenhouse versus field experiments. First, compared with controlled environments in greenhouses or laboratories, field conditions are notoriously heterogeneous. In addition, some field environmental factors, for example, the soil environment, are difficult to simulate under controlled conditions, yet they are significant in plant growth and development. For instance, the amount of nutrients and water available to plants grown in pots is considerably smaller than in the field because of the smaller volume of soil available to roots within a pot (Poorter et al. 2012). In addition, plants constitute a canopy in the field instead of growing individually in pots, which will influence the light absorption and growth architecture and requires different strategies for image acquisition and image analysis. Thus, phenotyping results from controlled environments are difficult to extrapolate to the field.

### 6.3.2 *Current Phenotyping Tools for Field Conditions*

In recent years, remote sensing by unmanned aerial vehicles, including ground-based field phenotyping at the plot level or single-plant level with higher spatial resolution has been widely applied in crop breeding (Maes and Steppe 2018). Effective field phenotyping at the plot level involves the incorporation of several low-cost commercial sensors on a field vehicle, such as a sonar sensor to extract canopy height, an infrared radiometer sensor to obtain canopy temperature, and a multi-spectral sensor to measure canopy reflectance, and biomass can be estimated by combining canopy reflectance and height (Sanchez et al. 2014). Moreover, to acquire more traits with high spatial and spectral resolution, RGB color imaging and hyper-spectral imaging can also be added to the moving field-scan phenotyping platform. However, these imaging techniques are susceptible to variable environmental conditions, such as changing sunlight. One smart solution is to fix these imaging sensors on a black moving chamber carried by a vehicle, as is done with the BreedVision system (Busemeyer et al. 2013). Equipped with multisensors and specific trait calibrations, novel field-based phenotyping can nondestructively measure plant traits, including plant height, tiller density, grain yield, moisture content, leaf color, lodging and dry biomass, at an operating speed of  $0.5 \text{ ms}^{-1}$ . Using the novel traits obtained by BreedVision, the genetic variation in biomass accumulation was dissected, with the potential to reveal the dynamic genetics of complex traits (Busemeyer et al. 2013). In the Chinese Academy of Sciences, Guo's group developed a series of field phenotyping solutions to extract plant architecture and leaf traits in the field using lidar and other optical sensors, which can be loaded with mobile monitoring tools, mobile monitoring vehicles, unmanned ground vehicles (UGVs) and unmanned aerial vehicles (UAVs) (Fig. 6.3) (Jin et al. 2018).

To extract the root architectural traits in a few minutes in the field, Shovelomics, a high-throughput and labor intensive root phenotyping method (requires root excavation and rinsing) was proposed (Trachsel et al. 2011). A commercial portable root scanner (CI-600, CID Bio-Science Inc., USA) can provide a high-resolution color image of roots in the soil; however, the screening field of view is limited ( $21.59 \text{ cm} \times 19.56 \text{ cm}$ ), and the procedure is so inconvenient (clear tubes must be installed prior to inserting the imaging sensor) that it can hardly be applied in high-throughput screening of full-view RSA. In the future, non-destructive full-view screening of root growth in the field will be one of the biggest challenges in plant phenotyping, which will require the breakthrough of novel imaging techniques.

### 6.3.3 *Flexible Phenotyping Techniques in Field Conditions*

To further promote ground-based field phenotyping, some low cost and feasible methodologies should be popularized. One prospect is to carry a mobile phone equipped with a color camera and to use corresponding image calibration (with a



**Fig. 6.3 Field phenotyping tools for crops:** **a** mobile monitoring tool; **b** mobile monitoring vehicle; **c** unmanned ground vehicle (UGV); **d** unmanned aerial vehicle (UAV); **e** the individual segmented results of maize plant analysis from terrestrial lidar data using deep learning; **f** group data registered from six scanning stations for maize growth, and three representative maize plants of the three growth stages (jointing stage, heading stage, and ripening stage) are shown in the right corner. (Figure 6.3a–f are courtesy of Qinghua Guo, Chinese Academy of Sciences, China)

standard color card), a robust image segmentation algorithm, and traits for calculating the algorithm to extract the quantitative traits of growth status or disease response for crops. Combined with machine learning, a smartphone application was developed to detect several leaf diseases, including *Cercospora* leaf spot, rust and bacterial blight in sugar beet, and the distinguishing accuracy of the smartphone system was shown to be better than the accuracy of experts (Hallau et al. 2018). If the calculating ability of mobile phones is not satisfactory and the connection speed of wireless networks is fast enough, delivering the captured images to a workstation with a wireless network could be an alternative for image analysis. In addition, free-access databases of plant image analysis software, which can expediently guide crop researchers to identify solutions, are also recommended (Lobet et al. 2013). Another innovation is the small agri-robot, named Prospero, which functions like an ant (<http://www.cropscience.bayer.com/Magazine/Ripe-for-Robots.aspx>) to replace skilled workers in caring for crops and may someday measure and record crop phenotypic traits, which will alter our understanding of crop development.

## 6.4 High-Throughput Phenotyping for Crop Yield and Quality

Improvements in crop yield and quality are the ultimate goal of crop breeding and crop research. In recent years, crop functional genomics has entered a large-scale and high-throughput stage, and thus, high-throughput evaluation of crop yield and quality is urgently needed (Zhang and Wing 2013). Some open-source image analysis software for grain characteristics or panicle traits has been encouraged by utilizing a low-cost flatbed scanner or digital camera. SmartGrain is a free-use software to extract seed size and seed shape but not color-related traits (Tanabata et al. 2012). GrainScan could be a significant supplement for the rapid measurement of grain size and color (Whan et al. 2014). Following the manual processing of rice panicles, P-TRAP and PANorama are recommended as flexible tools to quantify several panicle traits with good accuracy (AL-Tam et al. 2013; Crowell et al. 2014).

Some research has demonstrated that integrated and fully automatic facilities can be developed for achieving yield trait scoring or grain quality evaluation (Fig. 6.4). The integrated SEA (Seed Evaluation Accelerator) facility, for example, can automatically thresh rice panicles, score yield traits, and pack filled spikelets, with a capability of up to 1440 plants per day and a mean absolute percentage error of less than 5% (Duan et al. 2011). To improve the measuring efficiency of ear traits, a high-throughput phenotypic method for maize ear was proposed, which obtains the panoramic image of a corn ear and total kernels, number of ear rows and kernels per row, and the efficiency of image acquisition is 15 ears per minute (Du et al. 2018). To inspect rice quality, another automatic inspection facility incorporating some optical sensors was established to extract parameters such as the protein content and moisture content (Kawamura et al. 2003). In the future, decreasing the cost of

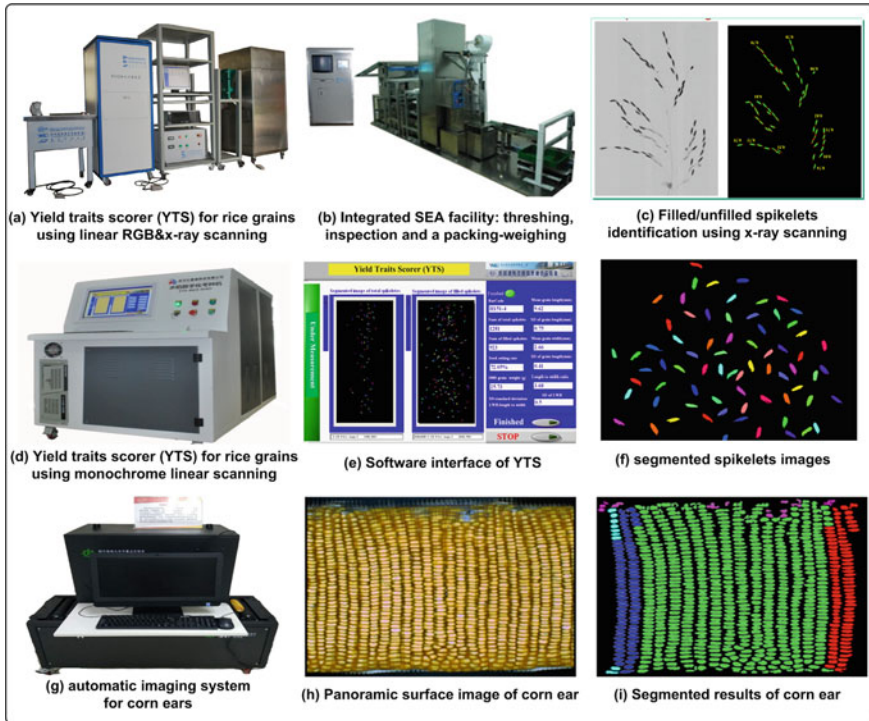


**Fig. 6.4 High-throughput phenotyping for yield-related traits in China:** **a** first generation yield traits scorer for yield-related traits using bimodal imaging (linear RGB and X-ray scanning); **b** SEA facility: an integrated phenotyping machine to extract yield-related traits, which mainly contains automatic threshing unit, automatic inspection unit and packing-weighing unit; **c** the panicle image acquired with X-ray scanning to identify and count filled/unfilled spikelet number; **d** prototype of a yield traits scorer (YTS) using linear RGB scanning; **e** software interface of YTS; **f** segmented spikelet images using YTS (Fig. 6.4a–f are courtesy of Wanneng Yang, Huazhong Agricultural University, China); **g** prototype of yield traits scorer for maize ear; **h** the scanned panoramic surface image of corn ear; **i** segmented results of corn ear (Fig. 6.4g–i are courtesy of Xinyu Guo, Beijing Research Center for Information Technology in Agriculture, China)

these novel photonics-based inspection techniques, improving their reliability, and providing more novel traits that are difficult to inspect manually could promote the popularization of these integrated tools and benefit more crop research groups.

## 6.5 High-Throughput Phenotyping and Genetic Mapping

### 6.5.1 *Genetic Study Using Traditional Phenotyping: Rice as a Case Study*

Green super rice (GSR) was first proposed by Qifa Zhang 10 years ago and should possess resistance to multiple insects and diseases, high nutrient efficiency, and drought resistance, reducing greenhouse gas emissions (Zhang 2007). To achieve this goal as soon as possible, it is important and necessary to better understand, manage and utilize the existing genes for resistance to diseases and insects, N- and P-use efficiency, drought resistance, grain quality, and yield. Before 2000, only approximately 130 genes were cloned in total. Hereafter, the number of cloned genes has gone up each year, especially after the draft sequence of the rice genome was released in 2002, and an increasing number of genes governing agricultural traits were isolated and functionally characterized, reaching 100 genes in 2005. By the end of 2007, a total of 3000 genes were well characterized through various traditional approaches (Yao et al. 2018) and have potential applications in breeding GSR. The cloned genes are involved in a wide variety of phenotypic traits. These traits were obtained by traditional phenotyping methods and can be classified into five categories: yield (number of panicles, number of grains per panicle, grain weight, plant architecture), grain quality (appearance/eating/nutritional quality), fertilizer efficiency (efficient nitrogen/phosphorus use), insect and disease resistance, and habitat adaptability (drought/flood/cold/heat resistance) (Zuo and Li 2014; Li et al. 2018; Meng et al. 2019). With the rapid development of high-throughput sequencing technology, digital genebanks (genotypic data) are easily and accurately obtained by all kinds of sequencing technologies. However, phenotyping is a serious bottleneck in functional genomics. Additionally, linking digital genebanks to phenotypes in a high-throughput format is of critical importance for rapid identification of new allele combinations suitable for the development of GSR cultivars. Thus, phenotypic data generated from various high-throughput phenotyping platforms (such as a facility, greenhouse or tractor gantry or drone in field) are necessary for mining new genes that could be used in 'Omics'-based strategies to develop GSR in the future (Wing et al. 2018).

With the rapid development of high-throughput sequencing technology, conventional quantitative trait locus (QTL) mapping based on linkage and genome-wide association studies (GWAS) based on linkage disequilibrium (LD) have been proven to be two powerful tools that are complimentary to each other in dissecting the genetic basis of complex traits in crops. In addition, many genes governing important traits have been cloned in crops. However, the fact that traditional crop phenotype detection methods are labor intensive, low-throughput in capacity, time consuming, costly and frequently destructive to plants still remains a limiting factor and is far behind the development of other omics studies, such as genomics (Chen et al. 2014).

## 6.5.2 Genetic Study Using High-Throughput Phenotyping

To solve this bottleneck and accelerate the development of functional genomics, in recent years, some research teams around the world have developed several high-throughput precision phenotype platforms or technologies to improve phenotyping efficiency. Based on these platforms or phenotyping technologies, some traits were phenotyped at the microscopic level to the whole plant level under normal and stress conditions that can be categorized as shoot apical meristem (SAM) morphology, root phenotyping traits, plant morphological traits, leaf architecture traits, color traits, biomass or yield-related traits, growth-related traits and so on. Meanwhile, many of these traits have been used in growth modeling, yield or biomass prediction, genetic mapping, genomic selection or machine learning. In particular, QTL mapping and GWAS have been conducted with many traits obtained in several crops (Table 6.1), including barley (Honsdorf et al. 2014), rice (Wu et al. 2018), triticale (Jin et al. 2018), wheat (Klukas et al. 2014; Rasheed et al. 2014), and maize (Zhang et al. 2017; Leiboff et al. 2015). Some major achievements in combining high-throughput phenotyping and genetic mapping in grain crops will be introduced in this section.

At the microscopic level, maize seedling shoot apical meristem (SAM) morphological traits (shape and size) were extracted using a high-throughput image-processing pipeline. In addition, GWAS and QTL mapping of the SAM morphological traits were conducted in an association panel and a backcross (BC) population, respectively. The results illustrate that the microscopic seedling SAM is a predictor for adult phenotypes and genes associated with SAM morphometric variation that not previously predicted contribute to regulating SAM size (Leiboff et al. 2015; Leiboff et al. 2016).

For root phenotyping, Topp et al. identified 89 univariate QTLs and 5 major multivariate QTLs associated with 25 root-related traits using semiautomatic *in vivo* 3D imaging and a digital phenotyping pipeline in a rice linkage mapping population (Wu et al. 2018). In addition, 15 rice root traits obtained from a root photography system were used in a GWAS and 19 and 78 significant associations were found at  $P < 1e-05$  and  $P < 1e-04$ , respectively. It should be noted is that most associations were detected for the number of deep roots and deep root mass, whereas no associations were found for total root biomass and deep root proportions (Courtois et al. 2013). In *Brassica napus*, a high-throughput root phenotyping method was also used to phenotype root architecture-related traits under high phosphate (Pi) and low Pi conditions and to identify QTLs controlling these traits (Shi et al. 2013).

For leaf phenotyping, two genetic mapping works for leaf traits in rice and maize were performed in cooperation of National Key Laboratory of Crop Genetic Improvement at Huazhong Agricultural University. They performed a GWAS for 29 leaf traits related to leaf size, shape, and color at three growth stages using a self-designed high-throughput leaf scoring (HLS) system on a panel of 533 rice accessions and identified 73, 123 and 177 new loci for traits associated with leaf size, color and shape, respectively. Interestingly, 9 loci containing known leaf-related genes were also detected (Yang et al. 2015). In addition, 22 leaf architecture traits of a maize recombinant



**Table 6.1** Combining high-throughput phenotyping and QTL mapping or GWAS in grain crops

ID	Traits category/environment	Crop	Platform	Phenotype	Population <sup>a</sup>	Sample size <sup>b</sup>	No. marker <sup>c</sup>	Methods	References
1	Agronomic and yield-related phenotyping/Controlled environment	Rice	HRPF	33 features, including projected area (A), 25 morphological features and 7 texture features,	IAP	533	4,358,600 SNPs	GWAS	11
2		Maize	IPK	biomass, growth traits, growth rate	IAP	252	50 K SNP array	GWAS & GS	76
3		Rice	PANorama	49 panicle phenotypes	IAP/RIL	242/168	700,000 SNPs/30,984 SNPs	GWAS & Linkage analysis	74
4		Maize	RAP-Maize	106 traits: 10 plant morphological traits, 22 leaf architecture traits, one plant color trait, three biomass-related traits, six histogram texture traits, and 64 growth-related traits,	RIL	167	2,496 recombinant bins	Linkage analysis	69
5		Rice	High-throughput hyperspectral imaging system (HHIS)	1,540 hyperspectral indices, i.e., chlorophyll content	IAP	529	4,358,600 SNPs	GWAS	80

(continued)

Table 6.1 (continued)

ID	Traits category/environment	Crop	Platform	Phenotype	Population <sup>a</sup>	Sample size <sup>b</sup>	No. marker <sup>c</sup>	Methods	References
6		Rice	high-throughput micro-CT-RGB (HCR) imaging system, YTS	74 phenotypic traits: tiller traits, shoot dry weight, etc.	IAP	234	2,863,169 SNPs	GWAS	33
7	Yield-related traits/Field	Bread wheat	A semiautomatic sensing system	Yield-component traits: modified canopy adjusted ratio index 2 ((MCARI2), normalized difference vegetation index (NDVI), MERIS terrestrial chlorophyll index (MTCI) at N deficiency-induced response	IAP	211	68,958 SNP	functional mapping, GWAS	75
8	Biomass/Field	Triticale	BreedVision	Biomass	DH	647	1710 DArT markers	GWAS	48
9	Drought tolerance/Controlled environment	Wild barley	LemnaTec 3D Scanalyzer	14 traits: shoot area, caliper length, height, color, biomass, etc.	ILs	42	1,536 SNPs	Linkage analysis	14

(continued)

Table 6.1 (continued)

ID	Traits category/environment	Crop	Platform	Phenotype	Population <sup>a</sup>	Sample size <sup>b</sup>	No. marker <sup>c</sup>	Methods	References
10	Drought tolerance/Controlled environment and field	Wheat	LemmaTec 3D Scanalyzer	Biomass, leaf area, growth (rate) and transpiration	RIL	250	–	Linkage analysis	77
11	Drought tolerance/Controlled environment	Rice	HRPF, HLS	51 image-based traits (t-traits) and traditional drought resistance (DR) traits	IAP/RIL	507/192	4,358,600 SNPs/2499 bins	GWAS	79
12	Salinity tolerance/Controlled environment	Rice	LemmaTec 3D Scanalyzer system	Plant growth and transpiration	IAP	553	700 k SNP	GWAS	78
13	Leaf phenotyping	Rice	HLS	29 leaf traits related to leaf size, shape, and color	IAP	533	4,358,600 SNPs	GWAS	73
14	Microscopic level/Controlled environment	Maize	High-throughput image-processing pipeline	Shoot apical meristem (SAM) morphology	IAP	369	1.2 M SNPs	GWAS	70
15		Maize	Axio Imager.Z10	Shoot apical meristem (SAM) morphology	BC	841	–	Linkage analysis	71
16	Root phenotyping/Field	Rice	3D root imaging and analysis platform	25 Root system architecture (RSA)	RIL	171	–	Linkage analysis	26
17	Root phenotyping/Controlled environment	Rice	Rhizoscope phenotyping platform	15 traits: Root system architecture and biomass traits	IAP	167	16,664 markers (9,727 DArTs and 6,717 SNPs)	GWAS	28

(continued)

Table 6.1 (continued)

ID	Traits category/environment	Crop	Platform	Phenotype	Population <sup>a</sup>	Sample size <sup>b</sup>	No. marker <sup>c</sup>	Methods	References
18		<i>Brassica napus</i>	Flatbed scanner	Primary root length (PRL), lateral root length (LRL), lateral root number (LRN), lateral root density (LRD) and biomass traits under low Pi (LP) and high Pi (HP) conditions	DH	190	798 markers	Linkage analysis	72

<sup>a</sup> IAP, inbred association panel (consists of a set of inbred lines); RIL, recombinant inbred lines; DH, double haploid population; BC, backcross population; NIL, near isogenic lines; ILs, introgression lines

<sup>b, c</sup> The values separated by a slash (/) indicate sample size (b) or marker numbers (c) corresponding to multiple populations, respectively. '-', not mentioned in reference

inbred population (RIL) at each of 16 time points were obtained and mapped to the QTLs governing these traits via linkage analysis (Zhang et al. 2017). In addition, novel traits have proven to play important roles in predicting digital biomass accumulation or as indicators of final yield prediction and an ideal plant type concept based on phenotypic traits in the early growth stage has been proposed, which provided a new strategy for breeders to optimize plant architecture towards an ideotype in breeding maize or other crops (Zhang et al. 2017).

Yield improvement is a central goal of breeding for most grain crops. Thus, dissection of the genetic bases of yield and its component traits will aid in understanding the genetics and molecular characteristics of yield traits and accelerating crop genetic improvement. In fact, most genetic mapping studies with high-throughput phenotyping focus on agronomic and yield-related traits under normal or abiotic stress conditions. For agronomic and yield-related traits, PANorama was used to phenotype inflorescence architecture-related traits and 49 panicle phenotypes, and then GWAS and QTL mapping was performed to test the biological validity of these traits (Crowell et al. 2016). QTL mapping with SmartGrain software in rice and GWAS with digital image analysis in synthetic hexaploid wheat was performed to understand the genetic control of grain morphology (Tanabata et al. 2012; Rasheed et al. 2014). In bread wheat (*Triticum aestivum* L.), by integrating functional mapping and high-throughput phenotyping data of yield-component traits under N deficient conditions, several QTLs were detected as determining the pattern and magnitude of response to low N stress and normal N supply throughout the wheat life cycle (Jiang et al. 2018). Additionally, the biomass of 252 maize inbred lines was obtained using the IPK (Leibniz Institute of Plant Genetics and Crop Plant Research) automated noninvasive plant phenotyping system at four time points; 12 main effect marker-trait associations by GWAS and four additional marker loci affecting growth dynamics using nonparametric functional mapping and multivariate mapping approaches were detected (Muraya et al. 2017).

For the study of abiotic stress, many drought or salinity tolerance QTLs in grain crops can be detected based on these phenotype platforms and novel image-based traits (Table 6.1). For example, 44 drought tolerance (DR) QTLs were found in a set of 47 six-week-old wild barley introgression lines with a LemnaTec 3D Scanalyzer (Honsdorf et al. 2014). Using the LemnaTec 3D Scanalyzer, QTL mapping related to biomass, leaf area, growth (rate) and transpiration in a wheat RIL population under water stress was performed and 20 QTLs for these traits were identified (Parent et al. 2015). In another study, GWAS was conducted on plant growth and transpiration traits in a rice association panel under salinity stress, and several significant loci and candidate genes underlying these QTLs were found (Al-Tamimi et al. 2016). Under the HRPF (high-throughput rice phenotyping facility) and HLS (high-throughput leaf scoring), GWAS and linkage analysis on 51 image-based traits (i-traits) and traditional DR traits were carried out in 507 rice diverse accessions and arice biparental mapping population (Guo et al. 2018). In total, 470 association loci were identified for i-traits and traditional DR traits, and 443 loci (94%) were identified using i-traits. More importantly, 69 i-trait locus associations were identified by both GWAS and linkage analysis of the biparental population. A DR gene, *OsPPI5*, its role in DR

was confirmed by transgenic experiment, which proved that a combination of HTP and genetic mapping provides a powerful method for mining causal genes for DR (Guo et al. 2018).

Furthermore, several other studies identified many loci governing different agronomic and yield-related traits through GWAS or linkage analysis in different grain crops based on different phenotype platforms (Table 6.1). Under field conditions, Busemeyer et al. developed a phenotyping platform to study dynamic changes in biomass in triticale and then performed GWAS to understand the complex dynamic regulation of biomass (Busemeyer et al. 2013). Combining a high-throughput rice phenotyping facility (HRPF) and GWAS for 15 important traits (including biomass-related traits and yield-related traits) in rice, some new significant traits not amenable to traditional phenotyping (e.g., plant compactness, digital biomass, leaf rolling, and stay-green) were analyzed, and several significant loci were detected (Yang et al. 2014). Additionally, 1540 hyperspectral features of the same rice association panel at the whole plant level during tillering, heading, and ripening stages were obtained using a high-throughput hyperspectral imaging system (HHIS), and 989 significant loci were identified by GWAS (Feng et al. 2017).

## 6.6 High-Throughput Phenotyping and Genome Selection

Genome selection (GS) was first reported in cattle breeding, and it has been proven that selection based on genetic values predicted from markers can substantially increase the rate of genetic gain in animals and plants. However, building an accurate prediction model based on a dataset of individuals or lines that have been genotyped and phenotyped is necessary for GS (Meuwissen et al. 2001). In short, GS is actually using genome-wide markers and statistical modeling to select complex traits. As the cost of sequencing has decreased in recent years, GS has been widely used in plant breeding. Its advantage is to predict how a plant will perform before it is field-tested. Two factors, a training set and a validation set, need to be considered in GS. In detail, first, the ‘training set’ is genotyped and phenotyped, then the ‘training set’ is used to create the GS prediction model, and last, only genotypic information from the breeding material or remaining lines (the validation set) is then fed into the model to calculate genomic estimated breeding values (GEBV) for the validation set; prediction accuracy of the model is determined after comparison with the actual data (Heffner et al. 2009). When building an effective prediction model, a large dataset, including a large number of markers and traits, is needed. With the development of next generation sequencing technology, molecular markers are easily and accurately obtained by all types of sequencing technologies. However, phenotyping is a serious bottleneck in building an accurate model.

In coming years, phenotypic data collected with high-throughput phenotype platforms will have great potential in enhancing GS in grain crops. For example, an unmanned aerial vehicle (UAV) carrying different remote sensing units (RGB, near-infrared, green and blue (NIR-GB) camera) has been used for obtaining sorghum

plant height (PH) data that is used in different genomic prediction models. The results tell us that genomic prediction models were almost identical and that UAV remote sensing could replace traditional measurements in genomic prediction modeling. UAV remote sensing will be an indispensable tool in genomics-assisted plant breeding because it can increase the throughput of phenotyping and decrease its cost (Watanabe et al. 2017). In a wheat GS study, the authors found that without correcting for days to heading, secondary traits could increase accuracies for grain yield by 70% in genomic prediction models, on average. However, the accuracy of the model could increase slightly when considering replications or days to heading. In this study, we learned that secondary traits obtained with high-throughput methods could be used in genomic prediction to improve prediction accuracy (Rutkoski et al. 2016). Moreover, the International Maize and Wheat Improvement Center (CIMMYT) obtained dynamic high-throughput phenotyping (HTP) data of 1170 advanced wheat lines in two environments, drought in 2014 and 2015 and heat in 2015 (Watanabe et al. 2017). Combining 2254 genotyping-by-sequencing (GBS) markers with over 1.1 million phenotypic observations for GS, several GS methods were investigated to best model the phenotypic information and HTP traits improved model performance and increased selection accuracy. The results indicate that GS strategies are a tractable way for plant breeders to increase the rate of genetic gain and select superior higher yielding crop varieties more efficiently (Crain et al. 2018).

It is imperative to understand the biological meaning and genetic basis of new traits measured by multidisciplinary phenotyping technologies instead of traditional phenotyping in the future. However, high-throughput phenotyping has not been sufficiently successful for achieving gene loci discoveries, genomic selection (GS), and machine learning (ML), and the following issues should be considered. (1) Reliable phenotypic traits: high-throughput phenotyping does not mean full-automation, so proper pipeline checking is necessary, which means every piece of phenotypic data should be checked before GWAS, linkage analysis, GS or ML. (2) Proper mapping population: Population sometimes has more of an effect than novel phenotyping tools on gene discovery. (3) Sample size: Appropriately mapped populations usually have more statistical power in detecting loci or genes with true position; however, sample size is influenced by the throughput capacity and operational efficiency of phenotyping platforms. At present, it is difficult to complete the phenome of a large population, such as a nested association mapping (NAM) population, random-open-parent association mapping (ROAM) population or multiparent advanced generation intercross population (MAGIC) (Xiao et al. 2017). (4) Strict environmental control: Unwanted environmental variation alters phenotypic traits and leads to false-negative or false-positive QTL mapping or GWAS.

## 6.7 Conclusions

In recent years, plant phenomics has become an important discipline, and many high-throughput plant phenotyping methodologies have been developed to benefit

crop functional genomics and breeding. Using high-throughput techniques not only acquires phenotypic traits at different time points but can also detect dynamic development at those time points, which could be used to uncover the genetic architecture of complex traits (shown in Fig. 6.5). With genetic analysis tools (e.g., GWAS,

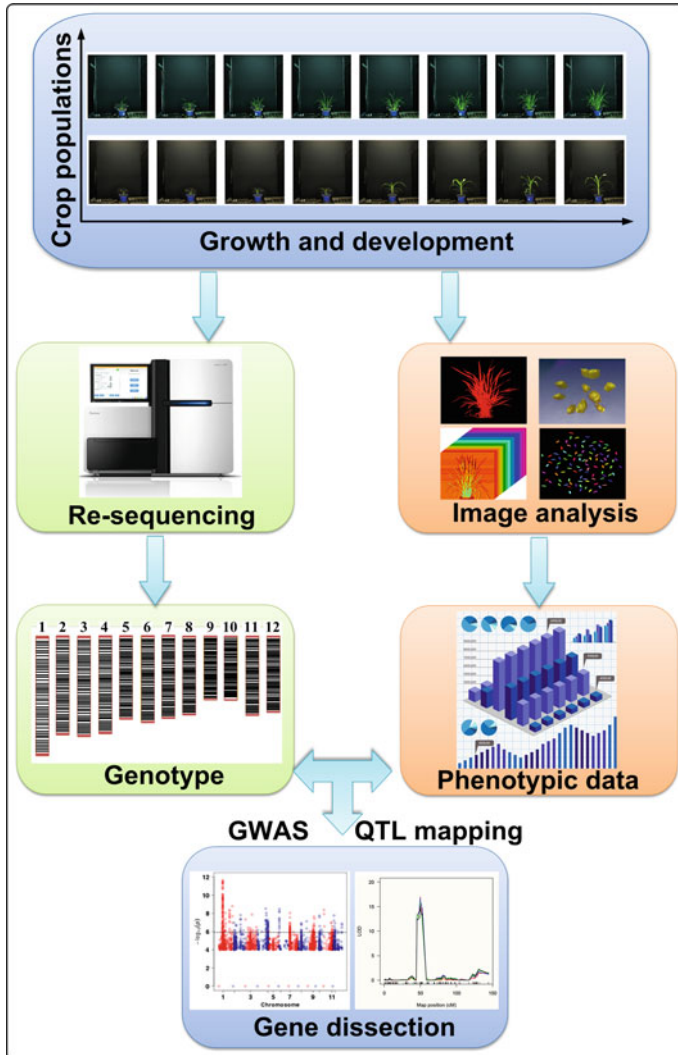


**Fig. 6.5** The combination of phenotypic traits and genetic analysis tools. Some significant traits (cannot be obtained by traditional phenotyping, e.g., plant compactness, grain projected area, 3D RSA in the soil) can be analyzed with novel photonics-based techniques. Moreover, using high-throughput techniques can acquire both phenotypic traits at different time points and dynamic development at those time points



linkage analysis, PheWAS (Denny et al. 2013)), more loci or genes with important function could be dissected with a combination of novel traits, which cannot be obtained by traditional phenotyping. In the future, low-cost phenotyping platforms and open-source image analysis networks should be encouraged and promoted, which calls for cooperative efforts between international plant phenotyping communities. For this purpose, an international plant phenotyping network (IPPN) has been organized (<http://www.plant-phenotyping.org>) and supports the development of concepts and technologies in plant phenotyping through interactions between major phenotyping centers. We believe that high-throughput phenotyping and plant phenomics will provide new insight for dissecting certain complex traits, such as those regulating abiotic stress responses and yield and will benefit crop genetic improvement and the next Green Revolution.

## References

- AL-Tam F, Adam H, Anjos A, Lorieux M, Larmande P, Ghesquière A, Jouannic S and Shahbazkia HR (2013) P-TRAP: a panicle trait phenotyping tool. *BMC Plant Biol* 13:122
- Al-Tamimi N, Brien C, Oakey H, Berger B, Saade S, Ho YS, Schmoekel SM, Tester M, Negrao S (2016) Salinity tolerance loci revealed in rice using high-throughput non-invasive phenotyping. *Nat Commun* 7:13342
- Araus JL, Cairns JE (2014) Field high-throughput phenotyping: the new crop breeding frontier. *Trends Plant Sci* 19(1):52–61
- Baker NR (2008) Chlorophyll fluorescence: a probe of photosynthesis in vivo. *Annu Rev Plant Biol* 59:89–113
- Barbagallo RP, Oxborough K, Pallett KE, Baker NR (2003) Rapid, non-invasive screening for perturbations of metabolism and plant growth using chlorophyll fluorescence imaging. *Plant Physiol* 132:485–493
- Brien CJ, Berger B, Rabie H, Tester M (2013) Accounting for variation in designing greenhouse experiments with special reference to greenhouses containing plants on conveyor systems. *Plant Methods* 9:5
- Busemeyer L, Mentrup D, Möller K, Wunder E, Alheit K, Hahn V, Maurer HP, Reif JC, Würschum T, Müller J et al (2013a) BreedVision — a multi-sensor platform for non-destructive field-based phenotyping in plant breeding. *Sensors* 13:2830–2847
- Busemeyer L, Ruckelshausen A, Möller K, Melchinger AE, Alheit KV, Maurer HP, Hahn V, Weissmann EA, Reif JC, Würschum T (2013b) Precision phenotyping of biomass accumulation in triticale reveals temporal genetic patterns of regulation. *Sci Rep* 3:2442
- Chen D, Neumann K, Friedel S, Kilian B, Chen M, Altmann T, Klukasa C (2014) Dissecting the phenotypic components of crop plant growth and drought responses based on high-throughput image analysis. *Plant Cell* 26(12):4636–4655
- Courtois B, Audebert A, Dardou A, Roques S, Herrera TG, Droc G, Frouin J, Rouan L, Gozé E, Kilian A et al (2013) Genome-wide association mapping of root traits in a japonica rice panel. *PLoS ONE* 8(11):
- Crain J, Mondal S, Rutkoski J, Singh RP, Poland J (2018) Combining high-throughput phenotyping and genomic information to increase prediction and selection accuracy in wheat breeding. *Plant Genome* 11. <https://doi.org/10.3835/plantgenome2017.05.0043>
- Crowell S, Falcão AX, Shah A, Wilson Z, Greenberg AJ, McCouch SR (2014) High-resolution inflorescence phenotyping using a novel image-analysis pipeline, PANorama. *Plant Physiol* 165:479–495

- Crowell S, Korniliev P, Falcao A, Ismail A, Gregorio G, Mezey J, McCouch S (2016) Genome-wide association and high-resolution phenotyping link *Oryza sativa* panicle traits to numerous trait-specific QTL clusters. *Nat Commun* 7:10527
- de Dorlodot S, Forster B, Pagès L, Price A, Tuberosa R, Draye X (2007) Root system architecture: opportunities and constraints for genetic improvement of crops. *Trends Plant Sci* 12(10):474–481
- Denny JC, Bastarache L, Ritchie MD, Carroll RJ, Zink R, Mosley JD, Field JR, Pulley JM, Ramirez AH, Bowton E, Basford MA, Carrell DS, Peissig PL, Kho AN, Pacheco JA, Rasmussen LV, Crosslin DR, Crane PK, Pathak J, Bielinski SJ, Pendergrass SA, Xu H, Hindorf LA, Li R, Manolio TA, Chute CG, Chisholm RL, Larson EB, Jarvik GP, Brilliant MH, McCarty CA, Kullo IJ, Haines JL, Crawford DC, Masys DR, Roden DM (2013) Systematic comparison of phenome-wide association study of electronic medical record data and genome-wide association study data. *Nat Biotechnol* 31:1102–1110
- Du J, Guo X, Wang C, Xiao B (2018) Assembly line variety test method and system for corn ears based on panoramic surface image. *Trans Chinese Soc Agric Eng* 34(13):195–202
- Duan L, Yang W, Huang C, Liu Q (2011) A novel machine-vision-based facility for the automatic evaluation of yield-related traits in rice. *Plant Methods* 7:44
- Duan L, Han J, Guo Z, Tu H, Yang P, Zhang D, Fan Y, Chen G, Xiong L, Dai M, Kevin W, Fiona C, John HD, Yang W (2018) Novel digital features discriminate between drought resistant and drought sensitive rice under controlled and field conditions. *Frontiers in Plant Science* 9:492
- Fabre J, Dauzat M, Nègre V, Wuyts N, Tireau A, Gennari E, Neveu P, Tisné S, Massonnet C, Hummel I, Granie C (2011) PHENOPSIS DB: an information system for *Arabidopsis thaliana* phenotypic data in an environmental context. *BMC Plant Biol* 11:7
- Feng H, Jiang N, Huang C, Fang W, Yang W, Chen G, Xiong L, Liu Q (2013) A hyperspectral imaging system for an accurate prediction of the above-ground biomass of individual rice plants. *Rev Scientific Instrum* 84(9): 095107–095107-10
- Feng H, Guo Z, Yang W, Huang C, Chen G, Fang W, Xiong X, Zhang H, Wang G, Xiong L, Liu Q (2017) An integrated hyperspectral imaging and genome-wide association analysis platform provides spectral and genetic insights into the natural variation in rice. *Sci Rep* 7:4401
- Fiorani F, Schurr U (2013) Future scenarios for plant phenotyping. *Annu Rev Plant Biol* 64:267–291
- Goff SA, Ricke D, Lan TH, Presting G, Wang R, Dunn M, Glazebrook J, Sessions A, Oeller P, Varma H et al (2002) A draft sequence of the rice genome (*Oryza sativa* L. ssp. *japonica*). *Science* 296:92–100
- Golzarian MR, Frick RA, Rajendran K, Berger B, Roy S, Tester M, Lun DS (2011) Accurate inference of shoot biomass from high-throughput images of cereal plants. *Plant Methods* 7:2
- Granier C, Aguirrezabal L, Chenu K, Cookson SJ, Dauzat M, Hamard P, Thioux JJ, Rolland G, Bouchier-Combaud S, Lebaudy A, Muller B, Simonneau T, Tardieu F (2006) PHENOPSIS, an automated platform for reproducible phenotyping of plant responses to soil water deficit in *Arabidopsis thaliana* permitted the identification of an accession with low sensitivity to soil water deficit. *New Phytol* 169:623–635
- Guo Z, Yang W, Chang Y, Ma X, Tu H, Xiong F, Jiang N, Feng H, Huang C, Yang P, Zhao H, Chen G, Liu H, Luo L, Hu H, Liu Q, Xiong L (2018) Genome-wide association studies of image traits reveal genetic architecture of drought resistance in rice. *Mol Plant* 11:789–805
- Hairmansis A, Berger B, Tester M, Roy SJ (2014) Image-based phenotyping for non-destructive screening of different salinity tolerance traits in rice. *Rice* 7:16
- Hallau L, Neumann M, Klatt B, Kleinhenz B, Klein T, Kuhn C et al (2018) Automated identification of sugar beet diseases using smartphones. *Plant Pathol* 67(2):399–410
- Hartmann A, Czauderna T, Hoffmann R, Stein N, Schreiber F (2011) HTPheno: an image analysis pipeline for high-throughput plant phenotyping. *BMC Bioinformatics* 12:148
- Heffner EL, Sorrells ME, Jannink JL (2009) Genomic selection for crop improvement. *Crop Sci* 49:1–12
- Honsdorf N, March TJ, Berger B, Tester M, Pillen K (2014) High-throughput phenotyping to detect drought tolerance QTL in wild barley introgression lines. *PLoS ONE* 9(5):

- Houle D, Govindaraju DR, Omholt S (2010) Phenomics: the next challenge. *Nat Rev Genet* 11(12):855–866
- Jahnke S, Menzel MI, van Dusschoten D, Roeb GW, Bühler J, Minwuyelet S, Blümner P, Temperton VM, Hombach T, Streun M et al (2009) Combined MRI–PET dissects dynamic changes in plant structures and functions. *Plant J* 59:634–644
- Jansen M, Gilmer F, Biskup B, Nagel K, Rascher U, Fischbach A, Briem S, Dreissen G, Tittmann S, Braun S, De Jaeger I, Metzclaff M, Schurr U, Scharf H, Walter A (2009) Simultaneous phenotyping of leaf growth and chlorophyll fluorescence via GROWSCREEN FLUORO allows detection of stress tolerance in *Arabidopsis thaliana* and other rosette plants. *Funct Plant Biol* 36:902–914
- Jiang L, Sun L, Ye M, Wang J, Wang Y, Bogard M, Lacaze X, Fournier A, Beauchene K, Gouache D, Wu R (2018) Functional mapping of N deficiency-induced response in wheat yield-component traits by implementing high-throughput phenotyping. *Plant J*
- Jin S, Su Y, Wu F, Pang S, Gao S, Hu T, Liu J, Guo Q (2018) Stem-Leaf segmentation and phenotypic trait extraction of individual maize using terrestrial LiDAR data. *IEEE T Geosci Remote*. <https://doi.org/10.1109/TGRS.2018.2866056>
- Jones HG, Serraj R, Loveys BR, Xiong L, Wheaton A, Price AH (2009) Thermal infrared imaging of crop canopies for the remote diagnosis and quantification of plant responses to water stress in the field. *Funct Plant Biol* 36:978–989
- Kawamura S, Natsuga M, Takekura K, Itoh K (2003) Development of an automatic rice-quality inspection system. *Comput Electron Agric* 40:115–126
- Keightley K, Bawden G (2010) 3D volumetric modeling of grapevine biomass using Tripod LiDAR. *Comput Electron Agric* 74:305–312
- Klukas C, Chen D, Pape JM (2014) Integrated analysis platform: an open-source information system for high-throughput plant phenotyping. *Plant Physiol* 165:506–518
- Kobori H, Tsuchikawa S (2009) Prediction of water content in *Ligustrum japonicum* leaf using near infrared chemometric imaging. *J Near Infrared Spectroscopy* 17:151–157
- Leiboff S, Li X, Hu HC, Todt N, Yang J, Yu X, Muehlbauer GJ, Timmermans MC, Yu J, Schnable PS, Scanlon MJ (2015) Genetic control of morphometric diversity in the maize shoot apical meristem. *Nat Commun* 6:8974
- Leiboff S, DeAllie CK, Scanlon MJ (2016) Modeling the morphometric evolution of the maize shoot apical meristem. *Front Plant Sci* 7:1651
- Li Y, Xiao J, Chen L, Huang X, Cheng Z, Han B, Zhang Q, Wu C (2018) Rice functional genomics research: past decade and future. *Mol Plant* 11:359–380
- Lobet G, Draye X, Périlleux C (2013) An online database for plant image analysis software tools. *Plant Methods* 9:38
- Maes WH, Steppe K (2018) Perspectives for remote sensing with unmanned aerial vehicles in precision agriculture. *Trends Plant Sci*. <https://doi.org/10.1016/j.tplants.2018.11.007>
- Mairhofer S, Zappala S, Tracy SR, Sturrock C, Bennett M, Mooney SJ, Pridmore T (2012) RooTrak: automated recovery of three-dimensional plant root architecture in soil from x-ray micro-computed tomography images using visual tracking. *Plant Physiol* 158:561–569
- Mairhofer S, Zappala S, Tracy S, Sturrock C, Bennett MJ, Mooney SJ, Pridmore TP (2013) Recovering complete plant root system architectures from soil via x-ray  $\mu$ -computed tomography. *Plant Methods* 9:8
- Meng F, Xiang D, Zhu J, Li Y, Mao C (2019) Molecular mechanisms of root development in rice. *Rice (N Y)* 12:1
- Meuwissen TH, Hayes BJ, Goddard ME (2001) Prediction of total genetic value using genome-wide dense marker maps. *Genetics* 157:1819–1829
- Muraya MM, Chu J, Zhao Y, Junker A, Klukas C, Reif JC, Altmann T (2017) Genetic variation of growth dynamics in maize (*Zea mays* L.) revealed through automated non-invasive phenotyping. *Plant J* 89:366–380
- Nagel KA, Putz A, Gilmer F, Heinz K, Fischbach A, Pfeifer J, Faget M, Blossfeld S, Ernst M, Dimaki C et al (2012) GROWSCREEN-Rhizo is a novel phenotyping robot enabling simultaneous

- measurements of root and shoot growth for plants grown in soil-filled rhizotrons. *Funct Plant Biol* 39:891–904
- Paulski A, Sirault X, Berry S, Furbank R, Fripp J (2012) A novel mesh processing based technique for 3D plant analysis. *BMC Plant Biol* 12:63
- Parent B, Shahinnia F, Maphosa L, Berger B, Rabie H, Chalmers K, Kovalchuk A, Langridge P, Fleury D (2015) Combining field performance with controlled environment plant imaging to identify the genetic control of growth and transpiration underlying yield response to water-deficit stress in wheat. *J Exp Bot* 66:5481–5492
- Paulus S, Dupuis J, Riedel S, Kuhlmann H (2014a) Automated analysis of barley organs using 3D laser scanning: an approach for high throughput phenotyping. *Sensors* 14(7):12670–12686
- Paulus S, Behmann J, Mahlein A-K, Plümer L, Kuhlmann H (2014b) Low-Cost 3D systems: suitable tools for plant phenotyping. *Sensors* 14(2):3001–3018
- Petrozza A, Santaniello A, Summerer S, Tommaso GD, Tommaso DD, Paparelli E, Piaggese A, Perata P, Cellinina F (2014) Physiological responses to Megafol® treatments in tomato plants under drought stress: a phenomic and molecular approach. *Sci Hortic* 174:185–192
- Poorter H, Fiorani F, Stitt M, Schurr U, Finck A, Gibon Y, Usadel B, Munns R, Atkin OK, Tardieu F, Pons TL (2012a) The art of growing plants for experimental purposes: a practical guide for the plant biologist. *Funct Plant Biol* 39:821–838
- Poorter H, Bühler J, van Dusschoten D, Climent J, Postma JA (2012b) Pot size matters: a meta-analysis of the effects of rooting volume on plant growth. *Funct Plant Biol* 39:839–850
- Rajendran K, Tester M, Roy S (2009) Quantifying the three main components of salinity tolerance in cereals. *Plant, Cell & Environ* 32(3):237–249
- Rasheed A, Xia X, Ogonnaya F, Mahmood T, Zhang Z, Mujeeb-Kazi A, He Z (2014) Genome-wide association for grain morphology in synthetic hexaploid wheats using digital imaging analysis. *BMC Plant Biol* 14:128
- Reuzeau C, Pen J, Frankard V, Wolf J, Peerbolte R, Broekaert W, Camp W (2010) TraitMill: a discovery engine for identifying yield-enhancement genes in cereals. *Plant Gene and Trait* 1(1):1–6
- Rutkoski J, Poland J, Mondal S, Autrique E, Perez LG, Crossa J, Reynolds M, Singh R (2016) Canopy temperature and vegetation indices from high-throughput phenotyping improve accuracy of pedigree and genomic selection for grain yield in wheat. *G3 (Bethesda)* 6:2799–2808
- Sanchez PA, Gore MA, Heun JT, Thorp KR, Carmo-Silva AE, French AN, Salvucci ME, White JW (2014) Development and evaluation of a field-based high-throughput phenotyping platform. *Funct Plant Biol* 41:68–79
- Schnable PS, Ware D, Fulton RS, Stein JC, Wei F, Pasternak S, Liang C, Zhang J, Fulton L, Graves TA (2009) The B73 maize genome: complexity, diversity, and dynamics. *Science* 326:1112–1115
- Shi L, Shi T, Broadley MR, White PJ, Long Y, Meng J, Xu F, Hammond JP (2013) High-throughput root phenotyping screens identify genetic loci associated with root architectural traits in *Brassica napus* under contrasting phosphate availabilities. *Ann Bot* 112:381–389
- Tanabata T, Shibaya T, Hori K, Ebana K, Yano M (2012) SmartGrain: high-throughput phenotyping software for measuring seed shape through image analysis. *Plant Physiol* 160:1871–1880
- Topp CN, Iyer-Pascuzzi AS, Anderson JT, Lee CR, Zurek PR, Symonova O, Zheng Y, Bucksch A, Mileyko Y, Galkovskiy T et al (2013) 3D phenotyping and quantitative trait locus mapping identify core regions of the rice genome controlling root architecture. *PNAS* 110(18):E1695–E1704
- Trachsel S, Kaeppler SM, Brown KM, Lynch JP (2011) Shovelomics: high throughput phenotyping of maize (*Zea mays* L.) root architecture in the field. *Plant Soil* 341:75–87
- Tracy SR, Black CR, Roberts JA, Sturrock C, Mairhofer S, Craigon J, Mooney SJ (2012) Quantifying the impact of soil compaction on root system architecture in tomato (*Solanum lycopersicum*) by X-ray micro-computed tomography. *Ann Bot London* 110:511–519
- Wagner B, Santini S, Ingensand H, Gärtner H (2011) A tool to model 3D coarse-root development with annual resolution. *Plant Soil* 346:79–96
- Walter A, Schar H, Gilmer F, Zierer R, Nagel KA, Ernst M, Wiese A, Virnich O, Christ MM, Uhlig B, Jünger S, Schurr U (2007) Dynamics of seedling growth acclimation towards altered

- light conditions can be quantified via GROWSCREEN: a setup and procedure designed for rapid optical phenotyping of different plant species. *New Phytol* 174:447–455
- Watanabe K, Guo W, Arai K, Takanashi H, Kajiya-Kanegae H, Kobayashi M, Yano K, Tokunaga T, Fujiwara T, Tsutsumi N, Iwata H (2017) High-throughput phenotyping of sorghum plant height using an unmanned aerial vehicle and its application to genomic prediction modeling. *Front Plant Sci* 8:421
- Whan AP, Smith AB, Cavanagh CR, Ral JPF, Shaw LM, Howitt CA, Bischof L (2014) GrainScan: a low cost, fast method for grain size and colour measurements. *Plant Methods* 10:23
- Wing RA, Purugganan MD, Zhang Q (2018) The rice genome revolution: from an ancient grain to Green Super Rice. *Nat Rev Genet* 19:505–517
- Wu J, Wu Q, Pages L, Yuan Y, Zhang X, Du M, Tian X, Li Z (2018) RhizoChamber-Monitor: a robotic platform and software enabling characterization of root growth. *Plant Methods* 14:44
- Wu D, Guo Z, Ye J, Feng H, Liu J, Chen G, Zheng J, Yan D, Yang X, Xiong X, Liu Q, Niu Z, Alan PG, John HD, Xiong L, Yang W (2019) Combining high-throughput micro-CT-RGB phenotyping and genome-wide association study to dissect the genetic architecture of tiller growth in rice. *J Exp Botany* 70(2):545–561
- Xiao Y, Liu H, Wu L, Warburton M, Yan J (2017) Genome-wide association studies in maize: praise and stargaze. *Mol Plant* 10:359–374
- Galkovskiy T, Mileyko Y, Bucksch A, Moore B, Symonova O, Price CA, Topp CN, Iyer-Pascuzzi AS, Zurek PR, Fang S, et al, GiA roots: software for the high throughput analysis of plant root system architecture. *BMC Plant Biol* 12:116
- Yang W, Duan L, Chen G, Xiong L, Liu Q (2013) Plant phenomics and high-throughput phenotyping: accelerating rice functional genomics using multidisciplinary technologies. *Curr Opin Plant Biol* 16(2):180–187
- Yang W, Guo Z, Huang C, Duan L, Chen G, Jiang N, Fang W, Feng H, Xie W, Lian X et al (2014) Combining high-throughput phenotyping and genome-wide association studies to reveal natural genetic variation in rice. *Nat Commun* 5:5087
- Yang W, Guo Z, Huang C, Wang K, Jiang N, Feng H, Chen G, Liu Q, Xiong L (2015) Genome-wide association study of rice (*Oryza sativa* L.) leaf traits with a high-throughput leaf scorer. *J Exp Bot* 66:5605–5615
- Yao W, Li G, Yu Y, Ouyang Y (2018) funRiceGenes dataset for comprehensive understanding and application of rice functional genes. *Gigascience* 7:1–9
- Zhang Q (2007) Strategies for developing Green Super Rice. *Proc Natl Acad Sci U S A* 104:16402–16409
- Zhang Q, Wing R (2013) Genome studies and molecular genetics: understanding the functional genome based on the rice model. *Curr Opin Plant Biol* 16:129–132
- Zhang X, Huang C, Wu D, Qiao F, Li W, Duan L, Wang K, Xiao Y, Chen G, Liu Q, Xiong L, Yang W, Yan J (2017) High-throughput phenotyping and QTL mapping reveals the genetic architecture of maize plant growth. *Plant Physiol* 173:1554–1564
- Zuo J, Li J (2014) Molecular dissection of complex agronomic traits of rice: a team effort by Chinese scientists in recent years. *Natl Sci Rev* 1:253–276

# Chapter 7

## High-Throughput Phenotyping in Soybean



**Asheesh K. Singh, Arti Singh, Soumik Sarkar,  
Baskar Ganapathysubramanian, William Schapaugh, Fernando E. Miguez,  
Clayton N. Carley, Matthew E. Carroll, Mariana V. Chiozza,  
Kevin O. Chiteri, Kevin G. Falk, Sarah E. Jones, Talukder Z. Jubery,  
Seyed V. Mirnezami, Koushik Nagasubramanian, Kyle A. Parmley,  
Ashlyn M. Rairdin, Johnathon M. Shook, Liza Van der Laan,  
Therin J. Young, and Jiaoping Zhang**

---

A. K. Singh (✉) · A. Singh · F. E. Miguez · C. N. Carley · M. E. Carroll · M. V. Chiozza ·  
K. O. Chiteri · K. G. Falk · S. E. Jones · T. Z. Jubery · K. A. Parmley · A. M. Rairdin ·  
J. M. Shook · L. Van der Laan · J. Zhang  
Department of Agronomy, Iowa State University, Ames, IA, USA  
e-mail: [singhak@iastate.edu](mailto:singhak@iastate.edu)

A. Singh  
e-mail: [arti@iastate.edu](mailto:arti@iastate.edu)

F. E. Miguez  
e-mail: [femiguez@iastate.edu](mailto:femiguez@iastate.edu)

C. N. Carley  
e-mail: [ccarley@iastate.edu](mailto:ccarley@iastate.edu)

M. E. Carroll  
e-mail: [carroll1@iastate.edu](mailto:carroll1@iastate.edu)

M. V. Chiozza  
e-mail: [mchiozza@iastate.edu](mailto:mchiozza@iastate.edu)

K. O. Chiteri  
e-mail: [kchiteri@iastate.edu](mailto:kchiteri@iastate.edu)

K. G. Falk  
e-mail: [falk@iastate.edu](mailto:falk@iastate.edu)

S. E. Jones  
e-mail: [sejones2@iastate.edu](mailto:sejones2@iastate.edu)

T. Z. Jubery  
e-mail: [znjubery@iastate.edu](mailto:znjubery@iastate.edu)

K. A. Parmley  
e-mail: [kparmley@iastate.edu](mailto:kparmley@iastate.edu)

A. M. Rairdin  
e-mail: [arairdin@iastate.edu](mailto:arairdin@iastate.edu)

**Abstract** Soybean [*Glycine max* (L.) Merr.] breeders and geneticists routinely evaluate thousands of plots per year in order to characterize various accessions and breeding populations for a multitude of traits, for example, morphological, physiological, abiotic and biotic stress, plant organs, and seed composition. Most of these trait evaluations require experienced raters to spend countless hours, recording phenotypes for each genotype in different filial generations. Plant breeders strive to work with increased population sizes, and improved accuracy of selection to increase the response to selection. These requirements have motivated the development of high-throughput phenotyping (HTP) methods and associated tools (i.e., hardware) and software solutions. This chapter consists of several topics related to HTP, including sensors, unmanned aerial systems, and ground robots, as these are important components of plant phenotyping in the new technological era. The advances in image-based analysis and machine learning methods have accompanied the improvements in phenotyping capabilities, both aerial and ground. This chapter includes the current state of the art in types of sensors, aerial, and ground-based HTP, in conjunction with machine learning-based analytics, particularly for physiological and morphological traits, abiotic and biotic stresses, and root-related traits. Advances in the integration of HTP with crop modeling are provided. Finally, the complementary relationship between HTP and genomic studies is explained with pertinent examples.

---

J. M. Shook  
e-mail: [jmshook@iastate.edu](mailto:jmshook@iastate.edu)

L. Van der Laan  
e-mail: [lizav@iastate.edu](mailto:lizav@iastate.edu)

J. Zhang  
e-mail: [jiaoping@iastate.edu](mailto:jiaoping@iastate.edu)

S. Sarkar · B. Ganapathysubramanian · S. V. Mirnezami · T. J. Young  
Department of Mechanical Engineering, Iowa State University, Ames, IA, USA  
e-mail: [soumiks@iastate.edu](mailto:soumiks@iastate.edu)

B. Ganapathysubramanian  
e-mail: [baskarg@iastate.edu](mailto:baskarg@iastate.edu)

S. V. Mirnezami  
e-mail: [vahid@iastate.edu](mailto:vahid@iastate.edu)

T. J. Young  
e-mail: [theriny@iastate.edu](mailto:theriny@iastate.edu)

W. Schapaugh  
Department of Agronomy, Kansas State University, Manhattan, KS, USA  
e-mail: [wts@ksu.edu](mailto:wts@ksu.edu)

K. Nagasubramanian  
Department of Electrical Engineering, Iowa State University, Ames, IA, USA  
e-mail: [koushikn@iastate.edu](mailto:koushikn@iastate.edu)

**Keywords** Phenomics · Sensors · Unmanned aerial systems · Ground robots · Machine learning · Crop modeling · Plant stress

Plant breeding can benefit from advances in phenotyping, with a better understanding of genetic architecture and the ability to integrate new insights and traits in improved lines. Depending on the region and market segment targeted by the breeder, this may encompass a broad range of traits including economic yield, agronomic, disease and insect resistance, herbicide tolerance, responses to abiotic factors such as water stress (drought or flooding), salt tolerance, seedling chill tolerance, and seed composition. With the advent of new sensors and carrying platforms (aerial and ground), remote and proximal sensing of plants and their parts have improved rapidly. These advances have opened up new avenues, while improving existing approaches for a number of practitioners, including plant breeders, agronomists, pathologists, physiologists, and farmers. Optical sensors and cameras are being deployed, enabling the logging of orders of magnitude more measurements, as well as realizing the ability to capture time-dependent changes throughout the growing season on large collections of genotypes (i.e., *phenomics*).

*We define the use of sensors or other tools to rapidly phenotype plants with some automation as “high-throughput phenotyping” or HTP.* While the term HTP can often be misinterpreted due to a lack of standardization for its classification as “High-Throughput”; for the purpose of this chapter, HTP is considered to encompass all situations (platforms-sensors-output combinations) where data collection is faster than done by a human acting alone. In addition to HTP-enabled selection for breeding decisions; by tracking the progression of phenotypes throughout the growing season, genetic underpinnings of developmental pathways are becoming clearer. With each additional trait that can be measured by proxy using sensors, more informed selections can be made. Given the long history of many plant selections based on visual appearance, image-based phenotyping has gained prominence for HTP applications. Using traditional RGB cameras, attached to ground-based systems or unmanned aerial systems (UAS), many traditionally measured traits are now collected digitally.

The adoption rate of HTP methods is affected by costs, ease of use, measurement accuracy, and correlation with traits of interest. The cost of these systems appears to be on a downward trend, easing the financial burden. Continual efforts are ongoing to improve measurement accuracies and establish trait correlations with new sensors. For example, multispectral and hyperspectral sensors provide an opportunity to focus on *phenes* of interest with increased insights on traits.

This chapter is split into nine research topics relevant to HTP, with a primary emphasis on field-based phenotyping.



## 7.1 Sensors in HTP

HTP sensors can be classified based on the source of the radiation detected (active or passive), the portion of the electromagnetic spectrum used, and further subdivided by the type of data that is returned (e.g., image or digital value). Both active and passive sensors measure reflected energy. The former type emits energy that is then detected, while the latter relies on solar radiation reflected off an object (Barmeier and Schmidhalter 2017). Popular active sensors used in HTP, such as LiDAR and ultrasonic sensors, are useful for generating 3D point clouds, which can be used for extraction of canopy architecture (Conn et al. 2017), plant height (Wang et al. 2018), and above-ground biomass (Pittman et al. 2015). Passive sensors consist of multi-spectral, hyperspectral, RGB (red, green, blue), fluorescence, and thermal infrared. Spectral sensors generate phenotypic trait information by leveraging the relationship between measured reflectance from a canopy or other plant tissue with many physiological traits that control the observed phenotypic response. Physiological traits are derived from reflectance values of regions of the electromagnetic spectrum (Parmley et al. 2019; Nagasubramanian et al. 2018), and vegetation indices that are associated with biochemical processes in the plant (Xue and Su 2017). RGB cameras are affordable and scalable sensors that have been used extensively in research for measuring canopy cover (Parmley et al. 2019; Yu et al. 2016; Xavier et al. 2017), above-ground biomass (Ballesteros et al. 2018), stress detection (Naik et al. 2017), disease scoring (Nagasubramanian et al. 2018; Naik et al. 2017; Dobbels and Lorenz 2019), and many other purposes. Gas exchange sensors used for measuring water use efficiency and photosynthetic capacity have seen limited application in HTP screening due to their limited throughput capacity. However, a recent study identified a wide range of genetic variability and correlation with seed yield (Lopez et al. 2019).

The main types of sensors used in HTP include the following:

- *RGB cameras*—RGB (Red, Blue, Green channel filters) cameras are typically the most inexpensive sensors and are the most popular. The benefits of an RGB camera include high resolution, and are usually easy to mount and incorporate onto a UAS (commonly referred to as a drone), especially if they are made by the same company as the UAS manufacturer. A drawback of the RGB camera is the lack of information in the near-infrared spectrum, which can provide valuable plant health information (Chaerle and Van Der Straeten 2001). Some of the traits that can be captured include height, stand counts, canopy coverage, biotic and abiotic stress symptoms, and visible spectrum computed reflectance indices. In maize (*Zea mays* L.), early-season plant counts using RGB imagery have been shown to be effective tools (Gnädinger and Schmidhalter 2017), but soybean stand counts have not been reported utilizing similar methods; however, it is not a limitation of the technology. Detection and quantification of iron deficiency chlorosis in soybean plants using RGB imagery taken from a UAS has proved to be an effective way to screen a large number of genotypes for susceptible and resistant lines in a breeding program (Dobbels and Lorenz 2019). Maturity date has also been estimated using an RGB camera (Narayanan et al. 2019).

- *Multispectral cameras*—these have 3 to 10 bands are typically not continuous, and have a wide spectral range. The benefit of these cameras is that they contain the visible light spectrum, which allows them to calculate the traits produced from an RGB camera, but they also contain bands in the near-infrared region (NIR), which can provide more information on overall plant health through the use of indices, such as the normalized difference vegetation index (NDVI). A multispectral camera was used for maturity date estimation (Zhou et al. 2019). Several manufacturers are now selling customizable multispectral cameras catering to individual needs.
- *Hyperspectral cameras* (image based)—these are similar to multispectral cameras in that they contain both visible and NIR bands, but the difference is that hyperspectral cameras capture reflectance data for a large number of continuous narrow bands (Yang et al. 2017). Much of hyperspectral imaging in soybean has been lab- or ground-based phenotyping for early disease detection (Nagasubramanian et al. 2018, 2019; Hatton et al. 2018). Hyperspectral data cubes have the advantage of generating a continuous spectrum of bands which can be studied to determine what bands provide the most valuable information for a given trait of interest, but this advantage can also represent a challenge given the data size that can be collected using UAS and the additional data processing requirements. At this time, UAS-mounted hyperspectral phenotyping in soybean is in a nascent stage, but has been shown to be effective in other plant species. For example, hyperspectral imagery from a UAS was used to map insect damage in Norway spruce (Näsi et al. 2015). Spectroradiometers have been routinely used in soybean for plant health estimation (Kovar et al. 2019), and even insect quantification (Alves et al. 2019), but these have not yet been used with a UAS or automated ground robot.
- *Thermal imaging cameras*—these cameras measure the heat that radiates from an object. They have been useful for monitoring canopy temperature in soybean, which can be correlated with tolerance to heat and drought stress (McKinney et al. 1989). Also, thermal imaging cameras have been used to characterize cultivar differences in resistance to sudden death syndrome (caused by *Fusarium virguliforme*) in soybean (Hatton et al. 2018). Thermal imagery is prone to give erroneous output if the height of the UAS, and weather conditions such as cloud cover and wind speed are not constant.
- *LiDAR*—it uses lasers to create dense 3D point clouds that can be used to track object geometries. Ground-based phenotyping has been accomplished with LiDAR, and has been capable of tracking plant height over time (Friedli et al. 2016). Elevation mapping using LiDAR collected via satellite data has also been successful (Gelder 2015), but small-sized LiDAR instruments mountable on UAS are new and not well researched. However, in forest mapping, good correlations with field inventory measurements have been reported using a UAV-LiDAR system (Wallace et al. 2012). It is expected that in coming years this technology will gain wider usage in soybean.

A multitude of sensors are available for HTP applications (Mahlein 2016); however, their usefulness depends on versatility, veracity to trait correlation, affordability, and throughput.

## 7.2 UAS-Based HTP

There are two commonly used platforms for UAS phenotyping: fixed-wing and multi-rotor drones. While satellite-based phenotyping has been utilized (Mfuka et al. 2019), the focus of this section will be on UAS. It seems that for research purposes in agriculture, multi-rotor drones are preferred, but for commercial agricultural mapping, fixed-wing aircraft may have an advantage. The benefits of multi-rotor drones over fixed-wing include vertical take-off and landing, usually lower purchase cost, higher payload capacity, and typically have the ability to customize payloads more easily. The disadvantages are that they typically have reduced “in-air” flight times because they have to generate all of their own lift, and are less stable in high wind speeds. To make up for shorter flight times, additional batteries are used for swapping (and re-charging) when flying for longer durations. Larger sized multi-rotor drones can help make up for stronger winds; however, for field-based phenotyping, high wind speeds create image processing challenges particularly image reconstruction due to moving plant organs. The fixed-wing UAS advantages and disadvantages are inverted compared to multi-rotor drones, as these have long flight times and are more stable at higher wind speeds. The disadvantages include a larger area needed for take-off and landing; higher costs; and for small fields, lower efficiency because they require more space to make turns in the flight pattern (DroneDeploy 2017). Researchers using UAS-based phenotyping carefully select the most appropriate sensors based on the trait of interest. The most commonly used sensors on UAS are RGB (i.e., digital camera), multispectral (generally more than three bands or filters), hyperspectral (generally more than 10 bands or filters), thermal imaging, and Light Detection and Ranging (LiDAR), as described earlier.

For new entrants in UAS-based phenotyping, several aspects are important to know. For obtaining high-quality images, Ground Control Points (GCPs) must be taken at Real-Time Kinematics (RTK) level accuracy (Do more GCPs equal more accurate drone maps? In: Pix4D [Internet]. 5 Nov 2018). GCPs should capture the variation in elevation and terrain across the area to be phenotyped (Oniga et al. 2018). Generally, four GCPs at the corner of fields and an additional point in the middle of the field increase vertical accuracies of reconstruction, but more GCPs may be required depending on field size. Sufficient GCPs are included to allow the stitching software to create a highly accurate reconstruction of the map, especially for time-series analyses. This ensures that when producing spatial files for plot extraction, the same files for each time point are used. If these are not included, the accuracy of the orthomosaic images may be slightly different each time reconstruction is completed.

Orthomosaic images are commonly used when utilizing UAS imagery, as they help to reduce data size and ease the visualization of the field of interest. Orthomosaic

images rely on point matching, which is somewhat of a black box process, so using the same dataset can lead to slightly different reconstructed images. In the absence or near absence of canopy movement at the time of data capture, reconstructions should be very similar; however, if imaging is done when substantial canopy movement is occurring, less reliable reconstructions are accomplished, i.e., outputs ghost plant leaves. After orthomosaic construction, plot extraction is completed and image processing is accomplished using the user-chosen software. Many applications with some human supervision have been developed that are capable to extract individually labeled plots, and usually provide some basic traits such as plant canopy extraction and coverage (Khan and Miklavcic 2019; Haghghattalab et al. 2016; Tresch et al. 2019). Efforts are ongoing to completely automate plot extraction from orthomosaics in plant sciences.

Most image processing software will output a 3D point cloud of an imaged field along with an orthomosaic, and a digital surface map. The 3D point cloud is similar to the type of data received from LiDAR, but does not have return values that can help determine the type of material being sensed. These files tend to be large, and not as dense as LiDAR data, because it is using structure from motion, which utilizes multiple camera angles of the same plant to reconstruct multiple 2D images into a 3D image. Digital surface maps are smaller files than point clouds, but also represent the height at a given spatial point, which is done by using the pixel value to represent the height. While UAS can capture several plant traits, few trait measurements or estimations are not feasible when using UAS due to occlusion or angle of view. These include many soybean disease traits that require “in the canopy” evaluations (Coser et al. 2017; Moellers et al. 2017), where disease symptoms are expressed on stems and petioles.

### 7.3 Ground-Based HTP

Precision agriculture has been greatly influenced by agricultural machinery specifically designed for row crop application, and more recently, these use local and global sensors for autonomous driving to improve on-farm production (R Shamshiri et al. 2018). Tractor-mounted sensors can improve throughput, but repeated phenotyping across the field comes with a serious cost of soil compaction that can lower yield and increase flooding tendencies (Batey 2009; Nawaz et al. 2013). Lightweight mobile phenotyping platforms capable of carrying multiple sensors have been constructed to alleviate the compaction factor and increase the rate of data collection (Gao et al. 2018; Crain et al. 2018). These mobile phenotyping platforms increase throughput while maintaining the accuracy of phenotyping. However, the current challenges in developing mobile robotic field phenotyping units for soybean include a lack of full autonomy and few software solutions that enable easy on-board real-time decision-making.

Researchers are making strides in developing ground-based robots or rovers (running in between canopies) to collect field data; however, limited studies have

been reported in soybean. Riera et al. (2020) utilized ground robots and developed a multi-view image-based soybean yield estimation framework utilizing Deep Learning (DL) architectures. A diverse collection of soybean accessions were phenotyped using RGB camera on ground robots that were run on breeding experiments. The DL methods were successfully deployed to isolate individual plants from the background and neighboring plants, and for pod counting estimate seed yield, as well as rank soybean genotypes for application in breeding decisions (Riera et al. 2020). In non-soybean examples, two methods (vision, vision + LiDAR) successfully measured sorghum stem width in a cluttered field environment and were then tested and amended for maize and hemp (Choudhuri and Chowdhary 2018). A ground robot with LiDAR was used to produce a 3D reconstruction of maize fields in order to extract plant architecture and biomass trait information (Gage et al. 2019). A multi-agent strategy combining a team of “weeder bots” to locate and mechanically control weed pressure in the field increased system performance (McAllister et al. 2019). In soybean, researchers reported a collaborative multi-robot system for phenotypic collection using lightweight robots and a saliency-driven informative path planning technique for navigation (Gao et al. 2018).

Ground rover-based phenotyping is built on proximal, non-destructive, and non-invasive approaches that sense visible/near-infrared radiation (reflected or transmitted) and far-infrared radiation (thermal radiation) emitted by the crop. Although ground rover -based HTP is more time-consuming than UAS, higher phenotypic resolution can be obtained. In current practice, available mounts for these sensors can be stationary towers, customized platforms, vehicles, or rovers.

- *Stationary Tower/Gantry System*: The advantage of stationary towers or a gantry system is that they can be quite robust, making them ideal choices for larger payloads and adverse atmospheric conditions. Kirchgessner et al (2016) achieved this by developing a cable-suspended field phenotyping platform, equipped with a point spectrometer, RGB camera, modified three-band NDVI camera, 40 band spectral image camera (16 Visible, 25 NIR), thermal camera, and a terrestrial laser scanner. Sensors were positioned 2–5 m above the canopy for high-resolution phenotyping. The system was deployed in soybean for monitoring canopy cover, canopy height, and traits related to thermal and multispectral imaging. However, the disadvantage of using towers is that they are restricted to a given field site and generally on their own, non-HTP.
- *Manual Cart*: A more lightweight proximal sensing cart or a manual cart with a multi-sensor system has been used for phenotyping. They cost less to manufacture and are often constructed in a narrow wheeled manner, which can cause minimal soil and crop disturbances. They are also highly maneuverable and can be designed to accommodate specific crop heights and row spacings. The system made by Bai et al. (2016) had five sensor modules (ultrasonic distance sensors, thermal infrared radiometers, NDVI sensors, portable spectrometers, and RGB web cameras) to measure crop canopy traits. Geo-referencing was accomplished using a Global Positioning System (GPS) device. Two environmental sensors (solar radiation and air temperature/relative humidity sensors) were also integrated into the system.

While high-resolution and extensive sensors provide advantages; as with any manually intensive operation, this method is slow and prone to operator errors and fatigue, which can affect data quality.

- *Customized Tractor*: When it comes to maneuverability, sensor-equipped tractors are advantageous over stationary mounted systems. A tractor equipped with a boom system allows for the precise positioning of sensors. In Barker III et al. (2016), the frame included up- and down-welling optical fibers, GPS antenna, infrared thermometer, pyranometer, quantum sensor, and down-looking digital camera. Phenotyping was done for foliar pigment contents (chlorophyll, carotenoids, and anthocyanins), green vegetation cover, fraction of absorbed photosynthetically active radiation, green leaf area index (LAI), green leaf biomass, total canopy chlorophyll content, and gross primary production. Using a tractor in such a manner can cause soil compaction. If sensors are mounted for use as a top view, it precludes in-between canopy trait measurements. Also, tractors are generally not amenable for later crop growth stages in between the row phenotyping without changing tires or damaging plants in the rows of movement.
- *Motorized and Autonomous Robot*: The most flexible ground-based HTP are motorized or autonomous. The emerging robotic systems are autonomous, work on demand (even at night), and can be equipped with multiple sensors enabling multiple traits phenotyping simultaneously. Gao et al. (2018) fabricated and deployed an all-terrain lightweight robot to capture images to phenotype foliar diseases, flowers, pods, etc. of soybean. It was equipped with RGB cameras (field of view 78 degrees) and RTK-GPS that provided centimeter accuracy and a differential GPS to facilitate better navigation under dynamic, heterogeneous field conditions, and crop status. To overcome the issue of coverage (by a single rover), a swarm of lightweight robots was deployed and connected wirelessly to a central hub guiding the path and action of the robots via a pre-programmed algorithm.

While ground robots have been developed (Gai et al. 2019; Birrell et al. 2019), the use of robotics for agricultural row crop research and production is still in its infancy, but rapidly gaining prominence. For successful robotic-based HTP, sturdy construction of software and hardware capable of adaptability to multiple infield situations and environments such as crop type, lighting, rain, mud, and debris is needed.

Plant breeders utilize both aerial- and ground-based systems for data capture, leading to plant breeding decisions (Fig. 7.1).

## 7.4 Use of Machine Learning in HTP

High-through put phenotyping creates a data deluge requiring sophisticated data analytics methods. Machine learning (ML) and deep learning (DL) algorithms are promising approaches for faster, more efficient, and better analytics for meaningful insights (Fig. 7.2). Machine learning methods are adept in extracting patterns and



**Fig. 7.1** Plant breeder taking field notes which can be complemented with, or independently collected using pushcart, ground robots, and an aerial system

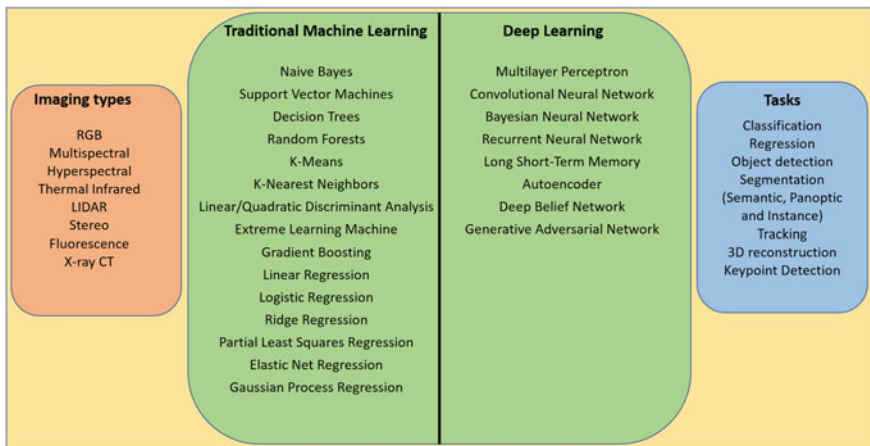


**Fig. 7.2** Illustration of some of the commonly used imaging, machine learning, and deep learning techniques used for plant phenotyping tasks

features from a large corpus of data, inherent from HTP platforms. Machine learning has brought rapid improvements in the ability to identify, classify, quantify, and predict traits (Singh et al. 2016, 2018, 2020). Machine learning requires a training dataset as an input to create the desired output. The size and features extracted from the dataset need to be customized for each ML algorithm. Hence, the dataset plays an important role in phenotyping using ML. Generally speaking, DL models require large amounts of labeled data; however, to overcome this challenge, active learning algorithms have been proposed that reduce the amount of labeling to achieve good predictive performance (Nagasubramanian et al. 2020).

For more details on ML and DL tools in plant phenotyping, refer to (Singh et al. 2016, 2018, 2020). These reviews provide practitioner guides on the implementation of ML and DL tools.

*Trait Extraction:* Plant traits can be measured using three different main approaches. (A) Manual phenotyping is utilized in the absence of robust platforms including imaging devices and computing nodes. This method is time-consuming, costly, inconsistent, and generally involves destructive sampling. (B) Semi-automated phenotyping: this came into fruition due to collaborations between plant scientists, engineers, and computer scientists that created different interactive applications to enable trait measurements. Examples of such software include Aria (Pace et al. 2014), DIRT (Das et al. 2015), and GiaRoot (Galkovskyi et al. 2012) among other phenotyping applications. Although these computer vision programs are not crop species specific, user intervention is needed to measure traits (Merchuk-Ovnat et al. 2019; Zhou et al. 2019). (C) Fully automated plant phenotyping requires robust image processing and/or ML algorithms to measure traits (Ghosal et al. 2018; Ubbens and Stavness 2017).

*Image processing:* Researchers designed and implemented algorithms using image processing tools to measure different plant traits (Pace et al. 2014; Zhou et al. 2019; Gage et al. 2017; Ma et al. 2019). Segmentation, classification, feature extraction, skeletonization, graph-based algorithm, and morphological operation are the most popular tools that researchers have used to measure traits.

*Machine Learning in soybean phenotyping:* Diverse examples exist on the ability of ML algorithms and applications in soybean. Some of the commonly used regression-based methods used in soybean phenotyping applications include linear regression, logistic regression, stepwise regression, ridge regression, partial least squares regression, elastic net regression, piecewise regression, tree regression, and Gaussian process regression. Some of the commonly used classification methods for soybean phenotyping applications include Naive Bayes classifier, decision trees, random forests, K-nearest neighbor, linear discriminant analysis, quadratic discriminant analysis, support vector machines, and extreme learning machine.

*Deep learning in soybean phenotyping:* Machine learning algorithms were a promising approach for deriving useful information from plant phenotype data. Recent advancements in automation, computation, and sensor technology have enabled the collection of high-resolution phenotype data across a large geographical area with high temporal resolution. This deluge of data has made it possible to



apply Deep Learning (DL) algorithms successfully in a wide variety of plant phenotyping tasks. With an increase in annotated training data, DL algorithms were able to perform better than traditional ML algorithms for many plant phenotyping problems. For example, plant disease classification is one of the challenging phenotyping tasks in which deep learning methods like Convolutional Neural Networks (CNN) have achieved success (Singh et al. 2018). DL methods have also achieved state-of-the-art performance in complex image-based plant phenotyping problems like root and shoot feature identification and localization (Pound et al. 2018). Multilayer Perceptrons (MLP), CNN, Recurrent Neural Networks (RNN), and Long Short-Term Memory (LSTM) are some of the deep learning models commonly used in soybean phenotyping applications. Current active areas of investigations include super-resolution, dehazing, and spectral reconstruction, which will advance the phenotype-based information from sensors (Arad et al. 2018; Shoeiby et al. 2019). Table 7.1 includes some of the research papers where ML- and DL-based methods have been used in soybean.

## 7.5 HTP for Physiological and Morphological Traits

The pursuit to improve the rate of genetic gain in crop species by plant researchers requires disentangling the underlying mechanisms involved in the observed phenotype. The aim of this is to: (a) assemble a relationship matrix of the underlying physiology and morphological traits with the trait of interest, (b) identify genetic drivers of such traits, and (c) leverage the aforementioned points to optimize the breeding or research workflow. Researchers are often focused on complex quantitative phenotypes measured sparsely during the growing season (e.g., seed yield, biomass accumulation, seed quality), and thus have little information on the framework of physio-morphological traits underlying the traits of interest. Several barriers have prevented past research into these traits as they can be difficult to quantify, require destructive sampling, expensive to collect, or were previously unable to be collected in an analog era. With advancements made in modern sensor technology and HTP, these bottlenecks are beginning to be removed, empowering researchers with high-dimensional data on physio-morphological processes on a spatio-temporal scale. This is enabling scientists to gather a full perspective of a phenotype to develop an understanding of the complex trait-of-traits interactions controlling important agronomic and quality traits, in turn enabling HTP-influenced breeding outcomes.

The adoption of HTP practices in plant breeding can be attributed to the simultaneous improvements in sensor technology, deployment platforms, and data processing techniques and capabilities. The pace of new sensor technology has allowed the adoption of these sensors for greenhouse, growth cabinet, and field-based measurements as broadly demonstrated in past research (Das Choudhury et al. 2019; Araus et al. 2018). An expanding area of research in soybean has been to use phenomic data for yield prediction during the growing season. Initial research has shown moderate-to-high levels of yield prediction using an RGB camera to estimate canopy coverage (Parmley et al. 2019; Yu et al. 2016; Xavier et al. 2017;

**Table 7.1** Examples of studies that reported ML/DL methods for the study of soybean traits

ML/DL architecture	Trait studied	References
Linear regression and logistic regression	Soybean flowering date using temperature and photoperiod	Sinclair et al. (1991)
Logistic regression	Predict sclerotinia stem rot ( <i>Sclerotinia sclerotiorum</i> ) using weather information	Mila et al. (2004)
Stepwise regression	Soybean rust epidemic; Predict soybean yield from hyperspectral image reflectance values	Yang et al. (1990), Jang et al. (2006)
Ridge regression	Identify phenological variables associated with soybean yield	Williams et al. (1979)
Partial Least Squares Regression (PLSR)	Drought stress using hyperspectral fluorescence imaging	Mo et al. (2015)
Elastic net regression	Predict soybean plant resistance to <i>Phytophthora sojae</i> using phenotype, genotype, and gene expression data	Loh et al. (2011)
Segmented regression	Effect of liming on soybean yield	Shuai et al. (2003)
Convolutional Neural Network (CNN)	Soybean Root phenotyping	Falk et al. (2020)
Multivariate regression tree	Effectiveness of phosphorous application	Zheng et al. (2010)
Gaussian process regression	Select the most useful spectral bands for chlorophyll content and green Leaf Area Index (gLAI)	Verrelst et al. (2016)
Random Forest (RF), Support Vector Machine (SVM)	LAI using UAV-based hyperspectral remote sensing	Yuan et al. (2017)
Naive Bayes classifier, Gaussian mixture clustering	Isolating weeds in soybeans using features extracted from RGB images	De Rainville et al. (2014)
Decision tree	Model soybean productivity using weather data	Veenadhari et al. (2011)
Classification and regression tree	Yield variability due to phosphorus application rates under drought conditions	Zheng et al. (2009)
K-Nearest Neighbors (K-NN) classifier	Brown spot and frogeye leaf spot using mobile phone-based RGB images	Shrivastava and Hooda (2014)

(continued)

**Table 7.1** (continued)

ML/DL architecture	Trait studied	References
Linear Discriminant Analysis (LDA)	Detection of pitted morning glory weed using hyperspectral reflectance signals	Koger et al. (2003)
LDA	Identification of symptomatic soybean seeds on features extracted from RGB images	Ahmad et al. (1999)
Saliency Maps, SmoothGrad, Guided Backpropagation, Deep Taylor Decomposition, Integrated Gradients, Layer-wise Relevance Propagation, and Gradient times Input	Diseases—interpretability of ML models	Nagasubramanian et al. (2020)
LDA and Quadratic Discriminant Analysis (QDA)	Detection of <i>Callosobruchus maculatus</i> (F.) infestation	Chelladurai et al. (2014)
Local descriptors and Bag of Visual Words model (BOVW) with SVM	Detecting mildew and rust	Pires et al. (2016)
Extreme Learning Machine (ELM)	Variety classification from remote sensing-based hyperspectral images	Moreno et al. (2014)
SVM, K-NN, and Probabilistic Neural Network (PNN)	Classification of six types of soybean diseases	Shrivastava et al. (2017)
Hopfield network and perceptron	Classification of individual leaflet shapes	Oide and Ninomiya (2000)
PLSR	Seed damage due to weather, frost, sprout, heat, and mold using the reflectance data	Wang et al. (2004)
Long Short-Term Memory (LSTM)	Yield prediction across multiple years and locations	Shook et al. (2020)
Spectral Angle Mapper (SAM), Minimum Euclidean Distance (MED) and Fisher's linear likelihood	Detection of weed species using UAV-based multispectral images	Gibson et al. (2004)
Adaboost, K-NN, J48, NB, RF, and Sequential Minimal Optimization (SMO)	Prediction of soybean foliar diseases from UAV RGB images	Castelão Tetila et al. (2017)
CNN (GoogLeNet)	Classify 79 diseases (9 diseases from soybeans) in 14 plant species (Arnal Barbedo 2019)	Arnal Barbedo (2019)
CNN (AlexNet, VGG, and ResNet)	Predicting soybean defoliation	da Silva et al. (2019)
CNN (Inception-V3, ResNet, VGG, and Xception)	Identify soybean leaf disease from UAV images	Castelão Tetila et al. (2019), Amorim et al. (2019)

(continued)

**Table 7.1** (continued)

ML/DL architecture	Trait studied	References
Deep Gaussian process	County-level soybean yields using satellite data	You et al. (2017)
3D-CNN	Soybean yield prediction using satellite data	Terliksiz and Altýlar (2019)
CNN/Fourier transforms	Root trait architecture traits	Falk et al. (2020)
CNN (AlexNet)	Weed detection using UAV-based images	dos Santos Ferreira et al. (2017), Tang et al. (2017), Sivakumar (2019), Etienne (2019)
Autoencoder	Segment and count soybean cyst nematode eggs	Akintayo et al. (2018)
Single Shot Detection (SSD)	Stomatal density	Sakoda et al. (2019)
RetinaNet, U-Net	Soybean nodule counts and localization	Jubery et al. (2020)
CNN	Estimate number of seeds in soybean pods	Uzal et al. (2018), Li et al. (2019)
CNN (SegNet)	Segmentation of root traits	Wang et al. (2019)
LSTM	Soybean crop yield prediction using satellite images	Wang et al. (2018)
CNN (DeepLabv3+)	Soybean leaf coverage estimation from UAV images	Keller et al. (2018)
3D-CNN	Early detection of disease utilizing hyperspectral imaging	Nagasubramanian et al. (2019)
RF	Seed yield prediction using phenomic predictors	Parmley et al. (2019)
RF/genetic algorithm	Seed yield	Parmley et al. (2019)

Hoyos-Villegas et al. 2014; Maimaitijiang et al. 2017). However, researchers are beginning to rely on multi-sensor platforms to capture a spectrum of physiological traits. Recent studies used information on multiple physiological traits collected throughout the growing season to assemble yield prediction models (Parmley et al. 2019; Maimaitijiang et al. 2017). A major finding from both studies revealed that high levels of yield prediction can be achieved when multiple sources of data are included throughout the growing season. It is important to point out that while these studies have demonstrated their utility to predict yield during the growing season, little research has been conducted on how these approaches can be used to optimize breeding pipelines. These studies, while including temporal scale, had time-series sparsity. This is expected to change as more rapid ways of data capture and analytics become routine.

A combination of ground-based and UAV imaging to measure canopy coverage at multiple time points throughout the growing season using the SoyNAM panel (Xavier et al. 2017) identified quantitative trait loci (QTL) for increased canopy

coverage, which is positively correlated with seed yield and may help with early-season weed suppression. Parmley et al. (2019) collected canopy-level traits such as canopy temperature, area, and reflectance through a broad range of wavelengths in order to phenotype a diverse soybean collection. Their results showed the potential for using high-throughput canopy measurements to capture useful data related to genotype-specific differences in water status, heat tolerance, chlorophyll concentration, and canopy size, each of which can be used to assist in selections within a breeding program at a low cost, with rank correlations as high as 0.6–0.8, depending on growth stage. Bai et al. (2016) used a ground-based multi-sensor approach to measure height, NDVI, temperature, reflectance, and canopy coverage throughout the growing season to examine well-watered versus drought plots in soybean. Early-season measurements were more correlated due to the effect of canopy closure differences, with maturity effects at the end of the season causing a clear drop in measurements such as NDVI and evaporation. Differences in plant height throughout the growing season were found.

Vegetation indices (VIs) computed from hyperspectral reflectance wavebands have been associated with yield using different statistical methods (Parmley et al. 2019; Maimaitijiang et al. 2017). For example, Multiple Linear Regression (MLR), Partial Least Squares (PLS), and ML algorithms (i.e., random forest, artificial neural network) have been used in the selection process of vegetation indices importance and yield prediction. Christenson et al. (2016) selected significant wavebands from the spectrum using the PLS method and then computed different VIs (NDVIs). Authors found associations between the different NDVIs computed and soybean yield using MLR. Machine learning algorithms (i.e., random forest) have also been used for the prediction of soybean seed yield using VIs as predictors. Among the VIs, the Vogelmann Red Edge Index 2 (VREI2) had the largest correlation with seed yield during the two measured soybean growth stages ( $r_g = -0.75$ ) (Parmley et al. 2019). These phenotypic measurements were taken with a human-operated sensor; however, the potential of integration with UAS or a ground-based phenotyping system is promising. Fused data from multi-satellite imagery have also been used to compute VIs for yield associations where a simple linear regression between two VIs, the Normalized Difference Vegetation Index (NDVI) and the Enhanced Vegetation Index (EVI2), and soybean yield was reported (Gao et al. 2018). Moreover, a combined use of different sensors has been implemented for the prediction of different crop biophysical and biochemical variables. Multispectral and thermal data fusion provided an estimate of nitrogen concentration and chlorophyll *a* content with RMSE of 9.9% and 17.1%, respectively, whereas the estimation of chlorophyll *a* + *b* content was obtained by fusion of information from three sensors (RGB, thermal, and multispectral) with an RMSE of 11.6% (Keller et al. 2018). RGB and thermal fused data was the best predictor of LAI, while multispectral and thermal data fusion were the best predictors of biomass (Keller et al. 2018). In the same study, it was determined that the Extreme Learning Machine-based Regression (ELR) technique performed better than Partial Least Squares Regression (PLSR) and Support Vector Regression (SVR) for the estimation of these crop variables.

## 7.6 HTP and Crop Modeling

Phenotypic evaluation (e.g., seed yield) of new varieties involves biological complexities emerging from genetic by environment interactions that challenge our ability to develop accurate predictions in a new testing environment. At the core of this challenge is the large uncertainty in the variables that define the new environment, which might differ substantially from the previously observed environment. This need for extrapolation has been realized with variable success through the use of comprehensive dynamic mathematical descriptions of crop behavior and the interaction with the soil and atmosphere environment. These mathematical descriptions, known as “crop simulation models,” have been used to predict the agronomic performance of genotypes under diverse environmental conditions. These crop simulation models require daily inputs of meteorological data and soil characteristics to integrate and describe the basic processes of crop growth and development. Crop models also require crop- and cultivar-specific coefficients, for example, Radiation Use Efficiency (RUE), maximum number of leaves or leaf expansion rate, and calculate state variables (e.g., Leaf Area Index) for predicting the final output (e.g., above-ground biomass or seed yield). Accurate yield prediction requires a careful parameterization of genetic coefficients and high-quality weather and soil environment descriptions. Several authors have proposed that HTP and statistical models can complement and improve crop simulation models and as a result yield prediction, making them an effective tool in decision-making within plant breeding programs (Moulin et al. 1998; Betbeder et al. 2016; Jin et al. 2018).

Data assimilation is a method that aims to integrate, both in space and time, canopy state variables which can be derived from field observations or remote sensed data for optimizing crop models (Jin et al. 2018). In general, this process involves calibration, forcing, and updating and the final product is a combination of observations, remotely sensed data, and crop simulation models which borrow strength from the different sources of information. As an example, LAI and biomass crop state variables from satellite images were integrated into a crop simulation model to improve the prediction accuracy of soybean yields (Betbeder et al. 2016). LAI retrieval from hyperspectral data was evaluated using different statistical regression models (RF, ANN, and SVM) and compared using PLS regression (Yuan et al. 2017). Similarly, vegetation indices were extracted from complex multi-sensors data that were combined (fused) to model and predict LAI and biomass (Maimaitijiang et al. 2017). Prediction of crop state variables was conducted using PLSR, SVR, and ELR techniques. The importance of crop-specific VIs associated to LAI predictions was assessed and best-fit relationships were evaluated between the VIs and LAI for soybean and maize, with an algorithm that identifies and ranks potential regression models (Eureqa) was developed (Nguy-Robertson et al. 2012).

The application of high-throughput measurements for estimating crop model genetic parameters is also another application of phenomics to facilitate the use of crop simulation models (Fig. 7.3). Usually, estimating genetic parameters for a large group of genotypes or large breeding populations is a major limitation to the use

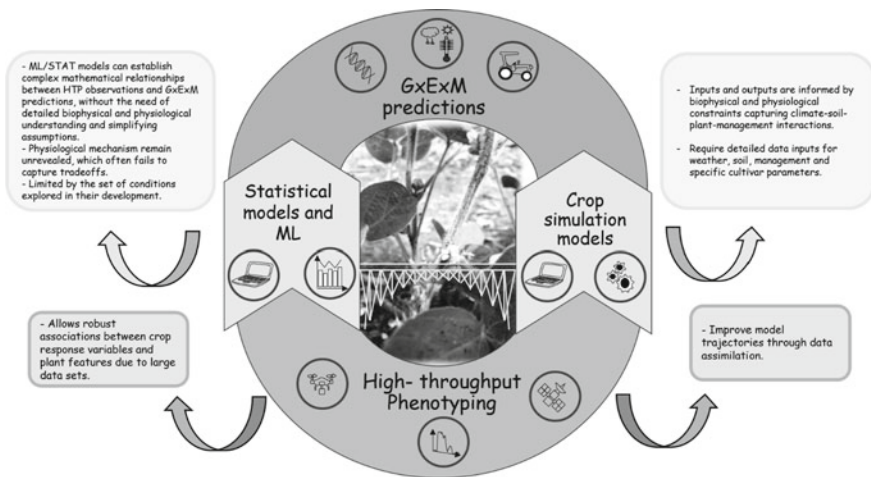


**Fig. 7.3** Diagram showing the connection between high-throughput phenotyping (HTP) and the prediction of the genotype by environment by management interaction mediated by the use of statistical models and ML and/or crop simulation models. Both approaches can be used in tandem (illustrated by the bridge connecting them)

of crop growth models in breeding. The relationship between RUE (a crop-specific parameter) and photochemical reflectance index in soybean leaves has been reported (Inoue and Peñuelas 2006). Incorporating this reflectance index in a high-throughput framework might be a possible alternative to retrieve RUE in a large set of genotypes. Other examples of the link between phenomics and crop modeling are the use of hyperspectral information to estimate water use efficiency (Thorp et al. 2018), and the development of phenotyping platforms and managed stress environments to estimate variety-specific parameters such as leaf expansion and transpiration rates (Gosseau et al. 2018). These last two examples were focused on species other than soybean; however, there is no impediment to expand these approaches to soybean breeding.

The use of HTP for the direct estimation of yield, LAI, and biomass has been well documented for soybean. However, the assimilation of intermediate crop state variables (i.e., LAI, biomass) into crop simulation models for soybean yield prediction is less studied. Similarly, little information is available on the use of HTP for retrieval of variety-specific coefficients and incorporating this information into crop simulation models is a crucial and limiting step to generalize the use of models for agronomic and breeding efforts. In addition, the estimation of parameters using HTP at large scale and high resolution has enormous potential for selection of cultivars in soybean breeding efforts. Predictions of soybean seed composition together with yield predictions could drive selection based on the Estimated Processed Value (EPV), which takes into account soybean meal and oil relative prices and, together with yield, incorporates an end-user and economic component for cultivar selection or for farmer management decisions before harvesting. Finally, the use of HTP

for soybean output traits such as seed composition will advance breeding efforts to develop higher yielding and high protein cultivars.

## 7.7 HTP of Soybean Stress-Related Traits

In field production, biotic and abiotic factors such as plant disease, insects, weeds, and unpredictable environmental conditions can limit production output. In the United States, it is estimated that disease (including SCN) alone impacts crop yield up to 11% on average each year, not including insects, weed pressure, poor environmental conditions, or nutrient deficit and water stress (Hartman et al. 2015). It was estimated that diseases cost North American soybean producers on average 5.2 billion each year from 2010 to 2014 (Allen et al. 2017). Other studies have emphasized that higher producing regions are more vulnerable to disease loss (Bandara et al. 2019). Farmers and researchers alike strive to limit the effect of these negative impacts by improving crop varieties and introducing management strategies to produce the highest yield and quality product possible.

Plant phenotyping is an integral part of developing genetic material resistant or tolerant to stresses. Visual ratings based on varied scales are common for research trials and field scouting to record the presence and severity of a particular stress. However, a reliance on human labor for stress identification and severity measurements leads to a few issues, including subjectivity and a lack of scalability. Quality of visual ratings suffer from human error due to inter- and intra-rater variation, experience level, field conditions, inherent bias, and fatigue, (Bock et al. 2010). Visual ratings can also vary in accuracy, speed, precision, agreement, and reliability. With the amount of lines that must be tested in breeding programs and the extensive acreage in production, it becomes a necessity to have a higher throughput solution to evaluate the impact of stress on soybean and image-based output to reduce rater variability.

High-throughput phenotyping methods have been developed for a wide range of stresses in soybean including herbicide injury, nematodes, nutrient deficiencies, and bacterial and fungal pathogens in multiple testing environments to help speed up the processes in phenotyping for plant stress (See examples in Table 7.1). Machine learning (Singh et al. 2016), especially DL methods (Singh et al. 2018), have shown extensive promise in handling and extracting detailed information from the expansive data provided by HTP systems (Singh et al. 2020).

Early identification of stress symptoms in the field can be beneficial to stress mitigation to promote early decision-making. These have been reported using hyperspectral cameras. Using two separate approaches, ML and deep learning methods, early symptom development of charcoal rot was identified on the interior of the soybean stem from plants grown in the greenhouse (Nagasubramanian et al. 2018, 2019). Application of these findings could save time in rating for charcoal rot severity in soybean by eliminating the need for cutting the stem open to examine interior lesions. Band selection, as demonstrated in the study (Nagasubramanian et al. 2018),



would streamline data collection and analysis by removing confounding hyperspectral bands, while the second related study provided saliency-based maps giving user confidence in interpretability (Nagasubramanian et al. 2019). An HTP approach for disease detection involved hyperspectral data collection in the field on a tractor-mounted system and through a handheld system to detect pre-visual foliar symptoms of *Fusarium virguliforme* (causal pathogen of sudden death syndrome) infection in soybean (Herrmann et al. 2018). These studies demonstrate the ability of extended hyperspectral wavelengths to detect pre-visual disease symptom development in greenhouse and field studies and show great promise for early disease mitigation that could be transferred to other stresses and in other crops.

Large-scale datasets have also helped fuel the data analytics innovation in plant stress trait phenotyping. One study utilized the publicly available PlantVillage dataset of over 54,000 digital images of both healthy and diseased leaves in order to develop a deep learning CNN solution to identify 14 crop species and 26 diseases (Hughes and Salathe 2015; Mohanty et al. 2016). Deep-CNN has also been implemented with a dataset of over 25,000 RGB soybean leaf images to identify eight soybean stresses, including nutrient deficiencies, fungal diseases, bacterial diseases, and herbicide injury (Ghosal et al. 2018). This study went one step further to develop an explainability model mapping the features of the leaves that were used for stress identification, removing the mystery and suspicion surrounding many “black box” ML techniques. Furthermore, this method was employed on canopy images under different illumination conditions showing the potential of transfer learning to increase the flexibility of ML algorithms (Ghosal et al. 2018).

In the field, weeds are a major issue in crop production. Researchers developed a portable hyperspectral imaging system and analysis protocol for successful segmentation between soybean and weed species in field images, enabling weed control (Suzuki et al. 2008). Advancements in phenotyping are needed in the field as well as in lab settings. For example, in working with Soybean Cyst Nematode (SCN), egg counts must be quantified under a microscope to determine the severity level of SCN in a field soil sample, in soil-mix from greenhouse experiments, or even of eggs removed from soybean roots to determine colonization severity and plant resistance. Implementation of deep learning and RGB imaging has created a framework capable of counting these microscopic eggs to a high degree of accuracy (Akintayo et al. 2018). This relieves experienced scientists from the time-consuming monotony of manually counting eggs under a microscope. One notable nutrient deficiency in soybean called Iron Deficiency Chlorosis (IDC) is caused by a lack of usable iron in the soil. Zhang et al. (2017) utilized computer vision and ML to translate RGB images of a diverse set of plant canopies into a numerical rating scale and subsequently used the ratings for Genome-Wide Association Studies (GWAS)-based QTL discovery (Zhang et al. 2017), proposing that rapid data collection through smart technologies can improve the rate of uncovering the genetic architecture and detecting QTL for breeding applications. Their work was built on a related study that combined image capture, image processing, and classification workflow into a real-time phenotyping smartphone app for IDC severity rating in the field that could be used by farmers and researchers alike to increase the repeatability of disease ratings (Naik et al. 2017).

Future implementation of this workflow on a ground vehicle or UAS supports HTP (Dobbels and Lorenz 2019).

Future work on stress-related traits and HTP-ML integration will benefit greatly from the application of high-quality and durable hyperspectral cameras (snapshot types) on UAS platforms for rapid data collection and early identification and mitigation of stress. Band selection will promote efficient use of computing resources. Finally, collaborative platforms and improved transfer learning will speed the development of high-quality, flexible ML algorithms trained to handle diverse datasets for real-life applications.

## 7.8 HTP for Root Traits

Roots provide the basis for primary and secondary nutrient uptake for plants. In addition to water acquisition and structural integrity, they play a critical role in the plant's growth and development. Yet, due to their complexity and difficulty to phenotype, they have often been neglected in research and in breeding. Until recently, few HTP methods had been developed to enable the evaluation of root traits. Additionally, recent developments in phenotyping (imaging, sensors, and automation) and application of image processing/ML-based methods have led to an increasing number of root phenotyping platforms. An ideal HTP system will be cost-effective and optimally use non-destructive methods to provide phenomic root growth data across a time series to use in genomics and plant breeding, with increased accuracy and efficiency than manual measurements. The possibility to combine improvements in above ground and root traits opens up exciting opportunities to develop high yielding and more resilient cultivars.

While HTP for above-ground phenotyping can deploy ground robots, drones, or even satellites, data acquisition below ground still ranges in breadth from traditional manual root extraction with shovels (*shovelomics*) (Trachsel et al. 2011; Burrige et al. 2016), ground-penetrating radar (Delgado et al. 2017), to expensive X-ray CT scanning (Jiang et al. 2018). Shovelomics is the primary root extraction method from soil; however, it is extremely labor-intensive, destructive, and not feasible for large experiments. Root traits have been evaluated in trash cans to simulate field trials (Hohmann et al. 2016), walk-in-field rhizotrons (Svane et al. 2019; Eberbach et al. 2013), blue paper evaluations (Atkinson et al. 2015), and even transparent soil (Ma et al. 2019). Moving toward high-throughput systems such as transparent soil imaging is non-destructive, and provides an opportunity to observe growth response with images collected across multiple time points (Ma et al. 2019).

Examples of root phenotyping studies include controlled (Rellán-Álvarez et al. 2015; Clark et al. 2011; Piñeros et al. 2016), semi-controlled (Zhao et al. 2004; Topp et al. 2013; Weaver and Frederick 1974), and field environments (Fenta et al. 2014; Abdel-Haleem et al. 2011; Ao et al. 2010) (Table 7.2).

Controlled environment approaches include both inexpensive cameras, capturing root growth on germination paper and agar plates, and integrated systems built using

**Table 7.2** Comparison of current root analysis methods

Factor\scale	Lab based	Greenhouse-based	Field based
<b>Throughput</b>	High	Medium	Low
<b>Software</b>	Many Available	Available	Few Available
<b>System</b>	Automated	Semi-automated	Primarily manual
<b>Overall costs</b>	Cheap -> Expensive	Affordable -> Expensive	Expensive
<b>Yield relevance</b>	Low	Medium	High
<b>Labor requirement</b>	Low	Medium	Medium -> High
<b>Automation</b>	Available	Possible	In development
<i>Examples:</i>	<i>Germination Paper</i>	<i>Transparent Pots</i>	<i>Shovelomics</i>
	<i>Agar Plate</i>	<i>Rhizotrons</i>	<i>Minirhizotrons</i>
	<i>Transparent Soil</i>	<i>X-Ray CT</i>	<i>Soil Cores</i>
	<i>Hydroponics</i>	<i>PVC Tubes</i>	<i>Excavation</i>

transparent soil (Downie et al. 2012; Lind et al. 2014). Studies conducted in controlled environment have advantages of scale, throughput, and reduced data noise while providing increased cost efficiency. However, these approaches do not have high conformity to field-based experiments. Semi-automated systems using desktop scanners have been adapted to inexpensive germination paper-based platforms. Hydroponics and aeroponic solutions allow for easy root observation; however, these lack representation of soil-based morphological structure. To augment the hydroponic approach, 3D printed plastic scaffolds were designed, allowing the root system to retain its morphology. Additionally, 3D root reconstruction in rice was conducted in a glass cylinder of gel-based media through the capture of multiple images (Clark et al. 2011). Transparent imaging is non-destructive with the advantage of capturing images at multiple time points, providing an opportunity to observe growth response and can somewhat simulate select field conditions (Clark et al. 2011; Lind 2018). Hydroponic root-scaffold systems have characterized root growth rates and structure in multiple crops with promising results (Piñeros et al. 2016). The current state-of-the-art approaches are advancing but not completely bridging the gap between controlled and field experiments. Improved methods and tools are needed to help provide a stronger correlation between lab-based and field experiments.

Semi-controlled environment studies bring advantages of scale, throughput, and data noise reduction through reduced soil heterogeneity and provide some balance with agronomic relevance. Greenhouse-based platforms using sand, soil, or other artificial material grown in pots or tubes allow for easy root removal while often sacrificing the structural morphology of the Root System Architecture (RSA) (Manavalan et al. 2010). Recently, root structure morphology has been captured using advanced 3D imaging approaches, for example, X-ray Computed Tomography (CT), Magnetic Resonance Imaging (MRI) (Rascher et al. 2011), and Positron Emission Tomography (PET) (Nagel et al. 2009). These 3D advances have increasing optimism to capture root system architecture non-destructively in an opaque environment. Tomographic

imaging technology is improving as research is underway to enhance the resolution and speed of these scans; however, such research is still in its infancy. The shortcomings of these technologies are the high-cost, low-throughput, immobile equipment, a need for specialized technicians, loss of information, and lower resolution (Metzner et al. 2015).

Field environments are used when agronomically relevant measurements of traits of interest are desired. However, they come with increased labor costs, difficulties associated with image and data capture (Atkinson et al. 2018), and reduced quality as plants and morphological features are often destroyed upon extraction. Original approaches include digging a trench adjacent to the plant, removal of the root from the soil (shovelomics) (Trachsel et al. 2011), and soil coring (Wasson et al. 2016). In another approach, transparent subterranean tubes buried at an angle in the soil require roots to intersect with the tube, which allows for non-invasive and repeated imaging (Majdi 1996). Scanners are placed inside the tube to identify the intersecting roots before being evaluated by software such as WinRhizo TRON. This approach requires a larger number of buried tubes to acquire an accurate estimate of rooting (Dupuy et al. 2010). Mechanistic solutions such as peanut, potato or tree diggers, underhoes, and tree spades have been tested with a general reduction in root quality being sacrificed for root quantity (Abdel-Haleem et al. 2011).

Automated sensor-to-plant systems for root phenotyping are limited, while manual systems such as minirhizotrons are not high throughput since numerous transparent subterranean tubes are required to achieve accurate phenotyping and their installation is not automated (Majdi 1996). Alternative sensor-to-plant systems include the use of desktop scanners connected in parallel to a single computer (Adu et al. 2014), or customized plant sensors in field (Benfey 2017). However, these require more space, cost, technical knowledge/expertise, and are generally not scalable or high-throughput. RootTracker, an electric plate equipped with tactile sensors, can monitor root touch in the field across a temporal growing season (Benfey 2017). Leaf elemental accumulation for deep roots (LEADER) evaluates deep rooting in cultivars in a short amount of time by comparing the elemental gradients of the soil with leaf measurements to determine root depth (Lynch and Hanlon 2019). X-ray Computed Tomography (CT) imaging within a high-throughput system has led to successful imaging of roots through solid (Turface®, sand and soil) media using pots grown in the greenhouse (Mairhofer et al. 2012; Paya et al. 2015). Coupling CT technology with budding high-throughput laboratory automation can merge large-scale genetic studies of root architecture and growth analysis in solid media with moderate affordability. As these lab-based methods become more field-like (soil or soil-like media, larger pots, increased duration of growth), researchers will be able to standardize the accuracy and precision, leading to increased field reliability. Frontier methods such as transparent media (gel), despite restricting root growth and oxygen availability, have generated positive root phenotyping results (Nagel et al. 2009; Iyer-Pascuzzi et al. 2010; Fang et al. 2009). Simpler, faster, and more affordable methods that can achieve similar correlation accuracies as those attained by X-Ray CT and other advanced methods are needed.

While advances in phenotyping and analytics of canopy-based traits is rapidly improving and increasing, root-related trait advances are still lacking primarily due to the lack of spatio-temporal limitation associated with root and related trait phenotyping. Therefore, studies need to be undertaken that attempt to link root-related traits and their direct role and influence on plant and crop yield. More importantly, there is a need for collective research efforts to build “true” HTP platforms for root studies, including sample acquisition, imaging/sensing, and trait extraction in a well-integrated pipeline. One of the most pressing needs is to develop automated root sampling methods with minimal organ damage from field studies. The optimal root phenotyping platform will include considerations for data quantity, quality, agronomic relevance, and applicability. Continual advances in hardware and ML-based methods and analytics are showing promise in root research involving phenotyping at higher throughput.

## 7.9 HTP Complementing Genetic Studies

Plant genetic studies have gone through a rapid transformation due to next-generation sequencing techniques enabling high-throughput genotyping that allows fast and accurate marker genotyping at a high density. These advances need to complement the rapid collection of robust phenotypic data with sufficient resolution for effective use of genomic data. High-throughput phenotyping using UAS and ground robotic systems followed by ML algorithms are transforming our understanding of phenotyping and is making a profound impact on genomic studies (Singh et al. 2016).

Collecting sufficient robust phenotypic data is the major challenge in plant genetic studies. Researchers can easily genotype a large number of individuals through a single nucleotide polymorphism (SNP) array, genotyping-by-sequencing (GBS), or re-sequencing analysis based on resource availability (Elshire et al. 2011; Song et al. 2013; Lijavetzky et al. 2007). Genotypic profiles are constant across different plant growth stages, with no need to test repeatedly. In contrast, phenotypic profiles are dynamic and vulnerable to environment changes. Phenotyping has to be conducted repeatedly over different environments, or at different crop growth stages to ensure meaningful statistical analysis and answer-specific genetic questions. The situation is exacerbated due to the need for large population sizes for most quantitative genetic studies. The literature is rapidly expanding on the advancements of phenotyping capabilities, but there is still a mismatch with the utilization of temporal phenotypic information for soybean genetic studies. It is promising to identify the dynamic profile of genomewide loci for crop development through HTP. The temporal QTL may shed light on the gene expression regulation, such as shut down or turn on at specific growth stages.

Jubery et al (2017) explored the diversity and inheritance of soybean canopy shape-related parameters through canopy image-based phenotyping of 446 diverse germplasm lines (Jubery et al. 2017). The author outlined and quantified soybean canopy shape descriptors by using Elliptical Fourier Transformation to study

extracted novel traits that are important but hard to measure through traditional phenotyping methods. In another study of soybean IDC, GWAS were carried out with both ML-generated score (ML score) and severity. It verified a major QTL for IDC on chromosome 3 in soybean (Zhang et al. 2017; Assefa et al. 2020). These studies illustrate the advantages of high-throughput image phenotyping in improving genomic study in soybean.

HTP provides high-quality phenotypic data for genomic prediction (GP) model development and improvement. Genomic prediction requires reliable phenotypic data to develop robust models. The accurate estimates of genome-wide effects, by default Genomic Estimated Breeding Value (GEBV), mainly rely on the accuracy of phenotypic data of the training population. Most GP models incorporate marker and/or pedigree information only, but not secondary traits information. HTP can evaluate secondary traits related to the target trait for potential integration into the prediction model and enhanced GP accuracy. Prediction models involving secondary traits can take advantage of correlations between traits (Zhang et al. 2017; Jia and Jannink 2012). Zhang et al. (2017) conducted GP for soybean resistance to IDC using ML score and severity. The GP model with genome-wide SNPs only had a prediction accuracy of 0.44 and 0.37 for the ML score and severity, respectively. The prediction accuracies were increased to 0.55 and 0.51 by adding the models with SPAD values as a covariant, which is a non-destructive measurement of leaf chlorophyll concentrations and is highly related to leaf chlorosis. HTP provides great opportunities to improve GP by including multiple traits into prediction models. In wheat, researchers have illustrated that a GP+HTP model with HTP traits as covariates provided equal or better prediction accuracy than the general GP model across three environments (Crain et al. 2018; Sun et al. 2019). HTP enables screening large training populations with multi-location tests, and ensures the accurate estimate of genotypic effects. Integrating HTP with GP is expected to improve the prediction accuracy and becomes more routine for breeding applications.

A major hurdle of collecting accurate phenomic data on a wide range of physiological traits has been alleviated by HTP, allowing for genomic studies to be conducted to identify associated genomic regions. A recent study by Kaler et al. (2018) identified associated genomic regions with canopy temperature, an important physiological trait associated with seed yield, and proposed that similar studies can be used to pyramid favorable alleles for other physiological traits. Similar genomic studies have been conducted using other HTP data for canopy coverage (Xavier et al. 2017; Kaler et al. 2018), canopy wilting (Kaler et al. 2017), photosynthetic capacity, water use efficiency (Lopez et al. 2019), and chlorophyll traits (Dhanapal et al. 2016). As researchers continue to identify the underlying genomic regions associated with the control of physiological processes (Shook et al. 2021), breeders will have the ability to integrate this information into selection decisions, and future crosses to assemble optimized genetic combinations.

## 7.10 Conclusions

HTP is rapidly becoming prominent in plant sciences, breeding, crop production, and precision agriculture (Singh et al. 2021). Technology advances in payloads (aerial and ground) and sensors (distal and proximal) along with data analytics (ML) are significantly improving HTP capabilities and the entire pipeline. Data analytics is fundamental to the success of HTP pipelines. While HTP is expected to see continued growth, it is important to note that HTP is a tool in a practitioner's toolbox. Sophisticated engineering solutions do not supersede the need for proper experimentation and appropriate choice of methods and tools that are context specific. Extensive validation and continual community effort are needed for proper and meaningful HTP implementation. "One common solution for all situations" may not be feasible. HTP can alleviate concerns of labor requirements for complex traits, remove or minimize inconsistencies in measurement, and improve our ability to collect more relevant data in a timely manner. Rapid adoption of these techniques within both the public and private sectors is facilitated by the ability to compare these measurements to ground truth data giving user confidence. Collaborations among different disciplines are needed to realize the potential offered by HTP.

**Acknowledgements** The support of USDA CRIS project IOW04714 (to A.K.S., A.S.), USDA National Institute of Food and Agriculture (NIFA) Food and Agriculture Cyberinformatics Tools (FACT) award 2019-67021-29938 (to A.S., A.K.S., B.G., S.S.), NSF S&CC award 1952045 (to A.K.S., S.S.), NSF CPS Frontier award CNS-1954556 (to S.S., B.G., A.K.S., A.S.), Iowa Soybean Association (to A.K.S.); Plant Sciences Institute (to A.K.S., B.G., S.S., F.E.M.); Bayer Chair in Soybean Breeding (to A.K.S.); and R F Baker Center for Plant Breeding (to A.K.S.) is sincerely appreciated.

## References

- Abdel-Haleem H, Lee G-J, Boerma RH (2011) Identification of QTL for increased fibrous roots in soybean. *Theor Appl Genet* 122:935–946
- Adu MO, Chatot A, Wiesel L, Bennett MJ, Broadley MR, White PJ et al (2014) A scanner system for high-resolution quantification of variation in root growth dynamics of *Brassica rapa* genotypes. *J Exp Bot* 65:2039–2048
- Ahmad IS, Reid JF, Paulsen MR, Sinclair JB (1999) Color classifier for symptomatic soybean seeds using image processing. *Plant Dis* 83:320–327
- Akintayo A, Tylka GL, Singh AK, Ganapathysubramanian B, Singh A, Sarkar S (2018) A deep learning framework to discern and count microscopic nematode eggs. *Sci Rep* 8:9145
- Allen TW, Bradley CA, Sisson AJ, Byamukama E, Chilvers MI, Coker CM et al (2017) Soybean yield loss estimates due to diseases in the United States and Ontario, Canada, from 2010 to 2014. *Plant Health Prog* 18:19–27
- Alves TM, Moon RD, MacRae IV, Koch RL (2019) Optimizing band selection for spectral detection of *Aphis glycines Matsumura* in soybean. *Pest Manag Sci* 75:942–949
- Amorim WP, Tetila EC, Pistori H, Papa JP (2019) Semi-supervised learning with convolutional neural networks for UAV images automatic recognition. *Comput Electron Agric* 164:

- Ao J, Fu J, Tian J, Yan X, Liao H (2010) Genetic variability for root morph-architecture traits and root growth dynamics as related to phosphorus efficiency in soybean. *Funct Plant Biol* 37:304–312
- Arad B, Ben-Shahar O, Timofte R, Van Gool L, Zhang L, Yang M-H, et al (2018) NTIRE 2018 challenge on spectral reconstruction from RGB Images. 2018 IEEE/CVF conference on computer vision and pattern recognition workshops (CVPRW), pp 1042–1049
- Araus JL, Kefauver SC, Zaman-Allah M, Olsen MS, Cairns JE (2018) Translating high-throughput phenotyping into genetic gain. *Trends Plant Sci* 23:451–466
- Arnal Barbedo JG (2019) Plant disease identification from individual lesions and spots using deep learning. *Biosyst Eng* 180:96–107
- Assefa T, Zhang J, Chowda-Reddy RV, Moran Lauter AN, Singh A, O'Rourke JA et al (2020) Deconstructing the genetic architecture of iron deficiency chlorosis in soybean using genome-wide approaches. *BMC Plant Biol* 20:42
- Atkinson JA, Wingen LU, Griffiths M, Pound MP, Gaju O, Foulkes MJ et al (2015) Phenotyping pipeline reveals major seedling root growth QTL in hexaploid wheat. *J Exp Bot* 66:2283–2292
- Atkinson JA, Robert J J, Bentley AR, Ober E, Wells DM (2018) Field phenotyping for the future. In: Roberts JA (ed) *Annual plant reviews online*. Chichester, UK: John Wiley & Sons, Ltd; pp 1–18
- Bai G, Ge Y, Hussain W, Baenziger PS, Graef G (2016) A multi-sensor system for high throughput field phenotyping in soybean and wheat breeding. *Comput Electron Agric* 128:181–192
- Ballesteros R, Ortega JF, Hernandez D, Moreno MA (2018) Onion biomass monitoring using UAV-based RGB imaging. *Precis Agric* 19:840–857
- Bandara AY, Weerasooriya DK, Bradley CA, Allen TW, Esker PD (2019) Dissecting the economic impact of soybean diseases in the United States over two decades. *bioRxiv*. p 655837. <https://doi.org/10.1101/655837>
- Barker J, Zhang N, Sharon J, Steeves R, Wang X, Wei Y et al (2016) Development of a field-based high-throughput mobile phenotyping platform. *Comput Electron Agric* 122:74–85
- Barmeier G, Schmidhalter U (2017) High-throughput field phenotyping of leaves, leaf sheaths, culms and ears of spring barley cultivars at anthesis and dough ripeness. *Front Plant Sci* 8:1920
- Batey T (2009) Soil compaction and soil management—a review. *Soil Use Manage* 25:335–345
- Benfey P (2017) Hi Fidelity genetics non-invasive field phenotyping device for plant roots. In: ARPA-E [Internet]. 2017. Available: <https://arpa-e.energy.gov/?q=slick-sheet-project/plant-root-phenotyping>
- Betbeder J, Fieuzal R, Baup F (2016) Assimilation of LAI and dry biomass data from optical and sar images into an agro-meteorological model to estimate soybean yield. *IEEE J Sel Topics Appl Earth Obser Remote Sens* 9:2540–2553
- Birrell S, Hughes J, Cai JY, Iida F (2019) A field-tested robotic harvesting system for iceberg lettuce. *J Field Robot*. <https://doi.org/10.1002/rob.21888>
- Bock CH, Poole GH, Parker PE, Gottwald TR (2010) Plant Disease Severity Estimated Visually, by Digital Photography and Image Analysis, and by Hyperspectral Imaging. *CRC Crit Rev Plant Sci*. 29:59–107
- Burridge J, Jochua CN, Bucksch A, Lynch JP (2016) Legume shovelomics: High—Throughput phenotyping of common bean (*Phaseolus vulgaris* L.) and cowpea (*Vigna unguiculata subsp, unguiculata*) root architecture in the field. *Field Crops Res* 192:21–32
- Castelão Tetila E, Brandoli Machado B, D S. Belete NA, Guimarães DA, Pistori H (2017) Identification of soybean foliar diseases using unmanned aerial vehicle images. *IEEE Geosci Remote Sens Lett* 14:2190–2194
- Castelão Tetila E, Brandoli Machado B, Menezes GK, d. S. Oliveira A, Alvarez M, Amorim WP, et al (2019) Automatic recognition of soybean leaf diseases using uAV images and deep convolutional neural networks. *IEEE Geosci Remote Sens Lett*, 1–5
- Chaerle L, Van Der Straeten D (2001) Seeing is believing: imaging techniques to monitor plant health. *Biochim Biophys Acta* 1519:153–166



- Chelladurai V, Karuppiyah K, Jayas DS, Fields PG, White NDG (2014) Detection of *Callosobruchus maculatus* (F.) infestation in soybean using soft X-ray and NIR hyperspectral imaging techniques. *J Stored Prod Res* 57:43–48
- Choudhuri A, Chowdhary G (2018) Crop stem width estimation in highly cluttered field environment. CVPPP. Available: [https://www.plant-phenotyping.org/lw\\_resource/datapool/systemfiles/elements/files/ce6e81f0-949b-11e8-8a88-dead53a91d31/current/document/0016.pdf](https://www.plant-phenotyping.org/lw_resource/datapool/systemfiles/elements/files/ce6e81f0-949b-11e8-8a88-dead53a91d31/current/document/0016.pdf)
- Christenson BS, Schapaugh WT, An N, Price KP, Prasad V, Fritz AK (2016) Predicting soybean relative maturity and seed yield using canopy reflectance. *Crop Sci* 56:625–643
- Clark RT, MacCurdy RB, Jung JK, Shaff JE, McCouch SR, Aneshansley DJ et al (2011) Three-dimensional root phenotyping with a novel imaging and software platform. *Plant Physiol* 156:455–465
- Conn A, Pedmale UV, Chory J, Navlakha S (2017) High-resolution laser scanning reveals plant architectures that reflect universal network design principles. *Cell Syst* 5(53–62):
- Coser SM, Chowda Reddy RV, Zhang J, Mueller DS, Mengistu A, Wise KA et al (2017) Genetic architecture of Charcoal Rot () resistance in soybean revealed using a diverse panel. *Front Plant Sci* 8:1626
- Crain J, Mondal S, Rutkoski J, Singh RP, Poland J (2018) Combining high-throughput phenotyping and genomic information to increase prediction and selection accuracy in wheat breeding. *Plant Genome*, 11. <https://doi.org/10.3835/plantgenome2017.05.0043>
- da Silva LA, Bressan PO, Gonçalves DN, Freitas DM, Machado BB, Gonçalves WN (2019) Estimating soybean leaf defoliation using convolutional neural networks and synthetic images. *Comput Electron Agric* 156:360–368
- Das Choudhury S, Samal A, Awada T (2019) Leveraging Image Analysis For High-Throughput Plant Phenotyping. *Front Plant Sci* 10:508
- Das A, Schneider H, Burrige J, Ascanio AKM, Wojciechowski T, Topp CN, et al (2015) Digital imaging of root traits (DIRT): a high-throughput computing and collaboration platform for field-based root phenomics. *Plant Methods*, 11. <https://doi.org/10.1186/s13007-015-0093-3>
- De Rainville F-M, Durand A, Fortin F-A, Tanguy K, Maldague X, Panneton B et al (2014) Bayesian classification and unsupervised learning for isolating weeds in row crops. *Pattern Anal Appl* 17:401–414
- Delgado A, Hays DB, Bruton RK, Ceballos H, Novo A, Boi E, et al (2017) Ground penetrating radar: a case study for estimating root bulking rate in cassava (*Manihot esculenta Crantz*). *Plant Methods*. <https://doi.org/10.1186/s13007-017-0216-0>
- Dhanapal AP, Ray JD, Singh SK, Hoyos-Villegas V, Smith JR, Purcell LC et al (2016) Genome-wide association mapping of soybean chlorophyll traits based on canopy spectral reflectance and leaf extracts. *BMC Plant Biol* 16:174
- Do more GCPs equal more accurate drone maps? In: Pix4D [Internet]. 5 Nov 2018 [cited 28 Aug 2019]. Available: <https://www.pix4d.com/blog/GCP-accuracy-drone-maps>
- Dobbels AA, Lorenz AJ (2019) Soybean iron deficiency chlorosis high throughput phenotyping using an unmanned aircraft system. *Plant Methods* 15:1–9
- dos Santos Ferreira A, Matte Freitas D, Gonçalves da Silva G, Pistori H, Theophilo Folhes M (2017) Weed detection in soybean crops using ConvNets. *Comput Electron Agric* 143:314–324
- Downie H, Holden N, Otten W, Spiers AJ, Valentine TA, Dupuy LX (2012) Transparent Soil for Imaging the Rhizosphere. *PLoS ONE* 7:
- DroneDeploy (2017) Choosing the Right Mapping Drone for Your Business Part I: Multi-Rotor vs. Fixed Wing Aircraft. In: Medium [Internet]. DroneDeploy's Blog; 16 Jun 2017 [cited 29 Aug 2019]. Available: <https://blog.dronedeploy.com/choosing-the-right-mapping-drone-for-your-business-part-i-multi-rotor-vs-fixed-wing-aircraft-6ec2d02eff48>
- Dupuy L, Vignes M, Mckenzie BM, White PJ (2010) The dynamics of root meristem distribution in the soil. *Plant, Cell & Environ* 33:358–369
- Eberbach PL, Hoffmann J, Moroni SJ, Wade LJ, Weston LA (2013) Rhizo-lysimetry: facilities for the simultaneous study of root behaviour and resource use by agricultural crop and pasture systems. *Plant Methods* 9:3

- Elshire RJ, Glaubitz JC, Sun Q, Poland JA, Kawamoto K, Buckler ES et al (2011) A robust, simple genotyping-by-sequencing (GBS) approach for high diversity species. *PLoS ONE* 6:
- Etienne A (2019) AUTOMATED WEED DETECTION USING MACHINE LEARNING TECHNIQUES ON UAS-ACQUIRED IMAGERY. 2019. Available: [https://hammer.figshare.com/articles/AUTOMATED\\_WEED\\_DETECTION\\_USING\\_MACHINE\\_LEARNING\\_TECHNIQUES\\_ON\\_UAS-ACQUIRED\\_IMAGERY/9108371](https://hammer.figshare.com/articles/AUTOMATED_WEED_DETECTION_USING_MACHINE_LEARNING_TECHNIQUES_ON_UAS-ACQUIRED_IMAGERY/9108371)
- Falk KG, Jubery TZ, Mirnezami SV, Parmley KA, Sarkar S, Singh A et al (2020a) Computer vision and machine learning enabled soybean root phenotyping pipeline. *Plant Methods* 16:5
- Falk KG, Jubery TZ, O'Rourke JA, Singh A, Soumik S, Ganapathysubramanian B, et al (2020) Soybean root system architecture trait study through genotypic, phenotypic, and shape-based clusters. *Plant*. 2020. Available: <https://spj.sciencemag.org/plantphenomics/2020/1925495/>
- Fang S, Yan X, Liao H (2009) 3D reconstruction and dynamic modeling of root architecture *in situ* and its application to crop phosphorus research: 3D dynamic modeling of root architecture *in situ*. *Plant J* 60:1096–1108
- Fenta B, Beebe S, Kunert K, BurrIDGE J, Barlow K, Lynch J et al (2014) Field phenotyping of soybean roots for drought stress tolerance. *Agronomy* 4:418–435
- Friedli M, Kirchgessner N, Grieder C, Liebisch F, Mannale M, Walter A (2016) Terrestrial 3D laser scanning to track the increase in canopy height of both monocot and dicot crop species under field conditions. *Plant Methods* 12:9
- Gage JL, Miller ND, Spalding EP, Kaeppeler SM, de Leon N (2017) TIPS: a system for automated image-based phenotyping of maize tassels. *Plant Methods*, 13. <https://doi.org/10.1186/s13007-017-0172-8>
- Gage JL, Richards E, Lepak N, Kaczmar N, Soman C, Chowdhary G, et al (2019) In-field whole plant maize architecture characterized by Latent Space Phenotyping. *bioRxiv*. p 763342. <https://doi.org/10.1101/763342>
- Gai J, Tang L, Steward BL (2019) Automated crop plant detection based on the fusion of color and depth images for robotic weed control. *J Field Robot*. <https://doi.org/10.1002/rob.21897>
- Galkovskiy T, Mileyko Y, Bucksch A, Moore B, Symonova O, Price CA et al (2012) GiA Roots: software for the high throughput analysis of plant root system architecture. *BMC Plant Biol* 12:116
- Gao T, Emadi H, Saha H, Zhang J, Lofquist A, Singh A et al (2018a) A Novel Multirobot system for plant phenotyping. *Robotics* 7:61
- Gao F, Anderson M, Daughtry C, Johnson D (2018b) Assessing the variability of corn and soybean yields in central iowa using high spatiotemporal resolution multi-satellite imagery. *Remote Sens* 10:1489
- Gelder BK (2015) Automation of DEM Cutting for Hydrologic/Hydraulic Modeling. Iowa State University; 2015. Report No.: IHRB TR-631. Available: [http://lib.dr.iastate.edu/cgi/viewcontent.cgi?article=1062&context=intrans\\_techtransfer](http://lib.dr.iastate.edu/cgi/viewcontent.cgi?article=1062&context=intrans_techtransfer)
- Ghosal S, Blystone D, Singh AK, Ganapathysubramanian B, Singh A, Sarkar S (2018) An explainable deep machine vision framework for plant stress phenotyping. *Proc Natl Acad Sci U S A* 115:4613–4618
- Gibson KD, Dirks R, Medlin CR, Johnston L (2004) Detection of weed species in soybean using multispectral digital images. *Weed Technol* 18:742–749
- Gnäding F, Schmidhalter U (2017) Digital counts of maize plants by unmanned aerial vehicles (UAVs). *Remote Sens* 9:544
- Gosseau F, Blanchet N, Varès D, Burger P, Campergue D, Colombet C et al (2018) Heliaphen, an outdoor high-throughput phenotyping platform for genetic studies and crop modeling. *Front Plant Sci* 9:1908
- Haghighatalab A, González Pérez L, Mondal S, Singh D, Schinstock D, Rutkoski J et al (2016) Application of unmanned aerial systems for high throughput phenotyping of large wheat breeding nurseries. *Plant Methods* 12:35

- Hartman GL, Rupe J, Sikora EJ, Domier LL, Davis JA, Steffey KL (2015) Compendium of soybean diseases and pests. 5th Edition. C. HGLRJ, editor. St. Paul, Minnesota: American Phytopathological Society
- Hatton N, Sharda A, Schapaugh W, Van der Merwe D (2018). Remote thermal infrared imaging for rapid screening of sudden death syndrome in soybean. 2018 ASABE annual international meeting. American Society of Agricultural and Biological Engineers, p 1
- Herrmann I, Vosberg SK, Ravindran P, Singh A, Chang H-X, Chilvers MI et al (2018) Leaf and Canopy Level Detection of *Fusarium virguliforme* (Sudden Death Syndrome) in Soybean. Remote Sens 10:426
- Hohmann M, Stahl A, Rudloff J, Wittkop B, Snowdon RJ (2016) Not a load of rubbish: simulated field trials in large-scale containers. Plant, Cell Environ 39:2064–2073
- Hoyos-Villegas V, Houx JH, Singh SK, Fritschi FB (2014) Ground-based digital imaging as a tool to assess soybean growth and yield. Crop Sci 54:1756–1768
- Hughes DP, Salathe M (2015) An open access repository of images on plant health to enable the development of mobile disease diagnostics
- Inoue Y, Peñuelas J (2006) Relationship between light use efficiency and photochemical reflectance index in soybean leaves as affected by soil water content. Int J Remote Sens 27:5109–5114
- Iyer-Pascuzzi AS, Symonova O, Mileyko Y, Hao Y, Belcher H, Harer J et al (2010) Imaging and analysis platform for automatic phenotyping and trait ranking of plant root systems. Plant Physiol 152:1148–1157
- Jang G-S, Sudduth KA, Hong S-Y, Kitchen NR, Palm HL (2006) Relating hyperspectral image bands and vegetation indices to corn and soybean yield. Korean J Remote Sens 22:183–197
- Jia Y, Jannink J-L (2012) Multiple-trait genomic selection methods increase genetic value prediction accuracy. Genetics 192:1513–1522
- Jiang N, Floro E, Bray AL, Laws B, Duncan KE, Topp CN (2018) High-resolution 4D spatiotemporal analysis reveals the contributions of local growth dynamics to contrasting maize root architectures. bioRxiv, p 381046. <https://doi.org/10.1101/381046>
- Jin X, Kumar L, Li Z, Feng H, Xu X, Yang G et al (2018) A review of data assimilation of remote sensing and crop models. Eur J Agron 92:141–152
- Jubery TZ, Shook J, Parmley K, Zhang J, Naik HS, Higgins R et al (2017) Deploying fourier coefficients to unravel soybean canopy diversity. Front Plant Sci 7:2066
- Jubery TZ, Carley CN, Singh A, Sarkar S, Ganapathysubramanian B, Singh AK (2020) Using Machine learning to develop a fully automated soybean nodule acquisition pipeline (SNAP). bioRxiv. 2020. Available: <https://www.biorxiv.org/content/10.1101/2020.10.12.336156v1.abstract>
- Kaler AS, Ray JD, Schapaugh WT, King CA, Purcell LC (2017) Genome-wide association mapping of canopy wilting in diverse soybean genotypes. Theor Appl Genet 130:2203–2217
- Kaler AS, Ray JD, Schapaugh WT, Asebedo AR, King CA, Gbur EE et al (2018a) Association mapping identifies loci for canopy temperature under drought in diverse soybean genotypes. Euphytica 214:135
- Kaler AS, Ray JD, Schapaugh WT, Davies MK, King CA, Purcell LC (2018b) Association mapping identifies loci for canopy coverage in diverse soybean genotypes. Mol Breed 38:50
- Keller K, Kirchgessner N, Khanna R, Siegwart R, Walter A, Aasen H (2018) Soybean Leaf coverage estimation with machine learning and thresholding algorithms for field phenotyping. Proc BMVC 2018:0032
- Khan Z, Miklavcic SJ (2019) An automatic field plot extraction method from aerial Orthomosaic images. Front Plant Sci. 10:683
- Kirchgessner N, Liebisch F, Yu K, Pfeifer J, Friedli M, Hund A, et al (2016) The ETH field phenotyping platform FIP: a cable-suspended multi-sensor system. Functional Plant Biol. Available: <http://www.publish.csiro.au/fp/fp16165>
- Koger CH, Bruce LM, Shaw DR, Reddy KN (2003) Wavelet analysis of hyperspectral reflectance data for detecting pitted morning glory (*Ipomoea lacunosa*) in soybean (*Glycine max*). Remote Sens Environ 86:108–119

- Kovar M, Brestic M, Sytar O, Barek V, Hauptvogel P, Zivcak M (2019) Evaluation of Hyperspectral reflectance parameters to assess the leaf water content in soybean. *Water* 11:443
- Li Y, Jia J, Zhang L, Khattak AM, Sun S, Gao W et al (2019) Soybean seed counting based on pod image using two-column convolution neural network. *IEEE Access* 7:64177–64185
- Lijavetzky D, Cabezas JA, Ibáñez A, Rodríguez V, Martínez-Zapater JM (2007) High throughput SNP discovery and genotyping in grapevine (*Vitis vinifera* L.) by combining a re-sequencing approach and SNPlex technology. *BMC Genomics*, 8:424
- Lind K (2018) Environments-by-design: developing new tools to bring “field conditions” to the laboratory. Cademartiri L, editor. Doctor of Philosophy, Iowa State University
- Lind KR, Sizmur T, Benomar S, Miller A, Cademartiri L (2014) LEGO® bricks as building blocks for centimeter-scale biological environments: the case of plants. *PLoS ONE* 9:
- Loh P-R, Tucker G, Berger B (2011) Phenotype prediction using regularized regression on genetic data in the DREAM5 systems genetics challenge. *PLoS ONE* 6:
- Lopez MA, Xavier A, Rainey KM (2019) Phenotypic variation and genetic architecture for photosynthesis and water use efficiency in soybean (*Glycine max* L. Merr). *Front Plant Sci* 10:680
- Lynch J, Hanlon M (2019) Identification of deep-rooted maize with X-ray fluorescence. In: *Roots Lab* [Internet]. 2019. Available: <https://plantscience.psu.edu/research/labs/roots/projects/deeper/research-projects-1/leader>
- Ma L, Shi Y, Siemianowski O, Yuan B, Egnér TK, Mirnezami SV et al (2019) Hydrogel-based transparent soils for root phenotyping in vivo. *Proc Natl Acad Sci USA* 116:11063–11068
- Mahlein A (2016) Plant Disease Detection By Imaging Sensors—Parallels And Specific Demands For Precision Agriculture And Plant Phenotyping. *Plant Dis* 100:241–251
- Maimaitijiang M, Ghulam A, Sidike P, Hartling S, Maimaitiyiming M, Peterson K et al (2017) Unmanned Aerial System (UAS)-based phenotyping of soybean using multi-sensor data fusion and extreme learning machine. *ISPRS J Photogramm Remote Sens* 134:43–58
- Mairhofer S, Zappala S, Tracy SR, Sturrock C, Bennett M, Mooney SJ et al (2012) RooTrak: automated recovery of three-dimensional plant root architecture in soil from X-Ray Microcomputed tomography images using visual tracking. *Plant Physiol* 158:561–569
- Majdi H (1996) Root sampling methods—applications and limitations of the minirhizotron technique. *Plant Soil* 185:255–258
- Manavalan LP, Guttikonda SK, Nguyen VT, Grover Shannon J, Nguyen HT (2010) Evaluation of diverse soybean germplasm for root growth and architecture. *Plant Soil* 330:503–514
- McAllister W, Osipychov D, Davis A, Chowdhary G (2019) Agbots: Weeding a field with a team of autonomous robots. *Comput Electron Agric* 163:
- McKinney NV, Schapaugh WT, Kanemasu ET (1989) Selection for canopy temperature differential in six populations of Soybean. *Crop Sci* 29:255
- Merchuk-Ovnat L, Ovnat Z, Amir-Segev O, Kutsher Y, Saranga Y, Reuveni M (2019) Coverage-Tool: A semi-automated graphic software: applications for plant phenotyping. *Plant Methods*, 15. <https://doi.org/10.1186/s13007-019-0472-2>
- Metzner R, Eggert A, van Dusschoten D, Pflugfelder D, Gerth S, Schurr U et al (2015) Direct comparison of MRI and X-ray CT technologies for 3D imaging of root systems in soil: potential and challenges for root trait quantification. *Plant Methods* 11:17
- Mfuka C, Zhang X, Byamukama E (2019) Mapping and quantifying white mold in soybean across south dakota using landsat images. *J Geogr Inform Syst* 11:331–346
- Mila AL, Carriquiry AL, Yang XB (2004) Logistic regression modeling of prevalence of soybean sclerotinia stem rot in the north-central region of the United States. *Phytopathology* 94:102–110
- Mo C, Kim MS, Kim G, Cheong EJ, Yang J, Lim J (2015) Detecting drought stress in soybean plants using hyperspectral fluorescence imaging. *J Biosyst Eng* 40:335–344
- Moellers TC, Singh A, Zhang J, Brungardt J, Kabbage M, Mueller DS et al (2017) Main and epistatic loci studies in soybean for *Sclerotinia sclerotiorum* resistance reveal multiple modes of resistance in multi-environments. *Sci Rep* 7:3554

- Mohanty SP, Hughes DP, Salathé M (2016) Using deep learning for image-based plant disease detection. *Front Plant Sci* 7:1419
- Moreno R, Corona F, Lendasse A, Graña M, Galvão LS (2014) Extreme learning machines for soybean classification in remote sensing hyperspectral images. *Neurocomputing* 128:207–216
- Moulin S, Bondeau A, Delecote R (1998) Combining agricultural crop models and satellite observations: From field to regional scales. *Int J Remote Sens* 19:1021–1036
- Nagasubramanian K, Jones S, Sarkar S, Singh AK, Singh A, Ganapathysubramanian B (2018) Hyperspectral band selection using genetic algorithm and support vector machines for early identification of charcoal rot disease in soybean stems. *Plant Methods* 14:86
- Nagasubramanian K, Jones S, Singh AK, Sarkar S, Singh A, Ganapathysubramanian B (2019) Plant disease identification using explainable 3D deep learning on hyperspectral images. *Plant Methods* 15:1–10
- Nagasubramanian K, Jubery TZ, Ardakani FF, Mirnezami SV, Singh AK, Singh A et al (2020) How useful is Active Learning for Image-based Plant Phenotyping? arXiv [cs.CV]. Available: <http://arxiv.org/abs/2006.04255>
- Nagasubramanian K, Singh AK, Singh A, Sarkar S, Ganapathysubramanian B (2020) Usefulness of interpretability methods to explain deep learning based plant stress phenotyping. arXiv [cs.CV]. 2020. Available: <http://arxiv.org/abs/2007.05729>
- Nagel KA, Kastenholz B, Jahnke S, van Dusschoten D, Aach T, Mühlich M et al (2009) Temperature responses of roots: impact on growth, root system architecture and implications for phenotyping. *Funct Plant Biol* 36:947–959
- Naik HS, Zhang J, Lofquist A, Assefa T, Sarkar S, Ackerman D et al (2017) A real-time phenotyping framework using machine learning for plant stress severity rating in soybean. *Plant Methods* 13:23
- Narayanan B, Floyd B, Tu K, Ries L, Hausmann N (2019) Improving soybean breeding using UAS measurements of physiological maturity. *Autonomous Air and Ground Sensing Systems for Agricultural Optimization and Phenotyping IV*. *Int Soc Opt Photon*. <https://doi.org/10.1117/12.2519072>
- Näsi R, Honkavaara E, Lyytikäinen-Saarenmaa P, Blomqvist M, Litkey P, Hakala T et al (2015) Using UAV-based photogrammetry and hyperspectral imaging for mapping bark beetle damage at tree-level. *Remote Sens* 7:15467–15493
- Nawaz MF, Bourrié G, Trolard F (2013) Soil compaction impact and modelling. *A Rev Agron Sustain Dev* 33:291–309
- Nguy-Robertson A, Gitelson A, Peng Y, Viña A, Arkebauer T, Rundquist D (2012) Green leaf area index estimation in maize and soybean: combining vegetation indices to achieve maximal sensitivity. *Agron J* 104:1336–1347
- Oide M, Ninomiya S (2000) Discrimination of soybean leaflet shape by neural networks with image input. *Comput Electron Agric* 29:59–72
- Oniga V-E, Breaban A-I, Stătescu F (2018) Determining the optimum number of ground control points for obtaining high precision results based on UAS images. *Multidisciplinary Digital Publishing Institute*, p. 352
- Pace J, Lee N, Naik HS, Ganapathysubramanian B, Lübberstedt T (2014) Analysis of Maize (*Zea mays* L.) seedling roots with the high-throughput image analysis tool ARIA (Automatic Root Image Analysis). *PLoS ONE* 9:e108255
- Parmley K, Nagasubramanian K, Sarkar S, Ganapathysubramanian B, Singh AK (2019a) Development of optimized phenomic predictors for efficient plant breeding decisions using phenomic-assisted selection in soybean. *Plant Phenomics* 2019:5809404
- Parmley K, Higgins RH, Ganapathysubramanian B, Sarkar S, Singh AK (2019b) Machine learning approach for prescriptive plant breeding. *Sci Rep* 9:17132
- Paya AM, Silverberg JL, Padgett J, Bauerle TL (2015). X-ray computed tomography uncovers root–root interactions: quantifying spatial relationships between interacting root systems in three dimensions. *Front Plant Sci*, 6. <https://doi.org/10.3389/fpls.2015.00274>

- Piñeros MA, Larson BG, Shaff JE, Schneider DJ, Falcão AX, Yuan L et al (2016) Evolving technologies for growing, imaging and analyzing 3D root system architecture of crop plants. *J Integr Plant Biol* 58:230–241
- Pires RDL, Gonçalves DN, Oruê JPM, Kanashiro WES, Rodrigues JF, Machado BB et al (2016) Local descriptors for soybean disease recognition. *Comput Electron Agric* 125:48–55
- Pittman JJ, Arnall DB, Interrante SM, Moffet CA, Butler TJ (2015) Estimation of biomass and canopy height in bermudagrass, alfalfa, and wheat using ultrasonic, laser, and spectral sensors. *Sensors* 15:2920–2943
- Pound MP, Atkinson JA, Townsend AJ, Wilson MH, Griffiths M, Jackson AS, et al (2018) Erratum to: Deep machine learning provides state-of-the-art performance in image-based plant phenotyping. *Gigascience*, 7. <https://doi.org/10.1093/gigascience/giy042>
- R Shamshiri R, Weltzien C, Hameed IA, J Yule I, E Grift T, Balasundram SK, et al (2018) Research and development in agricultural robotics: A perspective of digital farming. Available: <https://ntnuopen.ntnu.no/ntnu-xmlui/handle/11250/2595468>
- Rascher U, Blossfeld S, Fiorani F, Jahnke S, Jansen M, Kuhn AJ et al (2011) Non-invasive approaches for phenotyping of enhanced performance traits in bean. *Funct Plant Biol* 38:968–983
- Rellán-Álvarez R, Lobet G, Lindner H, Pradier P-L, Sebastian J, Yee M-C, et al (2015) GLO-Roots: an imaging platform enabling multidimensional characterization of soil-grown root systems. *Elife*, 4. <https://doi.org/10.7554/elife.07597>
- Riera LG, Carroll ME, Zhang Z, Shook JM, Ghosal S, Gao T, et al (2020) Deep multi-view image fusion for soybean yield estimation in breeding applications. arXiv [cs.CV]. 2020. Available: <http://arxiv.org/abs/2011.07118>
- Sakoda K, Watanabe T, Sukemura S, Kobayashi S, Nagasaki Y, Tanaka Y et al (2019) Genetic diversity in stomatal density among soybeans elucidated using high-throughput technique based on an algorithm for object detection. *Sci Rep* 9:7610
- Shoebly M, Robles-Kelly A, Timofte R, Zhou R, Lahoud F, Süsstrunk S, et al (2019) PIRM2018 challenge on spectral image super-resolution: methods and results. *Computer Vision—ECCV 2018 workshops*, pp 356–371
- Shook J, Gangopadhyay T, Wu L, Ganapathysubramanian B, Sarkar S, Singh AK (2020) Crop yield prediction integrating genotype and weather variables using deep learning. arXiv preprint arXiv. Available: <https://arxiv.org/abs/2006.13847>
- Shook JM, Zhang J, Jones SE, Singh A, Diers BW, Singh AK (2021) Meta-GWAS for quantitative trait loci identification in soybean, G3 Genes|Genomes|Genetics. jkab117. <https://doi.org/10.1093/g3journal/jkab117>
- Shrivastava S, Hooda DS (2014) Automatic brown spot and frog eye detection from the image captured in the field. *Amer J Intell Syst* 4:131–134
- Shrivastava S, Singh SK, Hooda DS (2017) Soybean plant foliar disease detection using image retrieval approaches. *Multimed Tools Appl* 76:26647–26674
- Shuai X, Zhou Z, Yost RS (2003) Using segmented regression models to fit soil nutrient and soybean grain yield changes due to liming. *JABES* 8:240–252
- Sinclair TR, Kitani S, Hinson K, Bruniard J, Horie T (1991) Soybean flowering date: linear and logistic models based on temperature and photoperiod. *Crop Sci* 31:786–790
- Singh A, Ganapathysubramanian B, Singh AK, Sarkar S (2016) Machine learning for high-throughput stress phenotyping in plants. *Trends Plant Sci* 21:110–124
- Singh AK, Ganapathysubramanian B, Sarkar S, Singh A (2018) Deep learning for plant stress phenotyping: trends and future perspectives. *Trends Plant Sci* 23:883–898
- Singh A, Jones S, Ganapathysubramanian B, Sarkar S, Mueller D, Sandhu K et al (2020) Challenges and Opportunities In Machine-Augmented Plant Stress Phenotyping. *Trends Plant Sci*. <https://doi.org/10.1016/j.tplants.2020.07.010>
- Singh DP, Singh AK, Singh A (2021) Plant breeding and cultivar development. 1st edition. Academic Press, p662

- Sivakumar ANV (2019) Mid to Late Season Weed Detection in Soybean Production Fields Using Unmanned Aerial Vehicle and Machine Learning. Shi Y, editor. MSc, University of Nebraska. 2019. Available: <https://digitalcommons.unl.edu/biosysengdiss/91/>
- Song Q, Hyten DL, Jia G, Quigley CV, Fickus EW, Nelson RL et al (2013) Development and evaluation of SoySNP50K, a high-density genotyping array for soybean. *PLoS ONE* 8:
- Sun J, Poland JA, Mondal S, Crossa J, Juliana P, Singh RP et al (2019) High-throughput phenotyping platforms enhance genomic selection for wheat grain yield across populations and cycles in early stage. *Theor Appl Genet* 132:1705–1720
- Suzuki Y, Okamoto H, Kataoka T (2008) Image segmentation between crop and weed using hyperspectral imaging for weed detection in soybean field. *Environ Control Biol* 46:163–173
- Swane SF, Jensen CS, Thorup-Kristensen K (2019) Construction of a large-scale semi-field facility to study genotypic differences in deep root growth and resources acquisition. *Plant Methods* 15:26
- Tang J, Wang D, Zhang Z, He L, Xin J, Xu Y (2017) Weed identification based on K-means feature learning combined with convolutional neural network. *Comput Electron Agric* 135:63–70
- Terlaksiz AS, Altıylar DT (2019) Use of deep neural networks for crop yield prediction: a case study of soybean yield in Lauderdale County, Alabama, USA. 2019 8th international conference on Agro-Geoinformatics (Agro-Geoinformatics), pp 1–4
- Thorp KR, Thompson AL, Harders SJ, French AN, Ward RW (2018) High-throughput phenotyping of crop water use efficiency via multispectral drone imagery and a daily soil water balance model. *Remote Sens* 10:1682
- Topp CN, Iyer-Pascuzzi AS, Anderson JT, Lee C-R, Zurek PR, Symonova O, et al (2013) 3D phenotyping and quantitative trait locus mapping identify core regions of the rice genome controlling root architecture. *Proc Natl Acad Sci U S A* 110:E1695–704
- Trachsel S, Kaeppler SM, Brown KM, Lynch JP (2011) Shovelomics: high throughput phenotyping of maize (*Zea mays L.*) root architecture in the field. *Plant Soil* 341:75–87
- Tresch L, Mu Y, Itoh A, Kaga A, Taguchi K, Hirafuji M et al (2019) Easy MPE: extraction of quality microplot images for UAV-based high-throughput field phenotyping. *Plant Phenomics* 2019:2591849
- Ubbens JR, Stavness I (2017) Corrigendum: Deep Plant Phenomics: a deep learning platform for complex plant phenotyping tasks. *Front Plant Sci* 8:2245
- Uzal LC, Grinblat GL, Namiás R, Larese MG, Bianchi JS, Morandi EN et al (2018) Seed-per-pod estimation for plant breeding using deep learning. *Comput Electron Agric* 150:196–204
- Veenadhari S, Mishra B, Singh CD (2011) Soybean productivity modelling using decision tree algorithms. *Int J Comput Appl Technol* 27:11–15
- Verrelst J, Rivera JP, Gitelson A, Delegido J, Moreno J, Camps-Valls G (2016) Spectral band selection for vegetation properties retrieval using Gaussian processes regression. *Int J Appl Earth Obs Geoinf* 52:554–567
- Wallace L, Lucieir A, Watson C, Turner D (2012) Development of a UAV-LiDAR system with application to forest inventory. *Remote Sens* 4:1519–1543
- Wang D, Dowell FE, Ram MS, Schapaugh WT (2004) Classification of fungal-damaged soybean seeds using near-infrared spectroscopy. *Int J Food Prop* 7:75–82
- Wang X, Singh D, Marla S, Morris G, Poland J (2018a) Field-based high-throughput phenotyping of plant height in sorghum using different sensing technologies. *Plant Methods* 14:53
- Wang AX, Tran C, Desai N, Lobell D, Ermon S (2018) Deep transfer learning for crop yield prediction with remote sensing data. *Proceedings of the 1st ACM SIGCAS conference on computing and sustainable societies*. New York, NY, USA: ACM, pp 50:1–50:5
- Wang T, Rostamza M, Song Z, Wang L, McNickle G, Iyer-Pascuzzi AS et al (2019) SegRoot: a high throughput segmentation method for root image analysis. *Comput Electron Agric* 162:845–854
- Wasson A, Bischof L, Zwart A, Watt M (2016) A portable fluorescence spectroscopy imaging system for automated root phenotyping in soil cores in the field. *J Exp Bot* 67:1033–1043
- Weaver RW, Frederick LR (1974) Effect of Inoculum Rate on Competitive Nodulation of *Glycine max* L Merrill. *I Greenhouse Studies. Agronomy J* 66:229

- Williams WA, Qualset CO, Geng S (1979) Ridge regression for extracting soybean yield factors. *Crop Sci* 19:869
- Xavier A, Hall B, Hearst AA, Cherkauer KA, Rainey KM (2017) Genetic architecture of phenomic-enabled canopy coverage in glycine max. *Genetics* 206:1081–1089
- Xue J, Su B (2017) Significant remote sensing vegetation indices: a review of developments and applications. *J Sens*. 2017. <https://doi.org/10.1155/2017/1353691>
- Yang XB, Royer MH, Tschanz AT, Tsai BY (1990) Analysis and quantification of soybean rust epidemics from seventy-three sequential planting experiments. *Phytopathology* 80:1421–1427
- Yang G, Liu J, Zhao C, Li Z, Huang Y, Yu H et al (2017) Unmanned aerial vehicle remote sensing for field-based crop phenotyping: current status and perspectives. *Front Plant Sci* 8:1111
- You J, Li X, Low M, Lobell D, Ermon S (2017) Deep gaussian process for crop yield prediction based on remote sensing data. Thirty-First AAAI Conference on artificial intelligence. 2017. Available: <https://www.aaai.org/ocs/index.php/AAAI/AAAI17/paper/viewPaper/14435>
- Yu N, Li L, Schmitz N, Tian LF, Greenberg JA, Diers BW (2016) Development of methods to improve soybean yield estimation and predict plant maturity with an unmanned aerial vehicle based platform. *Remote Sens Environ* 187:91–101
- Yuan H, Yang G, Li C, Wang Y, Liu J, Yu H et al (2017) Retrieving soybean leaf area index from unmanned aerial vehicle hyperspectral remote sensing: analysis of RF, ANN, and SVM regression models. *Remote Sens* 9:309
- Zhang J, Naik HS, Assefa T, Sarkar S, Chowda Reddy RV, Singh A et al (2017) Computer vision and machine learning for robust phenotyping in genome-wide studies. *Scientific Reports* 7:44048
- Zhao J, Fu J, Liao H, He Y, Nian H, Hu Y et al (2004) Characterization of root architecture in an applied core collection for phosphorus efficiency of soybean germplasm. *Chinese Sci Bull* 49:1611–1620
- Zheng H, Chen L, Han X, Zhao X, Ma Y (2009) Classification and regression tree (CART) for analysis of soybean yield variability among fields in Northeast China: The importance of phosphorus application rates under drought conditions. *Agric Ecosyst Environ* 132:98–105
- Zheng H, Chen L, Han X, Ma Y, Zhao X (2010) Effectiveness of phosphorus application in improving regional soybean yields under drought stress: a multivariate regression tree analysis. *Afr J Agric Res* 5:3251–3258
- Zhou J, Yungbluth D, Vong CN, Scaboo A, Zhou J (2019a) Estimation of the maturity date of soybean breeding lines using UAV-based multispectral imagery. *Remote Sens* 11:2075
- Zhou Y, Srinivasan S, Mirnezami SV, Kusmec A, Fu Q, Attigala L et al (2019b) Semiautomated feature extraction from RGB images for sorghum panicle architecture GWAS. *Plant Physiol* 179:24–37



# Chapter 8

## High-Throughput Phenotyping in Potato Breeding



**Jagesh Kumar Tiwari, Sushil S. Changan, Tanuja Buckseth, Rajesh K. Singh, Brajesh Singh, Satish K. Luthra, Shashi Rawat, and Manoj Kumar**

**Abstract** Increasing tuber yield, yield stability, biotic and abiotic stress resistance/tolerance, and improving nutritional quality characteristics are the important goals of potato breeding. Traditional phenotyping methods are comparatively lesser efficient than the high-throughput plant phenotyping (HTP) platforms for screening of elite genotypes. HTP platforms are image-based, non-destructive procedures that employ a series of electromagnetic-radiation wavelength bands and sensed by high-resolution cameras by visible and hyperspectral images and thermal sensors for capturing plant responses to environmental stimuli. Efficient HTP techniques are essential to develop new improved potato varieties for multiple traits like high yield potential, tuber quality traits, resistant to disease and pests, and abiotic stress (heat, drought, and nutrient use efficiency) to combat under climate change scenario. We speculate application of HTP with aeroponic culture for precised phenotyping for above- and underground plant parts in potato. For precision trait phenotyping, aeroponic-HTP technologies would be a good application for nutrient-based experiments and other traits as well, whereas HTP in soil-based pot cultivation would be promising technologies for investigation of heat and drought stress tolerance, and other biotic/abiotic stresses including tuber quality parameters. Besides, HTP application also uses RGB camera mounted with unmanned aerial vehicles for field trail studies. The purpose of this chapter is to present applications of HTP in potato could enhance selection efficacy for next-generation potato breeding.

**Keywords** Aeroponic · Breeding · Field · High-throughput phenotyping · Potato · Pot · Traits

---

J. K. Tiwari (✉) · S. S. Changan · T. Buckseth · R. K. Singh · B. Singh · S. K. Luthra · S. Rawat · M. Kumar  
ICAR-Central Potato Research Institute, Shimla 171001, Himachal Pradesh, India  
e-mail: [jagesh.tiwari@gmail.com](mailto:jagesh.tiwari@gmail.com)

© Springer Nature Switzerland AG 2021  
J. Zhou et al. (eds.), *High-Throughput Crop Phenotyping*,  
Concepts and Strategies in Plant Sciences,  
[https://doi.org/10.1007/978-3-030-73734-4\\_8](https://doi.org/10.1007/978-3-030-73734-4_8)

## 8.1 Introduction

Potato (*Solanum tuberosum* L.,  $2n = 4x = 48$ ) is the fourth most important food crop of the world after rice, wheat, and maize. Its annual production worldwide is more than 388 million tons (FAOSTAT 2017). Cultivated potato is a tetraploid and highly heterozygous crop which has the major application for food, feed, and industrial use. To meet the food demand of 9.1 billion population by 2050, a sustainable increase in food production is necessary (FAO 2009). Potato improvement through conventional breeding limited due to its tetrasomic inheritance and precised trait phenotyping (Muthoni et al. 2015). A conventional potato breeding program uses out-crossing and followed by subsequent phenotypic recurrent selection for a series of generations to identify desired traits (Bradshaw and Mackay 1994). Generally, large breeding populations are generated and further screened them through different field trials to screen superior phenotypes, thus reduce the population number, whereas on the other side increases the number of plants of each genotype (Bradshaw and Mackay 1994). During conventional breeding genotypes with desired phenotypic traits are identified to use them as parents in crossing program to generate new improved breeding lines (Bradshaw et al. 2007). These populations are then further screened over a series of clonal generations to get clones with desired traits, and this process takes more than 10 years (Bradshaw et al. 2007). About 40 traits are considered during the process of screening for improved variety identification (Gebhardt 2013). So, it is a very mammoth task to handle a huge population size and screen them for desirable traits. As conventional potato breeding is quite slow, laborious, and could be erroneous, there is need to utilize high-throughput phenotyping platform that can screen thousands of breeding populations in short time and thus accelerate the potato breeding. Increasing the genomics information puts pressure on the breeders to provide rapid and accurate phenotypic analysis. Precise and efficient phenotypic platform is important for potato breeders to develop new improved varieties. Various breeding techniques such as marker-assisted selection, quantitative trait loci (QTL) mapping, mutants population analysis, and association mapping require assistance of proper trait phenotyping. Manual collection of huge phenotypic data is laborious, time-consuming, erroneous, and requires a lot of man power. It is very difficult to manage and analyze this huge dataset. Thus, the major challenge for phenotyping is to develop tools that can collect, manage, access, organize, integrate, and analyze huge phenotypic dataset of breeding program. New advanced imaging techniques and bioinformatics/computational tools are now available that assist high-throughput phenotyping.

Various traits have been reported to be associated with biotic and abiotic stress tolerances; however, very few of them are used for screening a large pool of germplasm by traditional methods (Reynolds and Langridge 2016). Current phenotyping approaches are expensive, laborious, slow, and mostly destructive, and permit to study a few parameters at a time (Cobb et al. 2013; Virlet et al. 2017). Advancement in crop improvement techniques is necessary for plant breeders, biotechnologists, and geneticists to meet the world's increasing food production demands and tackle

abiotic and biotic stresses (Godfray et al. 2010; Sankaran et al. 2015). These non-destructive high-throughput phenotyping technologies are focusing on various traits that directly or indirectly show plant water content, chlorophyll content, biomass, and growth potential (Andrade-Sanchez et al. 2014) and also offer a new dimension that increase precision, speed, and analysis of captured data (Furbank and Tester 2011). Development of high yielding potato cultivars with improved tolerant to biotic and abiotic stresses required precise phenotyping for various morphological, structural, physiological, biochemical, and molecular traits (Zia et al. 2017). Therefore, breeders must be assisted by high-throughput phenotyping for functional analysis of specific genes, forward and reverse genetic studies, and generation of new improved varieties with desired traits. Thus, breeders can manage many trials in different growth conditions with use of different lines in mapping populations, breeding populations, mutant populations, and germplasm pool. Further advancement in high-throughput and accurate phenotyping, modeling, and association with potato breeders is major challenge particularly when developing new potato varieties and target environments.

## 8.2 High-Throughput Phenotyping (HTP) Platform

HTP platforms have been applied for non-destructive analysis of whole plant system in different crops under controlled or field conditions, which utilize advanced automation and robotics, imaging (2D, 3D) techniques, unique sensors, and hardwares and softwares to monitor various traits of plant growth and development (Table 8.1) (Prashar et al. 2013; Zia et al. 2017). HTP is based on the automated real-time measurement of plant growth and developmental stages, and physiological and biochemical responses in smart glasshouses (or field conditions by unmanned aerial vehicles) equipped with imaging system. The visible imaging system measures phenotypes like plant growth rates, biomass accumulation, architecture, canopy, phenology, pathogen lesion area, senescence and chlorophyll content, etc. Whereas hyperspectral imaging system allows measurements of internal traits such as sugar, starch, protein, moisture content, and several stress-related parameters (Slater et al. 2017). HTP platforms take multiple images at various time intervals at different wavelengths to generate data for software-based analysis. These imagery data is processed into a desired readable format using image analysis software. HTP platforms utilize application of visible light imaging system for estimation of various traits such as phenology, senescence, shoot biomass, plant height, leaf area, germination rate, flowering time, yield contributing traits, growth-related parameters, disease and pest symptoms (Backhaus et al. 2010; Clark et al. 2011; Li et al. 2014; Sugiura et al. 2016), thermal imaging for analyzing leaf/canopy temperature, leaf senescence, transpiration rate, heat dissipation, pathogen and disease detection (Jones et al. 2009; O'Shaughnessy et al. 2011; Li et al. 2014), fluorescence imaging for analyzing photosynthesis status of non-photochemical quenching (NPQ), plant health, shoot architecture drought, and heat stress (Burling et al. 2010; Brabandt et al. ; Tatagiba et al. ). Near-Infrared (NIR) hyperspectral and multispectral imaging techniques are used for

**Table 8.1** High-throughput phenotyping approaches in plants

Sr. no	Type of imaging	Tools/sensors/software/technique	Potential applications	References
1	Thermal infrared (IR) imaging	Thermal infrared thermometers	Leaf/canopy temperature, leaf senescence, transpiration rate, water deficit stress, heat dissipation, pathogen, and disease detection	Jones et al. (2009), O'Shaughnessy et al. (2011), Li et al. (2014), Manickavasagan et al. (2008)
2	Near-infrared NIR) imaging	Near-infrared cameras/Infrared thermography	Leaf area index (LAI), transpiration rate, water content, NDVI, and heat dissipation	Pask and Pietragalia (2012), Cook et al. (2012), Prashar et al. (2013)
3	Hyperspectral imaging	Hyperspectral Imaging sensors, thermal cameras, spectrometers	Chlorophyll fluorescence, leaf and canopy water content, leaf area, leaf density, plant health status, measure starch, protein, carbohydrate, and moisture content	Furbank and Tester (2011), Busemeyer et al. (2013), Yol et al. (2015)
4	Multispectral imaging	Multispectral scanning cameras	Nutrient status, pigment status, senescence, water content, and photosynthetic efficiency	Songsri et al. (2009), Moghaddam et al. (2011), Monneveux et al. (2013)
5	Visible light imaging	Visible spectral range digital cameras/LIDAR LAMINA SOFTWARE/LEAF PROCESSOR (leaf shape analysis tool)	Phenology, senescence, shoot biomass, height, leaf area, germination rate, flowering time, growth-related parameters, disease and pest symptoms, and yield contributing traits	Ikeda et al. (2010), Backhaus et al. (2010), Clark et al. (2011), Sugiura et al. (2016)

(continued)

Table 8.1 (continued)

Sr. no	Type of imaging	Tools/sensors/software/technique	Potential applications	References
6	Fluorescence imaging	Fluorescence capturing cameras	Status of photosynthesis, non-photochemical quenching (NPQ), drought and heat stress, plant health, and shoot architecture	Moshou et al. (2005), Burling et al. (2010), Brabandt et al. (2014), Tatagiba et al. (2015)
7	3D laser imaging	3D digital imaging system, RootReader 3D, X-ray CT (3D)	Root system architecture (RSA), plant architecture, canopy structure, leaf angle distributions, height, and leaf area	Biskup et al. (2007), Yazdianbakhsh and Fisahn (2009), Galkovskiy et al. (2012)

analyzing leaf area index (LAI), transpiration rate, water content, normalized difference vegetation index (NDVI), heat dissipation, plant health status, nutrient status, and photosynthetic efficiency (Pask and Pietragalla 2012; Busemeyer et al. 2013; Monneveux et al. 2013; Yol et al. 2015). 3D laser imaging is mostly used for assessment of root system architecture (RSA) (Yol et al. 2015). There are various image analysis software programs for high-throughput phenotyping, namely, LAMINA, LEAFPROCESSOR, RootReader2D and 3D, PlaRoM, LeafAnalyzer, Gia-Roots, GROWSCEEN 3D, LemnaTec 3D Scanalyzer, and TraitMill (Cobb et al. 2013). Study in Australia shows application of HTP technologies in field-grown crops applying LiDAR, multispectral and hyperspectral sensors, thermal sensors, ultrasonic sensors, data loggers, and RTK-GNSS receivers (Slater et al. 2017). Another new application of HTP demonstrates use of RGB camera coupled with unmanned aerial vehicles (UAV) for detection of late blight disease in potato (Chawade et al. 2019). Taken together, HTP technologies have been successfully applied in various crops for automated precision phenotyping to assist crop breeding (Table 8.1). Although successful application in potato is still limited till now but there is likely chances to speed up the potato breeding using HTP in future.

## 8.3 Application of HTP Platform in Potato Breeding

### 8.3.1 Target Traits

Breeding of potato is a difficult task because of its autotetraploid and heterozygous nature as over 40 different traits are measured while development of a new potato variety and also there are many market-specific and consumer-driven characters as well (Gebhardt 2013). These traits can be categorized into different groups like tolerance to biotic and abiotic stresses, yield-related traits, and nutritional and tuber quality features. For example, there are a number of breeding objectives under Indian conditions like early bulking and short duration, tolerance to high temperature and drought stresses, nutrient use efficient, resistance to diseases (late blight, viruses, bacterial wilt, etc.), and pests (aphid, white fly, mite, tuber moth, potato cyst nematode, etc.). Tuber quality traits are very much important for consumer and processing industry such as tuber dry matter content, storage behavior and keeping quality, nutritionally rich (Fe and Zn), and tuber traits (shape, size, and color), and processing traits like low reducing sugar. Most target traits like yield, tuber number, tuber size, specific gravity, and processing quality in potato are mainly influenced by genotype, environment, and interaction. As a result, more than 10 years needed for a conventional breeding program to select genotypes across several clonal populations in addition to many suitable sites for a variety of required traits (Gebhardt 2013). Hence, traits phenotyping based on HTP is essential for rapid potato breeding.

### 8.3.2 HTP for Traits Phenotyping

#### 8.3.2.1 Plant Phenotype

HTP technologies have been deployed in various crops such as Arabidopsis, rice, wheat, maize, soybean, legumes, beans, tomato, and sugar beet, and recently we have applied in potato also (Fig. 8.1). To develop high yielding improved potato cultivars with tolerance to various biotic and abiotic stresses, enhanced nutritional profile, nutrient use efficiency, and market-specific traits require precise phenotyping of various morphological, physiological, structural, biochemical, and molecular traits for marker or genomics-assisted breeding (Zia et al. 2017). Potato phenotyping has been reported under drought stress conditions by Monneveux et al. (2013) and Wishart et al. (2014). High-resolution aerial imaging system has been used as a high-throughput phenotyping technology for estimation of crop emergence in potato (Sankaran et al. 2017; Li et al. 2019). In potato, the frequent high-throughput phenotyping of plant growth and biomass accumulation using digital images of experimental fields would assist to detect a fast growing and early vigor genotypes which would be helpful in breeding for early maturing varieties. Earlier it could be very

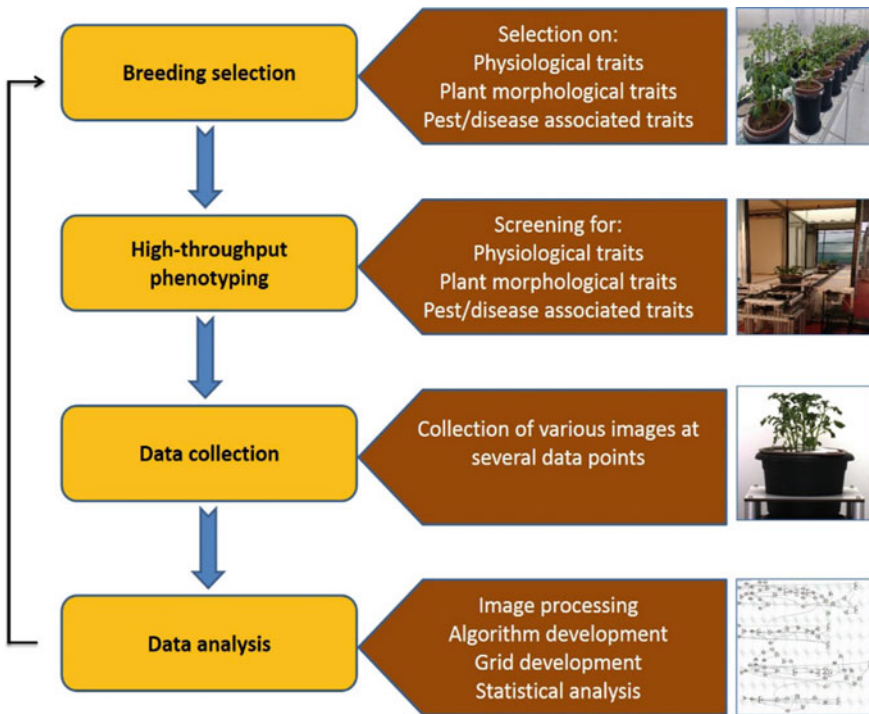


Fig. 8.1 High-throughput phenotyping platform for trait-specific potato breeding

difficult to manually measure these traits in a large pool of genotypes. This phenotyping approach could be utilized to detect foliar disease and pest symptoms, and also their level of infestation, time of arrival in potato field. This information could be used for effective management of disease and pest menace by designing package for control. Also, this phenotyping will assist to screen out susceptible genotypes in disease/pest resistance breeding program. Future advancement in sensor technology could also enable to unravel the underground traits like stolon and tuber initiation, and their growth and development. These traits could not be evaluated manually. Use of high-throughput phenotyping at harvesting stage will help to assess tuber characteristics, viz., tuber shape, size, skin color, texture, and number, and this information will be used to predict performance of each genotype in terms of yield and tuber distribution. Hyperspectral and multispectral imaging could be used to assess the tuber quality parameters, viz., carbohydrate, starch, protein, reducing sugar, and water content which are important for cooking performance. High-throughput visible near-infrared (NIR) and infrared (IR) range imaging of potato under controlled conditions are shown in Fig. 8.2.

### 8.3.2.2 Canopy Cover

Crop emergence and canopy cover are considered as important physiological traits for cultivar screening and nutrients management in potato. These traits are important for potato variety screening, field management, and prediction of yield (Spitters and Schapendonk 1990). Traditional manual assessment of these traits is laborious, time-consuming, and subjective as compared to high-throughput phenotyping. Many traits associated with potato emergence (uniformity and emergence rate) play important roles in screening of varieties, field management practices, and prediction of yield (Moran et al. 1997). These traits can be affected by various factors like potato seed quality, dormancy period, water deficit stress, nutrient deficiency, and soil temperature (Dyson and Watson 1971; Onder et al. 2005). Consistent monitoring of traits is important for efficient crop management. Crop canopy is one of the most commonly used traits for estimating crop canopy structure using remote sensing technology at the early stage of crop growth (Moran et al. 1997). Amount of sunlight interception is determined by crop canopy cover and thus affects photosynthetic efficiency. In crop breeding and precision agronomy, emergence rate and uniformity are crucial for field-scale phenotyping. Crop emergence is conventionally estimated by time-consuming and laborious manual counting practice, while canopy cover is assessed by subjective and inaccurate manual scoring method (Li et al. 2019). The repeatability and reproducibility of these manual assessment techniques are very low, and it is very difficult to execute these practices in thousands of trial plots of large agronomical and breeding experiments (Duan et al. 2017).

A non-destructive observation and phenotyping of individual plants in pot can be done using high-throughput phenotyping platform under controlled conditions. But, there are some bottlenecks to correlate results of controlled conditions with the field conditions. Potato crop possesses a large canopy and shows restricted growth



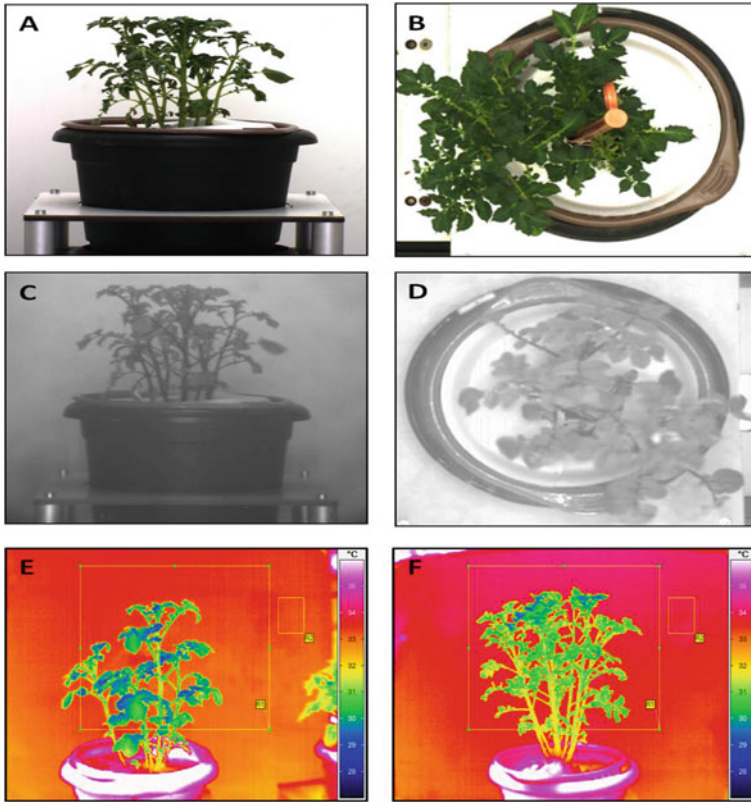


**Fig. 8.2** High-throughput potato imaging using LemnaTec Phenomics platform. Visible range imaging side (A) and top (B) view; Near-Infrared imaging side (C) and top (D) view, Infrared imaging side view (E, F)

and development in pots under controlled condition. Thus, there is need to develop a highly automated and non-destructive high-throughput platform for field condition. As breeding and genetic analysis of most crops comprising potato is generally carried out under natural environment, the field phenotyping approach provides better understanding of crop behavior (Prashar et al. 2013). A fully automated, high-throughput fixed site phenotyping platform, Field Scanalyzer, have been developed; it is equipped with multiple imaging sensors for non-destructive observation of plant growth and development (Sadeghi-Tehran et al. 2017; Virlet et al. 2017). The information generated by Field Scanalyzer may be utilized by potato breeders to screen large set of germplasm based on desired physiological and morphological traits. In potato, infrared thermography (IRT) was used to estimate stomatal conductance and canopy temperature (Prashar et al. 2013). Even under well-watered condition, the potato genotypes showed significant differences in canopy temperature. There was a negative correlation between canopy temperature and tuber yield (Prashar et al.

2013). These observations can be utilized to identify SNP (single nucleotide polymorphism) that control stomatal conductance and canopy temperature (Zia et al. 2017). Estimation of canopy temperature using thermal imagery was used to assess severity of water stress in maize (Han et al. 2016). Thus, stomatal conductance and canopy temperature traits can be used to screen potato germplasm for drought stress tolerance breeding.

The camera sensor phenotyping approach has been used to monitor green canopy coverage of potato and its correlation was established with fresh plant biomass and LAI (Dammer et al. 2016). Relative vegetation index (ratio of reflectance at 800 nm/650 nm) and NDVI (normalized difference vegetation index) ( $[\text{reflectance at } 800 \text{ nm} - \text{reflectance at } 650 \text{ nm}] / [\text{reflectance at } 800 \text{ nm} + \text{reflectance at } 650 \text{ nm}]$ ) were used to estimate leaf area index and biomass in potato (Schafleitner et al. 2007). It will be used to detect disease occurrence, severity and level of infestation, and also provides information to develop disease forecasting models and management practices (Zia et al. 2017). Thus, potato breeders can utilize this approach to identify biotic stress-tolerant (late blight of potato) genotype.

### 8.3.2.3 Biotic and Abiotic Stress-Related Traits

There is ample use of chemical fertilizers and pesticides to improve potato yield, which leads to potential economic waste and environmental pollution (Liang et al. 2018). Strategies for optimization of nutrient doses are required for potato cultivation. Heat and drought stress tolerance and nutrient use efficiency are the major abiotic factors in potato, which are complex phenomenon governed by various physiological, biochemical, and molecular factors. Among the biotic factors, diseases like late blight, viruses, bacterial wilt, and storage disease, and pests like aphid, white fly, mites, potato cyst nematodes, etc. are the devastating causes of yield losses in potato. Application of HTP could be possible to phenotype the traits for these above diseases pests. In potato, abiotic stress experiments are easily possible under HTP platforms under normal pot conditions by manipulation of temperature and photoperiod regulation for heat stress, soil water (moisture) control for drought stress, and nutrients doses for nutrient use efficiency studies. Moreover, HTP facility needs to be standardized for biotic stress studies, where challenge inoculations of pathogens or pests are applied to measure resistance/tolerance in plants that can be investigated by HTP imaging systems. The recently introduced high-throughput phenotyping technique provides advanced tools for precision screening by incorporation of innovative screening strategies that can assist the selection and pyramiding of drought-responsive genes appropriate for specific environmental conditions. Several methods for assessment of drought tolerance are available and used in cereal crops, and that could be also applicable to potato. These methods comprise fluorescence, thermometry, and reflectance. Chlorophyll fluorescence imaging provides a reliable technique for the study of changes in photosynthesis rate of potato under water deficit stress (Anithakumari et al. 2012), whereas the ratio of  $F_v$  and  $F_m$  and the differences in the

canopy temperature may be used to screen drought tolerance among potato genotypes (Prashar et al. 2013; Prashar and Jones 2014). Multispectral imaging has been used for determination of chlorophyll content in potato leaves (Borhan et al. 2004). In case of potato, genotypes with higher canopy temperature under irrigated conditions were more tolerant to drought stress as compared to genotypes with lower canopy temperature (Stark et al. 1991). Reflectance indices, calculated from the visible and near-infrared light reflected by vegetation, have been used in several crops to estimate biomass and changes in leaf water content (Ullah et al. 2014). These indices have proved accurate to assess drought-associated traits.

#### 8.3.2.4 Root System Architecture

Roots are an important underground plant part because plant's performance mainly depends on the healthy root system, thus root phenotyping is as important as shoot phenotyping (Wasaya et al. 2018). Root system architecture is largely associated with drought tolerance and nutrient uptake as compared to above-ground plant parts, and plays important role in maintaining crop yield under drought stress (Gupta et al. 2012). A non-invasive and non-destructive phenotyping techniques warrant special attention to more accurate assess of the response of various traits under drought condition. Different techniques have been developed for root phenotyping under controlled as well as field conditions. Root growth, development, architecture, and its functionality under water deficit stress must be the part of potato breeding programs (Iwama 2008). In situ root imaging technique is used to study root system in several crops and in potato also (Richner et al. 2000). Han et al. (2016) successfully used X-ray Computed Tomography (CT) technique to extract the architecture of first-order potato roots. Magnetic resonance imaging (MRI) technique can be used to assess root system architecture in early stages of potato development (Monneveux et al. 2013). Several root characters, i.e., morphological plasticity, primary root length, length and number of lateral roots, crown root number, root tip diameter, root hair density, root angles, root tissue density, and gravitropism help the plants to adapt and respond under various stress conditions and they might be important for improving water use efficiency in crop species (Fenta et al. 2014; Wasaya et al. 2018). Root phenotyping techniques comprise some degree of automation with imaging, image analysis, and processing. Various Imaging and its analysis techniques/software have been used as reliable tools for root phenotyping and they include WinRhizo, Smart Root, EZ-Rhizo, Image J, Root System Analyzer, Root Nav, IJ\_Rhizo, and Root Trace (Wasaya et al. 2018).

#### 8.3.2.5 Aeroponic Culture

Aeroponic is a soil-less crop cultivation system where nutrient solution is supplied through mist form to the plant roots under controlled chamber. Aeroponic technology

has been applied mostly for production of healthy minitubers. Application of aeroponic in seed potato production is recent in India and a few more; however, a decade back it was limited to countries like China and Korea for the commercial production of potato quality seeds. Nowadays, aeroponic is being applied in most parts of the potato-growing countries. Thus, aeroponic is an important technique of soil-less culture under controlled conditions for healthy quality seed potato production. Here, we have standardized phenotyping by manual method (semi-automated for nutrient supply) of potato for various plant parts like roots, shoots, and stolons under aeroponic (Tiwari et al. 2018, 2020d). Further, genomics approaches could be applied to study genes controlling nitrogen use efficiency in potato under controlled supply of nutrients (Tiwari et al. 2018, 2020a,b,c) (Fig. 8.3). Our recent studies indicate that aeroponic can be applied for screening of genotypes by measurement of root- and shoot-related traits and genes discovery. This technology allows dissection of full root system architecture of plants for various traits related to root, stolon, and minitubers. Further, it has advantages of year the round cultivation of potato and independent from crop season. Moreover, temperature and photoperiod are the key



**Fig. 8.3** Precision phenotyping in potato under aeroponic culture

environmental cues determining potato tuberization, which can be regulated under fully controlled environmental conditions (i.e., automated phenotyping platform or HTP). Further, data generated from aeroponic-HTP systems could be analyzed on similar pattern like earlier. Until now, HTP is mostly applied through pot culture experiments in various crops. Hence, here with the advancement in technologies, we propose that aeroponic could be integrated with HTP platform combined with multiple imaging systems and sensors for real-time monitoring of plant phenotypes. This would assist in measurement of above-ground parts (shoot/leaves/foilage) and underground parts (roots, stolons, and tubers) for a wide range of traits such as abiotic stresses like nutrient, heat and drought, and biotic stresses like disease and pests. This aeroponic-HTP platform would be a novel discovery for precision phenotyping in potato. In particular, nutrient stress-related study could be easily designed in aeroponic where amount of macro- and micro-nutrients can be monitored in the solution. Nevertheless, integration of aeroponic with HTP platforms would require designing of technologies equipped with imaging systems for whole plant image capture at different growth and developmental stages including tubers, and further data recording and analysis system.

## 8.4 Advantages of HTP

Application of HTP in potato breeding allows following advantages as schematically presented in Fig. 8.4 and summarized here:

- *Automated traits phenotyping*: Ease of traits phenotyping by HTP platform with automatic, non-invasive, non-destructive imaging coupled with UAV and analysis using advanced computing tools. HTP is integrated with various automated tools, sensors, imaging sensors, and camera for automatic image capture and their analysis using in-built software tools. Comparative analysis of crops by quantitative measurements of plant performance under controlled HTP and filed conditions could be done.
- *High accuracy*: With the advanced integrated technologies, HTP allows rapid and accurate screening of large set of genotypes for desired traits based on foliage and roots traits and less cumbersome than manual methods.
- *High precision*: Precise observation of complete plant life cycle and recording information at various time intervals in potato. Measurements are important at various growth stages like plant emergence, canopy cover, stolon initiation, tuber formation and growth, tuber bulking, and finally tuber harvest.
- *High selection efficiency*: Plant performance and phenotypic trait selection efficiency are greatly influenced by various environmental factors. The environmental influenced variations in traits can be assessed efficiently by high-throughput phenotyping techniques than traditional methods, thus improving selection efficiency (Sankaran et al. 2015; Virlet et al. 2017).

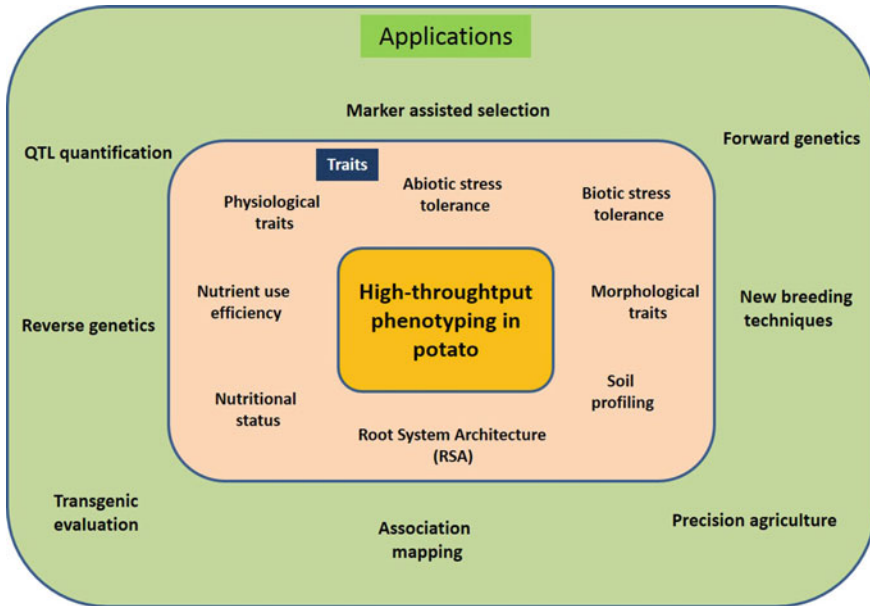


**Fig. 8.4** Applications of high-throughput phenotyping in potato breeding

- *Genomics-phenomics research advancement:* HTP has capacity to deliver genomics and phenomics research advancement in less time with accurate and precise traits phenotyping for speed breeding of potato. This technology facilitates genes and markers discovery for development of new potato varieties with desired traits in less duration and reduces breeding cycles.

## 8.5 Conclusions

In the present genomics era, HTP is becoming high priority research area due to its automation, precision, sensitivity, accuracy, repeatability, and reproducibility. Advanced plant breeding is a key factor to address the worldwide food security issue keeping in mind climate change, water scarcity, and diminishing land. High-throughput phenotyping in combination with advanced breeding approaches, viz., genomic selection, marker-assisted selection, QTL mapping, genotyping by sequencing, and genome editing are being used as next-generation breeding strategies for crop improvement. In potato, HTP using digital images at regular intervals of plant growth would enable early selection of genotypes with desirable traits. This high-throughput phenotyping could detect foliar diseases with different lesion areas using multispectral, hyperspectral, and thermal sensors on aerial vehicles without manual intervention. Further, these sensors are equipped to measure underground plant parts like tuber initiation, tuber characters (shape, size, number, color, etc.),

and quality traits (starch, reducing sugar, and moisture content). Moreover, RGB camera combined with UAV would be potential application of HTP in field trials. Such methods should maximize reproducibility and reliability of phenotyping experiments for enhancing precision in quantifying variation of plant trait expression. In order to do so, it is important to quantify features of both the plant and its growth environment that allows expression of desired trait. High-throughput genotyping and phenotyping can assist in faster, cheaper, and more effective potato breeding and also useful to capture genetic variation for several traits in breeding programs. For precisely extracting the desired information about the potato plant phenotype from these techniques, protocols need to be optimized for monitoring plant growth. Application of HTP techniques outlined in this chapter provides a roadmap for future rapid improvement in potato breeding. However, for maximum utilization of such HTP platforms, screening protocols should be standardized for different crop species and under different stress conditions.

**Acknowledgements** The authors thank the competent authorities for support under the Institute Biotechnology Programme and CABIn scheme, ICAR-IASRI, New Delhi.

## References

- Andrade-Sanchez P, Gore MA, Heun JT, Thorp KR, Carmo-Silva AE, French AN, Salvucci ME, White JW (2014) Development and evaluation of a field-based high-throughput phenotyping platform. *Funct Plant Biol* 41:68–79
- Anithakumari AM, Dolstra O, Vosman B, Visser RGF, van der Linden CG (2012) In vitro screening and QTL analysis for drought tolerance in diploid potato. *Euphytica* 181:357–369
- Backhaus A, Kuwabara A, Bauch M, Monk N, Sanguinetti G, Fleming A (2010) LEAFPRO-CESSOR: a new leaf phenotyping tool using contour bending energy and shape cluster analysis. *New Phytol* 187:251–261
- Biskup B, Scharr H, Schurr U, Rascher U (2007) A stereo imaging system for measuring structural parameters of plant canopies. *Plant Cell Environ* 30:1299–1308
- Borhan MS, Panigrahi S, Lorenzen JH, Gu H (2004) Multispectral and color imaging techniques for nitrate and chlorophyll determination of potato leaves in a controlled environment. *Am Soc Agric Eng* 47(2):599–608
- Brabandt H, Bauriegel E, Gaerber U, Herppich W (2014) PSII and NPQ to evaluate *Bremia lactucae*-infection in susceptible and resistant lettuce cultivars. *Sci Hortic* 180:123–129
- Bradshaw JE, Hackett CA, Pande B, Waugh R, Bryan GJ (2007) QTL mapping of yield, agronomic and quality traits in tetraploid potato (*Solanum tuberosum* subsp. *tuberosum*). *Theor Appl Genet* 116:193–211
- Bradshaw JE, Mackay GR (1994) Potato genetics. CAB International, Wallingford, pp 467–497
- Burling K, Hunsche M, Noga G (2010) Quantum yield of non-regulated energy dissipation in psii (y (no)) for early detection of leaf rust (*Puccinia triticina*) infection in susceptible and resistant wheat (*Triticum aestivum* L.) cultivars. *Precis Agric* 11:703–716
- Bussemeyer L, Mentrup D, Moller K, Wunder E, Alheit K, Hahn V, Maurer HP, Reif JC, Wurschum T, Muller J (2013) Breedvision—A multisensory platform for non-destructive field-based phenotyping in plant breeding. *Sensors* 13:2830–2847
- Chawade A, van Ham J, Blomquist H, Bagge O, Alexandersson E, Ortiz R (2019) High-throughput field-phenotyping tools for plant breeding and precision agriculture. *Agronomy* 9:258

- Clark RT, MacCurdy RB, Jung JK, Shaff JE, McCouch SR, Aneshansley DJ, Kochian LV (2011) Three-dimensional root phenotyping with a novel imaging and software platform. *Plant Physiol* 156:455–465
- Cobb JN, DeClerck G, Greenberg A, Clark R, McCouch S (2013) Next-generation phenotyping: requirements and strategies for enhancing our understanding of genotype-phenotype relationships and its relevance to crop improvement. *Theor Appl Genet* 126:867–887
- Cook JP, McMullen MD, Holland JB, Tian F, Bradbury P, Ross-Ibarra J, Buckler ES, Flint-Garcia SA (2012) Genetic architecture of maize kernel composition in the nested association mapping and inbred association panels. *Plant Physiol* 158:824–834
- Dammer KH, Dworak V, Selbeck J (2016) On-the-go phenotyping in field potatoes using camera vision. *Potato Res* 59:113–127
- Duan T, Chapman SC, Guo Y, Zheng B (2017) Dynamic monitoring of NDVI in wheat agronomy and breeding trials using an unmanned aerial vehicle. *Field Crops Res* 210:71–80
- Dyson PW, Watson DJ (1971) An analysis of the effects of nutrient supply on the growth of potato crops. *Ann Appl Biol* 69:47–63
- FAO (2009) How to feed the world in 2050 report, Food and Agriculture Organization of the United Nations, Rome, Italy
- FAOSTAT (2017) <https://www.fao.org/faostat/en/#data>. Accessed on 17th Aug 2019
- Fenta B, Beebe S, Kunert K, Burrige J, Barlow K, Lynch J, Foyer C (2014) Field phenotyping of soybean roots for drought stress tolerance. *Agronomy* 4:418–435
- Furbank R, Tester M (2011) Phenomics technologies to relieve the phenotyping bottleneck. *Trends Plant Sci* 16:635–644
- Galkovskiy MY, Bucksch A, Moore B, Symonova O, Price CA, Topp CN, Iyer-Pascuzzi AS, Zurek PR, Fang S (2012) GiA Roots: software for the high throughput analysis of plant root system architecture. *BMC Plant Biol* 12:116
- Gebhardt C (2013) Bridging the gap between genome analysis and precision breeding in potato. *Trends Genet* 29:248–256
- Godfray HCJ, Beddington JR, Crute IR, Haddad L, Lawrence D, Muir JF, Pretty J, Robinson S, Thomas SM, Toulmin C (2010) Food security: the challenge of feeding 9 billion people. *Science* 327:812–818
- Gupta PK, Balyan HS, Gahlaut V, Kulwal PL (2012) Phenotyping, genetic dissection, and breeding for drought and heat tolerance in common wheat: Status and prospects. In: Janick J (ed) *Plant breeding reviews*. Wiley, Hoboken, NJ, USA, pp 85–168
- Han M, Zhang H, DeJonge KC, Comas LH, Trout TJ (2016) Estimating maize water stress by standard deviation of canopy temperature in thermal imagery. *Agric Water Manag* 177:400–409
- Ikeda M, Hirose Y, Takashi T, Shibata Y, Yamamura T, Komura T, Doi K, Ashikari M, Matsuoka M, Kitano H (2010) Analysis of rice panicle traits and detection of QTLs using an image analyzing method. *Breed Sci* 60:55–64
- Iwama K (2008) Physiology of the potato: new insights into root system and repercussions for crop management. *Potato Res* 51:333
- Jones HG, Serraj R, Loveys BR, Xiong L, Wheaton A, Price AH (2009) Thermal infrared imaging of crop canopies for the remote diagnosis and quantification of plant responses to water stress in the field. *Funct Plant Biol* 36:978–989
- Li B, Xu X, Han J, Zhang L, Bian C, Jin L, Liu J (2019) The estimation of crop emergence in potatoes by UAV RGB imagery. *Plant Methods* 15(1):15
- Li L, Zhang Q, Huang D (2014) A review of imaging techniques for plant phenotyping. *Sensors* 14:20078–20111
- Liang SM, Ren C, Wang PJ, Wang XT, Li YS, Xu FH et al (2018) Improvements of emergence and tuber yield of potato in a seasonal spring arid region using plastic film mulching only on the ridge. *Field Crops Res* 223:57–65
- Manickavasagan A, Jayas D, White N (2008) Thermal imaging to detect infestation by *Cryptolestes ferrugineus* inside wheat kernels. *J Stored Prod Res* 44:186–192



- Moghaddam PA, Derafshi MH, Shirzad V (2011) Estimation of single leaf chlorophyll content in sugar beet using machine vision. *Turk J Agric* 35:563–568
- Monneveux P, Ramírez DA, Pino MT (2013) Drought tolerance in potato (*S. tuberosum* L.): can we learn from drought tolerance research in cereals? *Plant Sci* 205:76–86
- Moran MS, Inoue Y, Barnes EM (1997) Opportunities and limitations for image-based remote sensing in precision crop management. *Remote Sens Environ* 61:319–346
- Moshou D, Bravo C, Oberti R, West J, Bodria L, McCartney A, Ramon H (2005) Plant disease detection based on data fusion of hyper-spectral and multi-spectral fluorescence imaging using Kohonen maps. *Real-Time Imaging* 11:75–83
- Muthoni J, Kabira J, Shimelis H, Melis R (2015) Tetrasomic inheritance in cultivated potato and implications in conventional breeding. *Aust J Crop Sci* 9:185–190
- O'Shaughnessy SA, Hebel MA, Evett SR, Colaizzi PD (2011) Evaluation of a wireless infrared thermometer with a narrow field of view. *Comput Electron Agric* 76:59–68
- Onder S, Caliskan ME, Onder D, Caliskan S (2005) Different irrigation methods and water stress effects on potato yield and yield components. *Agric Water Manag* 73(1):73–86
- Pask A, Pietragalla J (2012) Leaf area, green crop area and senescence. In: Pask A, Pietragalla J, Mullan D, Reynolds M (eds) *Physiological breeding II: a field guide to wheat phenotyping*. CIMMYT, Mexico. pp 58–62
- Prashar A, Yildiz J, McNicol JW, Bryan GJ, Jones HG (2013) Infra-red thermography for high throughput field phenotyping in *Solanum tuberosum*. *PLoS ONE* 8:e65816
- Prashar A, Jones HG (2014) Infra-red thermography as a high-throughput tool for field phenotyping. *Agronomy* 4:397–417
- Reynolds M, Langridge P (2016) Physiological breeding. *Curr Opin Plant Biol* 31:162–171
- Richner W, Liedgens M, Bürgi H, Soldati A, Stamp P (2000) Root image analysis and interpretation. In: *Root methods*, Springer, Berlin, Heidelberg, pp 305–341
- Sadeghi-Tehran P, Sabermanesh K, Virlet N, Hawkesford MJ (2017) Automated method to determine two critical growth stages of wheat: heading and flowering. *Front Plant Sci* 8:252
- Sankaran S, Khot LR, Espinoza CZ, Jarolmasjed S, Sathuvalli VR, Vandemark GJ, Pavek MJ (2015) Low-altitude, high-resolution aerial imaging systems for row and field crop phenotyping: a review. *Eur J Agronomy* 70:112–123
- Sankaran S, Quirós JJ, Richard Knowles N, Knowles LO (2017) High-resolution aerial imaging based estimation of crop emergence in potatoes. *Am J Potato Res* 94:658–663
- Schafleitner R et al (2007) Field screening for variation of drought tolerance in *Solanum tuberosum* L. by agronomical, physiological and genetic analysis. *Potato Res* 50:71–85
- Slater AT, Cogan NOI, Rodoni BC, Daetwyler HD, Hayes BJ, Caruana B, Badenhorst PE, Spangenberg GC, Forster JW (2017) Breeding differently—the digital revolution: high-throughput phenotyping and genotyping. *Potato Res* 60:337–352
- Songsri P, Jogloy S, Holbrook CC, Kesmala T, Vorasoot N, Akkasaeng C, Patanothai A (2009) Association of root, specific leaf area and SPAD chlorophyll meter reading to water use efficiency of peanut under different available soil water. *Agric Water Manag* 96:790–798
- Spitters CJ, Schapendonk AH (1990) Evaluation of breeding strategies for drought tolerance in potato by means of crop growth simulation. In: *Genetic aspects of plant mineral nutrition* Springer, Dordrecht. pp 151–161
- Stark JC, Pavek JJ, McCann IR (1991) Using canopy temperature measurements to evaluate drought tolerance of potato genotypes. *J Am Soc Hortic Sci* 116:412–415
- Sugiura R, Tsuda S, Tamiya S, Itoh A, Nishiwaki K, Murakami N, Shibuya Y, Hirafuji M, Nuske S (2016) Field phenotyping system for the assessment of potato late blight resistance using RGB imagery from an unmanned aerial vehicle. *Biosyst Eng* 148:1–10
- Tatagiba SD, DaMatta FM, Rodrigues FA (2015) Leaf gas exchange and chlorophyll a fluorescence imaging of rice leaves infected with *Monographella albescens*. *Phytopathology* 105:180–188
- Tiwari JK, Plett D, Garnett T, Chakrabarti SK, Singh RK (2018) Integrated genomics, physiology and breeding approaches for improving nitrogen use efficiency in potato: translating knowledge from other crops. *Funct Plant Biol* 45:587–605

- Tiwari JK, Buckseth T, Devi S, Varshney S, Sahu S, Patil VU, Zinta R, Ali N, Moudgil V, Singh RK, Rawat S, Dua VK, Kumar D, Kumar M, Chakrabarti SK, Rao AR, Rai A (2020a) Physiological and genome-wide RNA-sequencing analyses identify candidate genes in a nitrogen-use efficient potato cv Kufri Gaurav. *Plant Physiol Biochem* 154:171–183
- Tiwari JK, Buckseth T, Zinta R, Saraswati A, Singh RK, Rawat S, Chakrabarti SK (2020b) Genome-wide identification and characterization of microRNAs by small RNA sequencing for low nitrogen stress in potato. *PLoS ONE* 15(5):e0233076
- Tiwari JK, Buckseth T, Zinta R, Saraswati A, Singh RK, Rawat S, Dua VK, Chakrabarti SK (2020c) Transcriptome analysis of potato shoots, roots and stolons under nitrogen stress. *Sci Rep* 10:1152
- Tiwari JK, Devi S, Buckseth T, Ali N, Singh RK, Zinta R, Dua VK, Chakrabarti SK (2020d) Precision phenotyping of contrasting potato (*Solanum tuberosum* L.) varieties in a novel aeroponics system for improving nitrogen use efficiency: in search of key traits and genes. *J Integr Agric* 19:51–61
- Ullah S, Skidmore AK, Ramoelo A, Groen TA, Naeem M, Ali A (2014) Retrieval of leaf water content spanning the visible to thermal infrared spectra. *ISPRS J Photogramm Remote Sens* 93:56–64
- Virlet N, Sabermanesh K, Sadeghi-Tehran P, Hawkesford MJ (2017) Field Scanalyzer: an automated robotic field phenotyping platform for detailed crop monitoring. *Funct Plant Biol* 44(1):143–153
- Wasaya A, Zhang X, Fang Q, Yan Z (2018) Root phenotyping for drought tolerance: a review. *Agronomy* 8(11):241
- Wishart J, George TS, Brown LK, White PJ, Ramsay G, Jones H, Gregory PJ (2014) Field phenotyping of potato to assess root and shoot characteristics associated with drought tolerance. *Plant Soil* 378:351–363
- Yazdanbakhsh N, Fisahn J (2009) High throughput phenotyping of root growth dynamics, lateral root formation, root architecture and root hair development enabled by PlaRoM. *Funct Plant Biol* 36:938–946
- Yol E, Toker C, Uzun B (2015) Traits for phenotyping. *Phenomics in crop plants trends, options and limitations*. Springer, India, pp 11–26
- Zia MAB, Naeem M, Demirel U, Caliskan ME (2017) Next generation breeding in potato. *Ekin J* 3:1–33

# Chapter 9

## High-Throughput Crop Phenotyping Systems for Controlled Environments



Jianfeng Zhou, Jing Zhou, Heng Ye, and Henry T. Nguyen

**Abstract** Increasing crop production through genetic improvements and crop breeding programs is a key solution for the expected food crisis in 2050. Crops with improved traits of high yield potential and resilience to biotic and abiotic stresses due to adverse environments can be developed at a faster speed by integrating crop genotypic data with phenotypic data. While the efficiency of breeding programs is limited by unpredictable environmental conditions in field conditions, facility with controlled environments and emerging technologies can provide a better alternative for the fast development of new crop varieties. This chapter introduces the high-throughput phenotyping systems used in controlled environments and their potentials to be used for fast characterization of plant traits. Various styles of automated phenotyping platforms are summarized and their features are compared to provide a vision on how to select such systems. The chapter also provides an introduction of some typical sensors that are typically used by researchers and commercial sectors for plant phenotyping in controlled environments. At the end of the chapter, a case study is provided to demonstrate how low-cost and automated plant phenotyping systems can be developed to suit customized studies. Methods of hardware development, data analysis, and results are discussed to show case the application of such a low-cost system. A vision of next-generation autonomous crop phenotyping system is provided too.

---

J. Zhou (✉) · J. Zhou

Division of Plant Science and Technology, University of Missouri, Columbia, MO 65211, USA  
e-mail: [zhoujianf@missouri.edu](mailto:zhoujianf@missouri.edu)

J. Zhou

e-mail: [jzmc3@mail.missouri.edu](mailto:jzmc3@mail.missouri.edu)

H. Ye · H. T. Nguyen

Division of Plant Science and Technology, University of Missouri, Columbia, MO 65211, USA  
e-mail: [yehe@missouri.edu](mailto:yehe@missouri.edu)

H. T. Nguyen

e-mail: [nguyenhenry@missouri.edu](mailto:nguyenhenry@missouri.edu)

© Springer Nature Switzerland AG 2021

J. Zhou et al. (eds.), *High-Throughput Crop Phenotyping*,  
Concepts and Strategies in Plant Sciences,  
[https://doi.org/10.1007/978-3-030-73734-4\\_9](https://doi.org/10.1007/978-3-030-73734-4_9)

**Keywords** Plant phenotyping · Controlled environments · Automation system · sensor

## 9.1 Introduction

By 2050, the global population is expected to reach 9.8 billion (Hincks 2018) and the current arable land is decreasing due to climate change, urbanization, soil degradation, water shortages, and pollution (Breene 2018). Food demand is expected to be 60% higher than it is today, resulting in a potential crisis in global food security. Crop breeding is a promising solution to the food crisis by developing new crop varieties with improved traits, including high yield potential and resilience to biotic and abiotic stresses due to adverse environments (Staton 2017). The rapid and continuous changes in climatic conditions increase the frequency of extreme weather including altered precipitation patterns and occurrence of drought and flood in the agricultural areas (Lesk et al. 2016). The U.S. National Climate Assessment conducted by the National Aeronautics and Space Administration (NASA) shows that the heavy precipitation events have increased by 42% in midwestern states and 55% in northeastern states from 1958–2016 (NASA 2019). Meanwhile, drought has been identified as one of the critical restraints for crop production (Marvel et al. 2019), and crops such as soybean have had a ~40% reduction in yield as a result of drought (Lesk et al. 2016). The frequent extreme weather significantly threatens crop production and global food security (Boyer et al. 2013). There is a pressing need to use the latest technological advances such as Artificial Intelligence (AI) to develop stress-resilient crops (i.e., soybean, corn, rice, maize, and others) to sustain agricultural production under unfavorable weather conditions.

Conventional crop breeding methods rely on field evaluations in multiple seasons and multiple locations based on statistical methods and experimental design. These conventional methods improve selection effort; however, they are time-consuming and rely on trial-and-error (one cycle per year, 6–12 breeding cycles for one variety), labor-intensive (mainly rely on people to conduct physical experiments, manage in field operations, and evaluate crop growth conditions,) and too slow to meet the expected yield gains (Bresseghele and Coelho 2013). Natural environment is highly variable, which significantly affects the stability of the expression of quantitative traits in plants. Based on previous reports on quantitative trait studies, more than 40% of the total phenotypic variations were usually explained by their environmental variations in field conditions (Weinig and Schmitt 2004). As crop phenotypes are interactions of their genotypes and environment factors, controlled environments, compared to field conditions, offer uniform growing conditions by controlling microclimate in a certain area and reduce the environmental effects to single factors, e.g., salty, drought, or flooding, to avoid the co-occurrence of these factors and to achieve more efficient and optimal crop breeding (Katsoulas et al. 2016). For example, modern greenhouses are set up for accurately controlled environments, such as temperature, light, humidity, and uniformity of soils, which allows us to minimize environmental

complexities and focuses exclusively on genetic effects. In addition, experiments can be conducted year-round in the greenhouse compared to only one season in the field advantaging greenhouse in achieving our research and breeding goals in a much shorter period. Therefore, it is important to conduct experiments in a modern greenhouse for accurate research and breeding. For example, Bayer, one of the largest seed companies in the world, has just invested more than \$100 million to build a 7-acre greenhouse facility in Marana, AZ to enhance their breeding programs (Gardner 2020). Meanwhile, the University of Missouri invested \$28.2 million to build a new greenhouse in 2019 to boost its research in crop breeding and genetics. Plant growth facility, including greenhouses, offers good opportunities to apply emerging technologies to accelerate crop breeding.

Recently plant breeders have started using high-resolution genome information for germplasm characterization and genetic dissection of major agronomic and stress-resilience traits. Along with the development of next-generation and cost-effective sequencing platforms, the speed of plant genome sequencing has been accelerated significantly. The top-of-the-line breeding programs need to utilize inexpensive, genome-wide data coupled with powerful algorithms that overcome limitations of the conventional methods and allow us to start breeding on predicted instead of measured phenotypes (Wallace et al. 2018). One of the 10 big ideas identified by U.S. National Science Foundation (NSF) is to address the issue of “our inability to look at an organism’s genetics and environment and predict its observable characteristics or phenotype”.

In the past few years, High-Throughput Phenotyping (HTP) approaches have been used for the fast measurement of plant traits in controlled environments. Efforts have been made by both academic and industrial sectors toward developing HTP systems under controlled environments to adapt various kinds of crops for different breeding purposes. For example, the GROWSCREEN FLUORO developed by Jansen et al. (2009) was used to detect the stress tolerance in rosette plants based on traits of leaf growth and chlorophyll fluorescence. The Phenovator designed by Flood et al. (2016) is capable of screening more than 1000 Arabidopsis plants for the measurements of photosynthesis, growth, and multispectral reflectance multiple times per day. The Scanalyzer HTS and three-dimensional (3D) system by LemnaTec GmbH were adopted by many studies to analyze plant leaf chemical properties (Pandey et al. 2017) and measure the diurnal patterns of leaf hyponasty and leaf size (Dornbusch et al. 2012).

High-throughput phenotyping platforms in controlled environments have been built and utilized in studies for various crops, such as Arabidopsis (De Diego et al. 2017), rice (Al-Tamimi et al. 2016), soybean (Zhang et al. 2017a; Zhou et al. 2018a), wheat (Zhang et al. 2017b), and maize (Bricchet et al. 2017). These studies mainly focused on measuring the temporal variations of crop growth and quantifying their genetic responses under biotic and abiotic stresses. Image features are commonly used to replace manual measurements and improve the efficiency of data collection (phenotyping) in crop studies (An et al. 2017; Horgan et al., 2015), combined in genomic analyses, e.g., Genome-Wide Association Studies (GWASs) or Quantitative

Trait Loci (QTLs) mapping to evaluate genetic variations in crops (Atieno et al. 2017; Yang et al. 2014; Zhang et al. 2017b) or predict crop performance under target environments (Fahlgren et al. 2015; Hairmansis et al. 2014).

Controlled environments in Plant Science usually refer to an enclosed area with certain environmental parameters controlled, such as temperature, humidity, light condition, and CO<sub>2</sub> level. Some examples of such facilities include greenhouses, growth chambers, climate room, and nursery room, which are widely used to study plant responses to controlled environmental conditions. Comparing to field conditions, controlled environments have a limited area (dimensions), protected regions, and well-equipped facility, which allow easy implementation of automated phenotyping systems. Automated plant phenotyping systems in controlled environments generally consist of sensors, automated control systems, data processing, management system, and computation software to accomplish an automated data collection in crop traits in a high-throughput manner. The experimental results from controlled environments usually will be tested and validated in field conditions. One example of modern automated phenotyping systems is shown in Fig. 9.1 that consists of hardware (phenotyping platform) and an advanced data processing pipeline. In this chapter, current high-throughput plant phenotyping systems in controlled environments and

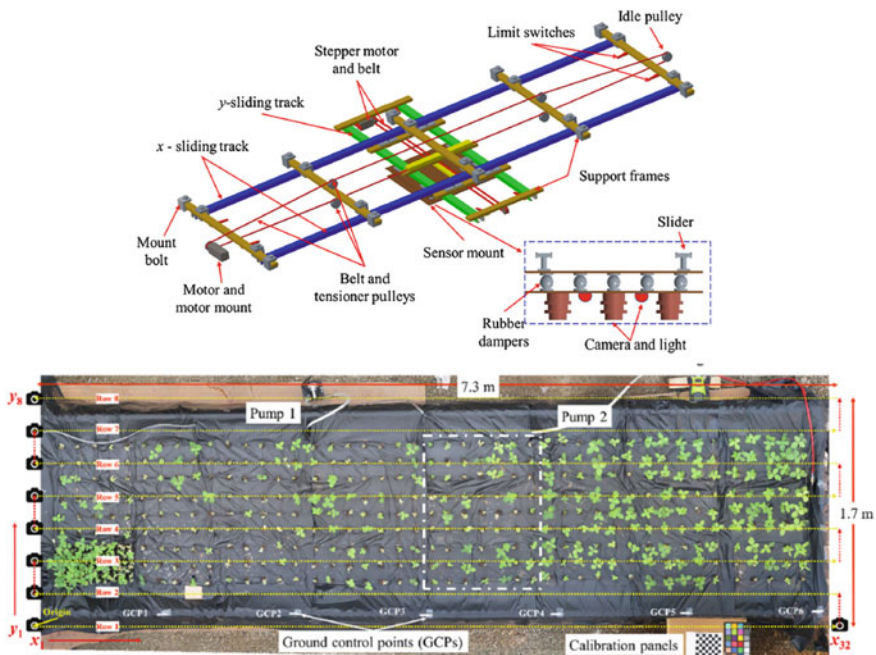


**Fig. 9.1** Example of an overhead platform with ceiling mounted track system (top) and stitched image from sequential images taken by a Red, Green, and Blue (RGB) camera with a yellow dotted line as the pre-defined path (bottom)

sensors used in such systems to quantify plant traits were summarized. In addition, a case study was included at the end of this chapter to explain how high-throughput phenotyping systems have been applied in crop breeding programs.

## 9.2 Automated Platforms for High-Throughput Crop Phenotyping Systems

The automated platforms for high-throughput crop phenotyping systems in controlled environments can be divided into two types according to the relative movement between sensors and plants, i.e., “sensor-to-plant” and “plant-to-sensor”. In Sensor-to-Plant (STP) systems, plants are in fixed positions while sensors are moved to approach plants. On the other hand, in Plant-to-Sensor (PTS) systems, plants are brought to sensors that are in a fixed location. The STP systems do not require complicated conveyor systems to transfer plants and have sufficient freedoms in system design; therefore, the STP systems are more commonly used in customized systems. However, the STP systems are less efficient than the PTS systems in terms of accommodation capacity for plants and time cost for screening individual plants. Therefore, the PTS systems have the advantage of being suitable for large-scale, highly automated, and non-destructive plant phenotyping; however, they usually require a large investment in facilities, hardware, and software.

### 9.2.1 *Sensor-To-Plant (STP) Phenotyping Systems*

The STP phenotyping systems are suitable for situations when plants are not preferred to move during the growth period. Some scenarios include plants growing in one testbed with treatments in water solution (Zhou et al. 2018b,2020b) and plants in large growth tubes for root observations (Ye et al. 2018a; b). Some other scenarios include the most traditional greenhouse setup with fixed testbeds, lights, and irrigation systems that are easily modified. In general, STP phenotyping systems are more flexible and easier to be adapted in existing plant growth facilities. The STP systems can be divided into three types, i.e., overhead platforms, ground platforms, and robotic systems. The overhead platforms move above plant canopies using rail track systems that are mounted on the ceiling or support by frames (An et al. 2016; Jansen et al. 2009; Zhou et al. 2018b). The ground platforms are operated on ground-based tracks (Polder et al. 2009), and the robotic systems offer free movement to sensors to mimic human activities (Scharr et al. 2014; Lu et al. 2017).

### 9.2.1.1 Overhead Platforms

Overhead platforms are the most widely used platforms in STP than the other two types (ground and robotic), especially for customized systems. The overhead platforms move sensors above plant canopies and capture their top view images with desired distances. One example of the overhead platforms is shown in Fig. 9.1, which consists of a sensor system, a track system (in  $x$ -,  $y$ -, and  $z$ -axis directions), a control system (to control the movement of the sensors on the tracks), and a lighting system. As the core component of a phenotyping system, the sensor system integrates non-contact sensors (e.g., cameras and LiDAR), controllers, and other accessories (e.g., power sources). Sensors are controlled using their integrated firmware or external controller to collect data periodically or continuously. The collected data could be directly stored to their onboard storage (e.g., SD card) or transmitted to external hard drives through a wireless network. Track systems usually consist of sliding tracks, rollers, belts or chains, and motors to move sensors to desired locations or following pre-defined moving paths.

There are two different operation modes of sensors in the overhead STP platforms, i.e., stop-and-go and continuously scanning. In the stop-and-go mode, sensors collect data at still conditions, i.e., sensors are driven to and then stop at pre-defined positions. The stop-and-go mode is particularly suitable for scenarios when particular light conditions are required for imaging. For example, images are taken under low light conditions in which sensors are required to stay still for a long-time exposure. Some examples include imaging small-scale plants growing in leaf discs or small pots (Jansen et al. 2009). Fluorescence imaging is another special application of the stop-and-go mode since lights have to be blocked for the dark adaptation for plants during the short period of imaging (Biskup et al. 2009).

On the other hand, in the continuously scanning mode, sensors take measurements (images) at a constant interval while they are moving along a pre-defined path. The path is usually defined in a serpentine shape along the  $x$ - and  $y$ -axis to cover the whole area of plants. The top image in Fig. 9.1 illustrates one exemplar architecture of a continuously scanning platform (Zhou et al. 2018b), where the yellow dot lines in the bottom image show the path commonly defined for cameras in this mode. Compared to the stop-and-go mode, continuous scanning has the advantages of higher data acquisition efficiency and the ability to obtain 3D geometric information (plant height, plant volume, etc.) using stereovision (Moons et al. 2010) or Structure from Motion (SfM) (Snavely et al. 2006) techniques. The SfM is one of the most widely used stereovision methods in many automatic phenotyping systems (Zhang et al. 2016; Zhou et al. 2018b), which reconstructs 3D structures of plants by extracting and matching feature points from two-dimensional (2D) images. The 2D images are usually taken by Red, Green, and Blue (RGB) cameras (due to their high image resolution) continuously following the pre-defined path with certain image forward and side overlaps. The popularity of SfM is due to the development of commercial software, such as Agisoft PhotoScan (Agisoft LLC, Russia) and Pix4D Mapper (Pix4D, Lausanne, Switzerland) that have integrated this method into a completed



process, increasing the accessibility and manipulability of users who are even not familiar with those techniques.

### 9.2.1.2 Ground Platform

Ground platforms use a ground-based track system to support and move sensor systems to desired positions for continuous or scheduled data collection. Their sensor systems can be positioned on top of plant canopies for shooting nadir-view images or vertically for side-view images. Compared to the overhead platforms, the height of sensor systems can be adjustable within a certain range on the ground platforms allowing flexible setups for plants with different sizes from as small as rosette plants (Pereyra-Irujo et al. 2012) to as large as grow-up wheat or even corn (Horgan et al. 2015). Crop architecture features (e.g., dimension and angle of stems and leaf) can also be revealed with side-view images. Some other advantages of ground platforms include that the ground track system can be easily modified or extended and the sensor systems are allowed to carry more and heavy devices. However, ground platforms need additional installation space and may need more modifications to install such systems in the existing greenhouse.

### 9.2.1.3 Robotic Platform

Robotic platforms here exclusively refer to standalone robotic systems that are not based on track systems described above, including robotic arms, autonomous robots, and others. Robotic systems are able to mimic human actions to take measurements of single plants but on a larger scale than manual operations. Depending on the integrated sensors, information of plant architecture (e.g., plant height, leaf area, angle), physiological characteristics based on spectral reflectance (e.g., normalized difference vegetation index or NDVI), fluorescence, and temperature can be acquired in real time. Detailed crop architecture and morphological features of single plants can be obtained, such as each single leaf area, angles between leaves and stem, leaf incline angles, stem width and height, and volume convex hull. However, data acquisition and processing time spent on single plants might be significantly higher than other systems. Figure 9.2 shows a robotic system developed in Iowa State University that can perform multi-type tasks of measurements on crops in different growth chambers.

## 9.2.2 Plant-To-Sensor (PTS) Phenotyping System

Plant-to-sensor platforms are designed as (imaging) sensor stations that include one or multiple sensors in an enclosed area with active lights and an automation system. The PTS platforms consist of an automated converter system that transfers single

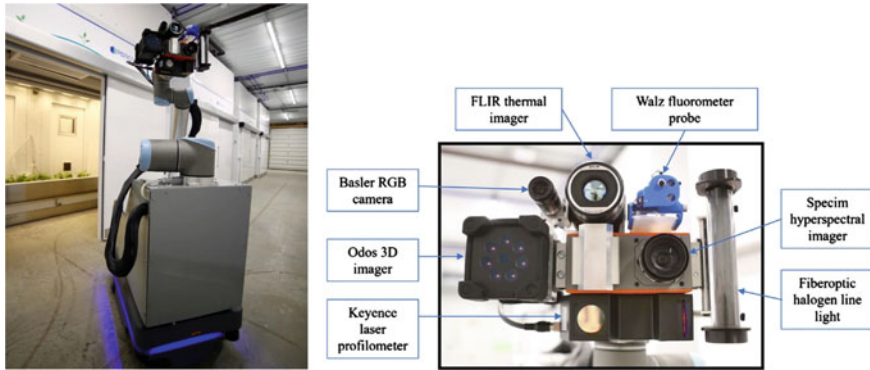


**Fig. 9.2** A robotic system consists of an unmanned ground vehicle, a six-axis robotic arm, and a sensing unit at the end of the arm. There are multiple sensing units are integrated to take multiple measurements simultaneously (Bao et al. 2019)

plants or plant pots to the sensor stations for taking measurements. The architecture and components vary for different PTS platforms developed by commercial sectors and research groups, which have many different capacities to handle a different number of plants from hundreds to thousands and various sizes of plants from single small-size plants (e.g., *Arabidopsis*, Junker et al. 2014) to midsize (e.g., sorghum, Neilson et al. 2015) or large-size plants (e.g., maize, Ge et al. 2016).

There are some advantages of PTS comparing to STP systems. First, sensors are housed in enclosed areas providing ideal environments for taking imagery data, such as controlled and uniform light conditions and clean background. For example, hyperspectral imaging systems have critical requirements for lights (full spectral, sufficient intensity, and uniform) (Lu et al. 2020) that are hard to meet in STP systems. Secondly, plants are transported to different locations of the growing facility during their life cycle, which may reduce the microclimate impacts due to the non-uniform light condition, temperature, and orientations to light (Ma et al. 2019a). Other benefits may include high security to sensor systems, easy installation, and highly automated and integrated systems.

Various kinds of sensors can be installed at any desired position in a sensor station to take the top- or side-view images of single plants. The sensor station is usually a closed chamber with controllable environments. Completely dark conditions can be applied as well as illuminations in certain ranges of spectrum wavelength, if necessary. Therefore, imaging environments in these platforms are favorable to all kinds of sensors due to the light conditions and smooth movements, especially to hyperspectral cameras. Applications of these platforms include the study of water use efficiency (Junker et al. 2014), diagnose of biotic and abiotic stresses (Atieno et al. 2017; Tschiersch et al. 2017), estimation of plant traits related to yield gain (Minervini et al. 2017), and modeling plant growth (Pradal et al. 2017).

Except for imaging plant shoots that are available in most of the automatic phenotyping systems, roots imaging can be achieved by replacing the traditional plant pots

with rhizotrons. Rhizotrons are laboratory constructed containers in order to study the root development of different crop cultivars under different conditions. They are typically equipped with a central corridor with viewing windows into the soil profiles on either side (Busch et al. 2006). Nagel et al. (2012) integrated rhizotrons to a commercial PTS platform by Maschinenbau Kitz GmbH (Troisdorf, Germany). This imaging platform enables imaging simultaneously plant shoot and root systems up to 60 rhizotrons per hour.

Currently, a number of PTS systems that have been developed by commercial sectors are available on the market with the price from hundreds of thousands to millions of dollars. One of the most popular PTS system providers is LemnaTec (LemnaTec GmbH, Aachen, Germany), which is able to acquire characteristics of plants using hyperspectral, fluorescence, thermal, multispectral, and RGB imagery. They have been utilized in studies of water use efficiency; stress diagnoses; estimation of biomass, nutrition, or production; and evaluation of root system development for crops like maize, soybean, Arabidopsis, and sorghum (Junker et al. 2014; Parlati et al. 2017; Tschiersch et al. 2017). There are similar commercial products available on the market, such as the Plant Accelerator by the Australian Plant Phenomics Facility in Australia and the Montpellier Plant Phenotyping Platforms by French National Institute for Agricultural Research in France.

### 9.3 Sensors

Sensors used in high-throughput crop phenotyping systems are primarily non-contact optical sensors that take non-invasive measurements of physical, chemical, and biological characteristics of plants. In general, the sensors primarily sense objects based on their radiation or spectral reflectance of natural or artificial light. When incident radiation (light source or natural light) hits the surface of an object, the radiation will either be absorbed, transmitted, or reflected (Lillesand et al. 2004). The reflected radiation can be expressed as the Electromagnetic Spectrum (EMS) with a range of wavelengths (Fig. 9.3). Different ranges of wavelength (waveband) are denoted to different names such as visible region (400–700 nm), near-infrared

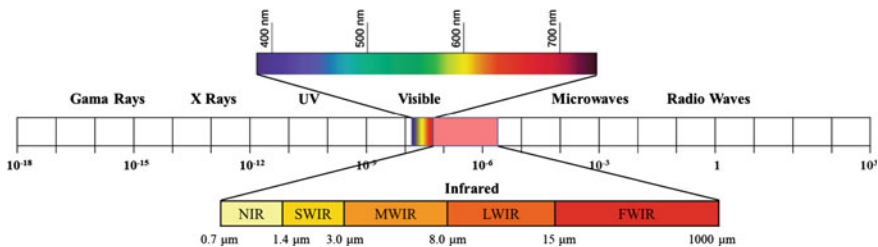
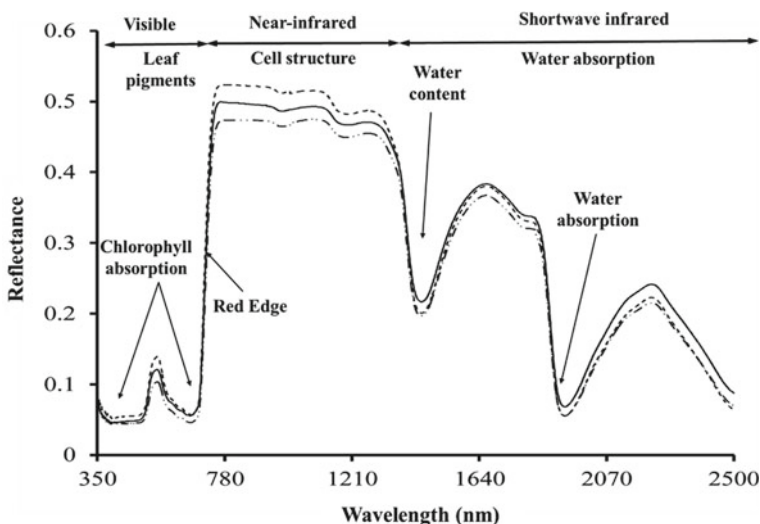


Fig. 9.3 Electromagnetic Spectrum (EMS) scheme (nm)

(NIR, 700–1,000 nm), short-wave infrared (SWIR, 900–2,500 nm), and long-wave infrared (LWIR, 7.5–14  $\mu\text{m}$ ) (Silván-Cárdenas et al, 2015).

When light interacts with a plant, it comes to a distinct set of physical processes, namely reflection, transmission, and absorption. A part of the incoming light is reflected from the surface of the plant, and after internal backscattering, some light is absorbed by plant tissue and another part of the light is transmitted through the plant tissue (Vogelmann 1993). In addition, there is an internal scattering of the reflected and transmitted light involved while it interfuses the plant tissue. The portion of incoming light that is reflected, transmitted, or absorbed varies with the wavelength of the incoming light and depends on the structural and chemical composition of a plant (Knippling 1970; Woolley 1971), which makes a spectral characteristic profile of plants associated with the structure of the leaf surface and the composition of the plant tissue (Vogelmann and Gorton 2014). Figure 9.4 shows an example of a typical curve of spectral reflectance characteristics of plant leaves. Plant pigments, such as chlorophyll, carotenoids, or anthocyanins, have well-known absorption patterns in the visible range of the EMS (Blackburn 2006). When a plant is subjected to stresses, such as drought, flooding, and pathogen, metabolic processes and the cellular structure of a plant change. This leads to an altered spectral profile of the plant and provides a possibility to detect plant diseases through observation of the plant's spectral characteristics (Bock et al. 2010; Mahlein et al. 2012). The spectral profile of plants may also offer a new way to quantify the genetic variations of crops due to target stress, which may be used to select crops with desired traits.

There are a large variety of sensors used in different research, and advanced sensors are emerging with the advance of technologies. This section summarizes



**Fig. 9.4** Spectral reflectance characteristics of leaves in the range of visible to short-wave infrared wavelength. Different lines show the crops under different nitrogen concentrations

some commonly used camera systems, including visible light (RGB) camera, spectral imager, fluorescence camera, infrared (IR) thermal camera, and time-of-flight (depth) camera.

### ***9.3.1 Visible Digital Camera***

Visible digital cameras are able to capture images in three bands of reflectance light of objects that are in the visible range of spectra (400–700 nm), namely red, green, and blue, also referring as RGB cameras. The RGB camera is the most widely used type of imaging sensor in crop phenotyping due to the features of low cost, high resolution, user-friendly operation, light weight, and adaptability to the working environment (Yang et al. 2017b). In the research of crop phenotyping, RGB cameras have been used to capture color information from plant root (Nagel et al. 2012), shoot (Honsdorf et al. 2014), and canopy (De Diego et al. 2017) and measure 2D geometric information (e.g., length of root, shoot, and area of leaf and canopy) (Lee et al. 2018). Additionally, 3D geometric information of plants can be obtained through reconstructing Digital Elevation Models (DEMs) based on 2D images using stereovision methods (Zhou et al. 2018b). The information of plant 3D architecture can provide many crop traits, such as a number of stems, angle of stems, and leaves that are not easy to acquire in conventional breeding programs, and shows great potential to precisely quantify the genetic variation of plants due to abiotic and biotic stresses (Zhou et al. 2018a).

### ***9.3.2 Spectral Cameras***

Visible cameras measure the spectral reflectance of objects in the visible range of 400–700 nm, which limits the ability to discover the spectral response of crops in the infrared spectral range that is “invisible” to human eyes. It has been found that the leaf of crops can reflect more spectral light in NIR than visible light, which makes the reflectance intensity of NIR light much stronger than that of visible light (as shown in Fig. 9.4). Currently, the most commonly used spectral features are reflectance in the spectra range of 400–2,500 nm, usually called visible-NIR or VNIR, due to the limitation in instruments. It can be seen from Fig. 9.4, spectral reflectance to vegetation at the NIR range is the highest in the VNIR spectra, and the difference in crops has been signified in this range. To signify the difference in spectral reflectance features of plants at different treatments, multiple spectral bands can be integrated to develop different vegetation indices (e.g., NDVI) (Humplík et al. 2015) or build predictive models using machine learning techniques (Zhou et al. 2018a). Spectral cameras can be divided into two categories according to the number of discrete wavebands or channels, i.e., multispectral camera and hyperspectral camera.

### 9.3.2.1 Multiple Spectral Cameras

Multispectral cameras generally refer to the type of spectral cameras that are able to capture images with two to fit discrete wavebands in the VNIR range (Humplík et al. 2015). The spectral wavebands are selected based on research results that show effectiveness in representing important crop traits. Some widely used wavebands include blue (450–520 nm), green (520–600 nm), red (630–690 nm), red edge (700–730 nm), and NIR (760–900 nm) (Hunt et al. 2013; Thenkabail and Lyon 2016). Depending on the waveband width (number of wavelengths) of every single channel, spectral cameras can also be divided into narrow waveband (e.g., 2–20 nm) or broad waveband (more than 50 nm) cameras (Hunt et al. 2005). For example, the multispectral camera Micasense RedEdge-M (Micasense, Seattle, WA, USA) consists of five narrow spectral bands of blue (475 nm center, 32 nm bandwidth), green (560 nm center, 27 nm bandwidth), red (668 nm center, 14 nm bandwidth), red edge (717 nm center, 12 nm bandwidth), and NIR (842 nm center, 57 nm bandwidth). The narrow-band spectral cameras are usually more accurate to pick up the difference of spectral signature for different plants, but more expensive than broad-band spectral cameras.

To signify the spectral reflectance signal, vegetation indices are calculated using multiple bands, such as NDVI, Normalized Difference RedEdge (NDRE, Barnes et al. 2000), and Photochemical Reflectance Index (PRI, Gamon et al. 1997). Vegetation indices have been widely used to quantify the difference of plants under different treatments and predict more complex crop traits, such as crop health condition, leaf chlorophyll content, and yield (Zhang et al. 2017a; Zhou et al. 2018a, 2020a).

### 9.3.2.2 Hyperspectral Camera

More powerful “multispectral cameras” are hyperspectral cameras that include more than 50 narrow wavebands in the range of 400–2,500 nm (Li et al. 2014). There are two different types of hyperspectral cameras based on their data collection methods, i.e., pushbroom (line scanning) hyperspectral cameras and snapshot (snapshotting) cameras. Pushbroom hyperspectral cameras consist of a line of spectroscopic sensors that acquire images using a line-by-line scanning method when the cameras are moving above the scene. On the other hand, a snapshot hyperspectral camera consists of a matrix of spectroscopic sensors that are able to acquire images of a scene without moving the camera. Pushbroom hyperspectral cameras usually have more narrow-band spectral wavebands or higher spectral resolution of narrow wavebands comparing to the snapshot cameras. However, pushbroom cameras require stabilized mounts and smooth movements to “reconstruct” the image, which becomes a limitation for scale-up research. In addition, a consistent artificial light source is always needed to provide extra light for hyperspectral cameras. It should be noticed that PTS platforms are preferable for pushbroom hyperspectral imaging as the camera is fixed to reduce movements, and translation stages for plants can be easily designed to provide a consistent speed and smooth movements.

The power of hyperspectral cameras is the large amount of acquired narrow-band spectral information of crops that provide more information of chemical and physiological information and provide the potential of applying advanced big data processing and analytical technologies, such as machine and deep learning. Applications of using hyperspectral cameras are mainly on plant photochemical and physiological features (Pandey et al. 2017; Yang et al. 2017a), health status (Knauer et al. 2017; López-Maestresalas et al. 2016), and biomass/yield estimation (Liang et al. 2018). Current hyperspectral imagers are primarily using 50–270 narrow spectral bands of VNIR (400–1,100 nm) due to the cost. Adding a Short-Wave Infrared spectral imager (SWIR, 900–2,500 nm) may greatly improve the spectral range and capacity of research; however, SWIR imaging sensors are made of indium gallium arsenide (InGaAs) and usually heavy and expensive. The SWIR bands have a minimum amount of atmospheric disturbance or noise and distinguished ability to separate different ground materials thereby helping in feature extraction accurately (Swathandran and Aslam 2019). Studies have shown great potential in quantifying plant response to different stresses using VNIR cameras (Rascher et al. 2011; Thomas et al. 2017; Yuan et al. 2014). The SWIR channel shows specific reflectance for vegetation water content and soil moisture (Everitt et al. 1989; Jacquemoud and Baret 1990; Tucker 1980; Ustin 2004). The most important applications of the SWIR include agricultural management by assessing the crop stress by the reflectance of different pigments in the leaves along with crop moisture estimation and mapping and quantifying the crop residue and predicting the quality of the soil (Galloza et al. 2013; Hively et al. 2018; Serbin et al. 2009). With regard to the spectral reflectance differences of moisture absorption properties, various drought indices using the backscatter energy from NIR and SWIR channels have been formulated for estimating vegetation water content using satellite remote sensing (Ji et al. 2011; Vescovo et al. 2012; Wang and Qu 2007), which may serve as reliable indicators for crop drought stresses, and potentially to be used in selecting drought-resistant varieties.

### 9.3.3 *Chlorophyll Fluorescence Imaging Sensor*

Chlorophyll fluorescence of plants is the light re-emitted by chlorophyll molecules during the returning from excited to non-excited states (Maxwell and Johnson 2000). The yield of chlorophyll fluorescence depends on the efficiency of converting absorbed light to fluorescence. For normal and healthy plants, a major part of light absorbed by chlorophyll molecules is used for photosynthetic quantum conversion, and only a small proportion is de-excited via emission as heat or as red and far-red chlorophyll fluorescence. However, the ability of the photosynthetic quantum conversion declines for plants under stresses, with a concomitant increase in red and far-red chlorophyll fluorescence (Lichtenthaler and Miehe 1997). Therefore, the analysis of chlorophyll fluorescence re-emitted from plant leaves can release information about plant health status and has been used as an important tool in plant research (Halbritter et al. 2020).

Fluorescence imaging sensors (cameras) are used to capture the re-emitted proportion of irradiation in a short wavelength such as Ultraviolet (UV) light (wavelength ranges from 340 to 360 nm) by plants (Li et al. 2014). Recently, a high-resolution, UV Laser-Induced Fluorescence (LIF) imaging system was developed to image all four fluorescence bands: blue, green, red, and far-red (Ortiz-Bustos et al. 2016). The inverse relationship between photosynthetic performance and chlorophyll fluorescence analysis has made a large contribution to the understanding of photosynthesis and electron transport reaction.

A fluorescence sensing system usually consists of one or more Charge-Coupled Device (CCD) cameras with filters to capture fluorescence signals (Wang et al. 2018). Active light sources, such as pulsed lasers, pulsed flashlight lamps, or Light Emitting Diodes (LEDs), provide irradiation in certain wavelengths (Baker 2008). The Pulse Amplitude Modulated (PAM) fluorometry method by Schreiber et al. (1986) is adopted in practical applications. In this method, a short (e.g., 1  $\mu$ s) pulse of light (also called a dark adaptation) is imposed on a targeted object. Following the dark adaptation, the minimum fluorescence value ( $F_o$ ) of the object can be measured. The object is then exposed to a saturating pulse of light so that the maximum amount of fluorescence ( $F_m$ ) can be measured. The difference between these two extreme values is the variable fluorescence ( $F_v$ ).  $F_v/F_m$  provides a measure of a certain photochemical efficiency which has been successfully related to plant status in many studies.

This proportion depends on the plant's metabolic capacity and is highly sensitive for plant photosynthetic activity yielding parameters closely related to photosynthetic functions (Serôdio et al. 2018). Therefore, fluorescence imaging is commonly used to detect stress symptoms induced by pathogen attack (Chaerle et al. 2007), monitor stress responses (Baker, 2008), and measure physiological phenomena relating to photosynthesis and metabolism and growth-related traits (such as the leaf area) (Baker and Rosenqvist 2004; Lenk et al. 2006).

To reach the needs of the dark adoption and light saturation, phenotyping platforms for fluorescence sensing have to provide controllable ambient light conditions to plants. Therefore, PTS platforms with enclosed imaging unit and illuminating light (Junker et al. 2014; Parlati et al. 2017) are the most suitable for sensing large- or medium-size plants, and overhead STP platforms are for small-scale plants (Biskup et al. 2009).

### 9.3.4 Thermal Infrared Cameras

Thermal infrared cameras capture the long-wave infrared radiation (7.5–14  $\mu$ m) of the EMS emitted from crops and convert such radiation to an electrical signal (Jones 2004). Leaf temperature measurement using thermal IR sensing is primarily used to study plant water relations and specifically stomatal conductance because a major determinant of leaf temperature is the rate of evaporation or transpiration from the leaf (Jones 2004). During evaporation, a substantial amount of energy is required to convert liquid water in leaves to water vapor, and this energy is then taken away



**Fig. 9.5** Different models of Time-of-Flight sensors



from the leaves resulting in a cool surface. When a plant experience abiotic or biotic stresses, the transpiration rate will change and as well as the temperature. Hence, thermal cameras are useful in detecting this kind of water-related stress (Balota and Oakes 2017). For example, canopy temperature depression which is calculated as the temperature difference between the canopy and the surrounding air was found being highly correlated with the canopy water mass, and it was used to capture response levels induced by stress treatments (Ludovisi et al. 2017).

### 9.3.5 Time-of-Flight Sensors

A Time-of-Flight (ToF) sensor is a range system that employs ToF techniques to resolve the distance between the sensor and the subject by measuring the round trip time of an artificial light signal provided by a laser or an LED (Lindner et al. 2010). The ToF ranging technology has been used in robotic systems, automation, and computer vision technologies for object detection, distance ranging, and 3D modeling (Lu et al. 2017). In crop phenotyping, ToF sensors are majorly used as a tool to directly measure the 3D architecture of plants (Busemeyer et al. 2013; Paulus 2019). Commonly used ToF sensors in crop phenotyping include Light Detection and Ranging (LiDAR) (Paulus et al. 2014), ultrasonic sensors (Fricke et al. 2011), Microsoft Kinect v2 (Ma et al. 2019b), and ToF cameras (Chaivivatrakul et al., 2014), which are used to quantify plant height, build the 3D structure, and estimate biomass or yield (Fig. 9.5).

LiDAR sensors measure the distance between objects and the sensors by actively emitting laser lights (600–1,000 nm) toward the objects and recording the reflected laser points by the objects. 3D point clouds representing the spatial structures of the objects can be generated by scanning objects at multiple viewpoints and merging the laser points based on the positions where they are collected. Morphological measurements such as plant height, stem height, leaf angle distribution, and leaf area density can be quantified and extracted, which are helpful in characterize plant growth. With the flexible degrees of freedom, the robotic STP platforms are extensively adopted for phenotyping small-scale plants in controlled environments to provide multiple scanning positions of laser scanning devices (Paulus et al. 2014; Wang et al. 2017).

## 9.4 Low-Cost and Customized Crop HTP System

Commercial crop phenotyping platforms are usually designed for generic applications to cover various applications. Although customized designs can be provided, the cost would be too high for most research groups, especially for early-stage research projects. The following case study introduces a low-cost and automated STP phenotyping system designed for an established greenhouse that has limited space and resources to install a complex phenotyping system. As shown in Fig. 9.6, the platform consisted of a frame (7.3 m  $\times$  1.7 m) built by two sets of aluminum sliding tracks (STA-BP250, Spokane Hardware Supply, Spokane, WA, USA), stepper motors (23HS30-2804S, StepperOnline, Nanjing, China), timing belts, motor pulleys, limit switches (MX-11, Sparkfun Electronics, Boulder, CO, USA), DC power supplies (Model S-360-12, Amazon.com, Seattle, WA, USA), and a camera holder. The camera holder is a rectangle frame (400 mm  $\times$  150 mm) built by aluminum solid angles, and cameras can be fixed to the frame. The camera holder was driven along a y-sliding track (horizontal) by a stepper motor through timing belts. The y-sliding track was attached to an x-sliding track (vertical) using four ball-bearing sliders and was driven by another stepper motor that was mounted directly to the greenhouse ceiling. Two sets of sliding tracks and driving systems allowed the camera holder to move at desired speeds and patterns in two perpendicular directions.

Sequential imagery data collected by the system are processed with three major steps, i.e., pre-processing to build orthomosaic images and DEM, image processing to extract image features of single plants, and data analysis to quantify plant traits (phenotypes). Commercial software, such as Agisoft and Pix4D, was used to process sequential images to simplify the procedure of data pre-processing. Both software packages are able to develop orthomosaic images and DEM based on the principle of SfM. Followed the pre-processing is to develop customized image processing algorithms to segment (separate) each plant from orthomosaic images and DEM, which are used to extract temporal high-dimensional data sets of each plant, such as 2D and 3D image features, color, spectral reflectance, and temperature, depending

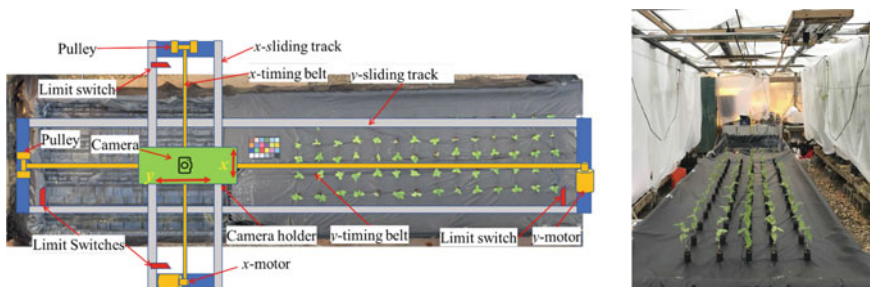


**Fig. 9.6** Illustration of the architecture of a low-cost and customized automated plant phenotyping platform. The left figure shows the details of the system and the right figure shows an example of the setup for a study of soybean salinity stress in a greenhouse

on the type of camera used. High-dimensional data sets are used to develop prediction models for desired crop traits (e.g., salt tolerance, drought tolerance) based on advanced machine learning and deep learning algorithms.

The automated phenotyping platform can be used in different studies to capture dynamic (temporal) responses of plants to abiotic and biotic stresses. Various image features can be extracted to quantify the variation of plants due to environmental stresses. The system is able to track plant growth (structural variations, such as height, canopy size) and quantify physiological and chemical characteristics (e.g., leaf chlorophyll content, spectral reflectance) that can be used to rate their tolerance to abiotic and biotic stresses. The following case study is regarding an application of a customized phenotyping system developed at the University of Missouri, where a consumer-grade digital camera (SX410, Canon U.S.A., Melville, NY) was used to quantify the genetic variation of soybean due to salinity stress. The system setup is shown in Fig. 9.6. Crops under salinity stress have reduced growth rate, plant height, shoot biomass, and ultimately reduced yield. Meanwhile, changes in ion level in plant shoots and leaves due to salinity may cause variations in leaf chlorophyll content, reflectance, and temperature. Quantification of variations in those stress symptoms is the key to developing soybeans with high salt tolerance and understanding the underlying mechanism regulating salt tolerance in plants.

The measurement accuracy in geometric dimensions of the system was firstly evaluated by comparing sensor estimation in dimensions with manual measurements of artificial objects. Figure 9.7 shows the estimated dimensions in height (vertical distance between the top and the base) and width (the horizontal length of edges at the top or base) of the artificial objects. It can be seen that the errors (standard deviation) in the horizontal direction were 1.4 mm and 1.2 mm at the base and top surfaces of the artificial object, while the error was 1.9 mm in the vertical direction (height).

An automated image processing pipeline was developed for images collected by the system, including background removal, plant separation, and feature extraction. Figure 9.8 shows the images of three soybean plants automatically processed from the first day after emerging (DAE) to the 23rd day and their height and shoot area

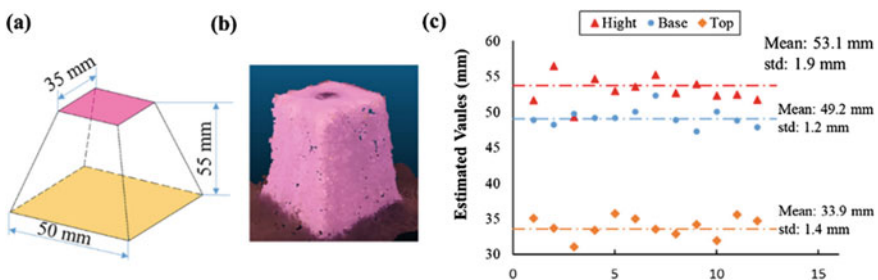


**Fig. 9.7** Measurement accuracy in geometric dimensions on artificial objects. **a** Illustration of real dimensions in artificial objects, **b** 3D dense point cloud of an artificial object, and **c** Measurement accuracy in the horizontal and vertical direction

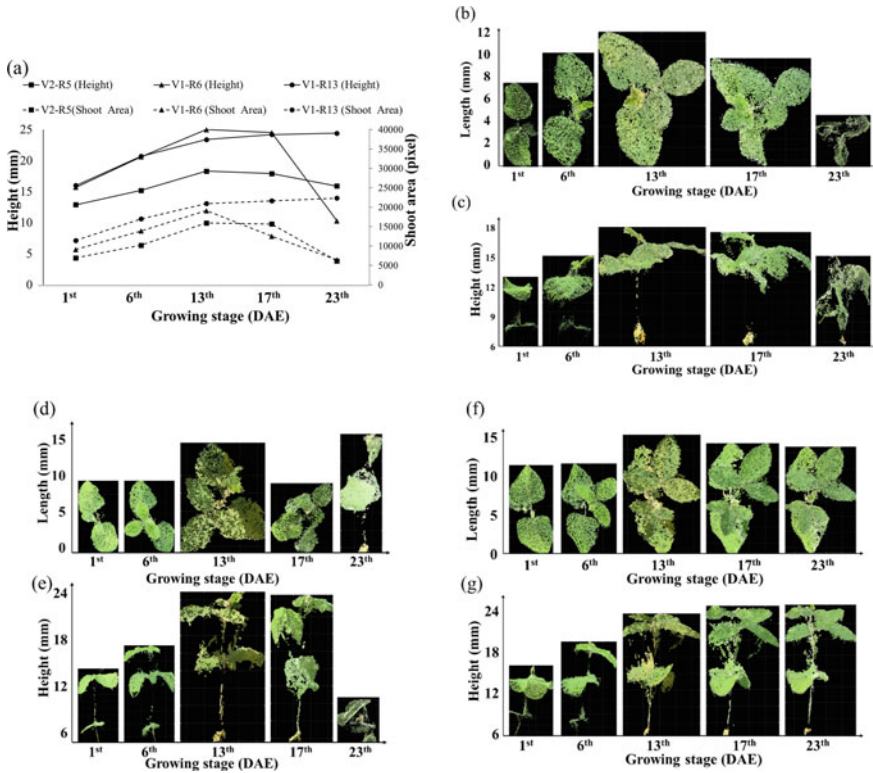


**Fig. 9.8** Soybean traits automatically acquired using the HTP system. **a** Height and shoot area of three soybean plants throughout their lifespan. **b, d, and f** are the top and front views of the plants. **c, e, and g** are the front view of the plants

extracted from images. The curves in Fig. 9.8a were able to not only track the growth (height and shoot area) of individual plants, but also quantify their difference that might be used to determine their level of resistance to salt stress.

A list of image features were extracted for the soybean plants throughout their lifespan to quantify their dynamic responses to salinity stress. The image features were first used to estimate leaf chlorophyll content that is one of the widely used traits in salt tolerance studies. The leaf chlorophyll was measured manually using a chlorophyll meter (Konica Minolta SPAD-502, Tokyo, Japan) on the 4th day after treatment. The correlation between the manual measurements and the estimated values is shown in Fig. 9.9a, indicating that the leaf chlorophyll content can be explained up to 85% with an average error of 0.6.

To quantify soybean tolerance under salinity stress, a Salt Tolerance Rating (STR) for each soybean line was scored by an expert at the end of the experiment (around two weeks). The STR scale was classified into five grades from 1 to 5, where 1 = no apparent chlorosis, 2 = slight (25% of the leaves showed chlorosis), 3 = moderate (50% of the leaves showed chlorosis and some necrosis), 4 = severe chlorosis (75%

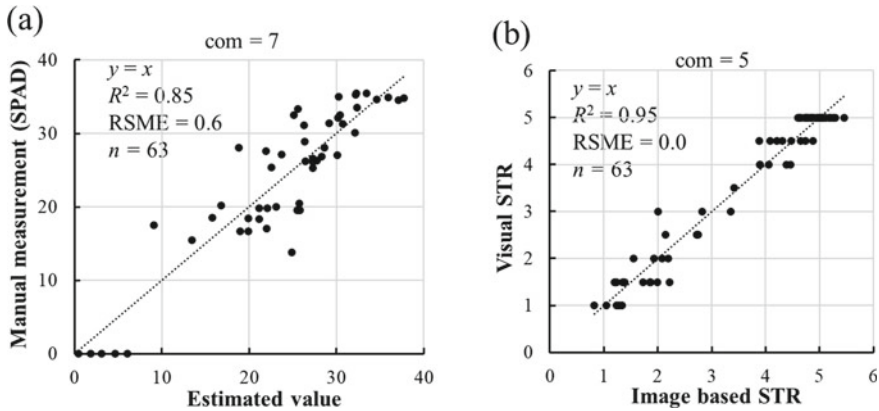


**Fig. 9.9** Quantify soybean responses to salinity stress **a** The correlation between leaf chlorophyll measurements and estimated values using seven Partial Least Square (PLS) components. **b** The agreement between the image-based and visual Salt Tolerant Rate (STR) using five PLS components

of the leaves showed chlorosis and severe necrosis), and 5 = dead (leaves showed severe necrosis and were withered). The potential of estimation of STR with multiple image features was also tested using the PLS regression, and the results are shown in Fig. 9.9b, indicating that 95% of STR could be explained by the image features.

### 9.5 Summary and Future Vision

Breeding crops in the controlled environment is gaining attention from industry and academic sectors because of the high efficiency and advantages of the controllable environment and treatments comparing to the field conditions. Thanks to the high-throughput phenotyping technology, now researchers and breeders can collect high-temporal and high-resolution data using emerging sensors that can be used to predict crop traits (predictive phenotypes). Recently plant breeders have started using high-resolution genomic information for germplasm characterization and genetic dissection of major agronomic and stress-resilience traits. Along with the development of cost-effective genotyping platforms, the speed of next-generation plant genome sequencing has also been accelerated. The top-of-the-line breeding programs need to utilize inexpensive, genome-wide data coupled with powerful algorithms that overcome limitations of the conventional methods and allow us to start breeding on predicted instead of measured phenotypes. The big data of crop phenotypes are expected to integrate with crop genotypic data to overcome the current barriers in fast crop breeding.

Based on the success in applying image-based phenotyping to crop breeding and genetics, we are envisioning that a next-generation plant phenotyping system will be an autonomous system that can scale up our current research capacity and provide

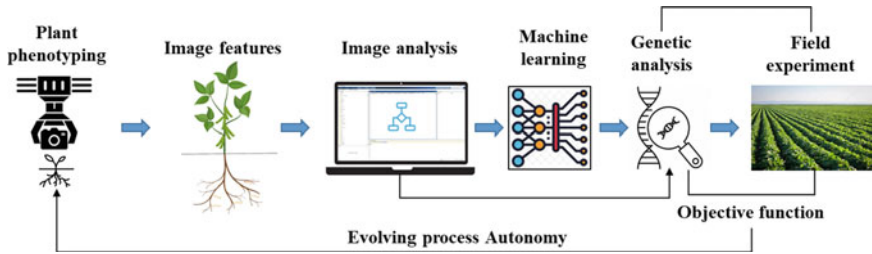


**Fig. 9.10** Illustration of vision of next-generation autonomous phenotyping system in controlled environments. It consists of a robotic imaging system to acquire images of plant root and shoot, which can be analyzed and used to train machine learning algorithms. Genetic analysis, genetic selection, and field studies will be used for further validation of selected crop traits

an innovative phenotyping paradigm. As shown in Fig. 9.10, an autonomous phenotyping system may consist of a robotic imaging system; an image processing and analysis pipeline; and a set of machine learning algorithms, genetic analyses, and field evaluations to validate the new knowledge established from the system. The robotic imaging system will collect images of plant shoots and roots, and rigorous image analysis will quantify image features, such as Root System Architecture (RSA), shoot 3D structure, and spectral and thermal characteristics (*descriptive phenotypes*). Machine learning algorithms will use experimental and numerical images to predict latent crop traits (*predicative phenotypes*) that are used in genetic analyses to identify functional gene loci associated with crop stress resistance. Field experiments will be used to evaluate the selected new breeding materials and the reliability of crop traits. The transition from “human-in-the-loop” to “human-out-of-the-loop” will occur gradually with AI-based expert system learning from human and knowledge base, leading to autonomous phenotyping (*prescriptive phenotyping*). Each of these phases of research will occur progressively and represent a significant contribution toward autonomous plant phenotyping and toward understanding the fundamental mechanisms governing the response of plants to environments.

## References

- Al-Tamimi N, Brien C, Oakey H, Berger B, Saade S, Ho YS et al (2016) Salinity tolerance loci revealed in rice using high-throughput non-invasive phenotyping. *Nat Commun* 7:13342. <https://doi.org/10.1038/ncomms13342>
- An N, Palmer CM, Baker RL, Markelz RC, Ta J, Covington MF et al (2016) Plant high-throughput phenotyping using photogrammetry and imaging techniques to measure leaf length and rosette area. *Comput Electron Agric* 127:376–394. <https://doi.org/10.1016/j.compag.2016.04.002>
- An N, Welch SM, Markelz RJC, Baker RL, Palmer CM, Ta J et al (2017) Quantifying time-series of leaf morphology using 2D and 3D photogrammetry methods for high-throughput plant phenotyping. *Comput Electron Agric* 135:222–232. <https://doi.org/10.1016/j.compag.2017.02.001>

- Atieno J, Li Y, Langridge P, Dowling K, Brien C, Berger B et al (2017) Exploring genetic variation for salinity tolerance in chickpea using image-based phenotyping. *Sci Rep* 7(1):1300. <https://doi.org/10.1038/s41598-017-01211-7>
- Baker N (2008) Chlorophyll fluorescence: a probe of photosynthesis in vivo, vol 59, pp 89–113
- Baker N, Rosenqvist E (2004) Applications of chlorophyll fluorescence can improve crop production strategies: an examination of future possibilities, vol 55, no 403, pp 1607–1621
- Balota M, Oakes J (2017) UAV remote sensing for phenotyping drought tolerance in peanuts. Paper Presented at the proceedings of SPIE-the international society for optical engineering. <https://doi.org/10.1117/12.2262496>
- Bao Y, Zarecor S, Shah D, Tuel T, Campbell DA, Chapman AVE et al (2019) Assessing plant performance in the Enviratron. *Plant Methods* 15(1):117. <https://doi.org/10.1186/s13007-019-0504-y>
- Barnes E, Clarke T, Richards S, Colaizzi P, Haberland J, Kostrzewski M et al (2000) Coincident detection of crop water stress, nitrogen status and canopy density using ground based multispectral data. Paper presented at the proceedings of the fifth international conference on precision agriculture, Bloomington, MN, USA
- Biskup B, Scharr H, Fischbach A, Wiese-Klinkenberg A, Schurr U, Walter A (2009) Diel growth cycle of isolated leaf discs analyzed with a novel, high-throughput three-dimensional imaging method is identical to that of intact leaves. *Plant Physiol* 149(3):1452–1461. <https://doi.org/10.1104/pp.108.134486>
- Blackburn GA (2006) Hyperspectral remote sensing of plant pigments. *J Exp Bot* 58(4):855–867
- Bock C, Poole G, Parker P, Gottwald T (2010) Plant disease severity estimated visually, by digital photography and image analysis, and by hyperspectral imaging. *Crit Rev Plant Sci* 29(2):59–107
- Boyer J, Byrne P, Cassman K, Cooper M, Delmer D, Greene T et al (2013) The US drought of 2012 in perspective: a call to action 2(3):139–143
- Breene K (2018) Food security and why it matters. Accessed from <https://www.weforum.org>
- Breseghello F, Coelho ASG (2013) Traditional and modern plant breeding methods with examples in rice (*Oryza sativa* L.). *J Agric Food Chem* 61(35):8277–8286. <https://doi.org/10.1021/jf305531j>
- Brichet N, Fournier C, Turc O, Strauss O, Artzet S, Pradal C et al (2017) A robot-assisted imaging pipeline for tracking the growths of maize ear and silks in a high-throughput phenotyping platform. *Plant Methods* 13:96. <https://doi.org/10.1186/s13007-017-0246-7>
- Busch J, Mendelsohn IA, Lorenzen B, Brix H, Miao SJF-M (2006) A rhizotron to study root growth under flooded conditions tested with two wetland Cyperaceae. *Distrib Funct Ecol Plants* 201(6):429–439
- Busemeyer L, Mentrup D, Möller K, Wunder E, Alheit K, Hahn V et al (2013) BreedVision— a multi-sensor platform for non-destructive field-based phenotyping in plant breeding. *Sensors* 13(3):2830–2847
- Chaerle L, Hagenbeek D, De Bruyne E, Van Der Straeten D (2007) Chlorophyll fluorescence imaging for disease-resistance screening of sugar beet. *Plant Cell Tissue Organ Cult* 91(2):97–106
- Chaivivatrakul S, Tang L, Dailey MN, Nakarmi AD (2014) Automatic morphological trait characterization for corn plants via 3D holographic reconstruction. *Comput Electron Agric* 109:109–123. <https://doi.org/10.1016/j.compag.2014.09.005>
- De Diego N, Fürst T, Humplík JF, Ugena L, Podlešáková K, Spíchal L (2017) An automated method for high-throughput screening of *Arabidopsis* rosette growth in multi-well plates and its validation in stress conditions. *Front Plant Sci* 8:1702. <https://doi.org/10.3389/fpls.2017.01702>
- Dornbusch T, Lorrain S, Kuznetsov D, Fortier A, Liechti R, Xenarios I et al (2012) Measuring the diurnal pattern of leaf hyponasty and growth in ‘*Arabidopsis*’—a novel phenotyping approach using laser scanning. *Funct Plant Biol* 39(11):860–869. <https://doi.org/10.1071/FP12018>
- Everitt J, Escobar D, Richardson A (1989) Estimating grassland phytomass production with near-infrared and mid-infrared spectral variables. *Remote Sens Environ* 30(3):257–261
- Fahlgren N, Feldman M, Gehan MA, Wilson MS, Shyu C, Bryant DW et al (2015) A versatile phenotyping system and analytics platform reveals diverse temporal responses to water availability in *Setaria*. *Mol Plant* 8(10):1520–1535. <https://doi.org/10.1016/j.molp.2015.06.005>

- Flood PJ, Kruijer W, Schnabel SK, van der Schoor R, Jalink H, Snel JFH et al (2016) Phenomics for photosynthesis, growth and reflectance in *Arabidopsis thaliana* reveals circadian and long-term fluctuations in heritability. *Plant Methods* 12(1):14. <https://doi.org/10.1186/s13007-016-0113-y>
- Fricke T, Richter F, Wachendorf M (2011) Assessment of forage mass from grassland swards by height measurement using an ultrasonic sensor. *Comput Electron Agric* 79(2):142–152. <https://doi.org/10.1016/j.compag.2011.09.005>
- Galloza MS, Crawford MM, Heathman GC (2013) Crop residue modeling and mapping using Landsat, ALI, Hyperion and airborne remote sensing data. *IEEE J Select Top Appl Earth Obs Remote Sens* 6(2):446–456
- Gamon J, Serrano L, Surfus J (1997) The photochemical reflectance index: an optical indicator of photosynthetic radiation use efficiency across species, functional types, and nutrient levels. *Oecologia* 112(4):492–501
- Gardner J (2020) Bayer greenhouse facility beginning operations. Tucson Bus. Accessed from [https://www.insidetucsonbusiness.com/news/bayer-greenhouse-facility-beginning-operations/article\\_d94862ee-41fa-11ea-a33b-b332b82ef6a3.html](https://www.insidetucsonbusiness.com/news/bayer-greenhouse-facility-beginning-operations/article_d94862ee-41fa-11ea-a33b-b332b82ef6a3.html)
- Ge Y, Bai G, Stoerger V, Schnable JC (2016) Temporal dynamics of maize plant growth, water use, and leaf water content using automated high throughput RGB and hyperspectral imaging. *Comput Electron Agric* 127:625–632. <https://doi.org/10.1016/j.compag.2016.07.028>
- Hairmansis A, Berger B, Tester M, Roy SJ (2014) Image-based phenotyping for non-destructive screening of different salinity tolerance traits in rice. *Rice* 7(1):16
- Halbritter AH, De Boeck HJ, Eycott AE, Reinsch S, Robinson DA, Vicca S et al (2020) The handbook for standardized field and laboratory measurements in terrestrial climate change experiments and observational studies (ClimEx). *Methods Ecol Evol* 11(1):22–37. <https://doi.org/10.1111/2041-210x.13331>
- Hincks J (2018) The world is headed for a food security crisis. Here's how we can avert it. Accessed from <https://www.un.org/development/desa/en/news/population/world-population-prospects-2017.html>
- Hively W, Lamb B, Daughtry C, Shermeyer J, McCarty G, Quemada M (2018) Mapping crop residue and tillage intensity using WorldView-3 satellite shortwave infrared residue indices. *Remote Sens* 10(10):1657
- Honsdorf N, March TJ, Berger B, Tester M, Pillen P (2014) High-throughput phenotyping to detect drought tolerance QTL in wild barley introgression lines. *PLoS ONE* 9(5):e97047. <https://doi.org/10.1371/journal.pone.0097047.g001>
- Horgan G, Song Y, Glasbey CA, van der Heijden GWAM, Polder G, Dieleman JA et al (2015) Automated estimation of leaf area development in sweet pepper plants from image analysis. *Funct Plant Biol* 42(5):486. <https://doi.org/10.1071/fp14070>
- Humplík JF, Lazár D, Husičková A, Spíchal L (2015) Automated phenotyping of plant shoots using imaging methods for analysis of plant stress responses—a review. *Plant Methods* 11(1):29
- Hunt ER, Cavigelli M, Daughtry CS, McMurtrey JE, Walthall CL (2005) Evaluation of digital photography from model aircraft for remote sensing of crop biomass and nitrogen status. *Precision Agric* 6(4):359–378
- Hunt ER Jr, Doraiswamy PC, McMurtrey JE, Daughtry CS, Perry EM, Akhmedov B (2013) A visible band index for remote sensing leaf chlorophyll content at the canopy scale. *Int J Appl Earth Obs Geoinf* 21:103–112
- Jacquemoud S, Baret F (1990) PROSPECT: a model of leaf optical properties spectra. *Remote Sens Environ* 34(2):75–91
- Jansen M, Gilmer F, Biskup B, Nagel KA, Rascher U, Fischbach A et al (2009) Simultaneous phenotyping of leaf growth and chlorophyll fluorescence via GROWSCREEN FLUORO allows detection of stress tolerance in *Arabidopsis thaliana* and other rosette plants. *Funct Plant Biol* 36(11):902–914
- Ji L, Zhang L, Wylie BK, Rover J (2011) On the terminology of the spectral vegetation index (NIR–SWIR)/(NIR+ SWIR). *Int J Remote Sens* 32(21):6901–6909



- Jones HG (2004) Application of thermal imaging and infrared sensing in plant physiology and ecophysiology. *Adv Bot Res* 41:107–163 (Academic Press)
- Junker A, Muraya MM, Weigelt-Fischer K, Arana-Ceballos F, Klukas C, Melchinger AE et al (2014) Optimizing experimental procedures for quantitative evaluation of crop plant performance in high throughput phenotyping systems. *Front Plant Sci* 5:770. <https://doi.org/10.3389/fpls.2014.00770>
- Katsoulas N, Elvanidi A, Ferentinos KP, Kacira M, Bartzanas T, Kittas C (2016) Crop reflectance monitoring as a tool for water stress detection in greenhouses: a review. *Biosys Eng* 151:374–398. <https://doi.org/10.1016/j.biosystemseng.2016.10.003>
- Knauer U, Matros A, Petrovic T, Zanker T, Scott ES, Seiffert U (2017) Improved classification accuracy of powdery mildew infection levels of wine grapes by spatial-spectral analysis of hyperspectral images. *Plant Methods* 13(1):47. <https://doi.org/10.1186/s13007-017-0198-y>
- Knipling EB (1970) Physical and physiological basis for the reflectance of visible and near-infrared radiation from vegetation. *Remote Sens Environ* 1(3):155–159
- Lee U, Chang S, Putra GA, Kim H, Kim DH (2018) An automated, high-throughput plant phenotyping system using machine learning-based plant segmentation and image analysis. *PLoS ONE* 13(4):e0196615. <https://doi.org/10.1371/journal.pone.0196615>
- Lenk S, Chaerle L, Pfündel EE, Langsdorf G, Hagenbeek D, Lichtenthaler HK et al (2006) Multi-spectral fluorescence and reflectance imaging at the leaf level and its possible applications. *J Exp Bot* 58(4):807–814
- Lesk C, Rowhani P, Ramankutty N (2016) Influence of extreme weather disasters on global crop production. *Nature* 529(7584):84–87. <https://doi.org/10.1038/nature16467>
- Li L, Zhang Q, Huang D (2014) A review of imaging techniques for plant phenotyping. *Sensors (basel)* 14(11):20078–20111. <https://doi.org/10.3390/s141120078>
- Liang Z, Pandey P, Stoerger V, Xu Y, Qiu Y, Ge Y et al (2018) Conventional and hyperspectral time-series imaging of maize lines widely used in field trials. *GigaSci* 7(2):1–11. <https://doi.org/10.1093/gigascience/gix117>
- Lichtenthaler HK, Miehé JA (1997) Fluorescence imaging as a diagnostic tool for plant stress. *Trends Plant Sci* 2(8):316–320. [https://doi.org/10.1016/S1360-1385\(97\)89954-2](https://doi.org/10.1016/S1360-1385(97)89954-2)
- Lillesand, T. M., Kiefer, R. W., & Chipman, J. W. (2004). *Remote Sensing and Image Interpretation* (Fifth Edition ed.): John Wiley & Sons, Inc.
- Lindner M, Schiller I, Kolb A, Koch R (2010) Time-of-Flight sensor calibration for accurate range sensing. *Comput vis Image Underst* 114(12):1318–1328. <https://doi.org/10.1016/j.cviu.2009.11.002>
- López-Maestresalas A, Keresztes JC, Goodarzi M, Arazuri S, Jarén C, Saeyes W (2016) Non-destructive detection of blackspot in potatoes by Vis-NIR and SWIR hyperspectral imaging. *Food Control* 70:229–241. <https://doi.org/10.1016/j.foodcont.2016.06.001>
- Lu B, Dao PD, Liu J, He Y, Shang J (2020) Recent Advances of Hyperspectral Imaging Technology and Applications in Agriculture. *Remote Sens* 12(16):2659
- Lu H, Tang L, Whitham SA, Mei Y (2017) A robotic platform for corn seedling morphological traits characterization. *Sensors (Basel)* 17(9). <https://doi.org/10.3390/s17092082>
- Ludovisi R, Tauro F, Salvati R, Khoury S, Mugnozza Scarascia G, Harfouche A (2017) UAV-based thermal imaging for high-throughput field phenotyping of black poplar response to drought. *Front Plant Sci* 8:1681
- Ma D, Carpenter N, Amatya S, Maki H, Wang L, Zhang L et al (2019a) Removal of greenhouse microclimate heterogeneity with conveyor system for indoor phenotyping. *Comput Electron Agric* 166:104979. <https://doi.org/10.1016/j.compag.2019.104979>
- Ma X, Zhu K, Guan H, Feng J, Yu S, Liu G (2019b) High-throughput phenotyping analysis of potted soybean plants using colorized depth images based on a proximal platform. *Remote Sens* 11(9):1085
- Mahlein A-K, Steiner U, Hillnhütter C, Dehne H-W, Oerke E-C (2012) Hyperspectral imaging for small-scale analysis of symptoms caused by different sugar beet diseases. *Plant Methods* 8(1):3. <https://doi.org/10.1186/1746-4811-8-3>

- Marvel K, Cook BI, Bonfils CJW, Durack PJ, Smerdon JE, Williams AP (2019) Twentieth-century hydroclimate changes consistent with human influence. *Nature* 569(7754):59–65. <https://doi.org/10.1038/s41586-019-1149-8>
- Maxwell K, Johnson GN (2000) Chlorophyll fluorescence—a practical guide. *J Exp Bot* 51(345):659–668. <https://doi.org/10.1093/jexbot/51.345.659>
- Minervini M, Giuffrida MV, Perata P, Tsaftaris SA (2017) Phenotiki: an open software and hardware platform for affordable and easy image-based phenotyping of rosette-shaped plants. *Plant J* 90(1):204–216. <https://doi.org/10.1111/tbj.13472>
- Moons T, Van Gool L, Vergauwen M (2010) 3D reconstruction from multiple images part 1: principles. *Found Trends® Comput Graph Vis* 4(4):287–404. <https://doi.org/10.1561/0600000007>
- Nagel KA, Putz A, Gilmer F, Heinz K, Fischbach A, Pfeifer J et al (2012) GROWSCREEN-Rhizo is a novel phenotyping robot enabling simultaneous measurements of root and shoot growth for plants grown in soil-filled rhizotrons. *Funct Plant Biol* 39(11):891. <https://doi.org/10.1071/fp12023>
- NASA (2019) Earth's freshwater future: extremes of flood and drought. Accessed from <https://www.nasa.gov/feature/goddard/2019/earth-s-freshwater-future-extremes-of-flood-and-drought>
- Neilson EH, Edwards AM, Blomstedt CK, Berger B, Moller BL, Gleadow RM (2015) Utilization of a high-throughput shoot imaging system to examine the dynamic phenotypic responses of a C4 cereal crop plant to nitrogen and water deficiency over time. *J Exp Bot* 66(7):1817–1832. <https://doi.org/10.1093/jxb/eru526>
- Ortiz-Bustos CM, Pérez-Bueno ML, Barón M, Molinero-Ruiz L (2016) Fluorescence imaging in the red and far-red region during growth of sunflower plantlets. Diagnosis of the early infection by the parasite *Orobanche cumana*. *Front Plant Sci* 7(884):1–10. <https://doi.org/10.3389/fpls.2016.00884>
- Pandey P, Ge Y, Stoerger V, Schnable JC (2017) High throughput in vivo analysis of plant leaf chemical properties using hyperspectral imaging. *Front Plant Sci* 8:1348. <https://doi.org/10.3389/fpls.2017.01348>
- Parlati A, Valkov VT, D'Apuzzo E, Alves LM, Petrozza A, Summerer S et al (2017) Ectopic expression of PII induces stomatal closure in *Lotus japonicus*. *Front Plant Sci* 8:1299. <https://doi.org/10.3389/fpls.2017.01299>
- Paulus S (2019) Measuring crops in 3D: using geometry for plant phenotyping. *Plant Methods* 15(1):103
- Paulus S, Schumann H, Kuhlmann H, Léon J (2014) High-precision laser scanning system for capturing 3D plant architecture and analysing growth of cereal plants. *Biosys Eng* 121:1–11. <https://doi.org/10.1016/j.biosystemseng.2014.01.010>
- Pereyra-Irujo GA, Gasco ED, Peirone LS, Aguirrezábal LA (2012) GlyPh: a low-cost platform for phenotyping plant growth and water use. *Funct Plant Biol* 39(11):905–913
- Polder G, Heijden GWAMVD, Glasbey CA, Song Y, Dieleman JA (2009) Spy-see-advanced vision system for phenotyping in greenhouses. Paper presented at the MINET conference: measurement, sensation and cognition, London, UK, 10–12 Nov 2009
- Pradal C, Artzet S, Chopard J, Dupuis D, Fournier C, Mielewicz M et al (2017) InfraPhenoGrid: a scientific workflow infrastructure for plant phenomics on the grid. *Futur Gener Comput Syst* 67:341–353. <https://doi.org/10.1016/j.future.2016.06.002>
- Rascher U, Blossfeld S, Fiorani F, Jahnke S, Jansen M, Kuhn AJ et al (2011) Non-invasive approaches for phenotyping of enhanced performance traits in bean. *Funct Plant Biol* 38(12):968–983
- Scharr H, Minervini M, Fischbach A, Tsaftaris SA (2014) Annotated image datasets of rosette plants. In European conference on computer vision. Zürich, Suisse, pp 6–12
- Schreiber U, Schliwa U, Bilger W (1986) Continuous recording of photochemical and non-photochemical chlorophyll fluorescence quenching with a new type of modulation fluorometer. *Photosynth Res* 10(1–2):51–62

- Serbin G, Daughtry CS, Hunt ER, Brown DJ, McCarty GW (2009) Effect of soil spectral properties on remote sensing of crop residue cover. *Soil Sci Soc Am J* 73(5):1545–1558
- Serôdio J, Schmidt W, Frommlet JC, Christa G, Nitschke MR (2018) An LED-based multi-actinic illumination system for the high throughput study of photosynthetic light responses. *PeerJ* 6:e5589–e5589. <https://doi.org/10.7717/peerj.5589>
- Silvan-Cardenas J, Corona N, Pizana J, Nunez JM, Madrigal J (2015) Geospatial technologies to support coniferous forests research and conservation efforts in Mexico, pp 67–123
- Snavely N, Seitz SM, Szeliski R (2006) Photo tourism: exploring photo collections in 3D. Paper presented at the ACM transactions on graphics (TOG)
- Staton M (2017) What is the relationship between soybean maturity group and yield? Accessed from [https://www.canr.msu.edu/news/what\\_is\\_the\\_relationship\\_between\\_soybean\\_maturity\\_group\\_and\\_yield](https://www.canr.msu.edu/news/what_is_the_relationship_between_soybean_maturity_group_and_yield)
- Swathandran S, Aslam MAM (2019) Assessing the role of SWIR band in detecting agricultural crop stress: a case study of Raichur district, Karnataka, India. *Environ Monit Assess* 191(7):442. <https://doi.org/10.1007/s10661-019-7566-1>
- Thenkabil PS, Lyon JG (2016) Hyperspectral remote sensing of vegetation. CRC Press
- Thomas S, Wahabzada M, Kuska MT, Rascher U, Mahlein A-K (2017) Observation of plant–pathogen interaction by simultaneous hyperspectral imaging reflection and transmission measurements. *Funct Plant Biol* 44(1):23. <https://doi.org/10.1071/fp16127>
- Tschiersch H, Junker A, Meyer RC, Altmann T (2017) Establishment of integrated protocols for automated high throughput kinetic chlorophyll fluorescence analyses. *Plant Methods* 13:54. <https://doi.org/10.1186/s13007-017-0204-4>
- Tucker CJ (1980) Remote sensing of leaf water content in the near infrared. *Remote Sens Environ* 10(1):23–32
- Ustin SL (2004) Remote sensing of environment: state of the science and new directions. Remote sensing of natural resources management and environmental monitoring, pp 679–729
- Vescovo L, Wohlfahrt G, Balzarolo M, Pilloni S, Sottocornola M, Rodeghiero M et al (2012) New spectral vegetation indices based on the near-infrared shoulder wavelengths for remote detection of grassland phytomass. *Int J Remote Sens* 33(7):2178–2195
- Vogelmann TC (1993) Plant tissue optics. *Annu Rev Plant Biol* 44(1):231–251
- Vogelmann TC, Gorton HL (2014) Leaf: light capture in the photosynthetic organ. The structural basis of biological energy generation, pp 363–377. Springer
- Wallace JG, Rodgers-Melnick E, Buckler ES (2018) On the road to breeding 4.0: unraveling the good, the bad, and the boring of crop quantitative genomics. *Ann Rev Genet* 52(1):421–444. <https://doi.org/10.1146/annurev-genet-120116-024846>
- Wang H, Lin Y, Wang Z, Yao Y, Zhang Y, Wu L (2017) Validation of a low-cost 2D laser scanner in development of a more-affordable mobile terrestrial proximal sensing system for 3D plant structure phenotyping in indoor environment. *Comput Electron Agric* 140:180–189. <https://doi.org/10.1016/j.compag.2017.06.002>
- Wang H, Qian X, Zhang L, Xu S, Li H, Xia X et al (2018) A method of high throughput monitoring crop physiology using chlorophyll fluorescence and multispectral imaging. *Front Plant Sci* 9(407). <https://doi.org/10.3389/fpls.2018.00407>
- Wang L, Qu JJ (2007) NMDI: a normalized multi-band drought index for monitoring soil and vegetation moisture with satellite remote sensing. *Geophys Res Lett* 34(20)
- Weinig C, Schmitt J (2004) Environmental effects on the expression of quantitative trait loci and implications for phenotypic evolution. *Bioscience* 54(7):627–635. [https://doi.org/10.1641/0006-3568\(2004\)054\[0627:Eeoteo\]2.0.Co;2](https://doi.org/10.1641/0006-3568(2004)054[0627:Eeoteo]2.0.Co;2)
- Woolley JT (1971) Reflectance and transmittance of light by leaves. *Plant Physiol* 47(5):656–662
- Yang G, Liu J, Zhao C, Li Z, Huang Y, Yu H et al (2017a) Unmanned aerial vehicle remote sensing for field-based crop phenotyping: current status and perspectives. *Front Plant Sci* 8. <https://doi.org/10.3389/fpls.2017.01111>
- Yang H, Inagaki T, Ma T, Tsuchikawa S (2017b) High-resolution and non-destructive evaluation of the spatial distribution of nitrate and its dynamics in Spinach (*Spinacia oleracea* L.) Leaves

- by Near-Infrared Hyperspectral Imaging. *Front Plant Sci* 8(1937). <https://doi.org/10.3389/fpls.2017.01937>
- Yang W, Guo Z, Huang C, Duan L, Chen G, Jiang N et al (2014) Combining high-throughput phenotyping and genome-wide association studies to reveal natural genetic variation in rice. *Nat Commun* 5:5087. <https://doi.org/10.1038/ncomms6087>
- Ye H, Roorkiwal M, Valliyodan B, Zhou L, Chen P, Varshney RK et al (2018a) Genetic diversity of root system architecture in response to drought stress in grain legumes. *J Exp Bot* 69(13):3267–3277
- Ye H, Song L, Chen H, Valliyodan B, Cheng P, Ali L et al (2018b) A major natural genetic variation associated with root system architecture and plasticity improves waterlogging tolerance and yield in soybean. *Plant Cell Environ* 41(9):2169–2182. <https://doi.org/10.1111/pce.13190>
- Yuan L, Zhang J, Shi Y, Nie C, Wei L, Wang J (2014) Damage mapping of powdery mildew in winter wheat with high-resolution satellite image. *Remote Sens* 6(5):3611–3623
- Zhang C, Gao H, Zhou J, Cousins A, Pumphrey OM, Sankaran S (2016) 3D robotic system development for high-throughput crop phenotyping. *IFAC-PapersOnLine* 49(16):242–247
- Zhang C, Pumphrey M, Zhou J, Gao H, Zhang Q, Sankaran S (2017a) Development of automated high-throughput phenotyping system for controlled environment studies. Paper presented at the 2017 ASABE annual international meeting, St. Joseph, MI. <https://doi.org/10.13031/aim.201700581>
- Zhang X, Huang C, Wu D, Qiao F, Li W, Duan L et al (2017b) High-throughput phenotyping and QTL mapping reveals the genetic architecture of maize plant growth. *Plant Physiol* 173(3):1554–1564. <https://doi.org/10.1104/pp.16.01516>
- Zhou J, Chen H, Zhou J, Fu X, Ye H, Nguyen HT (2018a) Development of an automated phenotyping platform for quantifying soybean dynamic responses to salinity stress in greenhouse environment. *Comput Electron Agric* 151:319–330. <https://doi.org/10.1016/j.compag.2018.06.016>
- Zhou J, Fu X, Schumacher L, Zhou J (2018b) Evaluating geometric measurement accuracy based on 3D reconstruction of automated imagery in a Greenhouse. *Sensors (Basel)* 18(7). <https://doi.org/10.3390/s18072270>
- Zhou J, Ye H, Ali ML, Nguyen H, Chen P, Zhou J (2020a) Yield estimation of soybean breeding lines using UAV multispectral imagery and convolutional neuron network. Manuscript submitted for publication
- Zhou S, Mou H, Zhou J, Zhou J, Ye H, Nguyen HT (2020b) Development of an automated plant phenotyping system for evaluation of salt tolerance in soybean. Manuscript submitted for publication

# Chapter 10

## Phenotyping Root System Architecture, Anatomy, and Physiology to Understand Soil Foraging



Larry M. York

**Abstract** Increasing plant resilience in the face of climate change is a major challenge for the next century. At the same time, combatting environmental pollution from fertilizer use in agriculture is necessary. Optimized root systems would allow crops to withstand drought and to more efficiently use fertilizer, which in turn would drive plant growth and yield performance. Because roots are difficult to access in the soil, they are difficult to measure, or phenotype. This “phenotyping gap” is a major impediment to research seeking to understand how roots forage and influence crop performance. At the same time, even known important root traits, or phenes, are difficult to incorporate into crop breeding programs that rely on selection pressure towards beneficial phene states. However, progress in root phenotyping has been made with accessible tools available now for root system architecture. Root anatomy and physiology are the new frontiers for high-throughput phenotyping of crop roots. This chapter highlights the most practical methods to use for field root phenotyping, with a focus on how these methods could be combined to phenotype multiple root phenes sequentially. Dense root phene datasets would allow statistical insights to be made for understanding how root phene integration is important for crop performance. These methods are ready to use today, so the way forward to address the “phenotyping gap” to understand and breed for root phenes is clear. We have to get in the field, get our hands dirty, dig harder, and dig deeper.

**Keywords** Breeding · Nutrients · Phenomics · Rhizosphere · Uptake · Water

### 10.1 Introduction

The population of Earth may increase to nine billion people by 2050 which would require increasing agricultural production by at least 60%, but by as much as 100% due to increasing livestock consumption per capita (Grafton et al. 2015). Planting more land area with crops is not a sustainable way due to fragmentation of natural

---

L. M. York (✉)  
Noble Research Institute, LLC, Ardmore, OK 73401, USA  
e-mail: [lmyork@noble.org](mailto:lmyork@noble.org)

© Springer Nature Switzerland AG 2021  
J. Zhou et al. (eds.), *High-Throughput Crop Phenotyping*,  
Concepts and Strategies in Plant Sciences,  
[https://doi.org/10.1007/978-3-030-73734-4\\_10](https://doi.org/10.1007/978-3-030-73734-4_10)

209

ecosystems (Pretty 2008). Increasing fertilizer use is also not sustainable because of the resulting water and atmospheric pollution (Jenkinson 2001). At the same time, climate models predict that water will become more and more scarce over the next decade, and that more farming land will be drought-stressed (Nezhadahmadi et al. 2013). Therefore, increasing the ability of crops to capture nutrients and soil from water to efficiently produce yield while minimizing pollution is imperative.

Roots serve as the interface between the plant and the complex soil environment with key functions of water and nutrient extraction from soils (Lynch 1995; Meister et al. 2014). Root system architecture (RSA) refers to the shape and spatial arrangement of root systems within the soil, which plays an important role in plant fitness, crop performance, and agricultural productivity (Lynch 1995; York et al. 2013; Rogers and Benfey 2015). RSA is shaped by the interactions between genetic and environmental components, and influences the total volume of soil that roots can explore (Rogers and Benfey 2015). Many root phenes (or elemental units of phenotype Lynch 2011; Pieruschka and Poorter 2012; York et al. 2013) shape the final RSA, including the number, length, growth angle, elongation rate, diameter, and branching of axial and lateral roots (Bishopp and Lynch 2015). Understanding the contribution of RSA phenes to crop performance is of key importance; however, it only gives part of the story.

While root system architecture determines *where* roots are located in the soil, less will be known about *what* the roots are doing. Root cross-sectional anatomy refers to the microscopic organization of cells into tissues of various functions (Wachsman et al. 2015). Roots can be thought of as living pipes divided into the cortex as an outer ring, which contains most of the living cells, and the stele in the center which contains the vascular bundle. Water and nutrients must travel from outside the root, across the cortex, and into the xylem within the vascular bundle to be transported to the leaves. Therefore, root anatomical phenes are central to understanding water flow, nutrient uptake, root carbon costs, and root associations with microorganisms, such as mycorrhizal fungi.

Finally, the most obscured root phenes are physiological and flux based. These are rarely measured in root research, and have been studied in “high-throughput” scenarios even less. Root respiration is a measure of root CO<sub>2</sub> released due to the metabolic activity of the roots (Jaramillo et al. 2013). Root nutrient uptake rates are the speed at which a localized area of root can acquire nutrient ions from solution, whether in soil or hydroponics (Griffiths and York 2020). Last, exudation rates and relative abundance provide the abundance and types of compounds that roots release into the rhizosphere in order to mobilize nutrients and interact with soil microbes (Walker et al. 2014). Root physiological phenes represent a vast, untapped frontier for root research with direct importance for agricultural frontiers such as soil health.

Roots grow in the soil so are difficult to study (Eshel and Beekman 2013). Because of this difficulty, the genetic and functional basis of root phenes lags behind aboveground phenes (Topp et al. 2016). Conceptually, progress is being made in the ecology of root traits (Freschet et al. In Press a), but phenotyping remains a major bottleneck in research and a lack of efficient methods for collecting root phenotypic data is limiting progress in using RSA for genetic studies and breeding (Das et al.

2015; Kuijken et al. 2015). To address this “phenotyping gap,” there has been a shift to image-based phenotyping for enabling relatively high-throughput and accurate measurements of roots. Many of the platforms use 2D imaging with cameras, and involve the use of seedlings on agar plates, germination paper, or fabric cloth in bins (Kuijken et al. 2015). Several recent reviews cover the range of root phenotyping methods available (Kuijken et al. 2015; Paez-Garcia et al. 2015; Topp et al. 2016; Atkinson et al. 2019; Tracy et al. 2019), and Tracy et al. (2019) nicely highlight successes of root phenotyping in crop breeding. Readers are also encouraged to review a new root phenology handbook that covers a suite of root measures as well their ecological significance (Freschet et al. In Press b), but does not focus on high-throughput phenotyping. Despite the usefulness of controlling environmental parameters for characterization of root phenotypes, this chapter focuses on methods that could be applied to field-grown plants.

## 10.2 Root System Architecture

Weaver and colleagues (Weaver 1925; 1926) excavated, drew, and photographed root systems nearly a century ago (Böhm 2012). Over the past decade, root crown phenotyping (York 2018) has become popular for field-grown plants because it combines field relevance with high-throughput capacity. Root crown phenotyping involves excavating the top portion of the root system (the root crown), cleaning the roots, and measuring phenes, using a variety of means. Root crown phenes, including root number (York et al. 2013; Gao and Lynch 2016; Slack et al. 2018) and growth angle (Wasson et al. 2012; Trachsel et al. 2013; York et al. 2015; Slack et al. 2018), have been reported to relate to aboveground production. Root crown phenotyping was popularized as “shovelomics” by Trachsel et al. (2011) using visual scoring. The term “shovelomics” is widely used, but debate exists whether it only refers to methods based on root crown washing and visual scoring in maize (*Zea mays* L.) or to other protocols. Therefore, “root crown phenotyping” is proposed for more general use. Root crown phenotyping has been used to investigate the roots of soybean (*Glycine max* L.), common bean (*Phaseolous vulgaris* L.), cowpea (*Vigna unguiculata* L.), wheat (*Triticum aestivum* L.), and maize (*Zea mays* L.) crops (Trachsel et al. 2010; Colombi et al. 2015; York et al. 2015; York and Lynch 2015; Burrige et al. 2016; Maccaferri et al. 2016; York et al. 2018; Le Marié et al. 2019).

Image-based root crown phenotyping was first developed by Grift et al. (2011) for more reliable measurements and increased throughput. Image-based phenotyping requires acquiring an image of the root crown, followed by image analysis. Image analysis generally first starts with identifying the object of interest in an image in a process known as segmentation. Successful segmentation is essential for all downstream analysis that provides computed phenes, and therefore acquiring the right image is crucial. Features of a good starting image include high contrast of the root with the background and homogenous lighting conditions (Fig. 10.1). Current root crown image analysis options include DIRT (digital imaging of root traits) that

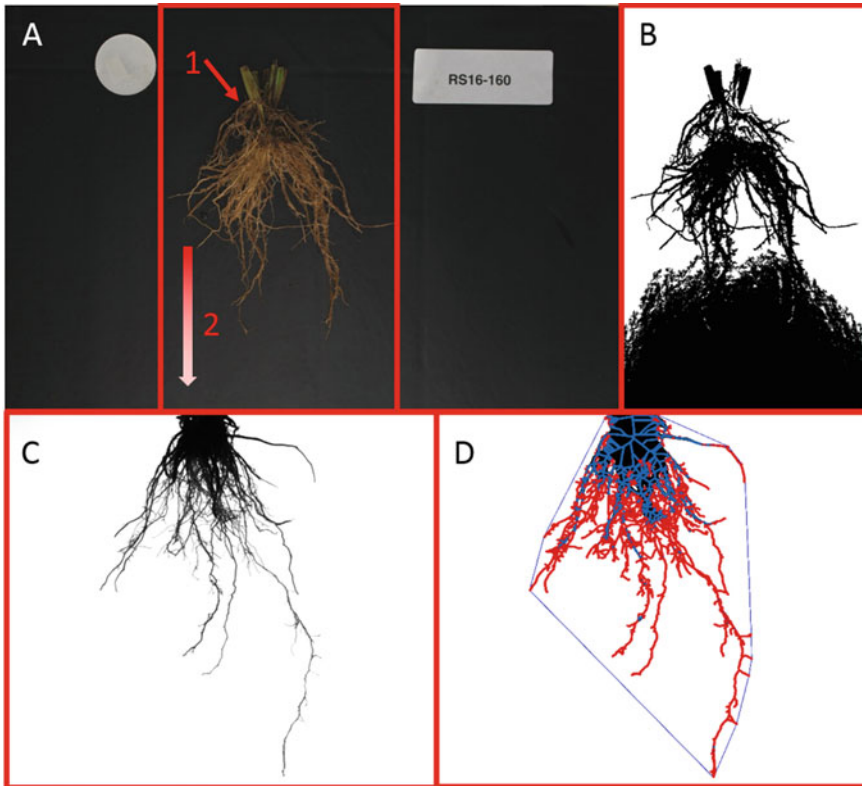


**Fig. 10.1** Even images that appear good quality by eye may not be suitable for reliable image analysis. Panel A shows the original color image with a wheat root crown on a black background, while B shows a segmentation that highlights possible problems. As seen in A, even within the root crown, self-shading and dark pigmentation prevent successful segmentation of all roots and stems (1), and a barely perceptible light intensity gradient (2) in the background also interferes. These challenges are completely solved by using a backlight, with a raw image of the root crown silhouette from the RhizoVision Crown platform shown in C with successful segmentation and analysis using RhizoVision Explorer in D. Getting the right image quickly and reliably is a crucial underpinning of phenotyping

requires uploading images to a cloud-based computational framework (Bucksch et al. 2014; Das et al. 2015) and REST (Root Estimator for Shovelomics Traits) that relies on proprietary MATLAB software (Colombi et al. 2015). The DIRT imaging protocol is designed to relax imaging conditions, but leads to the types of segmentation challenges presented in Fig. 10.1, and use of the cloud-based system can be slow and tedious. More recently, the RhizoVision Crown platform was developed as a state-of-the-art platform for root crown phenotyping that optimized every step of the process using a custom imaging unit, imaging software, and analysis software (Seethepalli et al. 2020). Root crowns are placed into the imaging unit with a clip-and-replace method in front of a Light-Emitting Diodes (LED) backlight such that the root crown



silhouette is captured by a monochrome camera resulting in nearly segmented raw images as shown in Fig. 10.1. The imaging software allows image acquisition to be triggered by barcode scanner, such that images are saved with the appropriate file name. While the original paper introduced RhizoVision Analyzer for analysis, this software has been greatly extended as RhizoVision Explorer (<https://doi.org/10.5281/zenodo.3747697>) for interactive, fast, and reliable root image analysis that works on Windows computers (Seethepalli and York 2020). Generally, analysis would be expected to be finished using RhizoVision Explorer before even uploading image files to a cloud-based platform would be completed. RhizoVision Explorer was shown to be very accurate for measurements of root length, diameter, surface area, and volume using, whereas the commercial WinRhizo substantially underestimated root volume (Seethepalli et al. 2021). Due to the use of barcodes and the output of the analysis software including the filenames, these data files can be ingested directly into data analysis scripts. Therefore, the RhizoVision Crown platform encourages several best practices for phenotyping to facilitate root research.

Still, root crown phenotyping is limited to only the upper portion of the root system, and while its properties have been shown to relate to deeper root measures (Trachsel et al. 2013), there is no substitute for sampling deep roots directly. Other field root phenotyping methods include minirhizotrons and soil coring, which both require a large amount of physical labor and setup time (Johnson et al. 2001; Böhm 2012; Wasson et al. 2016). Minirhizotrons require inserting clear acrylic tubes into the ground so that cameras can be inserted periodically to acquire images of roots growing along the face of the tube with the soil as a background. Inserting the tubes can be facilitated with machinery, and acquiring the images is relatively simple. However, a major bottleneck has been actually analyzing the images, which has generally been accomplished by manually tracing roots in software. However, in just the past couple years machine learning has been applied to successfully segment roots from the complex, soil backgrounds in minirhizotron images, so this bottleneck may be partially alleviated in the near future (Wang et al. 2019; Smith et al. 2020; Xu et al. 2020). Another new software facilitates manual annotation of roots, but importantly also the tracking for roots over time to provide birth and death rates (Möller et al. 2019). If automated segmentation could be coupled with automated time-series tracking of root population demography, then the field of root biology would be transformed. More recently non-destructive root phenotyping methods such as ground penetrating radar and electrical resistance tomography have shown promise; however, both techniques only provide indirect assessments of root length, do not provide RSA features, and have not been shown to be ready for reliable, large-scale use (Garré et al. 2013; Liu et al. 2018). Soil coring involves inserting metallic tubes into the ground to extract soil columns of 2–5 cm in diameter and 50–200 cm in depth. Typically, the soil core is divided into increments of equal length, roots are washed out, scanned, analyzed, and reported as root length distribution with depth (BurrIDGE et al. 2020). Arguably, the type of information provided by soil coring is the “holy grail” of field root phenotyping, and so methods that increase throughput, data density, and method reliability will be game-changers.

### 10.3 Root Anatomy

Root cross sections are readily observed by simply cutting a root in two, and have been extensively studied in root developmental biology. In the context of crop breeding, there are two major considerations for the importance of root anatomy (Fig. 10.2). Root construction and metabolic costs will both be influenced by the size of the cortical tissue (Jaramillo et al. 2013), which itself can be further divided into number and size of cortical cells with independent influence on metabolic cost (Chimungu et al. 2014a, b). Axial water flow is also an important component of plant–soil water relations, which is driven by the number and area of xylem vessels in the root (Passioura 1988). Sampling of root sections for anatomical phenotyping can be done in the field, using the same root crowns already excavated for architectural analysis. Generally, root sections should be sampled from the same root class and root type, such as second whorl nodal roots in monocots or first-order lateral roots in dicots (Burton et al. 2013) based on prior knowledge or preliminary studies. Short root sections a few centimeters in length can be excised and stored in 70% ethanol within labeled 1.5 ml tubes and stored for approximately 1 year in a refrigerator.

Anatomical imaging can be achieved in a variety of ways. Hand-sectioning involves using a razor blade to cut thin slices of roots to place on microscope slides. Roots can also be embedded and cut with a microtome for consistency. Atkinson and Wells (2017) describe a three-dimensional (3D)—printed block in which several roots can be embedded in agar in order to cut simultaneously on a microtome, and then imaged using various stains and fluorescence. Laser ablation tomography (LAT) represents a major advance by using a pulsed laser to ablate the root surface and a motorized stage to move the root surface into the imaging focal plane (Strock et al. 2019). By use of an ultraviolet (UV) laser, the root surface autofluoresces while

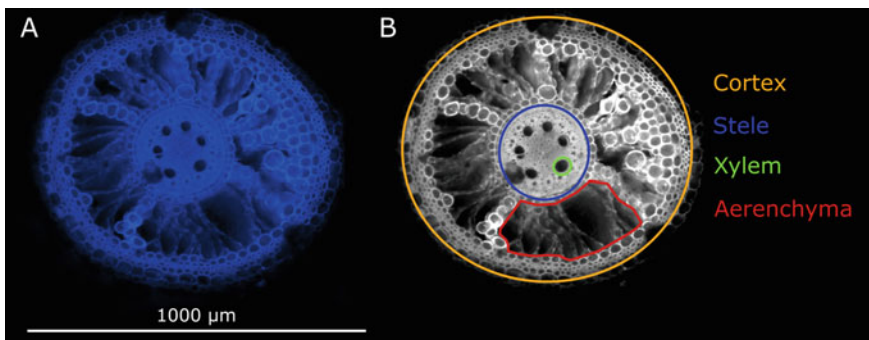


**Fig. 10.2** In panel A, a root cross section from switchgrass sectioned with a vibratome and imaged with a BioTek Lionheart microscope using fluorescence (imaged by Marcus Griffiths). In B, this same cross section is shown in white with areas drawn on major features. Total cortex and stele areas, along with their ratio, are commonly used, but can be refined. Average xylem vessel area, number of xylem vessels, and total xylem area relate to water relations, while living cortical area that is cortex area minus aerenchyma area gives a good indicator of metabolic costs

ablated, and this light is captured by a camera to generate a high-contrast image. As with root crown imaging, a researcher should take great care in optimizing an imaging protocol to generate clear, high-contrast anatomical images to facilitate downstream analysis.

A minimum set of relevant anatomical features would include cortex area, stele area, the number of xylem vessels, and the average xylem vessel area (see Fig. 10.2). These could be derived quickly from manual measurements in ImageJ (Schneider et al. 2012). Several semi-automated or automated tools have been developed for root anatomical phenotyping (Burton et al. 2012; Pound et al. 2012; Lartaud et al. 2014). The most successful may be RootScan, designed for use with the LAT method (Burton et al. 2012). This software provides very detailed analysis including cortical cell number, cortical cell area, aerenchyma area, xylem areas, and xylem number, among many others. However, the software suffers for specificity to the target species common bean and maize, and therefore more generalizable imaging and image analysis solutions are needed in order to integrate root anatomical phenotyping into research programs more routinely.

## 10.4 Root Physiology

Root physiological phenes that directly measure the influence of the root on the environment through gas, nutrient, or exudate flux are an important frontier for root biology. Specific root respiration is a measure of both root metabolic burden and also of root activity (Lynch 2015). Root respiration can be measured on samples quickly excised from excavated root crowns and placed in closed loops of an infrared gas analyzer for time-series measurement of CO<sub>2</sub> accumulation, from which a curve is fit to derive total respiration (see Fig. 10.3). These respiration measurements are standardized by fresh mass, dry mass, or scanned root length or volume for the measured sample. Root respiration is an important integrator of root anatomical phenes that affect metabolic burden, and is arguably faster and easier to measure than anatomy. Recently, specific root respiration was found to be heritable in winter wheat, and genetic mapping of the phene using a diversity panel discovered several gene candidates that possibly explain this variation and that could be used for selecting crops with lower root metabolic burden (Guo et al. In Press).

Root nutrient uptake is a critically understudied area of root biology, as reviewed by Griffiths and York (2020). Recently, 24 lines representing maize diversity were phenotyped for multiple nutrient uptake using nutrient solution depletion methods, and demonstrated substantial genetic variation that could potentially be used for plant breeding (Griffiths et al. 2021). Measuring root uptake in the field may be possible by placing excised roots in small volumes of nutrient solution with known starting concentrations, or by using stable isotopes such as <sup>15</sup>N as nitrate. While difficult to scale up, microdialysis could be used for confirmation of uptake abilities in situ with roots in soil (Shaw et al. 2014).

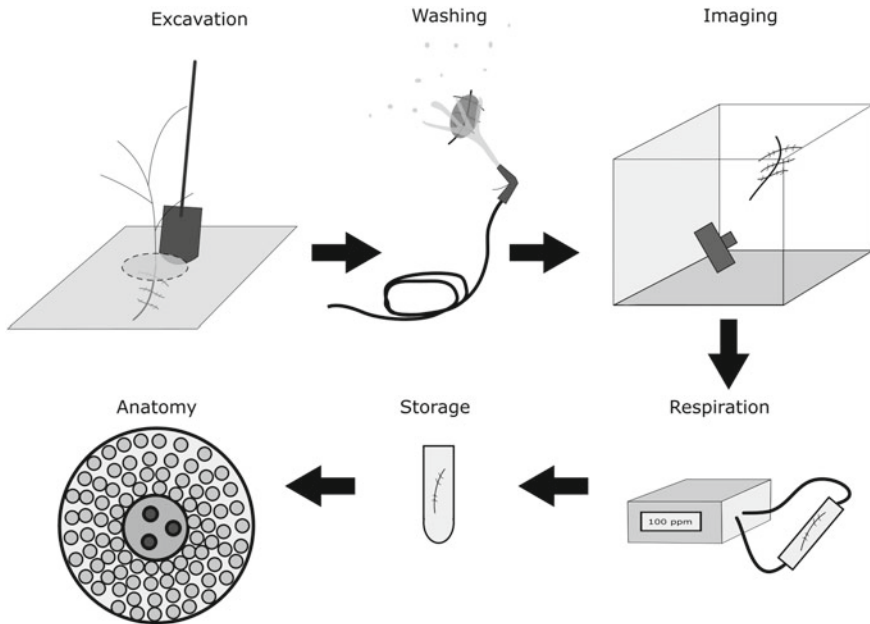


**Fig. 10.3** Next-generation root phenotyping from parallel phenotyping streams in the field. A root crown is excavated, cleaned, and imaged. Immediately a representative root (or several) is measured for a physiological function, like respiration, and then cold stored in 70% ethanol until root anatomical phenotyping occurs

Root exudation represents another important flux out of roots, yet little is known about genetic variation within or among species. However, there are a few reports of genetic mapping of exudation, for example, for acid exudation in common bean (Yan et al. 2004). Feasibly, exudate profiles including type and relative abundance could be measured from the same solutions as nutrient depletion above. Even quantifying the total carbon output of the root would be important for understanding the plant carbon balance as well as the potential for rhizodeposition and priming of the rhizosphere (Vranova et al. 2013).

## 10.5 Root Functional Phenomics and Phen Integration

Functional phenomics has recently been proposed as a new field that combines elements of physiology, phenotyping, and breeding to both increase understanding of fundamental plant processes and to use this understanding for trait-based, or ideotype, breeding (York 2019). Functional phenomics relies on a pipeline beginning with ideotype development, followed by phenotyping platform construction,

screening mapping populations, phenomic data analysis to link trait variation to function, detailed physiological work to uncover mechanisms, and simulation modeling. The knowledge gained feeds back to informing ideotype development and active use of traits of interest in breeding programs using the phenotyping platforms. This cycle is proposed to be central to how molecular biologists, physiologists, computer scientists, and breeders will solve this century's great agricultural challenges. By combining root phenotyping methods and utilizing the same germplasm, crop scientists can make phenotyping more efficient by reducing experimental redundancy. These efficiencies could include expanding collaboration and will be important to accelerate breeding gains.

One major flaw of many root studies is that either only a single root trait is reported, or even multiple are reported but no measurements of shoot traits are provided. Shoot mass and nutrient content are both very relevant metrics to include in crop studies along with root phenes. Recently, phenotyping of RSA and xylem anatomical traits was used to show how two legume species formed functional groups with differential plant performance in drought stress using multivariate clustering methods (Strock et al. 2021). This type of study should become the norm rather than the exception for phene integration (York 2019). Efficient phenotyping platforms using teams of collaborators could measure all the root phenes described in this chapter in the field by using sequential sample processing (Fig. 10.3). While non-destructive and 3D imaging technologies remain the long-term goals for root biology, in the short term even greater strides will be made by optimizing methods that can already be used in high throughput for field-grown roots. Enabling root researchers around the world with tools that democratize root biology will transform crop breeding.

## 10.6 Summary and Future Prospects

This chapter highlights phenotyping methods that can be used in the field now to greatly increase understanding of crop root biology. There are many additional methods to use in the greenhouse and lab that are not discussed to encourage crop scientists and breeders to go to the field directly. While most writing on roots highlights the laborious and time-consuming nature, the methods that are outlined here are possible to use on entire genetic mapping populations in hundreds or even thousands of plots. Innovations that increase throughput, measurement accuracy, and ease of data collection will allow further progress in field root research. While progress has been made on the study of roots in isolation, root phenes can only be understood in the context of other phenes, including the shoot's, and also with respect to plant ecology. Root phene integration and functional phenomics will require simultaneous phenotyping of multiple root phenes. Therefore, the root "phenotyping gap" will be addressed by taking standard protocols to the field and getting our hands dirty. To realize the potential of roots for transforming agriculture, we have to dig harder and dig deeper.

## References

- Atkinson JA, Wells DM (2017) An updated protocol for high throughput plant tissue sectioning. *Front Plant Sci* 8:1721
- Atkinson JA, Pound MP, Bennett MJ, Wells DM (2019) Uncovering the hidden half of plants using new advances in root phenotyping. *Curr Opin Biotechnol* 55:1–8
- Bishopp A, Lynch JP (2015) The hidden half of crop yields. *Nat Plants* 1:15117
- Böhm W (2012) Methods of studying root systems, vol 33. Springer Science & Business Media
- Bucksch A, BurrIDGE J, York LM, Das A, Nord E, Weitz JS, Lynch JP (2014) Image-based high-throughput field phenotyping of crop roots. *Plant Physiol* 166:470–486
- BurrIDGE J, Jochua CN, Bucksch A, Lynch JP (2016) Legume shovelomics: high—throughput phenotyping of common bean (*Phaseolus vulgaris* L.) and cowpea (*Vigna unguiculata* subsp. *unguiculata*) root architecture in the field. *Field Crops Research* 192:21–32
- BurrIDGE JD, Black CK, Nord EA, Postma JA, Sidhu JS, York LM, Lynch JP (2020) An analysis of soil coring strategies to estimate root depth in maize (*Zea mays*) and common bean (*Phaseolus vulgaris*). *Plant Phenomics* 2020:1–20
- Burton AL, Williams M, Lynch JP, Brown KM (2012) RootScan: software for high-throughput analysis of root anatomical traits. *Plant Soil* 357:189–203
- Burton AL, Lynch JP, Brown KM (2013) Spatial distribution and phenotypic variation in root cortical aerenchyma of maize (*Zea mays* L.). *Plant Soil* 367:263–274
- Chimungu JG, Brown KM, Lynch JP (2014a) Large root cortical cell size improves drought tolerance in maize (*Zea mays* L.). *Plant Physiol* 166:2166–2178
- Chimungu JG, Brown KM, Lynch JP (2014b) Reduced root cortical cell file number improves drought tolerance in maize. *Plant Physiol* 166:1943–1955
- Colombi T, Kirchgessner N, Le Marié CA, York LM, Lynch JP, Hund A (2015) Next generation shovelomics: set up a tent and REST. *Plant Soil* 388:1–20
- Das A, Schneider H, BurrIDGE J, Ascanio AK, Wojciechowski T, Topp CN, Lynch JP, Weitz JS, Bucksch A (2015) Digital imaging of root traits (DIRT): a high-throughput computing and collaboration platform for field-based root phenomics. *Plant Methods* 11:51
- Eshel A, Beeckman T (ed) (2013) *Plant roots: the hidden half*. CRC Press
- Freschet GT, Roumet C, Comas LH, Weemstra M, Bengough AG, Rewald B, Bardgett RD, De Deyn GB, Johnson D, Klimešová J, Lukac M, McCormack ML, Meier IC, Pagès L, Poorter H, Prieto I, Wurzbürger N, Zadworny M, Bagniewska-Zadworna A, Blancaflor EB, Brunner I, Gessler A, Hobbie SE, Iversen CM, Mommer L, Picon-Cochard C, Postma JA, Rose L, Ryser P, Scherer-Lorenzen M, Soudzilovskaia NA, Sun T, Valverde-Barrantes OJ, Weigelt A, York LM, Stokes A (In Press a) Root traits as drivers of plant and ecosystem functioning: current understanding, pitfalls and future research needs. *New Phytologist*
- Freschet GT, Pagès LL, Iversen C, Comas LH, Rewald B, Roumet C, Klimešová J, Zadworny M, Poorter H, Postma JA, Adams TS, Bagniewska-Zadworna A, Bengough AG, Blancaflor EB, Brunner I, Cornelissen JHC, Garnier E, Gessler A, Hobbie SE, Meier IC, Mommer L, Picon-Cochard C, Rose L, Ryser P, Scherer-Lorenzen M, Soudzilovskaia N, Stokes A, Sun T, Valverde-Barrantes OJ, Weemstra M, Weigelt A, Wurzbürger N, York LM, Batterman SA, Gomes De Moraes M, Janeček Š, Lambers H, Salmon V, Tharayil N, McCormack ML (In Press b) A starting guide to root ecology: strengthening ecological concepts and standardizing root classification, sampling, processing and trait measurements. *New Phyt*
- Gao Y, Lynch JP (2016) Reduced crown root number improves water acquisition under water deficit stress in maize (*Zea mays* L.). *J Exp Bot* 67:4545–4557
- Garré S, Coteur I, Wonglecharoen C, Hussain K, Omsunram W, Kongkaew T, Hilger T, Diels J, Vanderborght J (2013) Can we use electrical resistivity tomography to measure root zone dynamics in fields with multiple crops? *Procedia Environ Sci* 19:403–410
- Grafton RQ, Williams J, Jiang Q (2015) Food and water gaps to 2050: preliminary results from the global food and water system (GFWS) platform. *Food Security* 7:209–220

- Grift TE, Novais J, Bohn M (2011) High-throughput phenotyping technology for maize roots. *Biosys Eng* 110:40–48
- Griffiths M, York LM (2020) Targeting root uptake kinetics for increasing plant productivity and nutrient use efficiency. *Plant Physiol* 182:1854–1868
- Griffiths M, Roy S, Guo H, Seethepalli A, Huhman D, Ge Y, Sharp RE, Fritschi FB, York LM (2021) A multiple ion-uptake phenotyping platform reveals shared mechanisms that affect nutrient uptake by maize roots. *Plant Phys* 185:781–795
- Guo H, Ayalew H, Seethepalli A, Dhakal K, Griffiths M, Ma X-F, York LM (In Press) Functional phenomics and genetics of the root economics space in winter wheat using high-throughput phenotyping of respiration and architecture. *New Phytologist*
- Jaramillo RE, Nord EA, Chimungu JG, Brown KM, Lynch JP (2013) Root cortical burden influences drought tolerance in maize. *Ann Bot* 112:429–437
- Jenkinson DS (2001) The impact of humans on the nitrogen cycle, with focus on temperate arable agriculture. *1913*:3–15
- Johnson M, Tingey D, Phillips D, Storm M (2001) Advancing fine root research with minirhizotrons. *Environ Exp Bot* 45:263–289
- Kuijken RC, van Eeuwijk FA, Marcelis LF, Bouwmeester HJ (2015) Root phenotyping: from component trait in the lab to breeding. *J Exp Bot* 66:5389–5401
- Lartaud M, Perin C, Courtois B, Thomas E, Henry S, Bettembourg M, Divol F, Lanau N, Artus F, Bureau C, Verdeil J-L, Sarah G, Guiderdoni E, Dievart A (2014) PHIV-RootCell: a supervised image analysis tool for rice root anatomical parameter quantification. *Front Plant Science* 5:790
- Le Marié CA, York LM, Strigens A, Malosetti M, Camp K-H, Giuliani S, Lynch JP, Hund A (2019) Shovelomics root traits assessed on the EURoot maize panel are highly heritable across environments but show low genotype-by-nitrogen interaction. *Euphytica* 215 10(2019):1–22
- Liu X, Dong X, Xue Q, Leskovar DI, Jifon J, Butnor JR, Marek T (2018) Ground penetrating radar (GPR) detects fine roots of agricultural crops in the field. *Plant Soil* 423:517–531
- Lynch J (1995) Root architecture and plant productivity. *Plant Physiol* 109:7
- Lynch JP (2011) Root phenes for enhanced soil exploration and phosphorus acquisition: tools for future crops. *Plant Physiol* 156:1041–1049
- Lynch JP (2015) Root phenes that reduce the metabolic costs of soil exploration: opportunities for 21st century agriculture. *Plant Cell Environ*
- Maccaferri M, El-Feki W, Nazemi G, Salvi S, Canè MA, Colalongo MC, Stefanelli S, Tuberosa R (2016) Prioritizing quantitative trait loci for root system architecture in tetraploid wheat. *J Exp Bot* 67:1161–1178
- Meister R, Rajani M, Ruzicka D, Schachtman DP (2014) Challenges of modifying root traits in crops for agriculture. *Trends Plant Sci* 19:779–788
- Möller B, Chen H, Schmidt T, Zieschank A, Patzak R, Türke M, Weigelt A, Posch S (2019) rhizoTrak: a flexible open source Fiji plugin for user-friendly manual annotation of time-series images from minirhizotrons. *Plant Soil* 444:519–534
- Nezhadahmadi A, Prodhon ZH, Faruq G (2013) Drought tolerance in wheat. *Sci World J* 2013:12
- Paez-Garcia A, Motes C, Scheible W-R, Chen R, Blancaflor E, Monteros M (2015) Root traits and phenotyping strategies for plant improvement. *Plants* 4:334–355
- Passioura JB (1988) Water transport in and to roots. *Ann Rev Plant Physiol Plant Mol Biol* 39:245–265
- Pieruschka R, Poorter H (2012) Phenotyping plants: genes, phenes and machines. *Funct Plant Biol* 39:813–820
- Pound MP, French AP, Wells DM, Bennett MJ, Pridmore TP (2012) CellSeT: novel software to extract and analyze structured networks of plant cells from confocal images. *Plant Cell* 24:1353–1361
- Pretty J (2008) Agricultural sustainability: concepts, principles and evidence. *Philos Trans Royal Soc Lond Ser B, Biol Sci* 363:447–465
- Rogers ED, Benfey PN (2015) Regulation of plant root system architecture: implications for crop advancement. *Curr Opin Biotechnol* 32:93–98

- Schneider CA, Rasband WS, Eliceiri KW (2012) NIH Image to ImageJ: 25 years of image analysis. *Nat Methods* 9:671–675
- Seethepalli A, York LM (2020) RhizoVision explorer—interactive software for generalized root image analysis designed for everyone (version 2.0.2). Zenodo. <https://doi.org/10.5281/zenodo.3747697>
- Seethepalli A, Guo H, Liu X, Griffiths M, Almtarfi H, Li Z, Liu S, Zare A, Fritschi FB, Blancaflor EB, Ma X-F, York LM (2020) RhizoVision crown: an integrated hardware and software platform for root crown phenotyping. *Plant Phenomics* 1–15
- Seethepalli A, Dhakal K, Griffiths M, Guo H, Freschet GT, York LM (2021) RhizoVision Explorer: Open-source software for root image analysis and measurement standardization. *bioRxiv*: 2021.2004.2011.439359
- Shaw R, Williams AP, Jones DL (2014) Assessing soil nitrogen availability using microdialysis-derived diffusive flux measurements. *Soil Sci Soc Am J* 78:1797
- Slack S, York LM, Roghazai Y, Lynch J, Bennett M, Foulkes J (2018) Wheat shovelomics II: revealing relationships between root crown traits and crop growth. *bioRxiv*
- Smith AG, Petersen J, Selvan R, Rasmussen CR (2020) Segmentation of roots in soil with U-Net. *Plant Methods* 16:13
- Strock CF, Schneider HM, Galindo-Castaneda T, Hall BT, Van Gansbeke B, Mather DE, Roth MG, Chilvers MI, Guo X, Brown K, Lynch JP (2019) Laser ablation tomography for visualization of root colonization by edaphic organisms. *J Exp Bot* 70:5327–5342
- Strock CF, Burrige JD, Niemiec MD, Brown KM, Lynch JP (2021) Root metaxylem and architecture phenotypes integrate to regulate water use under drought stress. *Plant Cell Environ* 44:49–67
- Topp CN, Bray AL, Ellis NA, Liu Z (2016) How can we harness quantitative genetic variation in crop root systems for agricultural improvement? *J Integr Plant Biol* 58:213–225
- Trachsel S, Kaeppler SM, Brown KM, Lynch JP (2010) Shovelomics: high throughput phenotyping of maize (*Zea mays* L.) root architecture in the field. *Plant Soil* 341:75–87
- Trachsel S, Kaeppler SM, Brown KM, Lynch J (2011) Shovelomics: high throughput phenotyping of maize (*Zea mays* L.) root architecture in the field. *Plant Soil* 341:75–87
- Trachsel S, Kaeppler S, Brown K, Lynch J (2013) Maize root growth angles become steeper under low N conditions. *Field Crops Res* 140:18–31
- Tracy SR, Nagel KA, Postma JA, Fassbender H, Wasson A, Watt M (2019) Crop improvement from phenotyping roots: highlights reveal expanding opportunities. *Trends Plant Sci* 25(1):105–118
- Vranova V, Rejsek K, Skene KR, Janous D, Formanek P (2013) Methods of collection of plant root exudates in relation to plant metabolism and purpose: a review. *J Plant Nutr Soil Sci* 176:175–199
- Wachsman G, Sparks EE, Benfey PN (2015) Tansley review genes and networks regulating root anatomy and architecture. *New Phytologist* 208(1):26–38
- Walker TS, Bais HP, Grotewold E, Vivanco JM (2014) Update on root exudation and rhizosphere biology. *Root Exudation Rhizosphere Biol* 1(132):44–51
- Wang T, Rostamza M, Song Z, Wang L, McNickle G, Iyer-Pascuzzi AS, Qiu Z, Jin J (2019) SegRoot: a high throughput segmentation method for root image analysis. *Comput Electron Agric* 162:845–854
- Wasson AP, Richards R, Chatrath R, Misra S, Prasad SS, Rebetzke G, Kirkegaard J, Christopher J, Watt M (2012) Traits and selection strategies to improve root systems and water uptake in water-limited wheat crops. *J Exp Bot* 63:3485–3498
- Wasson A, Bischof L, Zwart A, Watt M (2016) A portable fluorescence spectroscopy imaging system for automated root phenotyping in soil cores in the field. *J Exp Bot* 67:1033–1043
- Weaver JE (1925) Investigations on the root habits of plants. *Am J Bot* 12:502–509
- Weaver JE, Bruner WE (1926) Root development of field crops. McGraw-Hill
- Xu W, Yu G, Zare A, Zurweller B, Rowland D, Reyes-Cabrera J, Fritschi FB, Matamala R, Juenger TE (2020) Overcoming small minirhizotron datasets using transfer learning. *Comput Electron Agricult* 175:105466



- Yan X, Liao H, Beebe SE, Blair MW, Lynch JP (2004) QTL mapping of root hair and acid exudation traits and their relationship to phosphorus uptake in common bean. *Plant Soil* 265:17–29
- York LM (2018) Phenotyping crop root crowns: general guidance and specific protocols for maize, wheat, and soybean. In Ristova D, Barbez E (eds) *Root development: methods and protocols*. Springer, pp 23–32
- York LM (2019) Functional phenomics: an emerging field integrating high-throughput phenotyping, physiology, and bioinformatics. *J Exp Bot* 70:379–386
- York LM, Lynch JP (2015) Intensive field phenotyping of maize (*Zea mays* L.) root crowns identifies phenes and phene integration associated with plant growth and nitrogen acquisition. *J Exp Bot* 66:5493–5505
- York LM, Nord E, Lynch J (2013) Integration of root phenes for soil resource acquisition. *Front Plant Sci* 4:355
- York LM, Galindo-Castaneda T, Schussler JR, Lynch JP (2015) Evolution of US maize (*Zea mays* L.) root architectural and anatomical phenes over the past 100 years corresponds to increased tolerance of nitrogen stress. *J Exp Bot* 66:2347–2358
- York LM, Slack S, Bennett MJ, Foulkes MJ (2018) Wheat shovelomics I: a field phenotyping approach for characterising the structure and function of root systems in tillering species. *bioRxiv* 280875

# Chapter 11

## Got All the Answers! What Were the Questions? Avoiding the Risk of “Phenomics” Slipping into a Technology Spree



Vincent Vadez, Jana Kholova, Grégoire Hummel, and Uladzimir Zhokhavets

**Abstract** For many crops, the genomics revolution has given hope that breeding would become easier, faster, and more efficient. Relevant phenotyping is now the main bottleneck and new technologies provide opportunities for easier, faster, more sensitive, and more informative phenotyping. However, the phenotyping agenda must be driven by scientific questions rather than by a technological push, especially for complex constraints, such as drought. In this chapter, we provide a viewpoint on phenotyping and what it should take into account. Phenotyping is a full-fledge research effort, calling for a multidisciplinary effort between technology providers and several research disciplines, and which needs to address the issue of linking scales. Two phenotyping platforms are described; a lysimetric platform (LysiField) to assess the patterns of plant water use and relate these to grain yield, and an imaging platform (LeasyScan) to characterize crop canopy traits responsible for water savings. In both cases, the chapter discusses the thought process and the hypotheses around key traits for drought adaptation that were put in the development of these platforms. The chapter concludes with perspectives on the integration of high-throughput phenotyping (HTP) technology with breeding, starting with an analysis of the cost as a prerequisite to decide on its usage and adoption in breeding. It takes a few examples of current opportunities in the domain of imaging, trying to bring closer together what the technology can bring and what breeding pragmatically needs. In conclusion, while new technologies provide opportunities to make phenotyping easier, faster, better, cheaper, the risk of becoming the end that justifies the means can be avoided by driving the technology with research questions, made

---

V. Vadez (✉)

Institut de Recherche pour le Développement (IRD), UMR DIADE, University of Montpellier, 911 Av Agropolis BP65401, 34394 Montpellier, France  
e-mail: [vincent.vadez@ird.fr](mailto:vincent.vadez@ird.fr); [v.vadez@cgiar.org](mailto:v.vadez@cgiar.org)

J. Kholova

Crop Physiology Laboratory, ICRISAT, Greater Hyderabad, Patancheru 502324, Telangana, India  
URL: <http://www.icrisat.org>

G. Hummel · U. Zhokhavets

Phenospex, Jan Campertstraat 11/NL-6416 SG, Heerlen, The Netherlands  
URL: <https://www.phenospex.com>

© Springer Nature Switzerland AG 2021

J. Zhou et al. (eds.), *High-Throughput Crop Phenotyping*,  
Concepts and Strategies in Plant Sciences,  
[https://doi.org/10.1007/978-3-030-73734-4\\_11](https://doi.org/10.1007/978-3-030-73734-4_11)

223

possible through a cross-discipline approach between genetics, breeding, modeling, engineering, physiology, and statistics.

**Keywords** Multi-discipline trait · Drought · Breeding · Genetic gain · Transpiration

## 11.1 Introduction

Although we know more and more about the "genotype," obtaining information on the "phenotype" remains a challenge due to the complexity of biological systems and the requirement for physical measurement of plant traits that are difficult to perform quickly. Obtaining phenotypic information that is relevant, accurate, fast, repeatable, and manageable in large numbers has been, and will remain, a basic challenge of any breeding program. There is also a need, and may be an opportunity with new technologies, to move away from the very "integrated" phenotypes that have been the bulk of phenotyping so far (e.g., yield, biomass, height) towards the causal building blocks of these integrated phenotypes. In the past few years, a revolution in plant phenotyping is taking place and technological progress has made possible an increase in the throughput and precision of phenotyping. We argue that the current phenotyping revolution while creating fantastic opportunities to capture phenotypic traits quickly and non-destructively, is also running the risk of becoming driven by the technology itself, rather than being driven by research questions around the critical plant traits to phenotype. This chapter analyzes the opportunities and challenges facing this phenotyping revolution, presents two phenotyping platforms that break up phenotypes in smaller building blocks, and addresses the link to breeding applications and forthcoming opportunities.

The first section is a viewpoint on the principles that should be applied to plant phenotyping. At present, phenotyping is seen as a tool to generate data for the breeding community. Contrary to this view, we argue that phenotyping is a full-fledged scientific approach that requires a careful analysis of the traits to be measured and their relevance for the targeted constraint (especially for complex traits). This calls for a multidisciplinary approach if "phenomics" is to be relevant for crop improvement, a view that is shared by many others (e.g., Deery et al. 2014; White and Snow 2012; Araus and Cairns 2014). In this section, we discuss the fact that some phenotypes are "consequential" (for instance, staygreen), whereas others are "causal" (for instance, leaf developmental traits). This section then explores the challenges and opportunities of linking information at different levels of plant organization, i.e., from either specialized phenotyping platforms, targeting predominantly traits at a lower level of plant organization, up to the field for agronomic trait phenotyping. The issue of scale in phenotyping is addressed by bringing up crop simulation modelling as an integration tool to bridge these scales, advocating linkages between trait-based and field-based evaluations of genotypes (Chapuis et al. 2012).

The following section presents the LysiField and LeasyScan platforms. The LysiField platform is a lysimeter platform that measures plant water use over the entire cropping cycle, instead of measuring roots per se, with a throughput of about 500–600 cylinders weighted per day since it remains a manual operation. The LeasyScan platform is a three-dimensional (3D) laser scanning system that generate 3D images from which several canopy features are extracted, like the leaf area, and that includes a lysimeter component for an automatic pot weighing to assess plant transpiration. This section will detail the thought process and research questions that led to the development of LysiField, how these research questions have shaped how the platform stands (Vadez et al. 2014). It then goes on describing how the knowledge gained from LysiField generated new research questions that have led to the development of another phenotyping platform (LeasyScan) to measure traits at a lower level of biological organization (crop canopy traits) more quickly and precisely. This section presents the principles of the scanning operation plant transpiration in situ. Scans are obtained at a high rate (approximately 2500 plots scanned per hour) on several parameters per plant, while tray weights are polled every 15'. Data management then becomes a major challenge (Cobb et al. 2013) and a description is given of the data handling process. This section presents the web-based interface that is used to visualize the data, and the data management tools are used to query data from the database and initiate the data analysis. We also discuss critical planning aspects during the development of a phenotyping platform such as the need to test the technology prior to acquisition and the need for a close user-provider relationship during and after the development of platforms.

The last section addresses phenotyping costs, and how this becomes a critical factor in the adoption of modern and technology-intensive methods in the breeding process. This section also presents a few examples using imaging technology to mirror what the technology can provide and what the immediate needs of breeding programs are.

## **11.2 Phenotyping: Basic Principles**

### ***11.2.1 Phenotyping is a Research Approach***

Understand the basic biological and physiological processes behind phenotypes is critical, especially for complex phenotypes. For instance, canopy temperature measurements can be used as a proxy phenotype for the transpiration capacity of genotypes. However, done at a late stage in a crop exposed to drought, this transpiration capacity could reflect: (i) the capacity to extract water from deep soil layer thanks to deeper rooting, or (ii) the fact that there is water remaining in the soil profile. In turn, the latter could be the consequence of a slower water use at earlier stages and have different causes, including (ii-a) a smaller leaf canopy size; and/or (ii-b) a lower canopy conductance under certain conditions. A smaller canopy size

could come from reduced tillering or branching, a lower leaf number, a smaller leaf or leaflet size. This example illustrates how a phenotype can be explained by a cascade of possible other phenotypes reflecting biological processes underneath. Similarly, the expression of a staygreen phenotype is actually the consequence of several phenotypes having contributed to differences in plant water use much earlier (Borrell et al. 2014). The concept of “phenes,” i.e., the phenotypic equivalent of genes (Lynch and Brown 2012), representing building blocks of more complex phenotypes, with a cause/consequence order between phenes measured at different levels of plant organization, reflects the difficulty and complexity of choosing the “right” phene (Fig. 11.1). As such, several “causal” phenes could influence a “consequential” trait (for instance, tillering and leaf size on staygreen (Borrell et al. 2014)), or how phene-to-phene interactions could influence a “consequential” trait (e.g., leaf size and leaf thickness effect on transpiration rate (Kholova et al. 2012), in a similar manner than pleiotropy and epistasis in genetics. We think there is no alternative to carefully ordering the cause-consequence structure of phenes to make phenotyping relevant and useful to genetics and breeding. Therefore, phenotyping is not only about generating trait data using well-set protocols, it is truly a scientific approach that involves the deciphering of complex biological cause/consequence relationships in a phenotype.

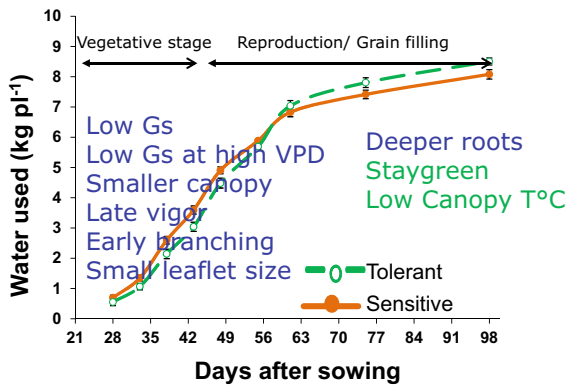


**Fig. 11.1** Profile of water extraction under terminal drought conditions in a set of terminal drought tolerant ( $n = 12$  lines) and sensitive ( $n = 8$  lines) chickpea genotypes having a narrow range of flowering time (re-drawn from Vadez et al. 2014—J Exp. Bot. <https://doi.org/10.1093/jxb/eru040>). Tolerant genotypes extracted less water during vegetative stage and more during reproduction and grain filling. The figure lists possible “causal” canopy phenotypes (in blue), and “consequential” phenotypes (in green), possibly explaining the differences in the patterns of water use

### ***11.2.2 Research-Driven, not Technology-Driven Development of Phenotyping Platforms***

In the past decade, the capacity to image plants has progressed dramatically. This includes simple digital measurement with RGB (Red-Green-Blue) cameras, more specific measurement of temperature with Infrared (IR)-cameras, more complex multi-spectral sensors including the simpler versions to assess vegetative index (e.g., Normalized Difference Vegetation Index (NDVI)), and highly complex hyperspectral or fluorescence measurements. The revolution in phenotyping tools offers both a terrific opportunity and also a major challenge. The opportunity is to extract information from genetic material on “phenotypes” that are non-visible to the human eye, visible but too complex to be measured from simple observations, or new phenotypes that were not considered before. However, the risk is of losing perspective on the target phenotype in favor of the many phenotypes that can be acquired and may be unrelated to the target phenotype.

### ***11.2.3 People-Skills, Cross-Discipline Interactions***

Phenotyping is also a cross-road where technology providers, physiologists, pathologists, geneticists, breeders, data analysts, statisticians, and others, come to interact. It calls for a multidisciplinary effort. For instance, scientists working in the area of stomata patchiness (stomata at the leaf level are regulated by patches that are interconnected) have provided evidence of a close relationship between these processes and those in computation (Peak et al. 2004), and this was only possible because biologists interacted with computer scientists. Linking phenomics information to genomics is a first step as we learn more about “phenes.” However, there is much to be done to make this link workable and useful, first in terms of data format, suitable databases, meta-data informing trials, ontologies, and statistical tools to analyze complex data (Cobb et al. 2013) or multi-trait analysis (Brown et al. 2014; Korol et al. 2001). Linking these dimensions goes beyond finding a technical fix to connect these spheres of information: It is about co-designing the linkages across disciplines and their technical features so that the linkage can be truly functional, leading to new and relevant knowledge. For instance, designing marker-trait analysis that takes into account environmental conditions as a covariate, or discussing population size beforehand to avoid logistical constraints of phenotyping populations larger than, say, 500 individuals, or defining what precision is needed in the measurements. Last but not least, a very close and iterative interaction between technology suppliers and biologists is needed to ensure the phenotyping platforms/sensors truly address the phenotyping needs.

### ***11.2.4 An Issue of Scales: Combining Platform- and Field-Based Phenotyping***

Earlier, we discussed the importance of deciphering phenotypes at different levels of biological organization, and then of structuring phenotypes into cause-consequence relationships. This is where specialized platforms have a role to play, in assessing the variation for critical causal traits and harnessing the genetics of these building blocks. Because such platforms cannot be developed in all breeding programs, there is a need to have a connection between platform-based trait phenotyping that the breeder can access in a simple and high-throughput manner and field-based phenotyping. The connection between trait and field phenotyping can also be established when traits can be measured in the field itself by imagery sensors, and then linked to agronomic assessment, e.g., grain or stover yield, in a network of testing locations. A few recent papers describe a number of such applications for trait phenotyping in the field (Araus and Cairns 2014; White et al. 2012; Deery et al. 2014), including tractor-based supporting devices and airborne devices. For instance, genotypic differences in the response of leaf expansion to vapor pressure deficit (VPD) (e.g., Welcker et al. 2011) could be proxied by NDVI measurements in the field. In this case, NDVI assessment in the field would integrate over time the cumulative effects of a physiological process that can be measured in a specialized platform. These applications also need to monitor the degree of causality/consequence of the different phenotypes that are measured (Fig. 11.1). The next step as we move up in the degree of plant integration is to establish links with agronomic assessments, where it can be tested in which environment a given trait, measured in a specialized platform, would have an effect on yield. Taking again the example of the sensitivity of leaf expansion to high VPD, it was shown that this trait was correlated to the drought sensitivity index measured in the field (Chapuis et al. 2012). In short, there is a great prospect for using the information from specialized platforms to inform and enrich field-based phenotyping application and use these traits in selection (see Fig. 11.2).

### ***11.2.5 Linking Phenotyping to Crops Simulation modeling***

Once traits benefitting crops under certain water stress patterns have been identified, testing their effects of traits via experimental means is restricted to a few traits at a time and a few environmental and climatic scenarios. In addition, the complexity in the resulting phenotypes originates from the interaction among traits and from their interactions with the environment (Buckler et al. 2009; Schuster 2011). This is where crop models can serve to “integrate” complex behavioral/developmental processes of plants that are all related through water need/use (Fig. 11.2). Models that are suitable for this must contain algorithms that reflect observable and quantifiable biological observations (Sinclair and Seligman 2000; Hammer et al. 2010). This is only then that models can be sensitive to changes in the conditions and can accurately predict

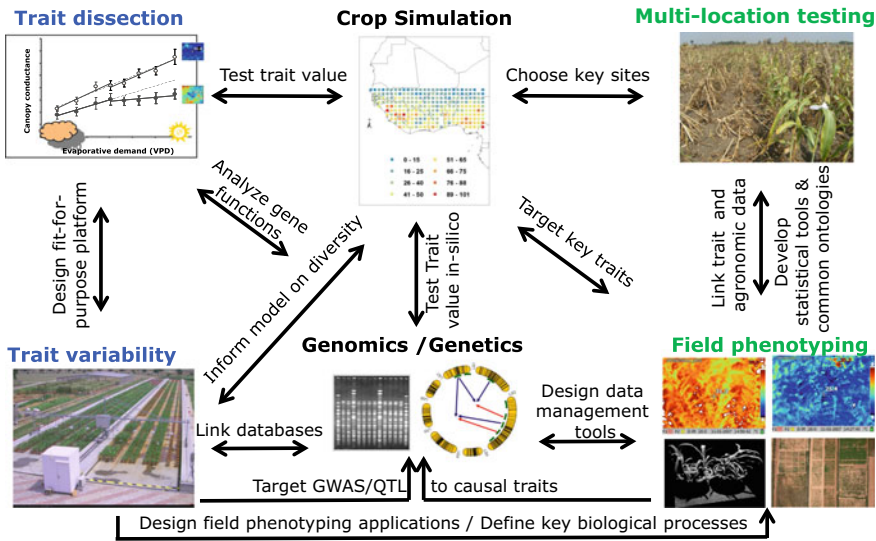


**Fig. 11.2** Schematic linkage relationships between disciplinary effort toward crop improvement. The left part of the schema deals with trait dissection variability (blue), and how specific platforms are designed to phenotype for critical traits at a large scale. The top left graph displays genetic variation for a water-saving trait (Kholova et al. 2010). The bottom right picture presents the LeasyScan platform (Vadez et al. 2015). The central part of the schema represents the interface with crop simulation and genetic analysis (black). The top central map represents the yield increase arising from the modification of a genetic trait, displayed in form of model output in  $1^\circ$  latitude  $\times$   $1^\circ$  longitude averaged across 50 years of weather information (Vadez et al. 2017). The right part of the schema are the field applications of phenotyping (green), where consequential phenotypes are measured along with agronomic traits. The top right picture represents the expression of a staygreen phenotype in sorghum lines introgressed with a staygreen QTL. The bottom right pictures represent different possible applications to field phenotyping. The different arrows represent the main linkage relationships between disciplinary domains and indicate the type of actions needed to make the links functional

effects. There is now convincing evidence that crop models are relevant to guide breeding targets (Kholová et al. 2014; Vadez et al. 2012; Reynolds et al. 2018). Using a mechanistic crop model, Soltani and colleagues (1999) showed that an early decline in leaf expansion and transpiration upon soil drying in chickpea led to about 5% yield increases under water stress conditions. Therefore, these traits had a limited interest where they were tested and did not justify an investment in breeding. In another study with chickpea, a rapid root growth rate decreased yield by an average of 5%, whereas an increase in the depth of root water extraction by 20 cm increased yield by an average of 10% (Vadez et al. 2012). This example shows the efficacy of a model for comparing genetic options, before deciding what to possibly invest in. In the last example in sorghum, the capacity to restrict transpiration under high VPD was simulated and showed yield advantage in all situations where it was tested, yet with higher effect in zones facing severe water stress (Kholová et al. 2014). The modeling approach is powerful because it is now possible to simulate the effects of



certain Quantitative Trait Loci (QTLs) on yield, based on the percentage effect of a given QTL on particular traits (Chapman et al. 2003; Welcker et al. 2007; Chenu et al. 2009; Cooper et al. 2009). We believe that investment in HTP platforms could be guided by prior crop simulation of the value of the trait that is targeted in these platforms.

## 11.3 Phenotyping Platforms

### 11.3.1 Lysimetric System to Assess Plant Water Use

Roots are intuitively basic for crops and especially for the adaptation of a crop to water deficit because nutrients and water are absorbed through them. However, they are difficult to work with (Vadez 2014). For water stress research, the root capacity to extract water was the basis of the idea to develop a lysimeter-based system (Vadez et al. 2008, 2014), in which consecutive weighings of lysimeters provide data on plant water extraction to support transpiration at different times (Fig. 11.3). Because the goal was to measure water use in crops grown under field conditions (something that is difficult to do precisely in the field) and with a high throughput, certain basic principles had to be followed. The platform was set outdoors and the tubes were designed and placed so that soil volume and surface area were similar to field population densities. Therefore, two types of tubes were developed to cater for different crops: Small lysimeters (1.2 m length and 20 cm diameters) were designed for crops sown at approximately 20 plant  $m^{-2}$  like chickpeas (Zaman-Allah et al. 2011b), whereas the large lysimeters (2.0 m length and 25 cm diameters) were designed for crops sown at approximately 10 plant  $m^{-2}$  (Vadez et al., 2011, 2013a). Lysimeters were also treated as micro-plots and kept undisturbed from one crop to the next, following a field-like rotation, alternating either experimental or fallow crops.

**Fig. 11.3** Overview of the lysimetric platform at ICRIASAT (LysiField), showing the large tubes (25 cm diameter, 2.0 m length), which are set in trenches and allow a planting density of about 10 plant  $m^{-2}$ . A pigeon pea crop is seen on the left trench and a sorghum crop in the central trench



The lysimetric platform was originally designed to screen genotypes for the capacity to extract water from the soil profile, instead of measuring roots. Genetic variation for total plant water extraction was found in all species that were tested (for a review see Vadez et al. 2014). However, the range of variation (30% among a subset of the sorghum reference collection) was not related to yield differences under stress conditions. The relationship between water extraction during the grain filling period and grain yield under stress conditions was much more critical (see Vadez et al. 2014 for a review), e.g., in pearl millet (Vadez et al. 2013a) chickpea (Zaman-Allah et al. 2011b) or peanut (Ratnakumar et al. 2009). For at least three crops, the availability of water during the grain filling period was not related to a higher capacity to extract water, but to earlier water-saving under non-stress conditions. For instance, tolerant chickpea genotypes had a smaller leaf canopy at the vegetative stage (Zaman-Allah et al. 2011a). Tolerant peanut genotypes also developed a smaller leaf canopy (Ratnakumar and Vadez 2011) and tolerant pearl millet had both a lower canopy conductance and the capacity to further reduce the conductance under high VPD conditions (Kholova et al. 2010). There have been similar findings in other crops such as cowpea (Belko et al. 2012) and sorghum (Borrell et al. 2014). In short, even if the cylinders were weighted only about once a week, the lysimetric system provided sufficient precision to pinpoint small but critical differences in the patterns of plant water use. From then on, the focus shifted towards traits that explain these small water use differences and influence the rate at which a crop uses the soil profile's moisture, including (i) canopy size and dynamic of canopy development; (ii) canopy conductance; and (iii) canopy conductance under high VPD (see a review in Vadez et al. 2013b). In other words, specific patterns of plant water use were a "consequential phenotype," and further attention shifted to the "causal phenotypes," which required a different type of measurement (see Fig. 11.1 for an example in chickpea).

### ***11.3.2 The LeasyScan Platform: 3D Scanning Plus Transpiration Assessment***

#### **11.3.2.1 Description**

LeasyScan's principle is to have a continuous and simultaneous monitoring of plant water use and leaf canopy development. In brief, the platform is using a set of scanners (PlantEye, Phenospex, Heerlen, Netherlands) which are moved above the plants using a carrier device and generate 3D point clouds of the crop canopy, from which the leaf area and several other plant parameters are extracted after a segmentation process of the 3D data cloud (Fig. 11.4). Validation of scanned leaf area versus observation has been successfully done before acquiring the equipment and has been re-validated later on while working on higher planting densities (Figs. 4 and 5 in Vadez et al. 2015). Leaf canopy development traits that influence plant water use are a combination of



**Fig. 11.4** Overview of the LeasyScan platform at ICRISAT. A groundnut crop is seen on side strips. The central strip shows the installation of load cells to allow the continuous weighing of the pots. Eight scanners (small white boxes) can be seen, attached to an irrigation boom that travels over the crop, on top of a center and two side walls. The central metal box has a key role to ensure a steady platform movement

(i) vigor, i.e., how quick the canopy develops; and (ii) size, i.e., how large a canopy develops (Fig. 1 of Vadez et al. 2013b).

The PlantEye sensor projects a very thin laser line in the near infrared (NIR) region of the light spectrum (940 nm) on plants and captures the reflected light with an integrated complementary metal oxide-semiconductor (CMOS)-camera. Since most of the light is reflected from plants, the device can operate day and night. All artifacts from sunlight or background noise are automatically removed with inter-graded optical- and algorithm-based sunlight filters. During the scanning process, the scanner linearly moves over the plants and generates 50 height profiles/s, those are then automatically merged into a 3D point cloud with a resolution of around  $0.8 \times 0.8 \times 0.2$  mm into the xyz-direction, respectively. The measurements are triggered and stopped via mechanical barcodes (metal plates 20 mm  $\times$  50 mm) positioned on the platform. PlantEye computes a diverse set of plant parameters on the flight by meshing neighboring points with a nearest neighbor search. From this triangle mesh a subsequent surface triangulation algorithm computes 3D leaf area (which is the area of the leaf independently of its position and orientation in the 3D space and relative to the sensor), plant height, leaf angle distribution within a second.

At the LeasyScan platform, the scanners are pre-set to image an area of 65 cm width and a length of either 40 or 60 cm. The volume in which the 3D image is generated is then a cuboid of 65  $\times$  40  $\times$  100 cm or 65  $\times$  60  $\times$  100 cm. Each scanning unit is referred to as a “sector.” Every 12 consecutive sectors constitute a “field.” Sector-wise binning of data point clouds is performed using a system of barcodes every 5 m (12 times 40 cm + 20 cm gap or 8 times 60 cm + 20 cm gap) to re-set the scanner position in height and length. As in the lysimetric facility, our choice was to remain as close as possible to the field conditions where plants are cultivated in each sector at a density similar to the field (for instance 24–32 plant m<sup>-2</sup>

chickpea or 16 plant  $\text{m}^{-2}$  for pearl millet or sorghum). The scanners are mounted on top of an irrigation boom, which is electronically controlled to be fully automated and speed-controlled. At a movement speed of  $3 \text{ m min}^{-1}$ , eight scanners are capable of scanning 4800 sectors (the name of an experimental unit) in slightly  $<2 \text{ h}$ .

These parameters can be visualized through a web-based software interface (HortControl<sup>R</sup>), which allows the selection of sectors and performs basic grouping functions to assess how the experiment is progressing. In addition, the platform is equipped with a set of 12 environmental sensors (Campbell Scientific, Logan, Utah, USA) that continuously monitor relative humidity (RH%) and temperature ( $T^{\circ}\text{C}$ ), integrating values every 30 min, one light sensor, one wind sensor. Each scanner is wirelessly connected to a local area network (LAN) through which the analyzed data are downloaded onto a server, along with the 3D images. 3D images can be reused at any time; for example, to re-calculate new parameters based on a new algorithm for additional plant traits or for better-optimized scanning software. Therefore, the scanning images become a repository of plant measurements that can be reused at a later date. An important factor to decide on the scanning system was to understand the signal-noise ratio for our targeted phenotype (leaf area), and then check not only the resolution of the sensor itself but also the noise of the environment, e.g., wind, diurnal rhythm of leaves, rain, reflection.

### 11.3.2.2 Integration of Canopy Growth with Plant Transpiration

A basic necessity in the development of the LeasyScan platform was to combine the measurements of leaf development parameters (which can be encapsulated in “volumetric growth”) with a continuous assessment of plant transpiration (or “massic growth” considering transpiration as a proxy for photosynthesis), to obtain a continuous measurement of the canopy conductance and shift from earlier destructive measurements (Kholova et al. 2012). In earlier studies, a low canopy conductance under high VPD was closely related to terminal drought stress adaptation in several crops (see a review in Vadez et al. 2014), but this phenotype depended on time-consuming leaf area measurements, especially in a crop like chickpea (Zaman-Allah et al. 2011b). One part of that phenotype, the leaf area, is described above. The other part of that phenotype, plant transpiration, is typically measured manually by gravimetrically determining transpiration (e.g., Zaman-Allah et al. 2011b). Using scales (also called load cells) then allowed to have a continuous weighing of the pots, avoiding time-consuming weighing of pots. Notably, in the development of this platform, we also sought the possibility to study intra- or inter-specific variations in crop water loss during the night (following recent results in wheat (Schoppach et al. 2014)), the interaction between water use and the 3D architecture of the crop canopy, possible relationships between leaf movements during the day (especially in legumes or, for example, in *Arabidopsis* (Dornbusch et al. 2012)), patterns of plant water use during the day, and of course the interplay between volumetric (leaf area dynamics) and massic (transpiration) growth.

The scales (PSX Rugged Scale 50, Phenospex, Heerlen, Netherlands) that were initially used had a capacity of 50 kg, with 0.02% accuracy. The accuracy of these temperature-corrected scales ( $-10^{\circ}\text{C}$  and  $+40^{\circ}\text{C}$  range) was tested under artificial rapid increase in temperature ( $14^{\circ}/\text{h}$ , i.e., much above our experimental conditions) and showed that the error remained within the stipulated 0.02% error range. The scales provided a reading with a 0.02% precision every second and these were integrated over one hour, giving readings with a precision of 0.1 g. An initial prototype of scale was developed where the frequency of measurements was limited to one every hour. After validation that key phenotypes like the capacity to restrict transpiration under high VPD could be measured (see Fig. 11.9 in Vadez et al. 2015), 1500 load cells were installed, each with a 150 kg capacity (Fig. 11.4). This increased capacity now allows to grow plants on large trays ( $60\text{ cm} \times 40\text{ cm} \times 30\text{ cm}$ , length-width-height) containing about 90 kg of soil and allowing to grow several plants in conditions that mimics the field. It also allows to irrigate at less frequent intervals, yet maintaining plants away from water stress.

### 11.3.2.3 Data Generation, Storage, and Visualization in HortControl

Scanning takes place every 2 h so that about 50,000 scans are captured every day and about 10 traits are calculated for each scan. This is in addition to the environmental data that are measured every minute. With regards to load cells, these are polled by a micro-processor every half-second and these data are integrated and loaded on the database every 15 min so that each load cell delivers 96 data points every day. All data gathered from PlantEye sensors, scales, and associated climate sensors are stored in a central PostgreSQL database. The data can be accessed and visualized with the web-based HortControl software that allows to follow up the progress in the different parameters that are measured. The three types of data collected in the platform, i.e., scan, weight, climate, are not collected at the same frequency. Therefore, the data are downloaded independently. R-scripts have then been developed to aggregate data at a time scale suited for all three types of data (Kar et al. 2020a). HortControl is used as a data visualization tool to monitor the experiment, for instance, to ensure scan data are properly computed, or possibly to detect load cell errors. In particular, the 3D image of any sector at any time during the experiment can be called for quality control, which is particularly useful to pinpoint possible outliers (for example, in case of sector to sector overlapping or other unexpected disturbance). It also allows the simultaneous plotting of the environmental conditions to the parameter evolution, for instance, to qualitatively estimate reasonable wind thresholds in each species.

### 11.3.2.4 Database Access, Processing, and Analysis

One major challenge of this platform, and of any high-throughput platform, is the analysis of the data. This issue was discussed at length in a recent review (Cobb et al. 2013). At the same time, well-documented datasets represent a potential treasure

trove to investigate plant growth processes on a large scale (for example, in meta-analysis (Poorter et al. 2010)). In that regard, we focused on linking measurement data with the most critical environmental parameters affecting plant growth (i.e., temperature, relative humidity, and light). It is also critical to have detailed meta-data accompanying the datasets if they are to be re-used in the future.

Processed data (e.g., leaf area) can be downloaded from a function in HortControl. These data are queried from the database via an R-command library interface working at the back-end (R, version 4.2.1, the R foundation) (Fig. 11.5). Among the essential features of the library is a process for smoothing data and for filtering the data to reject outliers. For instance, wind affects the quality of the 3D images. Data obtained when the wind is too high to have useful information (from shaky images) should be filtered out. The scanning data are tagged to the timing of each scan so that the time stamp can be linked to the environmental data provided. A data pre-processing and analysis pipeline has now been recently developed (Kar et al. 2020b) for scanning data, which allows to apply filters on raw data towards outlier detection, to input missing data, to choose for an optimal time window for genotype discrimination, and for spatially adjusting data. A similar pipeline has been developing to extract features from the transpiration profiles coming from the load cells and that characterize the transpiration response to high VPD conditions (Kar

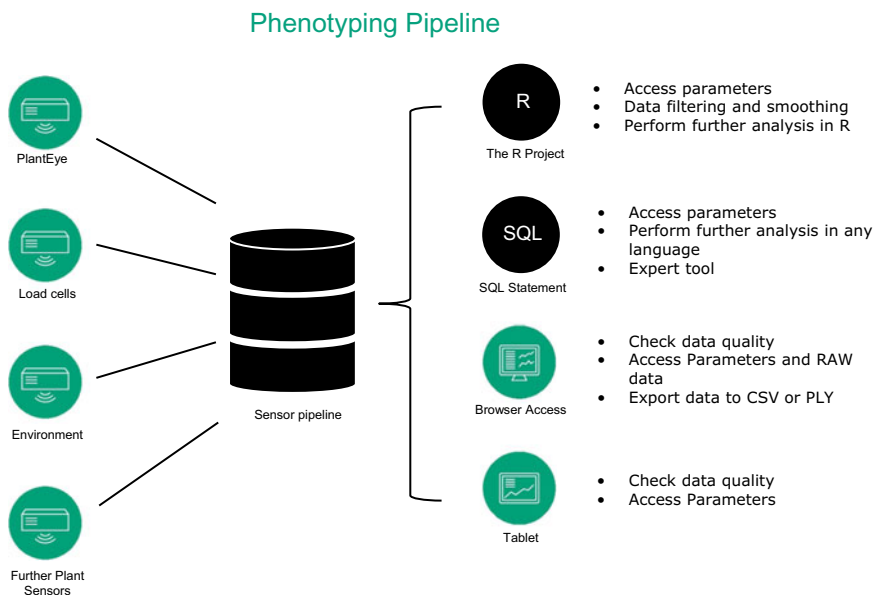


**Fig. 11.5** The phenotyping processes flow; the information generated by the PlantEye<sup>R</sup> scanners along with the information from the environmental sensors are connected to one another through time stamps and stored in the data repository system. Data can be called from the repository through various means: using R software, web-based interface browser (Hortcontrol<sup>R</sup>), and is also compatible with other analytical tools (SQL)

et al. 2020a). We are also planning to develop an alternative time stamp, right from the "R" interface, calculated from the temperature conditions and based on either thermal time or equivalent time at 20° (Parent et al. 2010). This feature would allow us to compare growth traces across experiments and analyze environmental effects on canopy development, independent of temperature effects. In this way, the analysis will increasingly become an exercise of statistical treatment of massive data series.

## 11.4 Cost of HTP Methods and Their Linkage to Breeding Efforts

### 11.4.1 Cost of HT Phenotyping

While new technologies offer precision and throughput, technology cost is an important decision factor. High-throughput phenotyping could directly contribute to breeding efforts but the choice made by breeders to adopt or not a given HTP approach will often/always be driven by a cost consideration. The "breeder's equation" is as follow:

$$\Delta G_{\text{year}} = i * r * \sigma / L$$

where  $\Delta G_{\text{year}}$  is the genetic gain per year,  $i$  is the selection intensity,  $r$  is the selection accuracy (or the heritability),  $\sigma$  is the genetic variance for the desired trait, and  $L$  is the length of one generation. The cost of achieving a given  $\Delta G_{\text{year}}$  per unit of phenotyping cost would then be

$$\Delta G_{\text{year}*\$} = i * r * \sigma / L * C$$

where  $C$  is the phenotyping cost per progeny. Breeding being a numbers' game, optimizing this ratio can be done in several ways where HT phenotyping has a role to play:

- The coefficient "r" proxies the accuracy of the trait. Breeders would always ask if a given trait is more accurate than those they measure already such as yield. Let's assume a trait is a good predictor of an increased yield, it could be given priority over yield assessment if its heritability was higher than yield heritability, provided its cost is not prohibitive. One could assume that the decision would depend on the ratio  $r/C$ . A heritability doubled by a HTP method would afford an increase in cost per progeny of a similar magnitude.
- The coefficient "i" here becomes important because it concerns the throughput at which phenotyping efforts are made. Let's assume here again a trait that is a good predictor of an increased yield. Its advantage could be in the fact that thousands

of progeny lines could be tested, instead of only a smaller number of lines that can be tested for yield. Therefore, any HTP method that could cater for a large number would allow to dramatically increase the selection accuracy. Here also the cost factor determines the choice within the boundaries of the  $i/C$  ratio.

- Finally, the coefficient " $\sigma$ " could be concerned in cases where there is large genetic variance for a given trait. A genetic variance for a given trait that is larger than the genetic variance for yield would potentially favor this trait over yield, provided that there is also a close association between this trait and yield under relevant scenarios.

### ***11.4.2 Integration of HTP Methods into Breeding***

This effort is a mix of being pragmatic while seeking the advantage of new technologies. Technology developer often propose high-end solutions while breeders want simple tools, easy to use, and cheap. So, efforts are needed to connect these two domains. Here, a few examples of existing cases showcase a possible fit between the "offer" from the HTP standpoint and the "demand" from the breeding side.

*Drone/remote sensing imaging—HTP methods at the service of yield trial quality control*—The use of drone imaging to acquire plant features that would be otherwise difficult or simply impossible to acquire has grown exponentially (Potgieter et al. 2016). Except for few programs the use of drone in routine breeding still remains at a research phase, although opportunities exist that would bring a lot of benefit. The first among these would be the use of drone imaging to support the quality control of plot measurements. Indeed, breeding networks in the National Agriculture Research Systems (NARS) could benefit from imaging technology to quickly assess the quality of testing fields. For instance, by measuring plant counts and ensuring these are in accordance with targeted density, or by measuring NDVI around canopy closure to ensure homogeneity in the plots. This information could be used to remove heterogeneous plots or parts of the field in the analysis and it would increase the accuracy of the evaluations. Quality standards during data acquisition will be needed to ensure the quality of drone images. For breeding programs to have an easy access to drone technology, data processing and analysis pipeline will also be needed, allowing breeding programs to easily load their images and receive data with a rapid turnover time to be part of the selection decisions. Then only more sophisticated measurements can be taken from the research stage to the scale of a breeding program. Additional such traits could be yield estimates (Guo et al. 2018), or indices that reflect on the crop development, functioning and efficiency with indices reflecting light interception, radiation use efficiency.



### 11.4.3 *Quality Analysis*

NIRS spectroscopy is being routinely used in the assessment of quality in grain and in stover. NIRS measurement currently take place in the lab using benchtop NIRS equipment in most cases. NIRS probes can also be mounted on combine harvesters, as is done in the private sector for major crops like maize. There is also an opportunity to insert NIRS probes in smaller harvesting equipment like the Harvest Master (Juniper System Inc, Logan, UT, USA). Different portable NIRS now exist and start being tested for a direct evaluation of quality in the field (Blummel, pers. Comm.). Raman spectroscopy is also appearing as a new opportunity technology, complementary to NIRS in the domain of quality analysis (Altangerel et al. 2017). X-ray fluorescence (XRF) equipment are used to measure mineral content of grain such as Fe or Zn, which are important but deficient component of the diet of poor rural populations of Africa and Asia.

For many breeding programs of the public system in crops others than the main commercial commodities like maize, wheat, or rice, breeding for quality to respond to a market or consumer demand, or to address a nutritional issue, imply a major shift in what is being evaluated. While the technologies above are available, they are still largely disconnected from the breeding process pipeline. That is, agronomic traits are measured at harvest while quality traits are measured after harvest, often too late to be taken into consideration in breeding selection decisions. Therefore, efforts here are needed to streamline the assessment of quality with the usual traits, allowing the combination of the probes above in the breeding process, here also accounting for time and cost of including these additional sensors and of making additional measurements. It requires the re-designing of harvesting pipelines, the possible re-development of harvesting tools including quality probes.

## 11.5 Conclusion

While new technologies provide opportunities to make phenotyping easier, faster, less expensive, and more informative, they also run the risk of becoming the end that justifies the means. We can avoid this by driving the technology with research questions, made possible through a cross-discipline approach between genetics, breeding, modeling, engineering, physiology, pathology, data management, and statistics. Combination of trait-based phenotyping targeting “building blocks” of critical phenotypes (phenes) to field-based phenotyping for capturing these traits or their consequences holds great promise to generate relevant phenotyping information to breeding programs and match up the load of genomic data available for finding genes behind the phenes. Last but not least, the cost of these HTP technologies has to be taken into consideration if these are to be used in breeding pipelines.

**Acknowledgments** The authors are thankful for the funding from ICRISAT for the capital investment in the LeasyScan facility and to the Kirkhouse Trust fund for contributing to the acquisition of additional scales.

## References

- Altangerel N, Walker JW, González PM, Bailey DW, Estell RE, O'Scullly M. M (2017) Comparison of near infrared reflectance spectroscopy and raman spectroscopy for predicting botanical composition of cattle diets. *Rangeland Ecol Manag* 70:781–786
- Araus JL, Cairns JE (2014) Field high-throughput phenotyping: the new crop breeding frontier. *Trends Plant Sci* 19:52–61
- Belko N, Zaman-Allah M, Cisse N, Diop NN, Zombre G, Ehlers JD, Vadez V (2012) Lower soil moisture threshold for transpiration decline under water deficit correlates with lower canopy conductance and higher transpiration efficiency in drought-tolerant cowpea. *Funct Plant Biol* 39:306–322
- Borrell AK, van Oosterom EJ, Mullet JE, George-Jaeggli B, Jordan DR, Klein PE, Hammer GL (2014) Stay-green alleles individually enhance grain yield in sorghum under drought by modifying canopy development and water uptake patterns. *New Phytol* 203:817–830
- Brown TB, Cheng R, Sirault XRR, Rungrat T, Murray KD, Trtilek M, Furbank RT, Badger M, Pogson BJ, Borevitz JO (2014) TraitCapture: genomic and environment modelling of plant phenomic data. *Curr Opin Plant Biol* 18:73–79
- Buckler ES, Holland JB, Bradbury PJ, Acharya CB, Brown PJ, Browne C, Ersoz E, Flint-Garcia S, Garcia A, Glaubitz JC, Goodman MM, Harjes C, Guill K, Kroon DE, Larsson S, Lepak NK, Li H, Mitchell SE, Pressoir G, Peiffer JA, Oropeza Rosas M, Rocheford TR, Romay MC, Romero S, Salvo S, Sanchez Villeda H, da Silva HS, Sun Q, Tian F, Upadaya N, Ware D, Yates H, Yu J, Zhang Z, Kresovich S, McMullen MD (2009) The genetic architecture of Maize flowering time. *Science* 325(5941):714–718. <https://doi.org/10.1126/science.1174276>
- Chapman S, Cooper M, Podlich D, Hammer G (2003) Evaluating plant breeding strategies by simulating gene action and dryland environment effects. *Agron J* 95:99–113
- Chapuis R, Delluc C, Debeuf R, Tardieu F, Welcker C (2012) Resiliences to water deficit in a phenotyping platform and in the field: how related are they in maize? *Eur J Agron* 42:59–67
- Chenu K, Chapman SC, Tardieu F, McLean G, Welcker C, Hammer GL (2009) Simulating the yield impacts of organ-level quantitative trait loci associated with drought response in maize: A “Gene-to-Phenotype” modeling approach. *Genetics* 183:1507–1523
- Cobb JN, DeClerck G, Greenberg A, Clark R, McCouch S (2013) Next-generation phenotyping: requirements and strategies for enhancing our understanding of genotype-phenotype relationships and its relevance to crop improvement. *Theor Appl Genet* 126:867–887
- Cooper M, van Eeuwijk FA, Hammer GL, Podlich DW, Messina C (2009) Modeling QTL for complex traits: detection and context for plant breeding. *Curr Opin Plant Biol* 12:231–240
- Deery D, Jimenez-Berni J, Jones H, Sirault X, Furbank R (2014) Proximal remote sensing buggies and potential applications for field-based phenotyping. *Agronomy* 5:349–379
- Dornbusch T, Lorrain S, Kuznetsov D, Fortier A, Liechti R, Xenarios I, Fankhauser C (2012) Measuring the diurnal pattern of leaf hyponasty and growth in Arabidopsis—a novel phenotyping approach using laser scanning. *Funct Plant Biol* 39:860–869
- Guo W, Zheng B, Potgieter AB, Diot J, Watanabe K, Noshita K, Jordan DR, Wang X, Watson J, Ninomiya S, Chapman SC (2018) Aerial imagery analysis—quantifying appearance and number of sorghum heads for applications in breeding and agronomy. *Front Plant Sci*. <https://doi.org/10.3389/fpls.2018.01544>

- Hammer GL, van Oosterom E, McLean G, Chapman SC, Broad I, Harland P, Muchow RC (2010) Adapting APSIM to model the physiology and genetics of complex adaptive traits in field crops. *J Exp Bot* 61:2002–2185
- Kar S, Tanaka R, Korbu LB, Kholova J, Iwata H, Durbha SS, Adinarayana J, Vadez V (2020a) Automated discretization of ‘transpiration restriction to increasing VPD’ features from outdoors high-throughput phenotyping data. *Plant Method* 16:140. <https://doi.org/10.1186/s13007-020-00680-8>
- Kar S, Garin V, Kholová J, Vadez V, Durbha SS, Tanaka R, Iwata H, Urban MO, Adinarayana J (2020b) SpaTemHTP: a data analysis pipeline for efficient processing and utilization of temporal high-throughput phenotyping data. *Front Plant Sci* (In press)
- Kholova J, Hash CT, Kumar PL, Yadav RS, Kocova M, Vadez V (2010) Terminal drought-tolerant pearl millet *Pennisetum glaucum* (L.) R. Br. have high leaf ABA and limit transpiration at high vapour pressure deficit. *J Exp Bot* 61:1431–1440
- Kholova J, Nepolean T, Hash CT, Supriya A, Rajaram V, Senthilvel S, Kakkera A, Yadav R, Vadez V (2012) Water saving traits co-map with a major terminal drought tolerance quantitative trait locus in pearl millet *Pennisetum glaucum* (L.) R. Br *Molecular Breeding* 30:1337–1353
- Kholová J, Tharanya M, Kaliamoorthy S, Malayee S, Baddam R, Hammer GL, McLean G, Deshpande S, Hash CT, Craufurd PQ, Vadez V (2014) Modelling the effect of plant water use traits on yield and stay-green expression in sorghum. *Funct Plant Biol* 41(10–11):1019–1034
- Korol AB, Ronin YI, Itskovich AM, Peng JH, Nevo E (2001) Enhanced efficiency of quantitative trait loci mapping analysis based on multivariate complexes of quantitative traits. *Genetics* 157:789–1803
- Lynch JP, Brown KM (2012) New roots for agriculture: exploiting the root phenome. *Philos Trans Royal Soc B-Biol Sci* 367:1598–1604
- Parent B, Turc O, Gibon Y, Stitt M, Tardieu F (2010) Modelling temperature-compensated physiological rates, based on the co-ordination of responses to temperature of developmental processes. *J Exp Bot* 61:2057–2069
- Peak D, West JD, Messinger SM, Mott KA (2004) Evidence for complex, collective dynamics and emergent, distributed computation in plants. *PNAS* 101:918–922. <https://www.pnas.org/cgi/doi/10.1073/pnas.0307811100>
- Poorter H, Niinemets U, Walter A, Fiorani F, Schurr U (2010) A method to construct dose-response curves for a wide range of environmental factors and plant traits by means of a meta-analysis of phenotypic data. *J Exp Bot* 61:2043–2055
- Potgieter AB, Lobell DB, Hammer GL, Jordan DR, Davis P, Brider J (2016) Yield trends under varying environmental conditions for sorghum and wheat across Australia. *Agric For Meteorol* 228:276–285. <https://doi.org/10.1016/J.AGRFORMET.2016.07.004>
- Ratnakumar P, Vadez V (2011) Groundnut (*Arachis hypogaea*) genotypes tolerant to intermittent drought maintain a high harvest index and have small leaf canopy under stress. *Funct Plant Biol* 38:1016–1023
- Ratnakumar P, Vadez V, Nigam SN, Krishnamurthy L (2009) Assessment of transpiration efficiency in peanut (*Arachis hypogaea* L.) under drought using a lysimetric system. *Plant Biol* 11:124–130
- Reynolds M, Kropff M, Crossa J, Koo J, Kruseman G, Molero Milan A, Rutkoski J, Schulthess U, Singh B, Sonder K, Tonnang H, Vadez V (2018) Role of modelling in international crop research: overview and some case studies. *Agronomy* 8:291. <https://doi.org/10.3390/agronomy8120291>
- Schoppach R, Clavierie E, Sadok W (2014) Genotype-dependent influence of night-time vapour pressure deficit on night-time transpiration and daytime gas exchange in wheat. *Funct Plant Biol* 41:963–971
- Schuster I (2011) Marker-assisted selection for quantitative traits. *CBAB* 11:50–55
- Sinclair TR, Seligman N (2000) Criteria for publishing papers on crop modeling. *Field Crops Research* 68:165–172
- Soltani A, Ghassemi-Golezani K, Khooei FR, Moghaddam M (1999) A simple model for chickpea growth and yield. *Field Crops Res* 62:213–224

- Vadez V (2014) Root hydraulics: the forgotten side of roots in drought adaptation. *Field Crops Res* 165:15–24
- Vadez V, Soltani A, Sinclair TR (2012) Modelling possible benefits of root related traits to enhance terminal drought adaptation of chickpea. *Field Crops Res* 137:108–115
- Vadez V, Kholova J, Yadav RS, Hash CT (2013a) Small temporal differences in water uptake among varieties of pearl millet (*Pennisetum glaucum* (L.) R. Br.) are critical for grain yield under terminal drought. *Plant Soil* 371:447–462
- Vadez V, Kholova J, Zaman-Allah M, Belko N (2013b) Water: the most important ‘molecular’ component of water stress tolerance research. *Funct Plant Biol* 40:1310–1322
- Vadez V, Kholova J, Medina S, Kakkera A, Anderberg H (2014) Transpiration efficiency: new insights into an old story. *J Experimental Botany*, eru040
- Vadez V, Rao S, Kholova J, Krishnamurthy L, Kashiwagi J, Ratnakumar P, Sharma K, Bhatnagar-Mathur P, Basu P (2008) Root research for drought tolerance in legumes: quo vadis. *J Food Legumes* 21:77–85
- Vadez V, Krishnamurthy L, Hash CT, Upadhyaya HD, Borrell AK (2011) Yield, transpiration efficiency, and water-use variations and their interrelationships in the sorghum reference collection. *Crop Pasture Sci* 62:645–655
- Vadez V, Kholova J, Hummel G, Zhokhavets U, Gupta SK, Hash CT (2015) LeasyScan: a novel concept combining 3D imaging and lysimetry for highthroughput phenotyping of traits controlling plant water budget. *J Exp Bot* 66(18):5581–5593. <https://doi.org/10.1093/jxb/erv251>
- Vadez V, Halilou O, Hissene HM, Sibiry-Traore P, Sinclair TR, Soltani A (2017) Mapping water stress incidence and intensity, optimal plant populations, and cultivar duration for african groundnut productivity enhancement. *Front Plant Sci* 8:432. <https://doi.org/10.3389/fpls.2017.00432>
- Welcker C, Bousuge B, Bencivenni C, Ribaut JM, Tardieu F (2007) Are source and sink strengths genetically linked in maize plants subjected to water deficit? A QTL study of the responses of leaf growth and of anthesis silking interval to water deficit. *J Exp Bot* 58:339–349
- Welcker C, Sadok W, Dignat G, Renault M, Salvi S, Charcosset A, Tardieu F (2011) A common genetic determinism for sensitivities to soil water deficit and evaporative demand: meta-analysis of quantitative trait loci and introgression lines of maize. *Plant Physiol* 157:718–729
- White TA, Snow VO (2012) A modelling analysis to identify plant traits for enhanced water-use efficiency of pasture. *Crop Pasture Sci* 63:63–76
- White JW, Andrade-Sanchez P, Gore MA, Bronson KF, Coffelt TA, Conley MM, Feldmann KA, French AN, Heun JT, Hunsaker DJ, Jenks MA, Kimball BA, Roth RL, Strand RJ, Thorp KR, Wall GW, Wang GY (2012) Field-based phenomics for plant genetics research. *Field Crops Res* 133:101–112
- Zaman-Allah M, Jenkinson DM, Vadez V (2011a) Chickpea genotypes contrasting for seed yield under terminal drought stress in the field differ for traits related to the control of water use. *Funct Plant Biol* 38:270–281
- Zaman-Allah M, Jenkinson DM, Vadez V (2011b) A conservative pattern of water use, rather than deep or profuse rooting, is critical for the terminal drought tolerance of chickpea. *J Exp Bot* 62:4239–4252

# Index

## A

- Abiotic and biotic stresses, 3, 40, 130, 167, 193, 199
- Abiotic stresses, 104, 119, 123, 132, 165–167, 170, 171, 174, 177, 183–185, 190
- Above Ground Biomass (AGB), 44–48, 56, 103
- Active sensors, 82, 132
- Aerial platforms, 39, 41, 90
- Aeroponic, 150, 165, 175–177
- Airborne systems, 73
- AKAZE, 56, 58, 59
- All-Terrain Vehicles (ATVs), 18
- Anthocyanins, 137, 192
- Artificial Intelligence (AI), 3, 7, 8, 15, 33, 184, 202
- Artificial selection, 4
- Atmospheric pollution, 210
- Automated traits phenotyping, 177
- Automatic phenotyping systems, 188, 190
- Autonomous mobile phenotyping robot, 13
- Autonomous phenotyping system, 202
- Auto-steer system, 18

## B

- Binary features, 30, 47, 56, 58
- Biological cause/consequence relationships, 226, 228
- Biomass, 17, 30–32, 45, 46, 79, 93, 103–105, 107, 109, 114–120, 132, 136, 137, 140, 144–146, 167, 168, 171, 174, 175, 191, 195, 197, 199, 224
- Biotic stresses, 79, 104, 132, 165, 167, 170, 171, 174, 177, 183–185, 190, 197

- Bootstrapped Structure-from-Motion (BSfM), 55, 65, 67
- Bootstrapping, 58, 61, 62
- Bottleneck, 6, 13, 40, 72, 113, 114, 120, 140, 172, 210, 213, 223
- Breeder's equation, 4, 5, 7, 8, 236
- Breeding, 2–8, 14, 40, 46, 51, 71–73, 79, 80, 92–94, 101, 109, 111, 113, 119, 120, 122, 130–132, 136, 140, 143–149, 153, 154, 165–167, 170–175, 177–179, 183–185, 187, 193, 201, 202, 209–211, 214, 216, 217, 223–226, 228, 229, 236–238
- BRISK, 56
- Bundle adjustment, 63

## C

- Cable suspended large-scale HTP facility, 39, 51
- Camera model, 60
- Canopy cover, 79, 132, 136, 172, 177
- Canopy height, 29, 30, 43, 45–47, 109, 136
- Canopy levels, 15, 40, 43
- Canopy-level traits, 144
- Canopy structure parameters, 43, 47
- Canopy temperature, 29, 43, 46, 73, 79, 108, 109, 133, 144, 153, 167, 168, 173–175, 225
- Canopy temperature depression, 197
- Carbon balance, 216
- Carotenoids, 137, 192
- Chlorophyll, 6, 7, 76, 79, 103, 115, 116, 137, 141, 144, 153, 167, 168, 175, 185, 192, 194–196, 199–201
- Chlorophyll fluorescence imaging, 103, 174

Chlorophyll fluorescence imaging sensor, 195

Classification methods, 139

Clip-and-replace method, 212

Cloud-based computational framework, 212

Computational perception, 31

Computed Tomography (CT), 6, 84, 103, 150, 151

Continuously scanning mode, 188

Controlled environments, 14, 72, 102, 108, 115–117, 149, 183–187, 197, 201, 202

Convolutional Neural Networks (CNNs), 32, 94, 140–143, 148

Coordinated Universal Time (UTC), 80, 90

Correlation coefficient ( $r$ ), 32

Correspondence establishment, 58

Crop architecture features, 189

Crop production equation, 1, 2

Crop segmentation, 43, 47

Crop simulation modelling, 224

Crop simulation models, 145, 146

Custom imaging unit, 212

**D**

Data acquisition systems, 80, 83

Data assimilation, 145

Data delivery pipeline, 43

Data loggers, 74, 75, 80, 170

Data management, 71, 84, 86, 87, 92, 94, 108, 225, 238

Data processing pipeline, 32, 72, 91, 186

3-d canopy architecture, 79

3d data cloud, 231

Deep Learning (DL), 7, 8, 33, 110, 136–143, 147, 148, 195, 199

Deep Neural Network (DNN), 56

Descriptive phenotyping, 8

2d geometric information, 193

Digital genebanks, 113

Digital surface map, 135

3-D imaging approaches, 150

Direct Linear Transformation (DLT), 62

Distance ratio matching, 59, 60

3D laser imaging, 169, 170

3d laser scanning, 105

3D point clouds, 22, 26, 32, 43, 56, 62, 65, 66, 132, 133, 135, 197, 231, 232

3D pose, 60

3D reconstruction, 48, 49, 60, 105, 107, 136

Drought sensitivity index, 228

Drought-stressed, 210

Drought tolerance (DR), 116, 117, 119, 174, 175, 199

## E

Election intensity, 5, 6, 8, 236

Electromagnetic Spectrum (EMS), 79, 132, 191, 192, 196

Environmental sensors, 73, 136, 233, 235

Epipolar line, 61, 64, 65, 67

Essential matrix, 61, 62

Exchangeable image file format (Exif), 86

Exposure time, 31

Extended Kalman Filter (EKF), 22

## F

Fabric, 211

Field based High Throughput Phenotyping (HTP), 39

Field of Views (FOV), 30, 45, 76, 82, 83, 109, 137

Field phenotyping, 39–41, 51, 84, 108–110, 135, 136, 173, 228, 229

Field Plant Phenotyping (FPP), 40, 49, 50

Field robotics, 16, 26

Field Scanalyzer, 15, 73, 84, 173

Fixed platforms, 14, 15

Fixed-wing, 73, 76, 134

Fluorescence imaging, 30, 107, 141, 167, 169, 188, 196

Fluorescent imaging, 107

Flux based, 210

Four-wheel-drive robot, 13

Front-view, 24, 200

Fully automated plant phenotyping, 139

Functional phenomics, 216, 217

Fused data, 144

Fusion method, 23

Fuzzy logic, 23

## G

Genetic gain, 1, 4–6, 8, 85, 92, 94, 120, 121, 140, 236

Genetic mapping, 114, 119, 120, 216, 217

Genome Selection (GS), 102, 120

Genome Wide Association Studies (GWAS), 7, 101, 102, 104, 113–117, 119–122, 148, 153, 185

Genomic Prediction (GP), 121, 153

Genomic Selection (GS), 4, 5, 72, 93, 94, 114, 115, 120, 121, 178

Genomics-phenomics research advancement, 178  
 Genotype-to-phenotype, 72  
 Genotypic profiles, 152  
 Georeferenced, 80, 85  
 Global optimization, 58  
 Global localization, 22  
 Global navigation satellite system, 74, 75, 80, 81, 84, 85, 170  
 Global Positioning System (GPS), 19, 21, 24, 26–29, 136, 137  
 Grain yield, 79, 89, 92, 109, 121, 223, 231  
 Greenhouse, 7, 14, 15, 40, 102–104, 107, 108, 113, 140, 147, 148, 150, 151, 184–187, 189, 198, 217  
 Greenhouse phenotyping, 108  
 Green Super Rice (GSR), 113  
 Green Vegetation Pixel Fraction (GVPF), 44, 45  
 Ground-based field phenotyping, 109  
 Ground-based platforms, 73  
 Ground-based robotic systems, 15  
 Ground-based systems, 87, 131, 137  
 Ground-based tracks, 187, 189  
 Ground Control Points (GCPs), 134  
 Ground robots, 18, 20, 32, 130, 133, 136–138, 149  
 Ground rover, 136  
 Ground sample distance, 83  
 Ground vehicles, 20, 39, 41, 149

## H

High contrast images, 215  
 Highly-variable parameters, 46  
 High-Performance Computing (HPC) cluster, 8, 23, 87, 90, 91  
 High resolution, 7, 31, 77, 78, 83, 105, 106, 109, 132, 136, 137, 139, 146, 165, 185, 193, 196, 201  
 High-resolution aerial imaging system, 171  
 High-speed interface (PCIe), 31  
 High-Throughput Crop Phenotyping (HTPP), 6, 13–20, 30, 32, 33, 187, 191  
 High-throughput crop phenotyping technology, 1  
 High-throughput fixed site phenotyping platform, 173  
 High-throughput Hyperspectral Imaging System (HHIS), 115, 120  
 High-throughput Leaf Scoring (HLS), 114, 117

High-Throughput Phenotyping (HTP), 1, 4, 6–8, 39–41, 49, 51, 71–74, 78–86, 88–95, 101, 102, 108, 111–115, 119–121, 123, 130–132, 134–137, 139, 140, 145–149, 152–154, 165, 167, 168, 170–172, 174, 177–179, 183, 185, 187, 198, 200, 201, 209, 211, 223, 236–238  
 High-throughput Rice Phenotyping Facility (HRPF), 103, 104, 115, 117, 120  
 High-throughput sequencing technology, 5, 113  
 Homogenous lighting conditions, 211  
 Hough transform, 25  
 Hyperspectral, 6, 7, 17, 43, 50, 81, 104, 120, 131–134, 141, 142, 145, 146, 148, 165, 170, 172, 178, 191, 227  
 Hyperspectral camera, 42, 43, 50, 73, 75, 81, 133, 147, 149, 190, 193–195  
 Hyperspectral imaging, 30, 49, 50, 74, 79, 107, 109, 133, 143, 168, 194  
 Hyperspectral imaging system, 148, 167, 190  
 Hyperspectral reflectance, 107, 142, 144

## I

Image analysis software programs, 170  
 Image-based analysis, 130  
 Image-based phenotyping, 131, 152, 201, 211  
 Image-based traits (i-traits), 117, 119  
 Image processing, 14, 32, 44, 82, 134, 135, 139, 148, 149, 198, 199, 202  
 Image processing work, 43  
 Image registration, 43  
 Indirect assessments, 213  
 Indium gallium arsenide (InGaAs), 195  
 Inertial measurement unit (IMU) sensor, 21, 23, 26  
 Infrared radiometer sensor, 109  
 Infrared (IR) range imaging, 172  
 Infrared thermometer, 74, 75, 79, 80, 82, 137, 168, 173  
 Integrated Analysis Platform (IAP), 108, 115–118  
 Integration, 7, 8, 29–31, 33, 39, 42, 72, 130, 144, 149, 153, 177, 209, 216, 217, 223, 224, 228, 233, 237  
 Interaction effects of GEM, 3  
 Internet of things, 3

**K**

Kalman filter, 25  
Kinematic model, 21, 22, 26

**L**

Large scale, 5, 15, 16, 41, 51, 72, 101, 102, 111, 146, 148, 151, 187, 213, 229, 235  
Large-scale ground systems, 39, 41  
Laster Ablation Tomography (LAT), 214, 215  
Leaf chlorophyll content, 200  
Leaf levels, 39, 41, 43, 48, 50, 51, 227  
Light Detection and Ranging (LiDAR), 6, 19, 25, 30, 42, 43, 45–48, 73, 75, 79, 84, 132–136, 168, 170, 188, 197  
Light Emitting Diodes (LEDs), 31, 196, 197, 212  
Lightweight mobile phenotyping platforms, 135  
Linear-Quadratic-Gaussian (LQG), 25  
Linear Quadratic Regulator (LQR), 23–25  
Local Area Network (LAN), 31, 233  
Localization-and-tracking strategy, 21  
Long-Wave Infrared (LWIR), 192, 196  
Lysimetric platform, 223, 230, 231

**M**

Machine learning, 6–8, 79, 94, 111, 114, 121, 130, 137–144, 146–149, 152–154, 193, 199, 202, 213  
Magnetic Resonance Imaging (MRI), 6, 107, 150, 175  
Manual Cart, 136  
Manual phenotyping, 40, 139  
Marker-Assisted Selection (MAS), 8, 93, 166, 178  
Maturity dates, 40, 44–46, 132, 133  
Metabolic activity, 210  
Metadata, 85–87, 90, 227, 235  
Microscopic level, 114, 117  
Microscopic organization, 210  
Mirror-scanning, 50  
Mobile platforms, 14, 17, 41  
Model Predictive Control (MPC), 24  
Modern breeding programs, 4  
Morphological features, 104, 151, 189  
Motorized and Autonomous Robot, 137  
Multi-angle RGB imaging, 49  
Multi-dimensional data, 81, 90  
Multi-rotor drones, 134  
Multi-row corn stand analyzing system, 18

Multispectral cameras, 42, 43, 76, 81, 133, 193, 194  
Multispectral imaging, 136, 167, 168, 172, 175  
Multispectral sensor, 75, 109  
Multi-view Stereo, 56, 60  
Mysql database, 74, 84

**N**

National Agriculture Research Systems (NARS), 237  
Navigation, 13, 20–22, 24–29, 80, 136, 137  
NDVI camera, 136  
Nearest neighbor matching, 59, 60  
Near-Infrared (NIR), 42, 43, 77, 107, 120, 132, 133, 136, 168, 175, 191, 193–195, 232  
Near-Infrared (NIR) hyperspectral imaging, 167  
Near Infrared (NIR) imaging, 107, 173  
Network-Attached Storage (NAS), 87, 91  
Next-generation plant phenotyping system, 201  
Non-contact sensors, 188  
Non-destructive measures, 80, 153  
Non-invasively measure, 72  
Non-invasive measurements, 191  
Nonlinear Model Predictive Control (NMPC), 24  
Normalized Difference Red Edge (NDRE), 194  
Normalized Difference Vegetation Index (NDVI), 30, 43–45, 74, 75, 90–93, 116, 133, 136, 144, 168, 170, 174, 189, 193, 194, 227, 228, 237  
Northern Leaf Blight (NLB), 56  
NU-Spidercam, 16, 41–44, 46, 47, 49–51  
Nutrients, 105, 108, 113, 147–149, 165, 168, 170–172, 174–177, 210, 215–217, 230

**O**

Off-the-shelf auto-steer module, 17  
Onboard instruments, 39, 42  
Operating system (ROS), 31  
Optical sensors, 109, 111, 131, 191  
Optimization-based algorithms, 24  
ORB, 56, 58  
Organ-level traits, 20, 30  
Orthomosaic, 134, 135, 198  
Ortho-mosaicking, 84  
Overhead platforms, 186–189



**P**

Pairwise incremental camera pose estimation, 62

Passive sensors, 82, 132

Perspective-n-Point (PnP), 62

Phene-to-phene interactions, 226

Phenomics, 39, 51, 72–74, 84, 85, 92, 102, 121, 123, 131, 140, 143, 145, 146, 149, 153, 173, 178, 191, 216, 217, 224, 227

Phenotype-genotype map, 107

Phenotypic parameters, 39–41, 46, 51

Phenotypic profiles, 152

Phenotyping gap, 209, 211, 217

Physiological traits, 106, 108, 132, 143, 153, 172

Plant 3D architecture, 193

Plant architecture, 30, 31, 105, 109, 113, 119, 136, 169, 189

Plant breeding, 8, 13, 14, 16, 39, 40, 71, 94, 120, 121, 131, 137, 140, 145, 149, 178, 215

Plant ecology, 217

Planting densities, 32, 44–46, 230, 231

Plant morphological measurements, 29

Plant organization, 72, 224, 226

Plant phenotyping systems, 43, 119, 183, 186

Plant-to-sensor, 14, 187, 189–191, 194, 196

Plot extraction, 134, 135

Plot level, 109

Plot-level traits, 29, 30

Point clouds, 25, 32, 47–49, 81, 84, 135, 199, 232

Positron Emission Tomography (PET), 6, 107, 150

Postgresql database, 234

Potential yield, 3

Precision agriculture, 3, 135, 154

Predicative phenotypes, 202

Predictive phenotyping, 8

Prescriptive phenotyping, 8, 202

Printed Circuit Board (PCB), 31

Proportional-Integral-Derivative (PID), 23

Protocols, 6, 26, 41, 44, 80, 83, 90, 92, 102, 148, 179, 211, 212, 215, 217, 226

Proximal sensing cart, 136

Pulse Amplitude Modulated (PAM) fluorometry, 196

Push-broom, 19, 50, 194

**Q**

Quantitative Trait Loci (QTL), 79

Quantitative Trait Loci (QTL) mapping, 85, 93, 114, 115, 119, 121, 166, 178

Quantitative Trait Locus (QTL), 7, 101, 102, 113

**R**

Radiometric calibration, 82, 84

Rail track systems, 187

Rapid breeding, 5, 170, 179

Real-time images, 22

Real-Time Kinematic Global Positioning System (RTK-GPS), 19–22, 137

Real-Time Kinematic (RTK), 81, 134, 170

Re-calculate, 233

Red, Blue, Green (RGB) cameras, 17, 19, 31, 43, 49, 74–77, 79, 82, 105, 131–133, 136, 137, 140, 165, 170, 179, 193

Reflectance, 7, 43, 49, 50, 109, 132, 133, 141, 142, 144, 146, 174, 175, 193–195, 199

Regions of interest, 17, 81, 82

Regression-based methods, 139

Remote sensing, 14, 49, 81, 109, 120, 121, 141, 142, 172, 195, 237

Rhizotrons, 103, 105, 149, 150, 191

Robotic systems, 7, 17, 26, 137, 152, 187, 189, 190, 197

Robot Operating System (ROS), 25–28, 31

Robust pose recovery, 62

Root cross-sectional anatomy, 210

Root crown phenotyping, 211–213

Root length, 118, 175, 213, 215

Root phenotyping, 105, 106, 109, 114, 117, 141, 149, 151, 152, 175, 209, 211, 213, 216, 217

Root physiological phenes, 210, 215

Roots imaging, 117, 175, 190

Root System Architecture (RSA), 102, 105, 106, 109, 117, 122, 150, 169, 170, 175, 176, 202, 209–211, 217

RTK level, 134

**S**

Satellites, 14, 49, 83, 133, 134, 143–145, 149, 195

Scanner, 76, 105, 109, 111, 118, 150, 151, 213, 231–233, 235

Selection accuracy, 4, 5, 121, 236, 237

Self-contained embedded design, 31

Self-navigating, 20

Semi-automated data processing, 72

Semi-automated phenotyping, 139

Semi-controlled environment, 150  
 Sensors, 3, 6–8, 13–31, 33, 40–44, 47, 51, 72–76, 78–87, 89–91, 94, 105, 106, 108, 109, 130–132, 134–137, 139, 140, 143–145, 149, 151, 154, 165, 167–170, 172–174, 177, 178, 183, 186–197, 199, 201, 227, 228, 232–234, 238  
 Sensor-to-plant, 14, 187, 188, 196–198  
 Sensor-to-plant systems, 151, 187, 190  
 Sequential sample processing, 217  
 Shoot Apical Meristem (SAM), 114, 117  
 Short-Wave Infrared (SWIR), 192, 195  
 Side-view sensing, 19  
 SIFT, 56, 58–60  
 Single-plant level, 109  
 Smartphone system, 111  
 Snapshot (snapshotting) cameras, 194  
 Soil profile, 191, 225, 231  
 Sonar sensor, 109  
 Spatial resolution, 42, 43, 81, 107, 109  
 Spatiotemporal resolutions, 8, 41, 46  
 Spatio-temporal scale, 140  
 Spectral cameras, 193, 194  
 Spectral reflectance, 42, 45, 73, 79, 93, 185, 189, 191, 193–195, 198, 199  
 Spectral reflectance characteristics, 192  
 Spectrometer-fiber system, 42, 45  
 Spectroscopic imaging, 30  
 Spectrum, 7, 32, 50, 79, 81, 90, 132, 133, 143, 144, 190, 232  
 Speed breeding, 5, 178  
 State-of-the-art, 8, 13, 14, 130, 140, 150, 212  
 Stationary Tower/Gantry System, 15, 73, 76, 136  
 Statistical tools, 227  
 Stereo vision, 31, 32, 188, 193  
 Stereo vision-guided robot manipulator, 20  
 Stop-and-go, 188  
 Structure Tensor, 67  
 Structure from Motion (SfM), 135, 188, 198  
 Support Vector Machines (SVMs), 139, 141, 142, 145  
 SURF, 56, 58, 59  
 Sustainable agricultural system, 4

**T**  
 Technology-intensive methods, 225  
 Temporal resolution, 14, 39, 41, 44, 46, 47, 51, 71, 139  
 Terrestrial Laser Scanning (TLS), 76, 136  
 TGRS, 59

Thermal imaging cameras, 133  
 Thermal infrared camera, 42, 43, 75, 196  
 Thermal infrared imaging (IR), 106  
 Thermal Infrared (IR) sensing, 196  
 Threshold-based matching, 60  
 Timed Elastic Band (TEB), 24  
 Time-efficient physical engine, 27  
 Time-of-Flight camera, 6, 74, 197  
 Time-of-Flight (ToF), 19–22, 25, 26, 193, 197  
 Time-of-Flight (ToF) sensor, 197  
 Time-series measurement, 215  
 Time-series tracking, 213  
 Top-viewing sensors, 17  
 Total carbon output, 216  
 Tractor-based supporting devices, 228  
 Trait extraction, 84, 106, 139, 152  
 Transpiration, 106, 117, 119, 146, 167, 168, 170, 196, 197, 225, 226, 229–231, 233–235  
 Triangulation, 232  
 Two-Dimensional (2D) images, 50, 135, 188, 193

**U**  
 Ultrasonic sensors, 74, 132, 170, 197  
 Ultraviolet (UV) Laser-Induced Fluorescence (LIF) imaging system, 196, 214  
 Unmanned Aerial Systems (UAS), 7, 130–136, 144, 149, 152  
 Unmanned Aerial Vehicles (UAV), 14, 73, 76, 78, 80, 82, 83, 86, 87, 90, 109, 110, 120, 121, 133, 141–143, 165, 167, 170, 177, 179  
 Unmanned Ground Vehicles (UGV), 19, 109, 110, 190

**V**  
 Vapor Pressure Deficit (VPD), 228, 229, 231, 233–235  
 Vegetation Indices (VIs), 29, 40, 43, 79, 81, 84, 85, 107, 132, 144, 145, 193, 194  
 Video Mosaicking and summarization (VMZ), 67  
 Visible digital camera, 193  
 Visible imaging, 30  
 Visible imaging system, 167  
 Visible light imaging, 103–105, 167, 168  
 Visible light spectrum, 133  
 Visible Near-Infrared (NIR), 172  
 Vision sensor, 13, 15, 25, 26

Visual ratings, [147](#)

**W**

Wavelengths, [42](#), [79](#), [144](#), [148](#), [165](#), [167](#),  
[190–192](#), [194](#), [196](#)

Wide Area Motion Imagery (WAMI), [65–67](#)

**X**

X-ray CT, [105](#), [106](#), [149–151](#), [169](#)

**Y**

Yield gains, [1](#), [3](#), [4](#), [8](#), [184](#), [190](#)

Yield gap, [3](#)